Lehrstuhl für Fluidverfahrenstechnik
Technische Universität München

Fluiddynamics and Mass Transfer of Single Particles and Swarms of Particles in Extraction Columns

Daniel Garthe

Vollständiger Abdruck der von der Fakultät für Maschinenwesen
der Technischen Universität München zur Erlangung des akademischen Grades eines
Doktor-Ingenieurs
genehmigten Dissertation.

Vorsitzender:	Univ.-Prof. Dr.-Ing D. Weuster-Botz
Prüfer der Dissertation:	1. Univ.-Prof. Dr.-Ing. Dr.-Ing. habil. J. Stichlmair
	2. Univ.-Prof. Dr.-Ing. Dr.-Ing. E.h. E. Blaß, emeritiert

Die Dissertation wurde am 19.01.2006 bei der Technischen Universität München eingereicht und durch die Fakultät für Maschinenwesen am 03.04.2006 angenommen.

Vorwort

Die vorliegende Arbeit entstand während meiner Tätigkeit als wissenschaftlicher Mitarbeiter am Lehrstuhl für Fluidverfahrenstechnik an der Technischen Universität München. Gefördert wurde diese Arbeit von der Arbeitsgemeinschaft industrieller Forschungsvereinigungen sowie der Technischen Universität München. Mein Dank gilt Herrn Prof. Dr.-Ing. J. Stichlmair für das mir entgegengebrachte Vertrauen während der Durchführung meiner Forschungen. Herrn Prof. Dr.-Ing. E. Blaß gebührt mein Dank für die Übernahme des Korreferats und Herrn Prof. Dr.-Ing. D. Weuster-Botz danke ich für die Übernahme des Vorsitzes der Prüfungskommission.

Mein besonderer Dank gilt Herrn P. Hocke, Herrn L. Hinterneder, Herrn B. Faltenbacher, Herrn N. Hodzic und Herrn P. Buchbauer für die umfangreichen konstruktiven Arbeiten, vor allem beim Auf- und Umbau meiner Forschungsanlagen. Ganz besonders möchte ich Herrn P. Hocke danken, der mir durch sein Interesse und Fachwissen bei der Konstruktion der Versuchsanlagen immer hilfreich zur Seite stand. Frau D. Styrnik danke ich für die präzisen und umfangreichen analytischen Laborarbeiten. Weiterhin möchte ich mich bei Frau R. Majewski und Frau M. Schmid bedanken, die mich bei zahlreichen Verwaltungsaufgaben unterstützten.

Bei den wissenschaftlichen Kollegen am Lehrstuhl möchte ich mich für das angenehme Arbeitsklima bedanken. Ganz besonders würdigen und danken möchte ich Herrn Dr.-Ing. M. Tourneau. Seine enorme Unterstützung, vor allem in den ersten Monaten meiner Tätigkeit am Lehrstuhl, seine ständige Hilfsbereitschaft und die zahlreichen wissenschaftlichen Diskussionen trugen maßgeblich zum Gelingen meiner Arbeit bei.

Ausdrücklich möchte ich mich bei den vielen Studenten bedanken, die mich in den letzten Jahren in Form von studentischen Hilfsarbeiten, Semester- und Diplomarbeiten unterstützten. Mein herzlichster Dank gilt Frau C. Fleischer, Frau L. Krauch, Frau F. Sabatier, Frau M. Schröpf, Herrn P. Baier, Herrn A. Bauer, Herrn M. Dopfer, Herrn M. Eberle, Herrn A. Eichner, Herrn H. Förster, Herrn J. Gooding, Herrn S. Holz, Herrn B. Kröss, Herrn J. Laupitz, Herrn T. Lohr, Herrn A. Maier, Herrn M. Notzon, Herrn V. Papaioannou und Herrn M. Rustler.

Mein größter Dank gilt meiner Familie, meiner Lebensgefährtin und meinen engsten Freunden, die mir in den letzten Jahren, vor allem in schwierigen Zeiten, immer zur Seite standen und mir immer wieder neue Kraft gaben.

München, im April 2006

Meiner Familie gewidmet.

Abstract

To this day a liquid/liquid-extraction column can be reliably dimensioned only from preliminary tests in pilot plant columns using the original fluids. The disadvantage of this procedure is that large quantities of fluids are necessary which are often difficult to provide. Furthermore, experiments in pilot plant columns are expensive and time-consuming, and thus reduce the profitability of liquid/liquid-extraction processes. For these reasons, the aim of the chemical industry is to develop new dimensioning techniques. To achieve this goal, attention has turned to the investigation of the fundamental behaviour of single drops. These investigations involve studies of the velocities, the breakage mechanisms and the mass transfer rates of single drops in extraction columns.

When the fundamental behaviour of single drops is properly understood, the interactions of drops in a swarm have to be studied. By understanding the basic principles of the motion of drop swarms, a more reliable dimensioning technique can be established. Single drop experiments combined with computer simulations of drop size distributions, hold-up distributions and concentration profiles can bring extraction processes cheaper to market and can reduce the time-to-market.

The objective of this work is the investigation of the influence of column internals on the behaviour of single particles and swarms of particles. Sieve trays, structured packings, rotating disc agitators and Kühni blade agitators are used as internals in pulsed or agitated extraction columns. Further objectives of this work are the modelling of the characteristic velocities of single particles and the modelling of the hold-up influence on the motion of a swarm. To develop models for the characteristic velocity and the swarm velocity, rigid polypropylene spheres as well as drops are studied. Using rigid spheres offers the advantage that investigations can be carried out in absence of breakage and coalescence effects, which are typical for drops.

The breakage of single drops is investigated to give information about the effects of energy input and drop size on the breakage probability, the number of generated drops and their size distribution. In addition, the influence of column internals, energy input and drop size on mass transfer can be seen from experiments with single drops and swarms of drops. Two different liquid/liquid-systems are used in this work: the standard systems toluene (d)/acetone/water and butyl acetate (d)/acetone/water, which are recommended by the “European Federation of Chemical Engineering“.

Zusammenfassung

Trotz der Vielzahl technischer Anwendungen und der intensiven Entwicklung unterschiedlicher Apparateausführungen in den letzten 50 Jahren ist die Auslegung von Flüssig/flüssig-Extraktionskolonnen immer noch mit erheblichen Problemen behaftet. Bis heute können Extraktionskolonnen nur basierend auf Vorversuchen im Technikumsmaßstab mit den später zum Einsatz kommenden Originalflüssigkeiten ausgelegt werden. Die dafür benötigten großen Mengen an Originalflüssigkeiten sowie die kostenaufwendigen Experimente verringern die Wirtschaftlichkeit eines Extraktionsprozesses.

Das Ziel der Industrie ist es deshalb, Extraktionskolonnen basierend auf experimentellen Untersuchungen mit einzelnen Tropfen in standardisierten Laboranlagen auszulegen. Dazu müssen die grundlegenden Vorgänge beim Tropfenzerfall, die Geschwindigkeiten einzelner Tropfen und die Stofftransportmechanismen von Einzeltropfen in unterschiedlichen Kolonnen bekannt sein. Ein weiterer wesentlicher Aspekt einer exakten Auslegung eines Extraktionsapparates stellt die Bestimmung des Einflusses eines Tropfenschwarms auf die Bewegung einzelner Tropfen dar. Nur durch eine genaue Bestimmung des Schwarmeinflusses, d. h. des Übergangs vom Einzeltropfen zum Tropfenschwarm, wird eine Auslegung von Extraktionskolonnen auf der Basis von Einzeltropfenexperimenten in Verbindung mit PC-unterstützten Simulationsprogrammen möglich. Die Kombination von Einzeltropfen-Untersuchungen und leistungsfähigen Simulationsprogrammen führt zu einer erheblichen Reduzierung der Kosten während einer Kolonnenauslegung und hilft, die immer wichtiger werdende time-to-market eines Extraktionsprozesses deutlich zu verkürzen.

Aus diesen Gründen beschäftigt sich diese Arbeit mit der Untersuchung des Einflusses unterschiedlicher Kolonneneinbauten auf das Verhalten von einzelnen Partikeln (starre Kugeln und Tropfen) und Partikelschwärmen. Das Hauptziel der Arbeit ist die Bestimmung der charakteristischen Geschwindigkeiten von einzelnen Partikeln und die Bestimmung des Schwarmeinflusses auf die Fluiddynamik in unterschiedlichen Extraktionsapparaten. Dazu werden experimentelle Untersuchungen mit einzelnen Partikeln und Partikelschwärmen sowohl in pulsierten Siebboden- und geordneten Packungskolonnen als auch in gerührten RDC- und Kühni-Kolonnen vorgestellt. In den einzelnen Kolonnen werden starre Polypropylen-Kugeln und Tropfen untersucht. Der entscheidende Vorteil bei der Verwendung von starren Kugeln liegt vor allem in der Vermeidung von Zerfalls- und Koaleszenz-Erscheinungen.

Die Untersuchungen zum Zerfall von Einzeltropfen dienen der Bestimmung der Zerfallswahrscheinlichkeiten sowie der Bestimmung der beim Zerfall eines Muttertropfens entstehenden Tochtertropfenanzahl und derren Tropfengrößenverteilung. Durch die Untersuchungen von Einzeltropfen und Tropfenschwärmen kann außerdem der Einfluss der unterschiedlichen Einbauten, des Energieeintrags und der Tropfengröße auf den Stoffübergang in Tropfen ermittelt werden. Als Flüssig/flüssig-Stoffsysteme werden die beiden Standardstoffsysteme Toluol (d)/Aceton/Wasser und Butylacetat (d)/Aceton/Wasser untersucht, die von der Europäischen Föderation für Chemie-Ingenieur-Wesen für experimentelle Untersuchungen in Extraktionskolonnen vorgeschlagen werden.

Contents

1 Introduction

Liquid/liquid-extraction, also referred to as solvent-extraction, is a widely-used separation technique in the metallurgical industry, in the oil industry, in conditioning of nuclear fuels and for wastewater treatments, see *Stichlmair and Steude 1990*, *Rydberg et al. 1992*, *etc*. In recent years liquid/liquid-extraction has also become a preferred separation technique for environmental, biotechnological and pharmaceutical processes, see also *Schmidt 1994*. Compared to distillation, its biggest competitor, extraction offers several advantages in the separation of azeotropic mixtures or the purification of liquids with small amounts of high boiling constituents. Extraction additionally provides considerable advantages in separating mixtures whose fractions have similar physical properties, see *Pilhofer 1989* and *Blaß 1997*. In an extractor one or more solutes of a multi-component liquid feed (raffinate phase) is separated through addition of an immiscible liquid solvent (extract phase). One of the phases, feed or solvent, is dispersed to increase the interfacial area and the mass transfer rates.

For economic reasons the solvent must be recycled, which is often achieved by distillation. Sometimes extraction is the only feasible process for a separation. However, if there is an alternative separation technique, for example distillation, an extraction process must offer distinct advantages. An extraction process is preferred if the energy demand for solvent regeneration is clearly lower than for distillation. Through careful solvent selection, the energy demand for solvent regeneration can be significantly reduced and for this reason, extraction is often used for the treatment of industrial wastewater. Direct separation of the aqueous feed through distillation would require large amounts of energy because of the high enthalpy of evaporation of water. Thus extraction is the preferred separation technique, see also *Goldmann 1986*.

In spite of the various advantages of extraction, it is often not considered in industry. This is mainly due to the fact that a large number of parameters influences the fluiddynamics and the mass transfer in extraction columns, which makes the dimensioning of such columns difficult.

1.1 Problems in Column Dimensioning

The fluiddynamics in counter current liquid/liquid-extraction columns with different internals is affected by many parameters. A very important factor is the drop size and drop size distribution of the dispersed phase along the column height. The drop size distribution is governed by breakage and coalescence mechanisms and can be relatively narrow or wide, depending on column internals and operating conditions. The drop size has great impact on the drop velocity. In addition, the drop velocity is controlled by the internals, which act as a hindrance to the drops, and the energy input. Furthermore, the velocity of a swarm of drops can significantly differ from the velocity of single drops. The influence of drop concentration (i. e. hold-up) on the velocity of a swarm, which is the so-called swarm influence, is not satisfactorily understood to this day. Hence, the prediction of the maximum throughput rates of the dispersed phase, which is strongly related to the velocities of the drops, is a complex issue.

Mass transfer also has a strong influence on fluiddynamics, and vice versa. The physical properties of the liquid/liquid-system change along the column height. For example, mass transfer has a strong effect on the interfacial tension of a liquid/liquid-system. For this reason, breakage and coalescence behaviour will change along the column height and different drop sizes and velocities will appear. Thus, the development of scale-up methods based on fluiddynamic evaluations without considering mass transfer seems insufficient.

Even though mass transfer in and out of single drops has been studied by several research groups, there still exists no reliable method for modelling the mass transfer rates in swarms of drops. Furthermore, the effect of surface instabilities (see *Blaß et al. 2000*) which cause convections or turbulent eruptions at the interface (Marangoni convections) and the effect of tensides are not well understood.

1.2 Ways to Solve the Problems

As mentioned, there are many parameters that influence fluiddynamics and mass transfer in extraction columns. It is obvious that the dimensioning of extraction columns without preliminary tests is not possible with the current standard of knowledge. For this reason, pilot plant tests are often carried out using the original liquids. Based on the results of these experiments, models can be developed for predicting the performance of pilot plant columns

and scale-up methods can be used. The disadvantage of this approach is that large amounts of liquids are needed and that experiments in pilot plant columns are time-consuming.

Nowadays, the aim of novel scale-up methods is to reduce the experimental effort of the preliminary tests by investigating the fundamental behaviour of single drops. The basic phenomena typically studied during experiments with single drops are the breakage mechanisms, the drop velocities, and the mass transfer rates. Experiments with single drops are performed in laboratory scale columns. These columns typically have a diameter of 80 mm and a height of 1 m. The volume of liquids required for these experiments is very low, for example, only a few litres. However, not only the quantity of liquids but also the time for the preliminary experiments is considerably reduced. Hence, enormous cost reductions are associated with these novel methods.

Finally, an extraction column is dimensioned from the results of the single drop experiments in combination with computer simulation programs. These simulation programs are normally based on drop population balance models (DPBMs). DPBMs describe the behaviour of discrete drop size classes in different column sections along the column axis. Using this procedure, the efficiency of pilot plant extractors can be predicted with an accuracy of 20 % of the actual column efficiency, see *Hoting 1996*, *Modes 1999*, *Henschke 2003*, *etc*.

1.3 Objectives of This Work

Objectives of this work are the investigation of the behaviour of single particles (rigid spheres and drops) and swarms of particles in extraction columns with different internals. The dependence of drop velocity, breakage and mass transfer on drop size, energy input and internals is of main interest. In addition, the influence of drop concentration on the motion of drops is of special interest. Through a correct description of the behaviour of both single drops and swarms of drops, hold-up distributions, drop size distributions and mass transfer rates can be accurately calculated by DPBMs.

The behaviour of single rigid spheres is investigated to gain information about the influence of column internals and energy input. Using rigid spheres allows the determination of the parameters that have the greatest influence on the velocities of single spheres in absence of breakage and coalescence. Furthermore, single drops are analysed to obtain information about velocity, breakage and mass transfer rates in compartments with different internals.

Swarms of rigid spheres and drops are also studied. A new swarm model for predicting the influence of particle concentration on fluiddynamics will be presented. In addition, mass transfer efficiencies of different extraction columns will be shown. For these reasons, rigid polypropylene spheres and two different liquid/liquid-systems will be studied in pulsed columns with sieve trays or structured packings as well as in agitated columns with rotating discs or Kühni blade agitators.

- *Annotation to this work*

The main part of this work resulted from work on an industry-funded project. Three research groups from three different universities were involved in the project and a new design method for different extraction columns was developed. While this work deals mainly with experimental investigations and the development of correlations to predict the velocities of single drops and swarms of drops, the other groups involved were mainly concerned with the development of simulation programs based on drop population balance models. In combination with the experimental data and the derived correlations, these simulation programs gave information about the accuracy of the new scale-up method. Parameters such as drop size distributions, hold-up distributions and concentration profiles obtained from experiments in different pilot plant extractors were compared with calculated parameters of the project partners. Exact information on the simulation programs and their validation can be found in the *Final Report AiF 40 ZN 2004*.

2 Critical Review of the Literature

The following sections provide an overview of different ways to model an extraction column and give information about the most important parameters which influence the behaviour of single drops and swarms of drops. In addition, the fluiddynamic and mass transfer models in the literature used to predict parameters such as drop size, hold-up and mass transfer rates in liquid/ liquid-extractors will be critically reviewed.

2.1 Modelling of Counter Current Liquid/Liquid-Extractors

The performance of extraction columns has been extensively investigated, see *Niebuhr 1982*, *Kumar 1985*, *Korchinsky and Ismail 1988*, *Nedungadi 1991*, *etc.* The objectives of many investigations were to simplify and improve the selection and dimensioning of extractors. For this purpose, physical models derived from these investigations describe integral parameters such as average drop size, total hold-up of dispersed phase, axial dispersion coefficients of both phases and overall mass transfer coefficients. Thus, the dispersed phase is treated as a mono-dispersed or a quasi-continuous fluid. The dispersion model and the backflow model are often used.

The deviations between these models and experiments, together with the problems associated with transferring the derived integral models to different column dimensions or liquid/liquid-systems, reveal that new ways of modelling extraction columns must be found. In particular, the consideration of the poly-dispersed character of the dispersed phase gives rise to a more realistic description of the two-phase flow and the mass transfer in extraction columns. Thus, drop population balance models are often used for dimensioning extractors. With these types of models the characteristic features of the dispersed phase, such as drop velocities, breakage behaviour and mass transfer mechanisms, are determined as a function of drop size distribution. Hence, the characteristic features of the dispersed phase are obtained for all drop size classes. In addition, the combination of drop population balance models with results of single drop experiments produce much more reliable results than integral models, see also *Olney 1964*. The basic features of integral models and drop population balance models are presented in the following sections. The backflow model is explained in detail as an example of an integral model.

2.1.1 Backflow Model

The determination of the mass transfer performance of an extractor is often carried out by modelling the column as a cascade of equilibrium stages. A very simple way is achieved assuming that plug flow exists for both phases, see also *Schweitzer et al. 1996*. For mass transfer from a continuous to a dispersed phase, the mass transfer performance is then determined by the number of equilibrium stages n_{th} per active column height H_{ac}:

$$\frac{n_{th}}{H_{ac}} = \frac{1}{H_{ac} \cdot ln\lambda} \cdot ln\left[\left(\frac{X_{in} - Y_{in}/m}{X_{out} - Y_{in}/m}\right) \cdot \left(1 - \frac{1}{\lambda}\right) + \frac{1}{\lambda}\right] \qquad when\ \lambda = \frac{m}{\dot{M}_c/\dot{M}_d} \neq 1 \qquad (2.1)$$

$$\frac{n_{th}}{H_{ac}} = \left(\frac{X_{in} - Y_{in}/m}{X_{out} - Y_{in}/m} - 1\right) \cdot \frac{1}{H_{ac}} \qquad when\ \lambda = \frac{m}{\dot{M}_c/\dot{M}_d} = 1 \qquad (2.2)$$

Here, the main mass flow rates of the continuous phase and of the dispersed phase are given by $\dot{M}_c$ and $\dot{M}_d$, respectively. The solute concentrations of the continuous phase at the inlet X_{in} and at the outlet X_{out} as well as the solute concentration of the dispersed phase Y_{in} are expressed in terms of mass fractions based on solute free bases. The parameter *m* is the distribution coefficient.

However, the assumption of plug flow is in contrast to the actual flow of both phases. In extraction columns a part of each main phase flow is mixed back. Thus, these back mixing currents, so-called axial mixing currents, flow in the opposite direction of the main phase flow. Axial mixing causes a reduction of the driving concentration difference for mass transfer. Subsequently, it reduces the mass transfer rates. In addition, axial mixing causes large uncertainties in the determination of the mass transfer rates in extraction columns with increasing column diameter.

To account for axial mixing, the backflow model is often used. The basic equations of backflow models are derived by the subdivision of the complete column height into several equilibrium stages, see *figure (2.1)*. The main mass flows ($\dot{M}_c$ and $\dot{M}_d$) to and from each stage are accompanied by axial back mixing currents. To account for axial back mixing in the material balances, back mixing coefficients for the continuous phase *f* and the dispersed phase *g* are used. Component balances for the solute in an intermediate stage, where the mass transfer direction is from the continuous to the dispersed phase and the dispersed phase represents the light phase, give:

$$\rho_c \cdot A_C \cdot h_s \cdot (1 - h_d) \cdot \frac{dX_k}{dt} = \tag{2.3}$$
$$\dot{M}_c \cdot [(1+f) \cdot (X_{k+1} - X_k) + f \cdot (X_{k-1} - X_k)] - \beta_{oc} \cdot \rho_c \cdot a \cdot A_C \cdot h_s \cdot \left(X_k - \frac{Y_k}{m}\right)$$

$$\rho_d \cdot A_C \cdot h_s \cdot h_d \cdot \frac{dY_k}{dt} = \tag{2.4}$$
$$\dot{M}_d \cdot [(1+g) \cdot (Y_{k-1} - Y_k) + g \cdot (Y_{k+1} - Y_k)] + \beta_{oc} \cdot \rho_c \cdot a \cdot A_C \cdot h_s \cdot \left(X_k - \frac{Y_k}{m}\right)$$

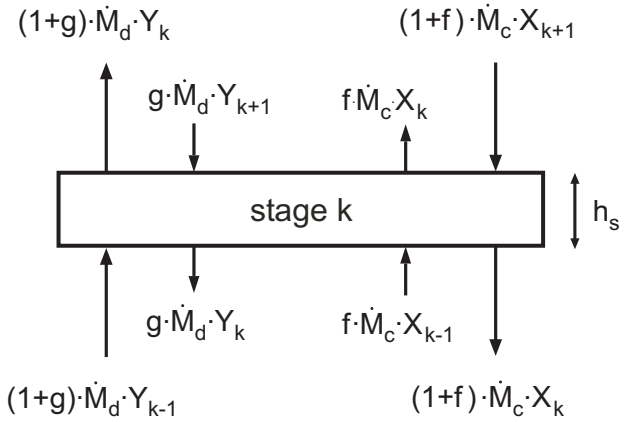

Figure 2.1: Characteristic stage of height h_s with convective and axial back mixing streams for both phases

The component balances in the first and last stages slightly differ, since it is assumed that there is no back mixing underneath the inlet of the dispersed phase and that there exists a concentration jump at the inlet of the continuous phase. For the case of steady state operation, this system of differential equations can be analytically solved if the two phases are immiscible and a linear phase equilibrium exists, see *Mecklenburg and Hartland 1966* and *Steiner 1988*. With the help of the backflow model the mass transfer rates in an extractor can be predicted. For this purpose, additional models have to be used to determine the back mixing coefficients f and g, the volumetric mass transfer area a and the integral overall mass transfer coefficient β_{oc}.

2.1.2 Drop Population Balance Models

The consideration of the dispersed phase as a quasi-continuous fluid is contradictory to the poly-dispersed character of the drops. As a result of the breakage and coalescence mechanisms, relatively wide drop size distributions often exist in extraction columns, see *figure (2.2)*. The drop size distribution can significantly alter along the column height until equilibrium between breakage and coalescence is reached.

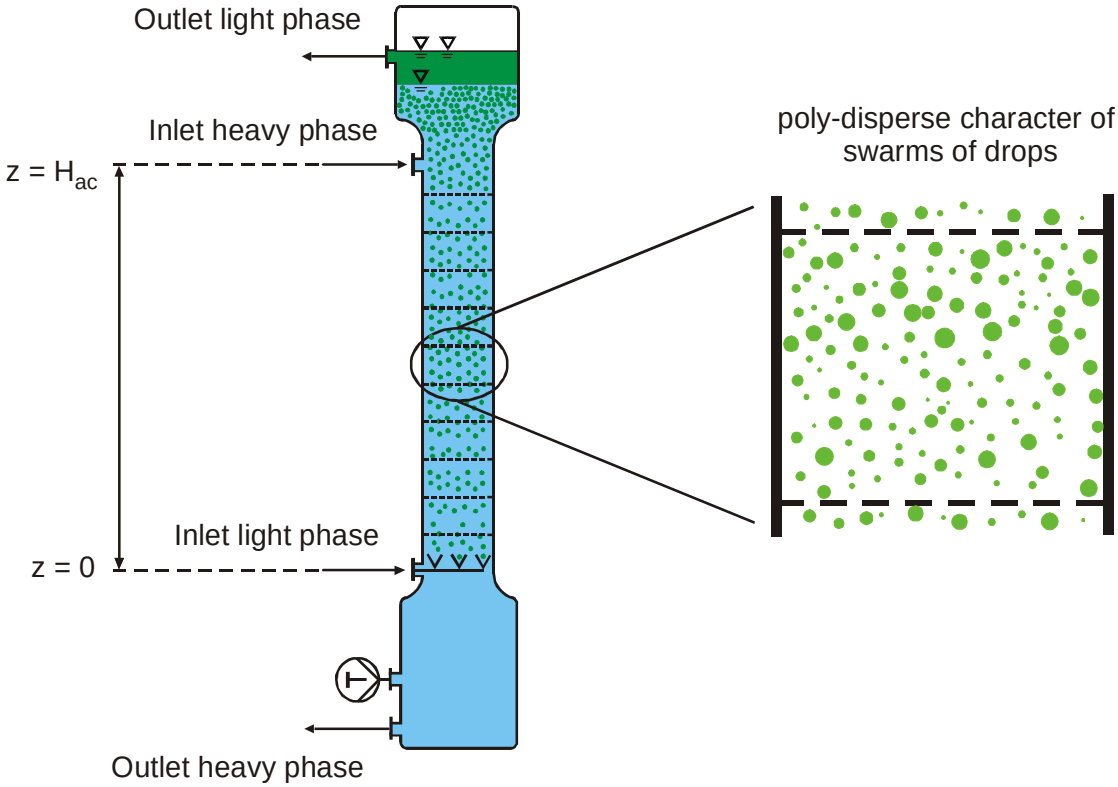

Figure 2.2: Scheme of an extraction column and characteristic drop size distribution

The influence of drop size distribution on residence time distribution of the dispersed phase strongly affects the mass transfer of single drop size classes. Many authors have demonstrated that the residence time of both phases in an extractor is a major factor for mass transfer, see *Reissinger 1985* and *Wagner 1999*. Drop population balance models (DPBMs) account for this interrelationship by considering all drop size classes.

According to *Casamatta and Vogelpohl 1985*, volume balances of a certain drop size class and the continuous phase result in the following equations:

$$\underbrace{\frac{\partial P(t,z,d_i)}{\partial t}}_{term1} + \underbrace{\frac{\partial}{\partial z}[v_{d,e}(t,z,d_i)\cdot P(t,z,d_i)]}_{term\ 2} = \underbrace{\frac{\partial}{\partial z}\left[D_{ax,d}\cdot\frac{\partial}{\partial z}P(t,z,d_i)\right]}_{term\ 3} + \underbrace{S_B + S_C + S_{F,d}}_{term\ 4} \tag{2.5}$$

$$\frac{\partial h_c(t,z)}{\partial t} + \frac{\partial}{\partial z}[v_{c,e}(t,z)\cdot h_c(t,z)] = \frac{\partial}{\partial z}\left[D_{ax,c}\cdot\frac{\partial}{\partial z}h_c(t,z)\right] + S_{F,c} \tag{2.6}$$

Here, the basic parameter $P(t,z,d_i)$ is a drop size distribution function that represents the volumetric fraction of drops of diameter d_i at column height z and time t. According to DPBMs, the volume balance for a certain drop size class is governed by convective transport (*term 2*), axial back mixing (*term 3*) of drops with diameter d_i and the loss and gain of drops with a diameter of d_i due to breakage S_B and coalescence S_C (*term 4),* see *equation (2.5)*. The factors $S_{F,d}$ of *term 4* and $S_{F,c}$ in *equation (2.6)* account for the feed inlet of the dispersed phase and the continuous phase and are normally characterised by a Dirac function.

In *equation (2.6)* the parameter $h_c(t,z)$ characterises the volume fraction of the continuous phase and depends on the hold-up $h_d(t,z)$:

$$h_c(t,z) = 1 - h_d(t,z) \quad \text{where} \quad h_d(t,z) = \int_0^{d_{max}} P(t,z,d_i)\,dd_i \tag{2.7}$$

While the equations above allow the determination of drop size and hold-up profiles, component mass balances make the evaluation of concentration profiles along the column height possible. A detailed description of the derivation of the following equations is given by *Al Khani et al. 1989*:

$$\frac{\partial}{\partial t}[y(t,z,d_i)\cdot P(t,z,d_i)] + \frac{\partial}{\partial z}[y(t,z,d_i)\cdot P(t,z,d_i)\cdot v_{d,e}(t,z,d_i)] = \tag{2.8}$$
$$\frac{\partial}{\partial z}\left(D_{ax,d}\cdot\frac{\partial}{\partial z}[y(t,z,d_i)\cdot P(t,z,d_i)]\right) + \frac{6}{d}\beta_{oc}(d_i)\cdot P(t,z,d_i)\cdot\left[x(t,z) - \frac{y(t,z,d_i)}{m}\right] + \int_0^{\infty} T_y\,dy$$

Here, $y(t,z,d_i)$ characterises the average concentration of all drops with diameter d_i at column position z and time t. The second term on the right side describes the mass transfer between a considered drop size class d_i and the continuous phase. The parameter T_y accounts for the mixing effects due to breakage and coalescence for the average concentration of the drop class

considered. Analogously, the concentration of the continuous phase is evaluated by:

$$\frac{\partial}{\partial t}[h_c(t,z)\cdot x(t,z)] + \frac{\partial}{\partial z}[v_{c,e}(t,z)\cdot h_c(t,z)\cdot x(t,z)] = \frac{\partial}{\partial z}\left(D_{ax,c}\cdot\frac{\partial}{\partial z}[h_c(t,z)\cdot x(t,z)]\right) - m_s(t,z) \tag{2.9}$$

where $m_s(t,z)$ takes the mass transfer of the solute between all drops and the continuous phase at column height *z* and time *t* into consideration:

$$m_s(t,z) = \int_0^{d_{max}} \frac{6}{d}\cdot\beta_{oc}(d_i)\cdot P(t,z,d_i)\cdot\left[x(t,z) - \frac{1}{m}\cdot y(t,z,d_i)\right]dd_i \tag{2.10}$$

To solve the system of equations above, boundary conditions for the inlet and outlet of both phases have to be formulated. According to *Korchinsky und Young 1986*, the following expressions hold:

$$z = 0: \qquad \frac{\partial x(t,z)}{\partial z} = 0 \quad and \quad y(t,z,d_i) = y_{in} \tag{2.11}$$

$$z = H_{ac}: \qquad \dot{M}_c\cdot x_{in} = \dot{M}_c\cdot x(t,z) - A_C\cdot\rho_c\cdot D_{ax,c}\cdot\frac{\partial}{\partial z}[h_c(t,z)\cdot x(t,z)]$$

Hence, the concentration of the continuous phase does not change beneath the position z = 0. Furthermore, a concentration jump appears at the inlet of the continuous phase due to axial back mixing.

Drop population balance models have been used by many groups for predicting the performance of extractors. For example, *Toutain et al. 1998* and *Henschke 2003* evaluated the operating mode of a pulsed sieve tray extractor (PSE) with the help of DPBMs. *Leu 1995* and *Hoting 1996* used DPBMs to predict the performance of a pulsed extractor with structured packings (PESP). The fluiddynamics and mass transfer rates of an agitated extractor with rotating discs (RDC) were determined by *Cruz-Pinto 1979* and *Modes 1999*. The operating conditions of an agitated extractor with blade agitators (Kühni) were investigated by *Zamponi 1996* and *Steiner et al. 1998*. Further information about the application of DPBMs and numerical solutions for the system of equations in DPBMs are described in *Ortner et al. 1995*, *Attarakih 2004* and *Attarakih et al. 2005*.

2.2 Fluiddynamics in Extraction Columns

Fluiddynamics in extractors are controlled by different parameters such as drop breakage and velocities of drops. DPBMs take these parameters into consideration principally on the basis of single drop experiments or correlations derived from single drop experiments. Thus, the following sections give a review of single drop phenomena and their descriptions in the literature as well as a presentation of correlations to predict characteristic features of swarms of drops like hold-up, axial back mixing and maximum throughput of extraction columns.

2.2.1 Drop Size

Drop size and drop size distribution have a significant influence on throughput and mass transfer in extractors. The drop size determines the velocity as well as the mass transfer rate of the drops. Swarms of drops can be characterised by average values of the drop size, for example by the sauter diameter. The sauter diameter is defined as the diameter of drops in a mono-dispersed swarm that has the same interfacial area per volume as the actual poly-dispersion:

$$d_{1,2} = \frac{\sum n_i \cdot d_i^3}{\sum n_i \cdot d_i^2} \tag{2.12}$$

To model the sauter diameter the theory of isotropic turbulence by *Kolmogorov 1958* is often used as a basis for the description of the average drop size of swarms, see *Fischer 1973*, *Coulaloglou and Tavlarides 1976*, *Niebuhr 1982*, *Sovova 1990*, *etc*. A number of other correlations can be found in the literature which evaluate the drop size by a set of dimensionless numbers, see *Laddha et al. 1978*, *Godfrey and Slater 1994* and *Kumar and Hartland 1996*.

In contrast to the description of swarms of drops by an average drop diameter, a more detailed investigation of liquid/liquid-extractors gives rise to the realisation that the width of the drop size distribution has a strong impact on mass transfer rates. A small number of large drops can hold a relatively large fraction of the dispersed volume and cause a large reduction of the interfacial area. Furthermore, small drops have poor mass transfer coefficients. Hence, relatively narrow drop size distributions are desired to enhance mass transfer. Because of the width of the drop size distributions, average diameters like the sauter diameter do not sufficiently characterise a poly-dispersed phase. Hence, DPBMs account for the dynamic change of the entire drop size distribution along the column height through breakage and

coalescence expressions for each drop size class. This leads to a more realistic description of the two-phase flow.

- *Drop breakage*

Breakage of drops with diameter d_i and production of drops with diameter d_i by the breakage of larger drops can be predicted by:

$$S_{B^-} = g(t, z, d_i) \cdot P(t, z, d_i) \tag{2.13}$$

$$S_{B^+} = \int_0^{d_{max}} q_3(d_M, d_{dd}) \cdot g(t, z, d_M) \cdot P(t, z, d_M) dd_M$$

where $g(t, z, d_i)$ represents a breakage frequency. The breakage frequency is defined by the ratio of the number of breaking drops to the initial number of drops and time:

$$g(t, z, d_i) = \frac{number\ of\ breaking\ drops}{initial\ number\ of\ drops \cdot t} \tag{2.14}$$

The production of drops with a diameter d_i further depends on the parameter $q_3(d_M, d_{dd})$. This parameter denotes the volumetric density distribution of the daughter drops of diameter d_{dd} generated by the breakage of a mother drop d_M. Hence, the volumetric density distribution in *equation (2.13)* has to be determined for a daughter drop with the same size as the considered drop class: $d_{dd} = d_i$.

There are numerous approaches for the evaluation of breakage frequencies in liquid/liquid-systems in the literature which are based on the assumption that local turbulence eddies cause breakage if the kinetic energy of the eddies is larger than the surface energy of the drop. In these approaches, the local turbulence eddies are considered to have approximately the same size as the drop, see *Narsimhan 1979, Tsouris and Tavlarides 1994, etc*. The breakage frequency is also often determined as a function of the breakage probability p_B:

$$g(t, z, d_i) = p_B(t, z, d_i) \cdot \frac{v_{d,e}(t, z, d_i)}{h_c} \tag{2.15}$$

The breakage probability p_B can be experimentally obtained by the fraction of breaking drops from a number of mother drops analysed in a laboratory scale column. The second term on the right side of *equation (2.15)* considers the time for breakage in a compartment height h_c.

Haverland 1988, Leu 1995 and *Hoting 1996* determine the breakage probability in single compartments with different sieve trays and structured packings as a function of the characteristic drop diameters d_{stab} and d_{100}. The diameter d_{stab} is the maximum stable diameter for a certain pulsation intensity and d_{100} defines the diameter of mother drops which will be split with 100 percent certainty in the compartment. *Figure (2.3)* shows the dependence of the characteristic drop diameters on the energy input in a pulsed compartment with a single sieve tray and in a pulsed compartment with a single structured packing.

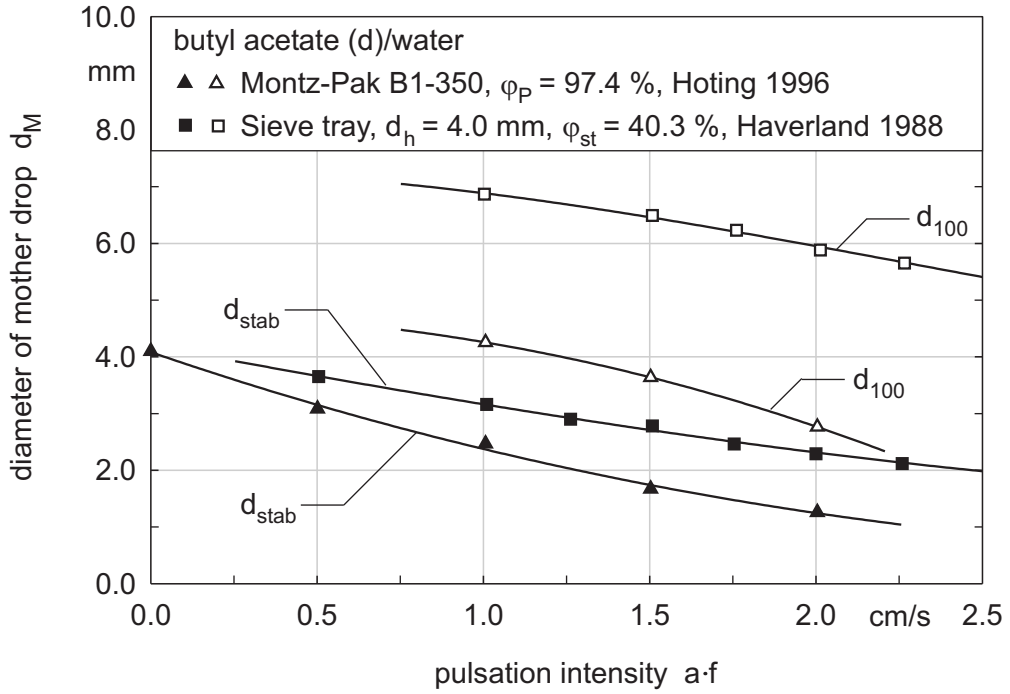

Figure 2.3: Characteristic diameters d_{stab} and d_{100} for the breakage of single drops in pulsed compartments with a single sieve tray and a single structured packing

While the values for d_{stab} are in close agreement for both types of internals there is a major difference in the values for d_{100}. Hence, breakage is higher in the structured packing than in a compartment with a sieve tray with 4 mm hole diameter.

Following *Haverland 1988* and *Leu 1995*, the breakage probability for drop diameters d_i in between the characteristic diameters can be evaluated by:

$$p_B(d_i) = \left(\frac{d_i - d_{stab}}{d_{100} - d_{stab}} \right)^C \tag{2.16}$$

where the exponent C is a function of the pulsation intensity. The breakage probability p_B in different pulsed compartments is illustrated in *figure (2.4)*. This figure reveals that breakage in

sieve tray columns strongly depends on the hole diameter of the sieve tray.

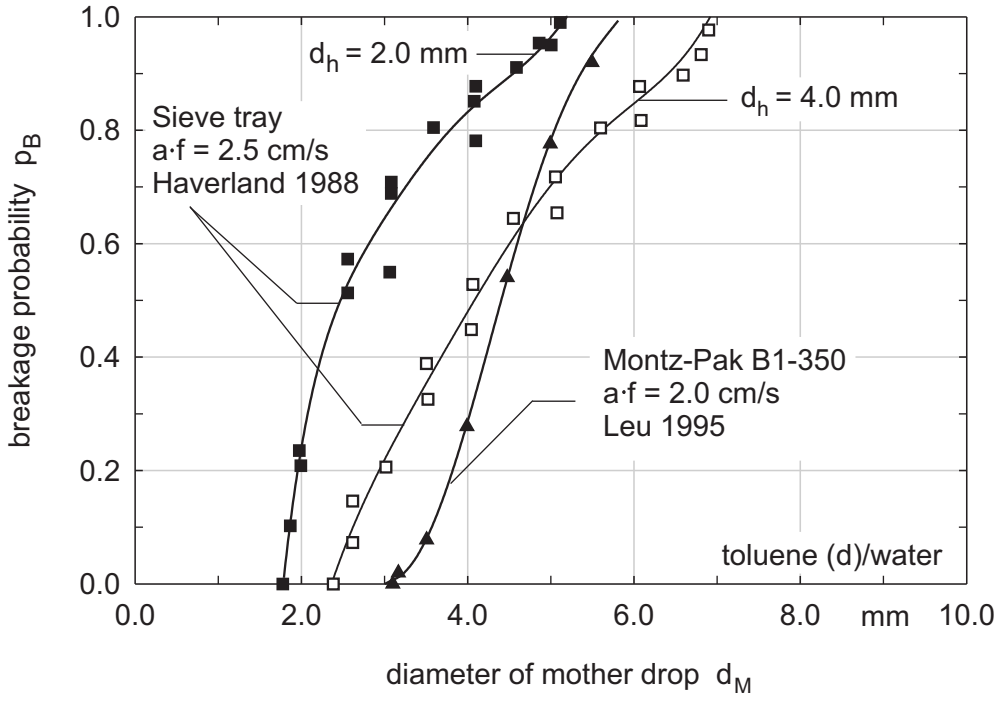

Figure 2.4: Breakage probability in pulsed compartments with single sieve trays and a single structured packing

In agitated columns the breakage probability can be determined as a function of the critical rotational speed $n_{R,crit}$ according to *Fang et al. 1995* and *Modes 1999*. The critical rotational speed $n_{R,crit}$ is the maximum rotational speed where no drop breakage appears for a drop of diameter d_i. Fang et al. investigated drop breakage in Kühni-compartments and found that the breakage probability is well described by:

$$\frac{p_B}{1-p_B} = 6.25 \cdot \left(\frac{\rho_c^{0.5} \cdot \eta_c^{0.5} \cdot d_i \cdot d_A \cdot [n_R^{1.5} - n_{R,crit}^{1.5}]}{\sigma} \right)^{1.32} \tag{2.17}$$

Plots of the breakage probability against the rotational speed were made in order to determine the critical rotational speed $n_{R,crit}$. Subsequently, the critical rotational speed in the Kühni-compartments was determined by an extrapolation of the breakage probability to zero for a certain mother drop diameter. Modes determined the breakage probability in compartments with rotating discs similar to Fang et al.:

$$\frac{p_B}{1-p_B} = 0.118 \cdot \left(\frac{\rho_c^{0.8} \cdot \eta_c^{0.2} \cdot d_i \cdot d_A^{1.6} \cdot [n_R^{1.8} - n_{R,crit}^{1.8}]}{\sigma} \right)^{1.595} \tag{2.18}$$

$$where \quad n_{R,\,crit} = 0.738 \cdot \left(\frac{\rho_c \cdot d_A^3}{\sigma}\right)^{-0.5} \cdot \left(\frac{d_i}{d_A}\right)^{-0.986} \tag{2.19}$$

Figure (2.5) presents a plot of breakage probabilities in single agitated compartments which shows that the use of Kühni blade agitators results in much larger numbers of breakage events than the use of rotating discs. Although the rotational speed in the RDC-compartment is 2.3 times higher than in the Kühni-compartment, breakage probabilities are still higher for the blade agitator.

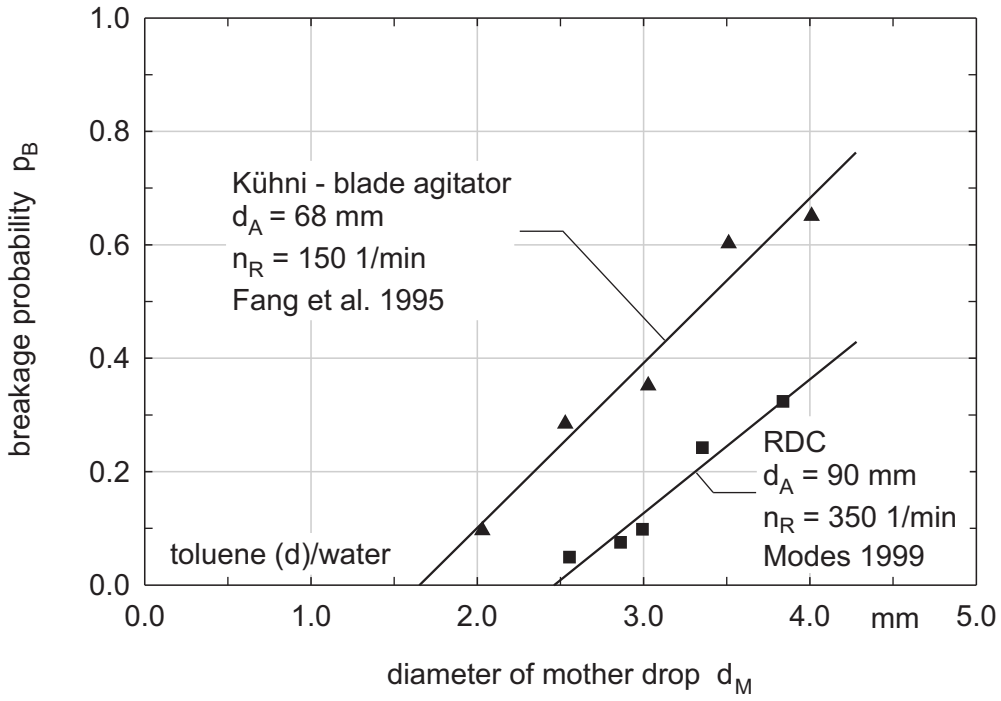

Figure 2.5: Breakage probability in a single compartment with different agitators

To model the drop breakage in extraction columns by DPBMs, the drop size density distributions q_3 of the daughter drops must be known. Drop size density distributions can be described by many different distribution functions. Normal, beta and Mugele-Evans distributions are often used. Beta distributions are described by:

$$q_3(x) = \frac{x^{p-1} \cdot (1-x)^{q-1}}{\int_0^1 x^{p-1} \cdot (1-x)^{q-1} dx} \quad where \quad x = \frac{d_{dd}}{d_M} \quad and \quad 0 \le x \le 1 \tag{2.20}$$

$$x_{1,3} = \frac{p}{p+q} \quad and \quad s_{1,3} = \frac{p \,.\, q}{(p+q)^2 + (p+q+1)}$$

The mean value of the dimensionless volume distribution of daughter drops is given by $x_{1,3}$ with the standard deviation $s_{1,3}$. The transformation of the dimensionless distribution function into a dimensional one is carried out by $q_3(d_M, d_{dd}) = q_3(x)/d_M$. While Haverland, Leu and Hoting used the equations above, Modes used a different structure of a beta function from *Bahmanyar and Slater 1991*:

$$q_3(d_M, d_{dd}) = 3 \cdot n_{dd} \cdot (n_{dd} - 1) \cdot \left[1 - \frac{d_{dd}^3}{d_M^3} \right]^{(n_{dd}-2)} \cdot \frac{d_{dd}^5}{d_M^6} \tag{2.21}$$

$$with \quad n_{dd} = 2 + 0.17 \cdot \left[\frac{d_M}{d_{crit}} - 1 \right]^{1.83} \tag{2.22}$$

Here, n_{dd} is the average number of daughter drops per breakage and d_{crit} is given by a rearrangement of *equation (2.19)*.

Henschke used a different approach to evaluate drop size profiles in pulsed sieve tray columns. The author considered all parameters that influence the stable drop diameter, the breakage probability, the number of daughter drops per breakage and daughter drop distributions. Detailed information about this model is given in *Henschke 2003*.

To simplify the modelling of drop breakage, some groups assumed that drops just split in two or at most three daughter drops. However, this is an oversimplification of the problem since particularly larger drops are fragmented in greater numbers with increasing energy input, see *Bahmanyar and Slater 1991*. *Figure (2.6)* depicts the number of daughter drops produced by drop breakage in a pulsed sieve tray compartment, which shows that more than two daughter drops are typically generated. For example, mother drops with a diameter of d_M = 5 mm break into 11 daughter drops at a pulsation intensity of 2.5 cm/s. Since drop distribution profiles react very sensitively to the number of daughter drops produced by breakage, all generated daughter drops should be considered, see also *Cruz-Pinto 1979*.

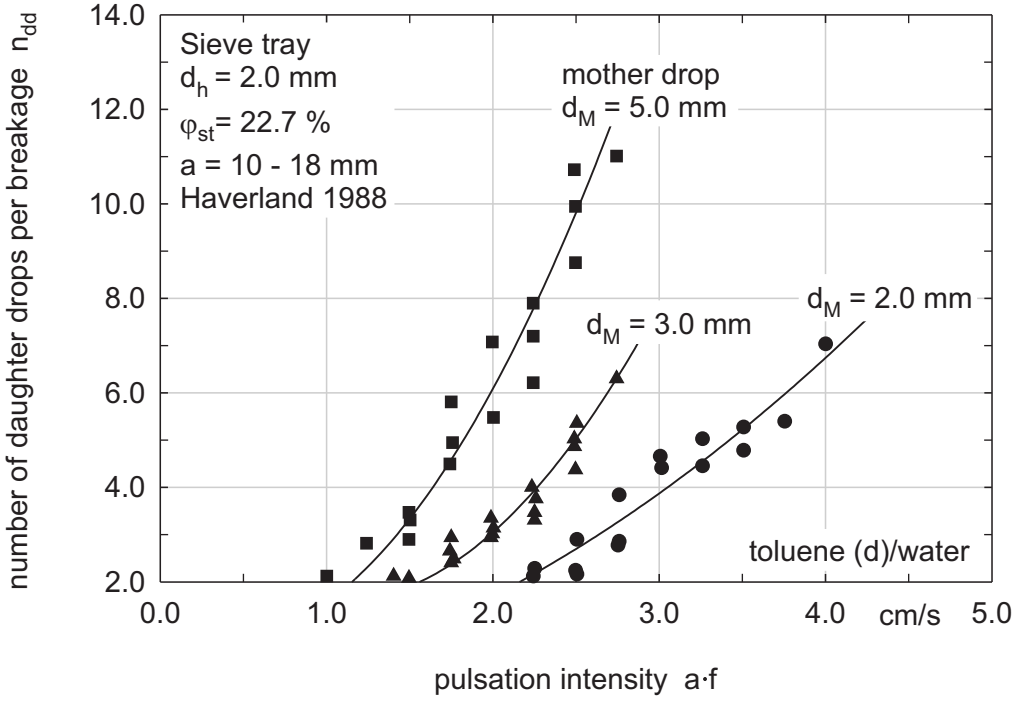

Figure 2.6: Number of daughter drops produced by breakage in a single pulsed sieve tray compartment

- *Drop coalescence*

Although the rate of coalescence is normally suppressed in technical applications through the choice of the mass transfer direction, coalescence must not be neglected, see *Henschke 2003*. However, the determination of the influence of coalescence in liquid/liquid-systems, especially in extraction columns with different internals, is one of the most challenging issues. For this reason, the influence of impurities or surfactants as well as the direction of mass transfer cannot be sufficiently described by theoretical considerations yet.

Investigations of coalescence phenomena make clear that drop/drop-coalescence strongly depends on the liquid/liquid-system and the size of the drops. Drop population balance models (DPBMs) allow a realistic description of the coalescence mechanisms in poly-dispersed swarms of drops. In DPBMs normally only binary coalescence is considered, which is described in terms of the number of drops with diameters of d_1 and d_2 which coalesce with a certain rate $w(d_1, d_2)$. The number of coalescence events per unit volume and time is given by $w(d_1, d_2) \cdot N(d_1) \cdot \Delta d \cdot N(d_2) \cdot \Delta d$, where $N(d_i) \cdot \Delta d$ denotes the number of drops per unit volume:

$$N(t, z, d_i) \cdot \Delta d = \frac{P(t, z, d_i)}{V(d_i)} \cdot \Delta d . \tag{2.23}$$

$V(d_i)$ describes the volume of a drop with diameter d_i. The gain and loss of drops of class d_i due to binary drop coalescence is given by:

$$S_{C^+} = \frac{V(d_i)}{2} \cdot \int_0^{d_i} w(d_1, d_2) \cdot \frac{P(t, z, d_1)}{V(d_1)} \cdot \frac{P(t, z, d_2)}{V(d_2)} \cdot \left(\frac{d_i}{d_2}\right)^2 dd_1 \tag{2.24}$$

$$S_{C^-} = P(t, z, d_i) \cdot \int_0^{\infty} w(d_i , d_1) \cdot \frac{P(t, z, d_1)}{V(d_1)} \, dd_1 \tag{2.25}$$

where d_2 is defined by $V(d_1) + V(d_2) = V(d_i)$, see also *Kronberger et al. 1995*. Hence, drop/ drop-coalescence is characterised by a single parameter, the coalescence rate. The coalescence rate is often described by the product of collision frequency $h(d_1, d_2)$ and coalescence efficiency $\lambda(d_1, d_2)$:

$$w(d_1, d_2) = h(d_1, d_2) \cdot \lambda(d_1, d_2) \tag{2.26}$$

According to *Coulaloglou and Tavlarides 1977*, the collision frequency $h(d_1, d_2)$ of two drops can be described in analogy to the collision frequency between gas molecules. In contrast to the collision frequency, the coalescence efficiency accounts for the time of contact between two drops and the time of coalescence. After a collision the contact time must exceed the coalescence time, which is given by the drainage time of the liquid film between the drops, see also *Blaß 1990*. According to the kinetic gas theory and the film drainage theory, Coulaloglou and Tavlarides evaluated the collision frequency and the coalescence efficiency as follows:

$$h(d_1, d_2) = \frac{C_1 \cdot \phi^{1/3}}{1 + h_d} \cdot (d_1^2 + d_2^2) \cdot (d_1^{2/3} + d_2^{2/3})^{1/2} \tag{2.27}$$

$$\lambda(d_1, d_2) = exp\left[-\frac{C_2 \cdot \eta_c \cdot \rho_c \cdot \phi}{\sigma^2 \cdot (1 + h_d)^3} \cdot \left(\frac{d_1 \cdot d_2}{d_1 + d_2}\right)^2 \right] \tag{2.28}$$

Here, ϕ is the energy dissipation. *Sovova 1981* describes the coalescence efficiency based on the assumption that the velocity and subsequently the kinetic energy with which two drops collide is greater than the surface energy of the drops. If the impact energy in a stirred vessel is higher than the surface energy, coalescence efficiency is described by:

$$\lambda(d_1, d_2) = exp\left[-\frac{C_3 \cdot \sigma}{\rho_d \cdot n_R^2 \cdot d_A^{4/3}(1 + h_d)^3} \cdot \frac{(d_1^2 + d_2^2) \cdot (d_1^3 + d_2^3)}{d_1^3 \cdot d_2^3 \cdot (d_1^{2/3} + d_2^{2/3})} \right] \tag{2.29}$$

By the combination of *equation (2.28)* and *equation (2.29)* Sovova gives a correlation which can also be applied when the collision energy is less than the surface energy of the drops, see also *Sovova and Prochazka 1981*.

To gain reliable results for the coalescence effects in liquid/liquid-systems, the constants in *equation (2.27), equation (2.28)* and *equation (2.29)* are evaluated from experimental investigations. The experimental investigation of coalescence phenomena is complicated and results have to be treated carefully. Often coalescence effects are examined in stirred vessels, see *Tobin and Ramkrishna 1999*. Drop size distributions are detected before and after switching off the agitator. The change of drop size distribution gives information about the coalescence effects and, in turn, the constants in the equations above. The determination of coalescence in this way is doubtful. Shearing rates are still high even after the agitator is powered down, resulting in further drop breakage events.

A better way to gain reliable results for the coalescence rate is to carry out experiments in columns where no drop breakage occurs. *Simon et al. 2003* investigated drop/drop-coalescence in a venturi tube. In this venturi tube, single drops with a defined size are generated by a two-phase nozzle. The continuous phase flows counter currently to the dispersed phase so that a swarm of mono-dispersed drops remains at a constant position in the tube due to their terminal velocity. After the formation of a swarm of drops with diameter d_1, single drops of diameter $d_2 > d_1$ are formed. If a single drop coalesces with a drop in the swarm, the generated drop moves upwards and is analysed by a photoelectrical suction probe, see *Pilhofer 1977*, and a high-resolution camera. Using this experimental set-up, drop/drop-coalescence can be determined as a function of drop size and hold-up in the column. Thus, the coalescence rate $w(d_1, d_2)$ is derived from the experimentally determined coalescence probability p_c and the residence time t_{res} of the drops in a volume V_{Comp} where coalescence occurs:

$$w(d_1, d_2) = \frac{p_c(d_1, d_2)}{t_{res}} \cdot V_{Comp} \quad where \quad p_c(d_1, d_2) = \frac{\sum_{i=1}^{k} n_{i,coal} \cdot V_{i,coal}}{V_{total}} \tag{2.30}$$

Figure (2.7) illustrates the coalescence probability p_c as a function of drop size and hold-up. The coalescence probability increases with the hold-up. In addition, swarms with drop diameters d_1

of 2.0 mm show higher coalescence probabilities than swarms with drop diameters d_1 of 1.5 mm. For drops larger than 2.0 mm in the swarm, constant or lower coalescence probabilities exist. According to Simon et al., this is due to the deformation of large drops. The deformation of drops leads to an increase of the space between adjacent drops and to an increase of film drainage time. Hence, the residence time of two adjacent deformed drops is often too short for a coalescence event. Although the experimental approach of *Simon et al. 2003* is promising, the experimental data only give information about the coalescence behaviour of single drops for a maximum hold-up of 12.5 %. Since the hold-up in extraction columns is often higher, the coalescence behaviour of single drops needs further investigation.

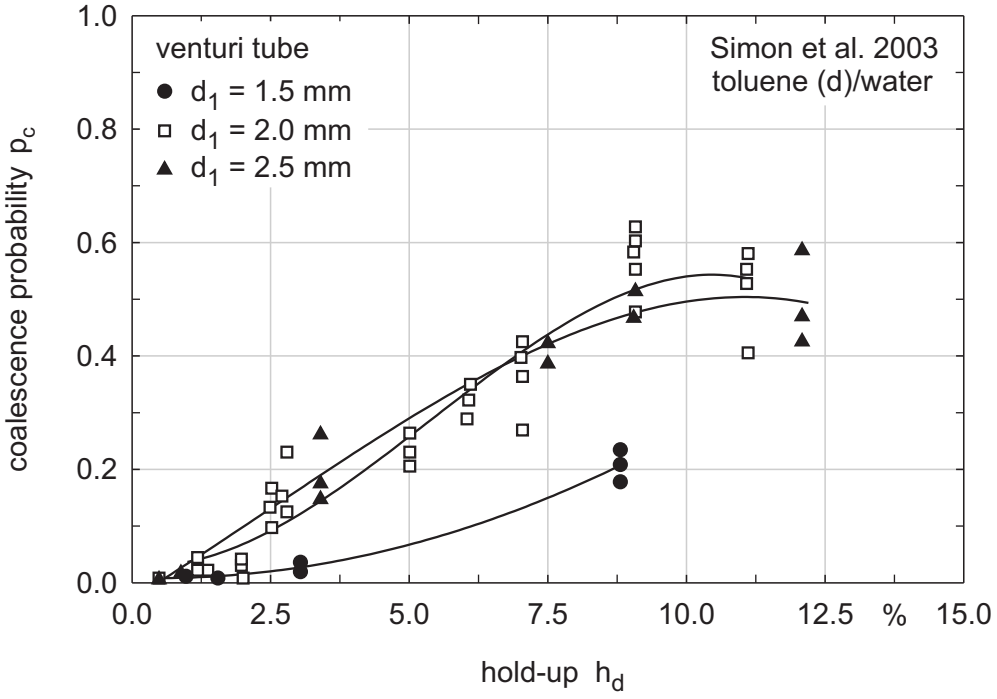

Figure 2.7: Coalescence probability of drops in mono-dispersed swarms with different drop diameters d_1 with respect to hold-up

It should be noted that reliable results for drop breakage as well as for coalescence are only gained by experimental investigations. Quantitative information about the influence of electrostatic repulsion, surfactants and the direction of mass transfer cannot be obtained by theoretical considerations. For this reason, the aim of further investigations must be the development of more reliable experimental techniques with lower operating expenses.

2.2.2 Single Drop Velocities

Although the velocity of drops in a swarm differs significantly from that of single drops, numerous investigations prove that the so-called swarm velocity can be modelled on the basis of single drop velocities.

- *Terminal velocity*

A single drop moving unhindered in a continuum, for instance, in an extraction column without internals, attains a constant velocity after a rather short distance. This velocity is often called the terminal velocity. The distance that a drop needs to reach its terminal velocity is approximately as short as 2 to 4 times of its own diameter, see *Stichlmair 2001*. The terminal velocity of single drops predominantly depends on the physical properties of the liquid/liquid-system and the drop diameter. Extensive investigations reveal that small drops behave like and move as fast as rigid spheres, see *Hu and Kintner 1955, Klee and Treybal 1956, Grace et al. 1976, etc.* This is due to the fact that small amounts of impurities accumulate on the surface and reduce the surface mobility. With increasing drop diameter the surface mobility increases and, in turn, circulation currents within a drop are generated. Drops with circulations move faster than rigid spheres, see *figure (2.8)*.

Large drops lose their stability and, in turn, show form oscillations. The flow resistance of drops with form oscillations, so-called oscillating drops, increases due to the large surface area exposed to the oncoming flow. The terminal velocity of oscillating drops decreases, and subsequently the drops move slower than rigid spheres of same volume. Very large drops lose their spherical shape completely and take the shape of deformed caps which again move slower than rigid spheres.

Although the free rise or fall of rigid spheres is well known, the determination of the terminal velocity of drops is still associated with some uncertainties. Currently, the effect of circulations within a drop, of surfactants as well as of the rate and direction of mass transfer can only be qualitatively described. This is surprising considering that the terminal velocity of single drops has been extensively investigated, see *Brauer 1971, Clift et al. 1978, Wesselingh and Bollen 1999, etc.*

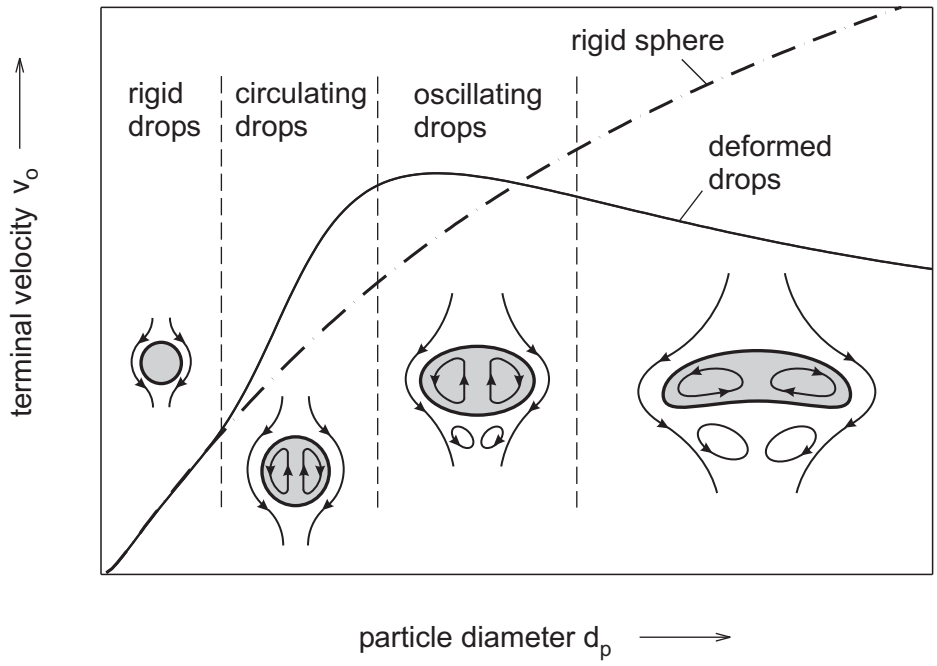

Figure 2.8: Terminal velocities of single drops and single rigid spheres versus particle diameter

Figure (2.9) illustrates the terminal velocity of single butyl acetate drops in water. The drops achieve a higher terminal velocity in the diameter range from 2.0 to 3.5 mm than rigid spheres of the same size. This effect is larger when no mass transfer occurs because mass transfer reduces the circulations within a drop by eruptions at the interface, for example induced by turbulent Marangoni convections.

A comparison of the experimental results of *Henschke 2003* with several models reveals that these models are unable to adequately describe the strong influence of circulations within a drop and mass transfer on drop velocity, see *figure (2.9)*. For this reason, the author developed a general model for the terminal velocity of rigid spheres, drops and bubbles. Although this model includes several fitting parameters, it offers a method for obtaining quantitative information on the effect of impurities and circulations within a drop.

The following section presents the application to liquid drops. According to *Henschke 2003*, the terminal velocity of single drops is determined by a transfer function between the velocity of spherical drops and oscillating or deformed drops:

$$v_o = \frac{v_{o,\,spherical} \cdot v_{o,\,os-de}}{\left(v_{o,\,spherical}^{C_1} + v_{o,\,os-de}^{C_1}\right)^{1/C_1}} \tag{2.31}$$

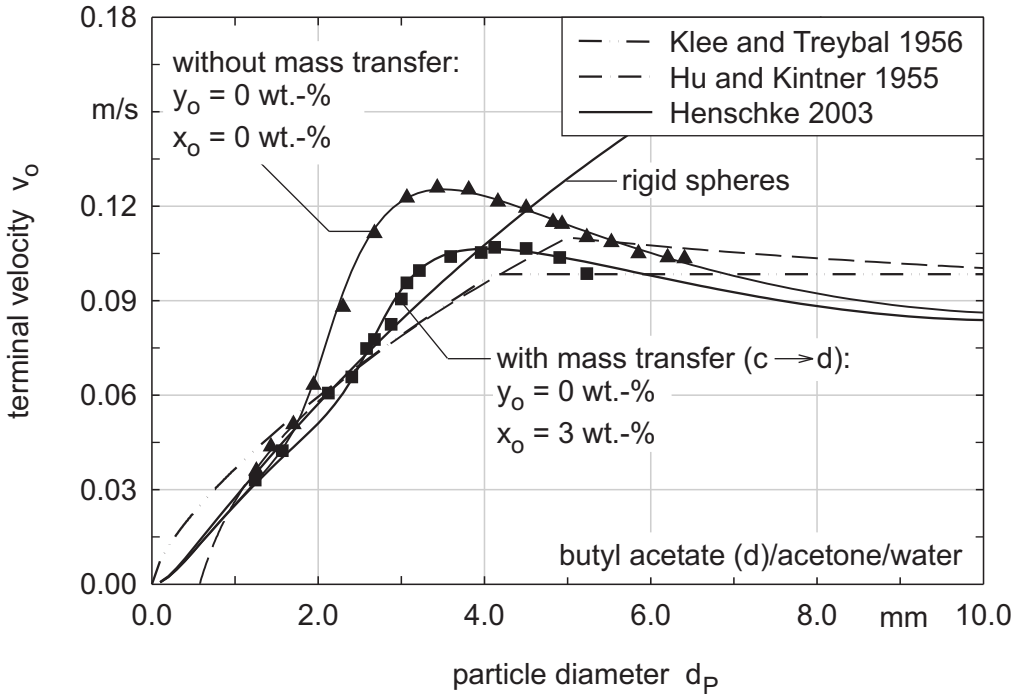

Figure 2.9: Terminal velocities of single drops with and without mass transfer; comparison of experimental results and model from Henschke 2003 with other models

The terminal velocity of a spherical drop is obtained from the velocity of a spherical rigid sphere and a spherical bubble since the Reynolds number of a spherical drop is given by an interpolation between these two limiting cases:

$$Re_{o,\,spherical} = (1 - f_1') \cdot Re_{o,\,rigid\,sphere} + f_1' \cdot Re_{o,bubble} \quad \text{where} \quad 0 < f_1' < 1 \tag{2.32}$$

Introducing the terms to determine the Reynolds number of a single rigid sphere and a bubble results in:

$$v_{o,\,spherical} = \left[(1 - f_1') \cdot \sqrt{\frac{4}{3} \cdot \frac{Ar}{c_{d,o\text{-}rigid\,sphere}}} + f_1' \cdot \frac{Ar}{12 \cdot (0.065 \cdot Ar + 1)^{1/6}} \right] \cdot \frac{\eta_c}{\rho_c \cdot d} \tag{2.33}$$

Here, the drag coefficient of a rigid sphere is given by:

$$c_{d,o\text{-}rigid\,sphere} = \frac{432}{Ar} + \frac{20}{Ar^{1/3}} + \frac{0.51 \cdot Ar^{1/3}}{140 + Ar^{1/3}} \tag{2.34}$$

Ar denotes the Archimedes number. The parameter f_1' depends on the Hadamard-Rybczynski-factor K_{HR}' which was modified subject to the diameter d_{r-c}:

$$f_1' = 2 \cdot (K_{HR}' - 1) \quad \text{with} \quad K_{HR}' = \frac{3 \cdot (\eta_c + \eta_d / f_2)}{2 \cdot \eta_c + 3 \cdot \eta_d / f_2} \quad \text{and} \quad f_2 = 1 - \frac{1}{1 + (d / d_{r-c})^{C_2}} \tag{2.35}$$

The diameter d_{r-c} is that diameter where drops change from rigid to circulating behaviour. The velocity of oscillating and deformed drops is given by the following equation:

$$v_{o,\,os-de} = \left(v_{o,\,os}^{C_3} + v_{o,\,de}^{C_3}\right)^{1/C_3} = \left(\left(\frac{2 \cdot C_4 \cdot \sigma}{\rho_c \cdot d}\right)^{\frac{C_3}{2}} + \left(\frac{\Delta\rho \cdot g \cdot d}{2 \cdot \rho_c}\right)^{\frac{C_3}{2}} \right)^{1/C_3} \tag{2.36}$$

The parameters C_1, C_2, C_3, C_4 and d_{r-c} are determined by fitting the model to experimental results. The parameter C_3 indicates the transition from oscillating to deformed drops and C_4 describes the extent of oscillation and its effect on the velocity of the drop. *Figure (2.9)* demonstrates that the model of Henschke accurately describes the velocity of single butyl acetate drops. In addition, the difference of the parameter d_{r-c} for both runs gives quantitative information about the effect of mass transfer on single drop velocity, where d_{r-c} is 2.2 mm in absence of mass transfer and d_{r-c} is 3.0 mm in presence of mass transfer.

- *Characteristic velocity*

Single drops move significantly slower through columns with internals than without internals. Thus, the so-called characteristic velocity of single drops in extraction columns is significantly lower than the terminal velocity. For instance, drops in pulsed columns collide with the sieve trays or the structured packings. The steady collisions of the drops with the column internals reduce their velocity. In agitated columns, drops circulate within the compartments due to the rotations of the agitators. In addition, for high rotational speeds the drops are sometimes pulled back into a compartment after they passed it.

The characteristic velocity is often determined by measuring the velocity of swarms of drops for different hold-up values and extrapolating the so-called swarm velocity to a hold-up of zero. Such derived characteristic velocities of single drops have to be treated with care since drops can act differently in swarms due to the different fluiddynamic conditions compared to single drops, see *chapter 2.2.3*. Against this background, single drops have been investigated in many extraction columns in recent years, e. g. to determine the effect of energy input by varying the pulsation intensity or the rotational speed. Thus, the description of the characteristic velocity is primarily based on semi-empirical and empirical correlations. Several correlations for the prediction of the terminal velocity as well as for the characteristic velocity in different extractors are given in *table (2.1)*.

A weak point of the correlations is that many of them do not include all relevant parameters or interpret the effect of certain parameters on the characteristic velocities differently. For example, the correlation of *Laddha et al. 1978* for RDC-columns disregards the influence of the drop diameter. The correlations of *Seibert 1986* and *Mackowiak 1993* for columns with structured packings include the drop diameter. However, these correlations show a different dependence on the drop diameter. Hence, a further development of correlations to determine the characteristic velocity of single drops must be pursued.

The characteristic velocity of single toluene drops in pulsed compartments with structured packings was studied in detail by *Leu 1995*. He found that the velocity of single drops cannot be correctly described considering the void fraction and the volumetric surface area of the packing only. It has to be related to a larger number of geometrical factors such as the gradient angle and the width of the flanks of the packing channels. By including all relevant geometrical parameters and considering the pulsation intensity $a \cdot f$, Leu derived a complex function for the characteristic velocity. Further information about this model can be found in *Leu 1995*.

The motion of single drops in a sieve tray extraction column was investigated by *Qi 1992* and *Wagner 1999*. The experiments with different perforated sieve trays demonstrate that the ratio of the drop diameter d to the diameter of the holes d_h mainly determines the characteristic velocity. However, no conclusions can be drawn about the impact of energy input on drop velocity from Wagner's experimental results. In contrast, the results of Qi show that the characteristic velocity of single drops is relatively independent of the pulsation intensity.

The energy input in pulsed packed columns has less influence on the velocity of single drops than on the drop breakage, see *Leu 1995* and *Hoting 1996*. In contrast, the energy input in agitated columns dominates the single drop velocities, see *Fang et al. 1995*, *Weiss et. al 1995*, *Modes 1999, etc.* An increase in the rotational speed leads to a decrease of the drop velocity.

The characteristic velocities of single drops in different extractors referred to their terminal velocities in columns without internals $v_{char,o}/v_o$ are shown in *figure (2.10)*. Single drops move considerably faster through sieve tray compartments or packings than through RDC-compartments. In pulsed compartments, the characteristic velocity of single drops is strongly influenced by the geometry of the internals. In agitated compartments, the rotational speed has great impact on the characteristic velocity. *Figure (2.10)* reveals that an increase of the rotational speed by 100 1/min causes a reduction of the velocity ratio $v_{char,o}/v_o$ of 10 % for drops in RDC-compartments. Because of the much higher energy input in Kühni-compartments

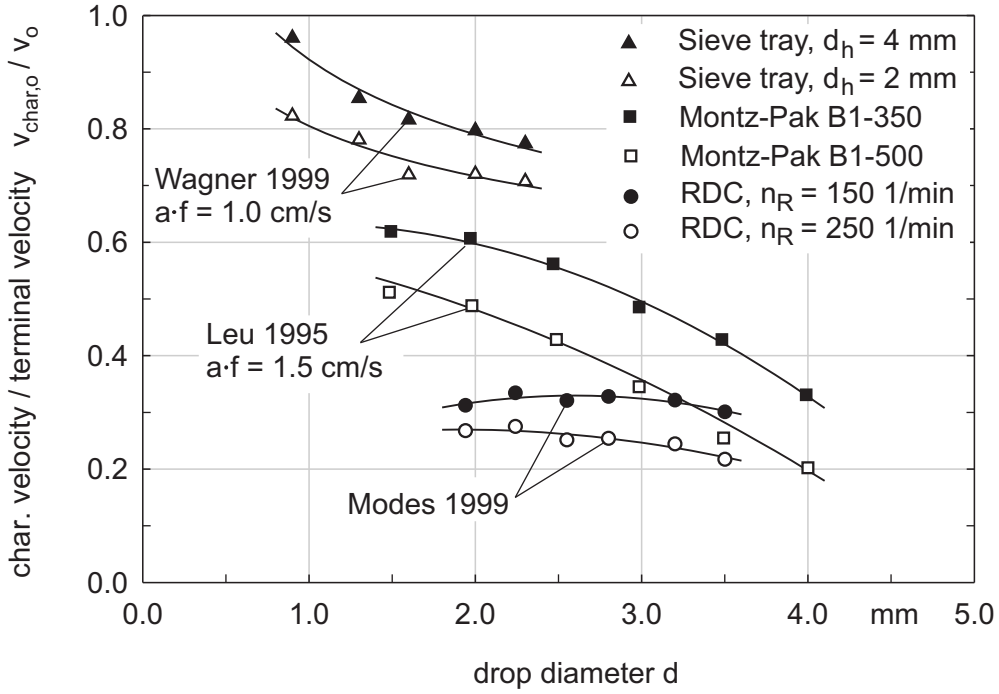

Figure 2.10: Influence of different internals on the characteristic velocities of single drops in reference to their terminal velocities. As liquid/liquid systems, Wagner 1999 used tridecanol (d)/water while Leu 1995 and Modes 1999 used toluene (d)/ water.

than in RDC-compartments, an increase of the rotational speed will affect the single drop velocity more strongly in Kühni-extractors than in RDC-extractors. This fact is confirmed by single drop experiments in agitated columns from *Wagner 1999*.

Table 2.1: Overview of correlations for the prediction of the terminal and characteristic velocity of single drops; PSE = pulsed sieve tray extractor, Karr = reciprocating plate extraction column, PESP = pulsed extractor with structured packings, PERP = pulsed extractor with random packings, RDC = rotating disc contactor, Kühni = stirred column with blade agitators

Literature source, column type	Correlations for the terminal velocity v_o and the characteristic velocity $v_{char,o}$ of single drops in different extraction columns
Hu and Kintner 1955 spray column	$v_o = \frac{\eta_c \cdot P^{0.15}}{\rho_c \cdot d} \cdot [0.798 \cdot Y^{0.784} - 0.75]$ *for* $2 < Y \leq 70$ $v_o = \frac{\eta_c \cdot P^{0.15}}{\rho_c \cdot d} \cdot [3.701 \cdot Y^{0.422} - 0.75]$ *for* $Y > 70$ *where* $Y = \frac{4 \cdot \Delta\rho \cdot d^2 \cdot g}{3 \cdot \sigma} \cdot P^{0.15}$ *and* $P = \frac{\rho_c^2 \cdot \sigma^3}{\eta_c^4 \cdot \Delta\rho \cdot g}$
Klee and Treybal 1956 spray column	$v_o = 3.042 \cdot \rho_c^{-0.45} \cdot \Delta\rho^{0.58} \cdot \eta_c^{-0.11} \cdot d^{0.7}$ *for small drops* $v_o = 4.96 \cdot \rho_c^{-0.55} \cdot \Delta\rho^{0.28} \cdot \eta_c^{0.1} \cdot \sigma^{0.18}$ *for large drops*
Wagner 1999 PSE	$v_{char,o} = 0.72 \cdot \left(\frac{d}{d_h}\right)^{-0.2} \cdot v_o$ *for* $a \cdot f = 1.0$ *cm/s*
Weiss et. al 1995 Karr	$v_{char,o} = 9.06 \cdot exp(-0.163 \cdot f) \cdot d^{0.856}$
Mackowiak 1993 PESP	$v_{char,o} = 0.565 \cdot \psi_m^{-1/6} \cdot \left(\frac{4 \cdot \varphi_P}{a_P \cdot d}\right)^{1/4} \cdot \left(\frac{d \cdot \Delta\rho \cdot g}{\rho_c}\right)^{1/2}$ *where* ψ_m *is a drag coefficient depending on the packing*
Mao et al. 1995 PESP	$v_{char,o} = C \cdot \left[1 - (1 + 0.163 \cdot Eö^{0.757})^{0.67} \cdot \left(\frac{d}{d_P}\right)^2\right]^{1.5} \cdot v_o$ *where* $Eö = \frac{g \cdot d^2 \cdot \Delta\rho}{\sigma}$ *and* $d_P = \left(\frac{4 \cdot A_P}{n \cdot \pi}\right)^{0.5} \cdot cos45°$ *(n is the number of channels per cross-sectional area* A_P *of packing)*
Seibert 1986 PESP	$v_{char,o} = cos\left(\frac{\pi}{4} \cdot \frac{\xi \cdot d}{2}\right) \cdot v_o$ *where* $\xi = \frac{6 \cdot \varphi_P}{d} + a_P$ *for a mass transfer direction from c to d and where* $\xi = a_P$ *for a mass transfer direction from d to c*

Rohlfing 1991 *PERP*	$v_{char,o} = \dfrac{v_o}{1 + 1.5 \cdot \left(\dfrac{v_o^2 \cdot \rho_d}{(d_{RP} - d) \cdot \Delta\rho \cdot g} \right)^{0.5}}$ *where d_{RP} denotes the diameter of a random packing and v_o is given by Mersmann 1980*
Spaay et al. 1971 *PERP*	$v_{char,o} = 6.32 \cdot 10^{-3} \cdot d^{0.727} \cdot \Delta\rho^{0.815} \cdot (a \cdot f^2)^{-0.254} \cdot [a_P \cdot (1 - \varphi_P)]^{-0.184} \cdot \eta_c^{-0.35}$ *for $L \leq 0.406$* $v_{char,o} = 2.57 \cdot 10^{-3} \cdot d^{-0.06} \cdot \Delta\rho^{0.56} \cdot (a \cdot f^2)^{-0.11} \cdot [a_P \cdot (1 - \varphi_P)]^{-0.61} \cdot \eta_c^{-0.35}$ *for $L > 0.406$* *where* $L = d^{0.787} \cdot \Delta\rho^{0.255} \cdot (a \cdot f^2)^{-0.144} \cdot [a_P \cdot (1 - \varphi_P)]^{0.426}$
Laddha et al. 1978 *RDC*	$v_{char,o} = C_1 \cdot \left[\left(\dfrac{g}{d_A \cdot n_R^2} \right) \cdot \left(\dfrac{\sigma^3 \cdot \rho_c}{\eta_c^4 \cdot g} \right)^{1/4} \cdot \left(\dfrac{\Delta\rho}{\rho_c} \right)^{0.6} \right]^{C_2} \cdot \left(\dfrac{\sigma \cdot \Delta\rho \cdot g}{\rho_c^2} \right)^{0.25} \cdot \left(\dfrac{h_c}{d_A} \right)^{0.9} \cdot \left(\dfrac{d_s}{d_A} \right)^{2.1} \cdot \left(\dfrac{d_A}{D_C} \right)^{2.1}$ *where C_1 and C_2 depend on the direction of mass transfer*
Modes 1999 *RDC*	$v_{char,o} = \left[1 - 2.95 \cdot (n_R^3 \cdot d_A^5)^{0.02} - 0.93 \cdot \left(\dfrac{d}{d_s - d_A} \right)^{1.38} + 2.92 \cdot \left(\dfrac{h_c}{D_C} \right)^{0.25} \right] \cdot v_o$
Weiss et. al 1995 *Kühni*	$v_{char,o} = 15.73 \cdot exp(-1.18 \cdot n_R) \cdot d^{1.14 \cdot exp(-0.225 \cdot n_R)}$
Fang et al. 1995 *Kühni*	$v_{char,o} = \left[1 - \dfrac{(1 - \varphi_s) \cdot \left(7.18 \cdot 10^{-5} \cdot \dfrac{Re_R}{\varphi_s} \right)}{1 + 7.18 \cdot 10^{-5} \cdot \dfrac{Re_R}{\varphi_s}} \right] \cdot v_o$ *where* $Re_R = \dfrac{n_R \cdot d_A^2 \cdot \rho_c}{\eta_c}$

2.2.3 Swarm Velocity and Hold-up

The velocity of particles in a swarm significantly depends on the size of the particles and the volume fraction of the dispersed phase, i. e. the hold-up h_d: $h_d = V_d/(V_d + V_c)$. The relative velocity between the particles and the continuous phase in the column is often called the relative swarm velocity or slip velocity. The relative swarm velocity v_{rs} is given by both effective phase velocities, see also *Gayler et al. 1953*:

$$v_{rs} = v_{d,e} + v_{c,e} = \frac{v_d}{h_d} + \frac{v_c}{1 - h_d} \tag{2.37}$$

Here, v_d and v_c characterise the superficial velocities of the dispersed and continuous phase, respectively. According to *Mersmann 1980*, *equation (2.37)* can be transformed in terms of superficial velocities:

$$v_s = v_d \cdot \frac{1 - h_d}{h_d} + v_c \quad \textit{where} \quad v_s = v_{rs} \cdot (1 - h_d) \tag{2.38}$$

By combining *equation (2.38)* with other models to predict the swarm velocity v_s in dependence of the hold-up, the swarm velocity and the hold-up can be iteratively determined. Many models for the prediction of swarm velocities in columns with and without internals exist: *Logsdail et al. 1957*, *Thornton 1957*, *Anderson 1961*, *Misek 1963*, *Yaron and Gal-Or 1971*, *Widmer 1973*, *Pilhofer 1974*, *Barnea and Mizrahi 1975*, *Marr et al. 1975*, *Pilhofer 1978*, *Ishii and Zuber 1979*, *Pietzsch and Blaß 1987*, *Godfrey and Slater 1991*, *etc*. The results of these research groups indicate that the velocity of particles in a swarm is normally lower than the velocity of a single particle. In addition, the velocity of particles in a swarm is reduced with an increase of the hold-up. Consequently, the swarm velocity can be determined subject to the velocity of a single particle v_o and the hold-up h_d. A widely used model which accounts for this interrelationship is that of *Richardson and Zaki 1954* who evaluated the swarm velocity for packed and fluidised beds of rigid spheres:

$$\frac{v_s}{v_o} = (1 - h_d)^n \quad \textit{where} \quad n = f(Re_o) \tag{2.39}$$

Here, *n* is the so-called swarm exponent which indicates the extent of the hold-up influence, i. e. the swarm influence. Thus, the essential influencing variables on the ratio of the velocities v_s/v_o are the hold-up h_d and the Reynolds number of a single particle Re_o. Richardson and Zaki developed correlations for the exponent *n* in different ranges of the Reynolds number. The

dependence of the swarm exponent *n* on the Reynolds number Re_o is shown in *figure (2.11)* by solid lines.

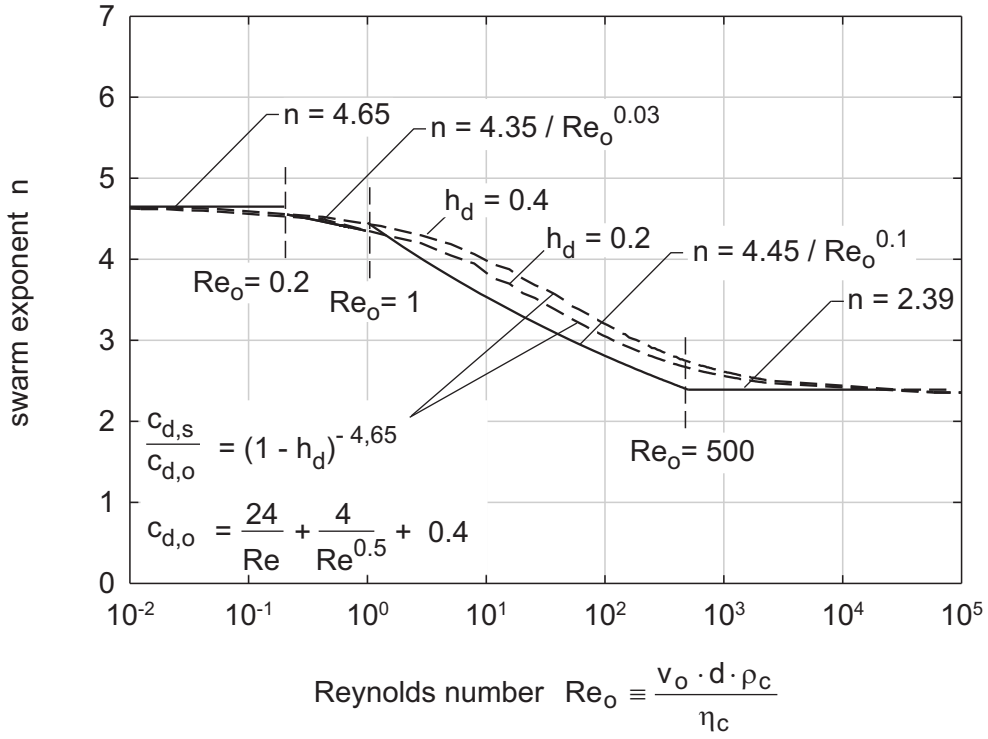

Figure 2.11: Swarm exponent n of rigid particle systems in dependence of the Reynolds number Re_o ; —— Richardson und Zaki 1954 , – – equation (2.44) in combination with the correlation of Kaskas 1971 for the drag coefficient of a rigid sphere

The swarm velocity can be better described when the influence of the swarm is related to the drag coefficient of the particles c_d and not to the velocity of the particles. According to *Stichlmair et al. 1989* the drag coefficient of a swarm of particles $c_{d,s}$ is given by:

$$\frac{c_{d,s}}{c_{d,o}} = (1 - h_d)^{-4.65} \quad \textit{where} \quad c_{d,o} = f(Re_o) \tag{2.40}$$

Again, there exists a dependence on hold-up h_d and Reynolds number Re_o of a single particle. However, the influence of the hold-up is now independent of the Reynolds number and is given by the constant exponent -4.65 . The influence of the Reynolds number is given by the well known relation between the drag coefficient of a single particle $c_{d,o}$ and the Reynolds number. The swarm influence description via the ratio of the drag coefficients $c_{d,s}/c_{d,o}$ has significant consequences for the description of the velocity ratio v_s/v_o , which can be written as:

$$\frac{v_s}{v_o} = \sqrt{\frac{c_{d,o}(Re_o)}{c_{d,o}(Re_s)} \cdot (1-h_d)^{4.65}} \tag{2.41}$$

Equation (2.41) reveals that the influence of the hold-up h_d on the swarm velocity is now exclusively determined by the drag coefficient of a single particle $c_{d,o}$. For this purpose, the drag coefficient $c_{d,o}$ has to be evaluated at the Reynolds number of a single particle Re_o and at the Reynolds number of a particle in the swarm Re_s. By examining the two limiting cases for laminar and turbulent flow, it is shown that:

$$\frac{v_s}{v_o} = (1-h_d)^{4.65} \qquad \textit{for laminar flow where } c_{d,o} \sim 1/Re \tag{2.42}$$

$$\frac{v_s}{v_o} = (1-h_d)^{4.65/2} \qquad \textit{for turbulent flow where } c_{d,o} = \textit{const.} \tag{2.43}$$

These results agree very well with the experimental results of Richardson and Zaki for the swarm exponent in rigid particle systems, see *figure (2.11)*. To compare both models for all relevant Reynolds numbers, swarm exponents according to Richardson and Zaki are obtained by combining *equation (2.41)* and *equation (2.39)*:

$$n = \frac{1}{ln(1-h_d)} \cdot ln \sqrt{\frac{c_{d,o}(Re_o)}{c_{d,o}(Re_s)} \cdot (1-h_d)^{4.65}} \tag{2.44}$$

Using the model of *Stichlmair et al. 1989* in combination with a correlation for the drag coefficient of a rigid sphere, e. g. the correlation of *Kaskas 1971*, allows the swarm exponent *n* to be determined in the whole range of the Reynolds number. This is illustrated in *figure (2.11)* by two dashed lines. It is obvious that both models agree very well in the whole range of the Reynolds number. However, the hold-up has some influence on the swarm exponent of *equation (2.44)*.

In contrast to Richardson and Zaki, the model of Stichlmair et al. allows the prediction of the swarm influence only from knowledge of the drag coefficient function of a single particle: $c_{d,o} = f(Re_o)$. This offers a promising approach for the prediction of the swarm influence in multiple drop systems, as will be shown later on.

As mentioned before, the combination of a model for the swarm velocity with *equation (2.37)* or *equation (2.38)* offers the possibility to evaluate the hold-up in an extraction column:

$$h_d = \frac{v_{rs} + v_d - v_c}{2 \cdot v_{rs}} - \sqrt{\left(\frac{v_{rs} + v_d - v_c}{2 \cdot v_{rs}}\right)^2 - \frac{v_d}{v_{rs}}} \tag{2.45}$$

$$h_d = \frac{v_d}{v_s + v_d - v_c} \tag{2.46}$$

The hold-up can only be iteratively determined from *equation (2.45)* and *equation (2.46)*. This is due to the implicit form of these equations since the swarm velocity (v_{rs} and v_s) depends on the hold-up. In contrast, there exist many correlations in the literature to predict the hold-up independent of the swarm velocity, see *Bell and Babb 1969, Hafez et al. 1974, Niebuhr 1982, Kumar and Hartland 1989, Godfrey and Slater 1994, etc.* Such explicit correlations principally consist of several dimensionless numbers whose effects on the hold-up are determined by regression analysis. In spite of the large quantity of experimental data used to derive these correlations, the application of such explicit functions is often problematic. *Kumar and Hartland 1995* developed a correlation to predict the hold-up in extraction columns using more than 1200 data points from several research groups. However, *Wagner 1999* found major deviations between his experimental hold-up data in a sieve tray column and the calculated values from this correlation. According to Wagner, the correlation overestimates the influence of the viscosity of the dispersed phase.

While correlations which include the velocity of single particles v_o indirectly account for the influence of the physical properties of the liquid/liquid-system, the application of explicit correlations is not advised. In contrast to explicit correlations, implicit correlations like the one of Richardson and Zaki additionally provide realistic results for the limiting cases $h_d \to 0$ and $h_d \to 1$.

2.2.4 Flooding Capacity

Extraction columns are often operated close to the maximum throughput, i. e. close to the flooding capacity. Flooding occurs if the counter current flow of the two phases breaks down. The flooding capacity of a column is reached if a slight increase of the flow rate of any phase causes an infinite increase of the dispersed phase hold-up:

$$\frac{\partial v_d}{\partial h_d} = 0 \quad or \quad \frac{\partial v_c}{\partial h_d} = 0 \tag{2.47}$$

To ensure that a column is operated with a sufficient safety margin, the flooding capacity must be known. Models for the flooding capacity are often derived by combining *equation (2.38)* with a model for the swarm velocity and by determining the first derivations according to *equations (2.47)*. Following *Mersmann 1980*, the superficial velocity of the continuous phase at flooding $v_{c,f}$ can then be determined using the model of *Richardson and Zaki 1954*:

$$\frac{v_{c,f}}{v_o} = (1-h_{d,f})^2 \cdot [(1-h_{d,f})^{n-1} - (n-1) \cdot h_{d,f} \cdot (1-h_{d,f})^{n-2}] \tag{2.48}$$

Because the evaluation of the flooding velocities of both phases cannot be solved explicitly by *equation (2.38)* and *equation (2.48)*, Mersmann developed an approximate solution:

$$\frac{v_{d,f}}{v_o} = X \cdot (1-X)^{n-1} - \frac{v_{c,f}}{v_o} \cdot \frac{X}{1-X} \quad \text{where} \quad X = \frac{1}{n} \cdot \left[1 - \left(\frac{v_{c,f}}{v_o}\right)^{0.6}\right] \tag{2.49}$$

The graphical evaluation of this equation is illustrated in *figure (2.12)*, which proves that the flooding velocities of both phases can be easily determined from the terminal velocity of a single particle v_o and the corresponding swarm exponent *n*.

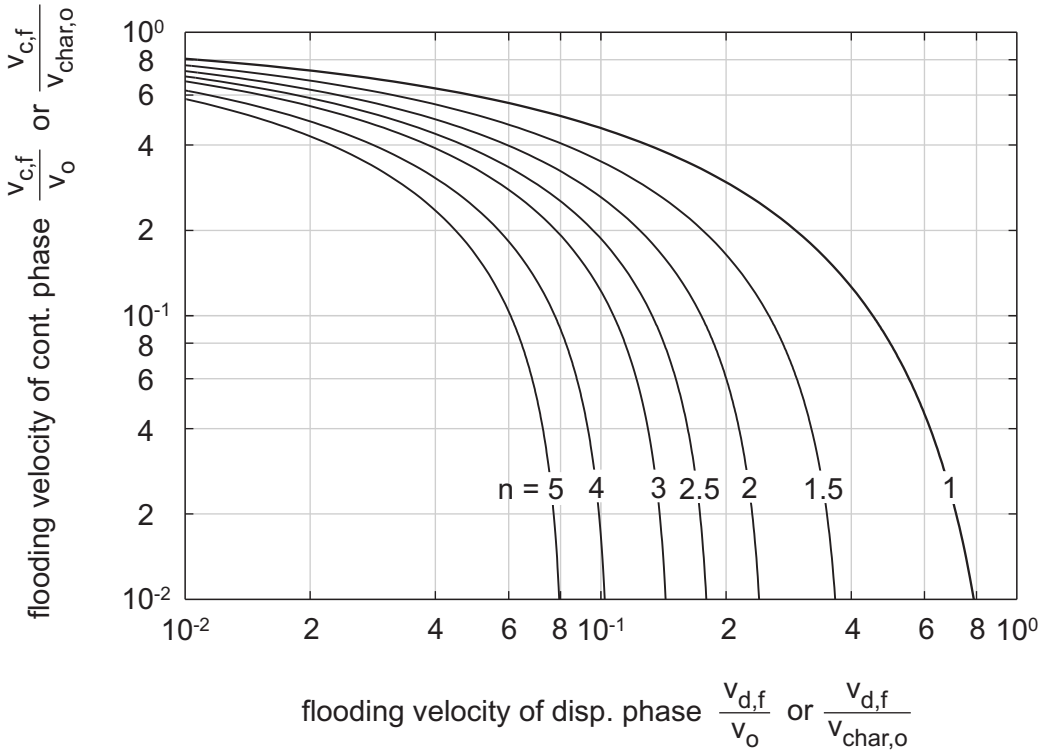

Figure 2.12: Flooding diagram according to Mersmann 1980

Applying Richardson and Zaki's equations to extraction columns with different types of internals is risky. Richardson and Zaki developed their model for rigid particle systems in columns without internals. In extraction columns the influence of internals has to be taken into account. *Mackowiak 1993* used the characteristic velocity of a single drop to determine the swarm velocity in packed extractors:

$$\frac{v_s}{v_{o,\,char}} = (1 - h_d)^n \tag{2.50}$$

To evaluate the flooding velocities of both phases, Mackowiak used the same procedure as Mersmann and made a comparison with experimental data. His results show that the swarm exponent *n* in columns with structured packings is significantly smaller than that of Richardson and Zaki. *Godfrey and Slater 1991* also found values of the swarm exponent *n* in different types of extractors which significantly differ from Richardson and Zaki's model.

Further models to predict the flooding capacity of extraction columns are given in *Seibert 1986, Kumar et al. 1986, Kirou et al. 1988, Lorenz 1990, Godfrey and Slater 1994, Delplancq and Delvosalle 1996, Wagner 1999, etc*. Some of these authors used *equation (2.38)* in combination with models for the swarm velocity. Others present empirical equations like the one of *McAllister et al. 1967*.

Drop population balance models (DPBMs) also allow the determination of the flooding capacity from knowledge of swarm velocities. Different criteria for the flooding capacity are often used. For example, simulation programs based on DPBMs are able to detect small drops retained in the compartments due to the counter current flow of the continuous phase. Thus, flooding capacity is predicted when the number of retained drops is higher than a critical value. Furthermore, DPBMs allow the determination of entrainment in the upper or bottom section of the column. Thus, flooding capacity can also be predicted when the calculated value of entrainment is too high. This proves again how powerful DPBMs are.

2.2.5 Axial Mixing

No plug flow of both phases exists in extraction columns. In fact, a part of each main phase flow is mixed back. Thus, these back mixing currents, so-called axial mixing currents, flow counter currently to the main phase flow. Axial mixing is generated by the formation of large eddies, the entrainment of the continuous phase in the wake of the drops (wake-effect: see *Wasowski and Blaß 1987*) and the different velocities of the drops due to their size distribution. In addition, axial mixing in extractors is caused by the forced transport of liquid in a direction opposite to its main phase. For instance, in agitated columns both phases are often pulled back into a compartment by the rotators after they passed it.

Axial mixing adversely affects the mass transfer in extractors. This is due to the fact that axial mixing significantly reduces the driving forces for mass transfer by reducing the concentration difference between the phases. This is particularly observed at both entries of a column where concentration jumps are produced due to axial mixing, see *figure (2.13)*.

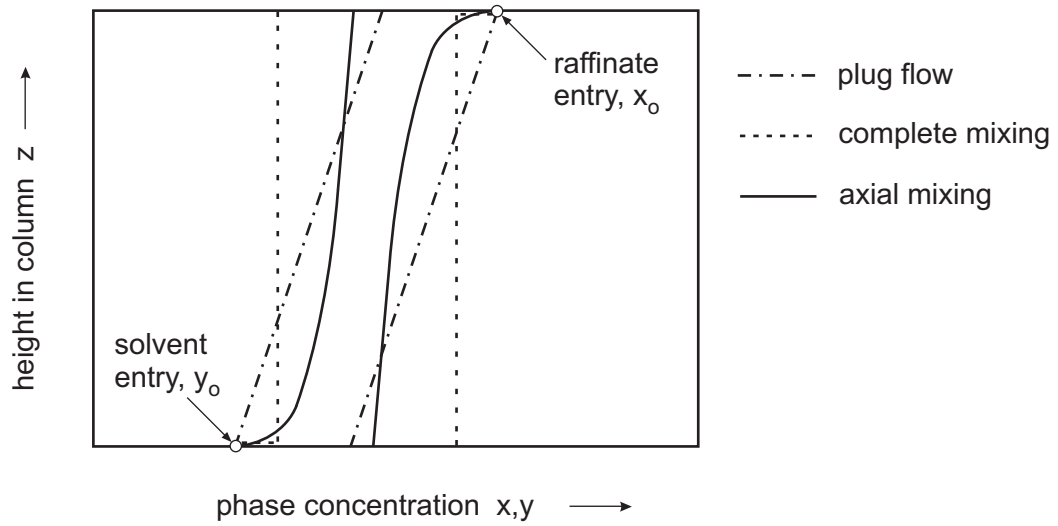

Figure 2.13: Influence of axial mixing on the concentration profile and its influence on mass transfer efficiency

The reduction of the concentration difference by axial mixing can be understood by analysing, for instance, the solute concentration of the raffinate phase. The solute concentration of the raffinate phase is reduced on its way through the column, see *figure (2.13)*. If a fraction of the raffinate phase which has already passed through a section of an extractor is mixed back into this section, it will be mixed with the new incoming raffinate. Since the back mixed raffinate has a lower solute concentration than the incoming raffinate, the concentration of the mixture is

reduced. Subsequently, the concentration difference between the main phases is reduced. Analogously, the solute concentration of the solvent phase is increased by axial mixing. This results again in a reduction of the driving concentration difference, see *figure (2.13)*.

Similar to the molecular diffusion model, axial mixing in extractors is considered by the axial dispersion model to be a result of macroscopic diffusion. All phenomena that causes axial mixing are then assumed to follow an eddy diffusion relationship where the diffusion coefficient is replaced by an axial dispersion coefficient D_{ax}, see also *Kumar 1985* and *Steiner 1988*. The axial dispersion model describes the solute concentration *x* in the raffinate phase by:

$$\frac{\partial x}{\partial t} = D_{ax,\,c} \cdot \frac{\partial^2 x}{\partial z^2} + v_{c,\,e} \cdot \frac{\partial x}{\partial z} - \frac{\beta_{oc} \cdot a}{(1 - h_d)} \cdot \left(x - \frac{y}{m} \right) \tag{2.51}$$

Analogously, the solute concentration *y* in the solvent phase is described by:

$$\frac{\partial y}{\partial t} = D_{ax,\,d} \cdot \frac{\partial^2 y}{\partial z^2} - v_{d,\,e} \cdot \frac{\partial y}{\partial z} + \frac{\beta_{oc} \cdot a}{h_d} \cdot \left(x - \frac{y}{m} \right) \tag{2.52}$$

The axial dispersion model is often given in dimensionless form, see also *Goldmann 1986*. For this purpose, the dimensionless Peclet numbers Pe_i of both phases are used:

$$Pe_d = \frac{v_{d,\,e} \cdot L}{D_{ax,\,d}} \quad and \quad Pe_c = \frac{v_{c,\,e} \cdot L}{D_{ax,\,c}} \tag{2.53}$$

The experimental determination of axial dispersion coefficients or Peclet numbers of the dispersed or the continuous phase is mainly carried out by tracer methods. Here, one phase is mixed with a liquid tracer, e. g. a potassium chloride solution or a phosphorescing dye. The tracer is injected at a certain column position and its concentration is then usually detected at two different downstream positions, see *Bauer 1976* and *Aufderheide 1985*. Subsequently, the axial dispersion coefficient is determined from a regression analysis comparing the calculated to the measured profiles. On the basis of these results, correlations are developed to predict axial dispersion coefficients for different operating conditions.

The application of axial dispersion coefficients for the characterisation of axial mixing in extractors is a contentious issue. Total radial mixing does not exist in all extractors, which is a precondition for the correct use of the axial dispersion model, see *Bauer 1976*. In addition, it is questionable whether this model can accurately describe effects like the accumulation of the dispersed phase under a stator or the development of large eddy circulations in a column. Nevertheless, many groups use this model for both phases, see *Miyauchi and Oya 1965, Rod*

1968, Rozen et al. 1970, Ingham et al. 1974, Häntsch and Weiss 1976, Niebuhr 1982, Kumar 1985, Rauscher 1992, Kumar and Hartland 1994, Rauber and Steiner 1997, etc.

With the help of DPBMs, axial mixing in the dispersed phase can be predicted only from the drop residence time distribution, which is determined by the drop size and drop velocity distribution, as is reported by *Henschke 2003.* For the prediction of axial mixing of the continuous phase by DPBMs, correlations for the axial dispersion coefficients are generally used. Henschke applied the following equation to predict the axial dispersion coefficient of the continuous phase in a pulsed sieve-tray column:

$$D_{ax,\,c} = 0.41 \cdot h_{st}^{2/3} \cdot D_C^{1/3} \cdot (v_c + v_d) \tag{2.54}$$

It is questionable whether *equation (2.54)* can predict the axial mixing in pulsed sieve-tray columns for a large range of operating conditions. This is due to the fact that it does not include relevant parameters such as the hole diameter and the relative free cross-sectional area of the sieve-trays as well as the energy input.

To account for axial mixing of the continuous phase in an agitated RDC-column by DPBMs, *Modes 1999* applied an empirical equation of *Kumar and Hartland 1994* which is valid over the entire range of agitation speeds, including the case of zero agitation:

$$D_{ax,\,c} = \left[0.42 + 0.29 \cdot \frac{v_d}{v_c} + \left(1.26 \cdot 10^{-2} \cdot \left(\frac{n_R \cdot d_A}{v_c} \right) + \frac{13.38}{3.18 + \left(\frac{n_R \cdot d_A}{v_c} \right)} \right) \cdot \left(\frac{v_c \cdot d_A \cdot \rho_c}{\eta_c} \right)^{-0.08} \cdot \left(\frac{D_C}{d_A} \right)^{0.16} \cdot \left(\frac{D_C}{h_c} \right)^{0.10} \cdot \frac{d_s^2}{D_C^2} \right] \cdot h_c \cdot \frac{v_c}{1 - h_d} \tag{2.55}$$

In contrast to Henschke, Modes also used the axial dispersion model to predict axial mixing of the dispersed phase. For this purpose, he determined the axial dispersion coefficient of the dispersed phase according to *Strand et al. 1962* as follows:

$$D_{ax,\,d} = \left[0.0138 + 8.26 \cdot 10^{-7} \cdot \left(\frac{n_R \cdot d_A}{v_d} \right)^{3.3} \right] \cdot h_c \cdot \frac{v_d}{h_d} \tag{2.56}$$

Analysing the published correlations for D_{ax} proves that large uncertainties are associated with the determination of axial mixing effects. Some of the models neglect essential influencing parameters or show different dependencies of the relevant variables. For example, *equation (2.56)* includes neither geometrical dimensions of the agitated cells nor the velocity of the continuous phase v_c. Considering that axial mixing is very important for the scale-up of extractors, it is surprising that so little effort has been expended in the investigation of this issue in recent years.

2.3 Mass Transfer in Liquid/Liquid-Systems

Mass transfer between drops and continuous phase is characterised by diffusion processes as well as by convective transport mechanisms in the interior and the external adjacent regions of the drops. The transfer rates are controlled by the mass transfer resistance in both phases, while mass transfer resistance in the interface is assumed to be zero. According to the film theory, see *Kumar 1985*, the mass transfer of a single component from the continuous to the dispersed phase is described by:

$$\dot{M} = A \cdot \rho_d \cdot \beta_d \cdot (y_{if} - y_b) = A \cdot \rho_c \cdot \beta_c \cdot (x_b - x_{if}) \tag{2.57}$$

Here, y_b and x_b denote the bulk weight concentration of the solute in the dispersed phase and the continuous phase, respectively. The concentrations y_{if} and x_{if} are the solute concentrations in each phase at the interface. The concentration at the interface is normally unknown. For this reason, the entire mass transfer resistance is formally put in one phase only by the overall concept. If the total mass transfer resistance is in the dispersed phase, the concentration of the dispersed phase at the interface can easily be determined from the bulk concentration of the continuous phase and the distribution coefficient *m*: $y_{if} = m \cdot x_b$. Similarly, the concentration of the continuous phase at the interface can be determined if the overall mass transfer resistance is only in the continuous phase: $x_{if} = y_b / m$. This allows the mass transfer rate to be described by the bulk concentrations of each phase according to:

$$\dot{M} = A \cdot \rho_d \cdot \beta_{od} \cdot (m \cdot x_b - y_b) = A \cdot \rho_c \cdot \beta_{oc} \cdot (x_b - y_b / m) \tag{2.58}$$

2.3.1 Mass Transfer Coefficients

The overall mass transfer coefficients β_{od} (overall dispersed phase) and β_{oc} (overall continuous phase) are related to the individual mass transfer coefficients β_d and β_c by:

$$\frac{1}{\beta_{od} \cdot \rho_d} = \frac{1}{\beta_d \cdot \rho_d} + \frac{m}{\beta_c \cdot \rho_c} \quad and \quad \frac{1}{\beta_{oc} \cdot \rho_c} = \frac{1}{\beta_c \cdot \rho_c} + \frac{1}{\beta_d \cdot \rho_d \cdot m} \tag{2.59}$$

The individual mass transfer coefficients mainly depend on drop size and flow conditions inside and outside the drop.

- *Individual mass transfer coefficient β_d in the dispersed phase*

In the following section, the mass transfer of a single drop in a stationary continuous phase is considered. If no circulations occur inside the drop and the drop behaves like a rigid sphere, the bulk concentration of the drop *y(t)* during mass transfer is described by the model of *Newman 1931*:

$$\frac{y(t) - y^*}{y_o - y^*} = \frac{6}{\pi^2} \cdot \sum_{n=1}^{\infty} \left(\frac{1}{n^2} \cdot exp[-(n \cdot \pi)^2 \cdot Fo_d] \right) \quad \text{with} \quad Fo_d = \frac{4 \cdot D_d \cdot t}{d^2} \tag{2.60}$$

In *equation (2.60)*, y_o is the initial concentration of the drop, y^* is the equilibrium concentration and Fo_d is the dimensionless time. An approximate solution of *equation (2.60)* for short and long contact times can be found in *Mersmann 1986*:

$$\frac{y(t) - y^*}{y_o - y^*} = \begin{cases} 1 - \frac{6}{\sqrt{\pi}} \cdot \sqrt{Fo_d} + 3 \cdot Fo_d; & for\ Fo_d < 0.1584 \\ \frac{6}{\pi^2} \cdot exp[-\pi^2 \cdot Fo_d]; & for\ Fo_d \geq 0.1584 \end{cases} \tag{2.61}$$

From knowledge of the change of drop concentration with time, the mass transfer coefficient β_d of rigid drops can be evaluated. For this purpose, the mass transfer rate of a drop with a constant volume is determined:

$$\dot{M} = \frac{\pi}{6} \cdot d^3 \cdot \rho_d \cdot \frac{dy}{dt} = \pi \cdot d^2 \cdot \rho_d \cdot \beta_d \cdot (y^* - y(t)) \tag{2.62}$$

This leads to:

$$\frac{y(t)-y^*}{y_o-y^*} = exp\left(-\frac{6\cdot\beta_d\cdot t}{d}\right) \tag{2.63}$$

Thus, the Sherwood number Sh_d and the mass transfer coefficient β_d of rigid drops are given by the combination of *equation (2.63)* and *equation (2.60)*:

$$Sh_d = \frac{\beta_d\cdot d}{D_d} = -\frac{d^2}{6\cdot D_d\cdot t}\cdot ln\left[\frac{6}{\pi^2}\cdot\sum_{n=1}^{\infty}\left(\frac{1}{n^2}\cdot exp[-(n\cdot\pi)^2\cdot Fo_d]\right)\right] \tag{2.64}$$

Equations (2.61) can also be used in combination with *equation (2.63)* to determine the Sherwood number Sh_d of rigid drops.

With increasing drop diameter circulations are generated within a drop. Such circulations improve the mixing of the drop interior and enhance the transport velocity of the solute. The effect of circulations within a drop on mass transfer is taken into account by *Kronik and Brink 1950*:

$$Sh_d = \frac{\beta_d\cdot d}{D_d} = -\frac{d^2}{6\cdot D_d\cdot t}\cdot ln\left[\frac{3}{8}\cdot\sum_{n=1}^{\infty}(C_n^2\cdot exp[-\lambda_n\cdot 16\cdot Fo_d])\right] \tag{2.65}$$

where C_n are constant factors and λ_n are eigen-values given by *Heertjes et al. 1954, Elzina and Banchero 1959, etc.*

Furthermore, the creation of turbulent eddies and, in turn, the high degree of mixing in the drop significantly enhance the mass transfer. The increase of the mass transfer is correlated with the degree of turbulence in the drop. The Sherwood number Sh_d of such drops can be determined according to *Handlos and Baron 1957*:

$$Sh_d = \frac{\beta_d\cdot d}{D_d} = -\frac{d^2}{6\cdot D_d\cdot t}\cdot ln\left(2\cdot\sum_{n=1}^{\infty}C_n^2\cdot exp\left[-\frac{\lambda_n\cdot v_o\cdot t}{128\cdot d\cdot(1+\eta_d/\eta_c)}\right]\right) \tag{2.66}$$

Considering only the first term of *equation (2.66)*, the mass transfer coefficient β_d is obtained by:

$$\beta_d = 0.00375\cdot\frac{v_o}{1+\eta_d/\eta_c} \tag{2.67}$$

The model of Handlos and Baron is often questioned in the literature because it shows no dependence on the diffusion coefficient D_d. However, many research groups have pointed out

that the application of this model results in a better correspondence with experimental data than other models.

There are many other models for the description of mass transfer coefficients for rigid, circulating and oscillating drops in the literature. For example, *Skelland and Wellek 1964* describe the mass transfer of non-oscillating and oscillating drops:

-) for non-oscillating drops:

$$Sh_d = \frac{\beta_d \cdot d}{D_d} = 31.4 \cdot Fo_d^{-0.338} \cdot Sc_d^{-0.125} \cdot \left(\frac{d \cdot v_o^2 \cdot \rho_c}{\sigma} \right)^{0.371} \quad \text{for } 37 < Re_o < 546 \qquad (2.68)$$

where $Sc_d = \eta_d / (\rho_d \cdot D_d)$ is the dimensionless Schmidt number of the dispersed phase.

-) for oscillating drops:

$$Sh_d = \frac{\beta_d \cdot d}{D_d} = 0.32 \cdot Re_o^{0.68} \cdot K_l^{0.1} \cdot Fo_d^{-0.14} \quad \text{for } 411 < Re_o < 3114 \qquad (2.69)$$

where $K_l = \frac{\sigma^3 \cdot \rho_c^2}{g \cdot \eta_c^4 \cdot \Delta\rho}$ is a dimensionless number characterising the liquid/liquid-system.

- *Individual mass transfer coefficient β_c in the continuous phase*

The mass transfer coefficient in the continuous phase β_c is often described by equations of the form:

$$Sh_c = \frac{\beta_c \cdot d}{D_c} = A + B \cdot Re_o^C \cdot Sc_c^D \qquad (2.70)$$

Here, $Sc_c = \eta_c / (\rho_c \cdot D_c)$ is the dimensionless Schmidt number of the continuous phase. The term A takes the mass transfer into account if only diffusion is responsible for the transport ($Re_o = 0$) and is often described by $A = 2$. The experimental examination of rigid spheres and rigid drops of several groups show that:

$$Sh_c = \frac{\beta_c \cdot d}{D_c} = 2 + B \cdot Re_o^{1/2} \cdot Sc_c^{1/3} \quad \text{where} \quad B = 0.6 - 1.1 \qquad (2.71)$$

Brauer 1971 and *Ihme et al. 1972* used the following empirical correlation to predict the Sherwood number Sh_c for rigid drops for $1 \le Re_o \le 100$:

$$Sh_c = \frac{\beta_c \cdot d}{D_c} = 2 + \left[\frac{0.66}{1 + Sc_c} + \frac{Sc_c}{2.4 + Sc_c} \cdot \frac{0.79}{Sc_c^{1/6}} \right] \cdot \frac{(Re_o \cdot Sc_c)^{1.7}}{1 + (Re_o \cdot Sc_c)^{1.2}} \tag{2.72}$$

For highly circulating drops ($Re_o \to \infty$) *Clift et al. 1978* suggested that Sh_c can be given by:

$$Sh_c = \frac{\beta_c \cdot d}{D_c} = \frac{2}{\sqrt{\pi}} \cdot (Re_o \cdot Sc_c)^{0.5} \tag{2.73}$$

which is the well known *Boussinesq* equation.

By analysing experimental data from different research groups *Steiner 1986* developed a model for the Sherwood number Sh_c that can be applied to a wide range of Reynolds and Schmidt numbers Sc_c. The actual Sherwood number is determined from the Sherwood number of a rigid and circulating drop by:

$$\frac{Sh_c - Sh_{c,rigid}}{Sh_{c,circ} - Sh_{c,rigid}} = 1 - exp[-4.18 \cdot 10^{-3} \cdot (Re_o \cdot Sc_c)^{0.42}] \tag{2.74}$$

for $10 \le Re_o \le 1200$ and $190 \le Sc_c \le 241000$. Thereby, $Sh_{c,circ}$ is given by *equation (2.73)* and $Sh_{c,rigid}$ is correlated by:

$$Sh_{c,rigid} = 2.43 + 0.775 \cdot Re_o^{1/2} \cdot Sc_c^{1/3} + 0.0103 \cdot Re_o \cdot Sc_c^{1/3} \tag{2.75}$$

- *Mass transfer coefficients in swarms of drops*

Since the hold-up changes the fluiddynamic conditions around drops, the influence of hold-up in the prediction of mass transfer rates in swarms of drops should be taken into consideration. An interesting approach to determine the mass transfer coefficients β_c and β_d in swarms of drops is given in *Kumar and Hartland 1999*. Analysing data from 596 measurements, the authors found a satisfactory agreement between their correlations and experimental results of swarms of drops in different extraction columns. Another possibility to predict the individual mass transfer coefficient β_c in swarms of drops was introduced by *Nishimura and Ishii 1980*:

$$Sh_c = \frac{\beta_c \cdot d}{D_c} = \frac{2}{(1 - h_d^{1/3})} + 0.6 \cdot Re_s^{1/3} \cdot Sc_c^{1/3} \cdot (1 - h_d^{-1/2}) \tag{2.76}$$

for $100 \le Re_s \le 1000$ with $Re_s \equiv \frac{v_s \cdot d \cdot \rho_c}{\eta_c}$

A summary of correlations for the prediction of mass transfer coefficients in swarms of drops can be found in *Slater 1994*. Most of these correlations are empirical. Analytical solutions for the mass transfer in swarms of drops are only possible if oversimplifying assumptions are made.

2.3.2 Experimental Investigations of Mass Transfer Between Single Drops and Continuous Phase

Numerous experimental investigations of mass transfer in and out of single drops have been carried out in recent years. To determine overall mass transfer coefficients in dependence of drop size and energy input, appropriate laboratory scale columns and mini plants have been developed. *Qi 1992*, *Wagner 1999* and *Hoting 1996* used a method with two measuring points within a laboratory scale column to determine the concentration change of rising drops. The experimental set-up and the operating procedure is described in detail by *Qi 1992*. Measuring the concentration of rising drops at a lower position 1 and at an upper position 2 as well as determining the concentration of the continuous phase leads to the evaluation of the overall dispersed phase mass transfer coefficient β_{od}:

$$\beta_{od} = \frac{d}{6 \cdot \Delta t} \cdot ln\left(\frac{y^* - y_1}{y^* - y_2}\right) \tag{2.77}$$

Here, Δt is the time a drop needs to pass a distance L between position 1 and position 2: $\Delta t = L/v_o$ *or* $L/v_{char,o}$. The results of the mass transfer measurements with organic drops in columns without internals are illustrated in *figure (2.14)* for different systems. The system butyl acetate (d)/acetone/water shows the highest overall mass transfer coefficients. In contrast, nonanol (d)/propanol/water and tridecanol (d)/propanol/water have much lower overall mass transfer coefficients. This can be attributed to the high viscosity of these organic phases compared to butyl acetate (*bu-ac*):

$\eta_{d,\,tridecanol} = 42.0 \cdot 10^{-3} Pa \cdot s$, $\eta_{d,\,nonanol} = 15.1 \cdot 10^{-3} Pa \cdot s$, $\eta_{d,\,bu\text{-}ac} = 0.7 \cdot 10^{-3} Pa \cdot s$

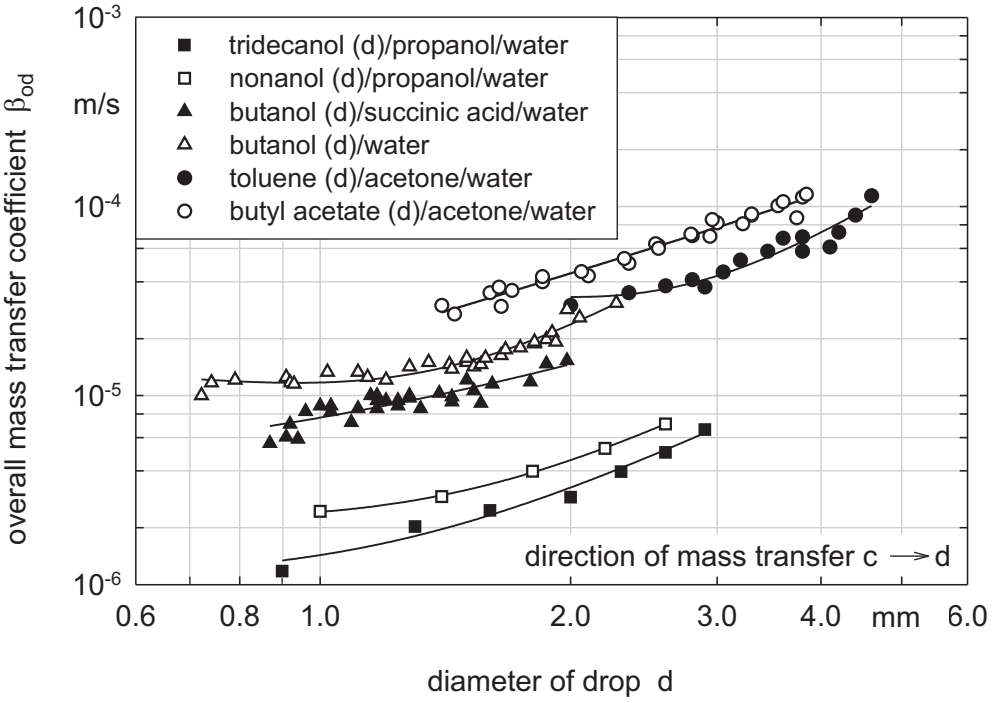

Figure 2.14: Overall mass transfer coefficients of different liquid/liquid-systems in columns without internals; Hoting 1996: butyl acetate (d)/acetone/water; Qi 1992: butanol (d)/water, butanol (d)/succinic acid/water, toluene (d)/acetone/water; Wagner 1999: nonanol (d)/propanol/water, tridecanol (d)/propanol/water

To evaluate the dependence of the overall mass transfer coefficient in different extractors on drop size and energy input, internals have to be installed inside a laboratory scale column. A plot of the experimental results of *Qi 1992* for a column with and without sieve trays is given in *figure (2.15)*. It is obvious that mass transfer in single drops in sieve tray columns is larger than in columns without internals. Unfortunately, the influence of the pulsation intensity in sieve tray columns was investigated by the author only to a maximum value of $a \cdot f = 1.0$ *cm/s* even though such columns are often operated at higher pulsation intensities.

The investigations of *Henschke 2003* of single toluene and butyl acetate drops in a pulsed column with different sieve trays reveal that mass transfer is significantly influenced by the drop residence time beneath the sieve trays. The flow around a drop for a given pulsation intensity is highly turbulent if the drop is positioned under a sieve tray for a certain time. In addition, the mass transfer is influenced by the ratio of the drop diameter to the hole diameter. The drop interior is better mixed if the drop is deformed when moving through the holes. Both effects result in higher mass transfer rates in sieve tray columns than in columns without internals.

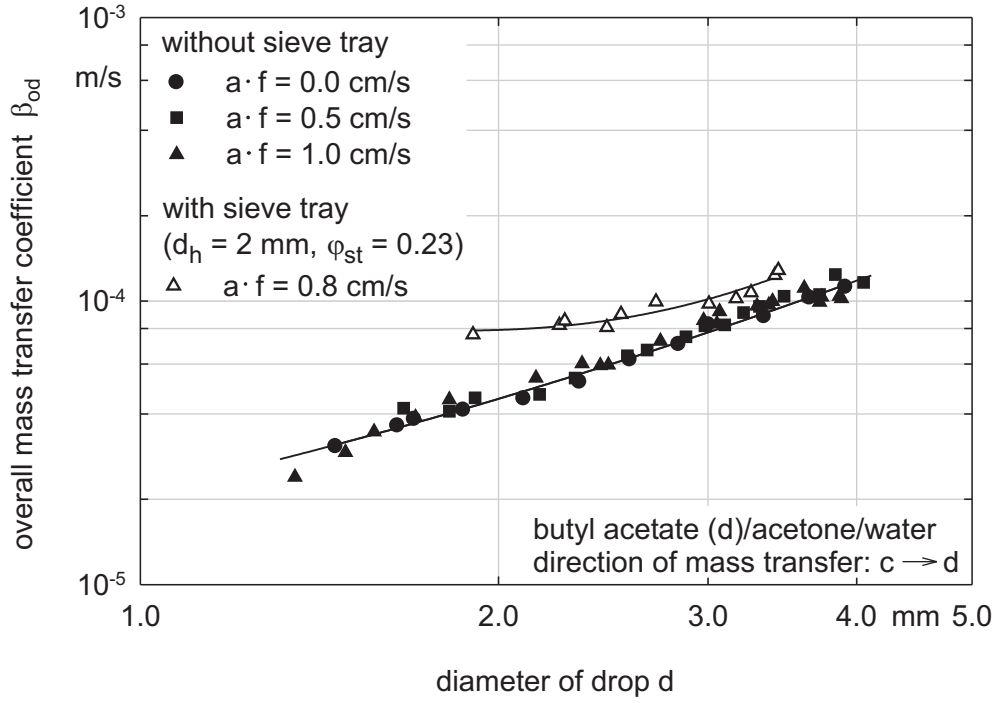

Figure 2.15: Influence of energy input on mass transfer in a column with and without sieve trays, Qi 1992

The experimental approach of Henschke differs from that of Qi. Qi and the authors mentioned above measured the mass transfer in a stationary aqueous fluid. In Henschke's experiments, the continuous water phase was in counter current contact with the dispersed organic phase. Due to the conic shape of the column, the drop residence time could be easily varied by changing the flow rate of the continuous phase. For this reason, the influence of drop residence time on mass transfer could be investigated. As an example, *figure (2.16)* shows data from *Grömping 2004*, who used Henschke's method. In this diagram, the dimensionless drop concentration is plotted versus the residence time of the drop in a column without internals. As expected, the concentration of the drops approaches the equilibrium concentration with increasing residence time.

According to Henschke, the experimental data can be used to evaluate an effective diffusion coefficient $D_{d,\,eff}$, which is defined by:

$$D_{d,\,eff} = D_d + \frac{v_o \cdot d}{C_{IP} \cdot (1 + \eta_d/\eta_c)} \tag{2.78}$$

The constant factor C_{IP} in *equation (2.78)* accounts for the influence of turbulent convections and eruptions at the interphase, so-called Marangoni convections. Marangoni convections

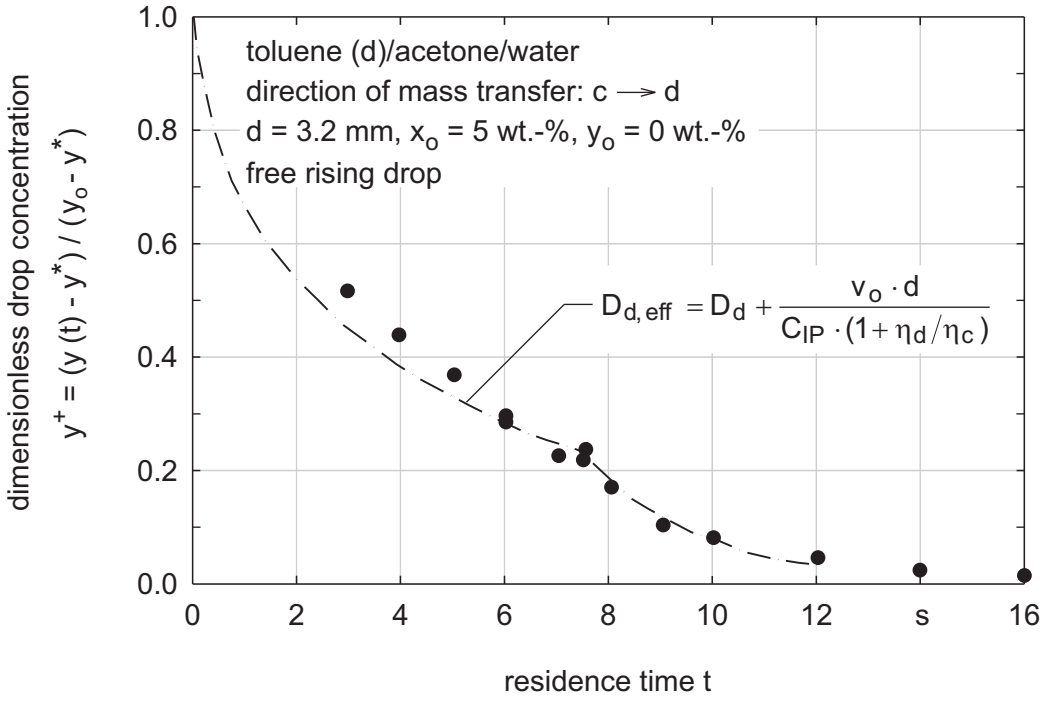

Figure 2.16: Dependence of drop concentration on residence time of a drop in a column without internals, comparison of experimental data (Grömping 2004) and model of Henschke 2003 (dashed line)

significantly increase the mass transfer. To determine the parameters C_{IP} and $D_{d,\,eff}$, the molecular diffusion coefficient D_d in the *equations (2.61)* is replaced by $D_{d,\,eff}$. Subsequently, regression analysis using experimental data and *equations (2.61)* is carried out.

The evaluation of the effective diffusion coefficient $D_{d,\,eff}$ for a certain drop size d_i allows the Sherwood number to be determined:

$$Sh_{od,\,i} = \sqrt{\frac{4 \cdot d_i^2}{\pi \cdot D_{d,\,eff,\,i} \cdot t} + \pi^4} \quad \Rightarrow \quad \beta_{od,\,i} = \frac{Sh_{od,\,i} \cdot D_{d,\,eff,\,i}}{d_i} \tag{2.79}$$

Based on the single drop experiments, the concentration of drops with diameter d_i in a swarm and of the continuous phase can be predicted from Henschke's drop population balance model for each time step *n* by:

$$y_i^n = y_i^{n-1} + \frac{6 \cdot \Delta M^n}{\pi \cdot d_i^3 \cdot \rho_d} \quad \text{and} \quad x_j^n = x_j^{n-1} - \frac{\Delta M^n}{V_c \cdot \rho_c} \tag{2.80}$$

where $\Delta M^n = \pi \cdot d_i^2 \cdot \rho_d \cdot \beta_{od,\,i}^n \cdot (m \cdot x_j^{n-1} - y_i^{n-1}) \cdot \Delta t$. Using this approach, the concentration of each single drop in the swarm is determined. Simultaneously, the lifetime of each drop due to breakage or coalescence is considered. Although this procedure is relatively

complex and time consuming, it represents a promising possibility for accurately predicting the mass transfer in extractors.

2.3.3 Marangoni Convections

As mentioned previously, turbulent convections at the drop surface, so-called Marangoni convections, significantly enhance the mass transfer rates. Orderly eddies or irregular eruptions occur which are shown in *figure (2.17)*.

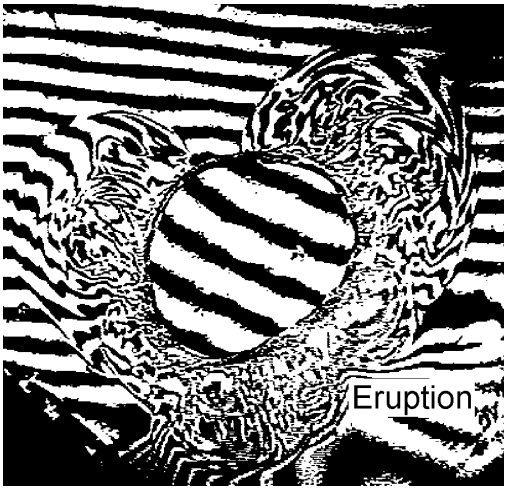

Figure 2.17: Eruptive interfacial convections caused by mass transfer, Wolf 1999

The influence of these interfacial convections and their effects on mass transfer was studied by *Golovin 1992*, *Wolf 1999* and *Tourneau 2004*. Tourneau compared the development of overall mass transfer coefficients with time for single drops and drops within a swarm. His experiments show that Marangoni convections essentially depend on the driving concentration difference and the flow of the continuous phase. The mass transfer rate is significantly increased if the initial driving concentration difference is higher than a critical value. According to Tourneau, the critical concentration difference of 3-chlortoluene (d)/acetone/water is *4 wt.-%*. Furthermore, the overall mass transfer coefficients of swarms $\beta_{od,\,s}$ are always higher than of single drops β_{od}.

2.3.4 Other Factors Influencing Mass Transfer

Several other factors influence the mass transfer in extractors. The influence of surfactants and small amounts of impurities in the column has been known for many years. The determination of the impact of surfactants on the mode of operation is still difficult. Because surfactants decrease the interfacial tension in a liquid/liquid-system and reduce the surface mobility of the drops, different mass transfer rates are expected. Information about the influence of surfactants on mass transfer can be found in *Liang and Slater 1990, Slater 1995* and *Chen and Lee 2000*.

3 Systems Used for the Experimental Investigations

Preliminary experiments are necessary for dimensioning extraction columns due to the large number of influencing factors, see *chapter 2*. The determination of these factors through single particle experiments represents a promising approach. Compared to tests in pilot plant columns, the use of single particle experiments reduces the amount of liquids and the time necessary for the experiments. For these reasons, single particles (rigid spheres and drops) were investigated in this work. Furthermore, experiments with swarms of particles were carried out to determine the influence of hold-up on the fluiddynamics and to obtain information about the mass transfer rates in different extractors.

The advantage of using rigid spheres in extraction columns for investigating the fluiddynamics is the absence of breakage and coalescence. In addition, mono-dispersed particle swarms can be studied.

3.1 Polypropylene-spheres/Water

Experiments with rigid spheres and water were conducted to determine the influence of internals and energy input on the characteristic velocity of single rigid spheres and on the velocity of swarms. The rigid spheres for these investigations were made of polypropylene (pp). Polypropylene is a suitable material for the spheres because it possesses a density that is very similar to the density of toluene and butyl acetate, both standard liquids for extraction tests.

When the velocity of a single rigid sphere is evaluated, the density distribution within the sphere has to be considered. A sphere with an irregular density distribution has a different velocity compared to a sphere of same size but with a uniformly distributed density. This is due to the fact that a sphere with an irregular density distribution shows a fluctuating motion in columns without internals. To control whether the density within a sphere is uniformly distributed or not, the rolling behaviour of the sphere on a smooth horizontal plane is investigated. The rolling behaviour of all pp-spheres used for the single particle experiments was controlled. Only particles with no preferred direction of rolling were used. The pp-spheres were further sorted so that only particles with the same size and density for a certain particle diameter were used.

The behaviour of mono-dispersed particle swarms in extraction columns was determined with precisely grounded pp-spheres from *Spherotech GmbH, Germany*. The diameter and density of the pp-spheres was checked by a random examination of 500 particles for each particle size to ensure that size and density distribution of the particles were sufficiently precise. The results revealed that the deviation of the particle size was lower than declared by the company and all pp-spheres had very similar densities for a certain particle size. Furthermore, the examined pp-spheres did not show any favoured direction of rolling. The size and density of both the single pp-spheres and the pp-spheres for the mono-dispersed swarms are given in *table (3.1)* and *table (3.2)*.

Table 3.1: Particle size and density properties of single pp-spheres

diameter d_p [mm]	1.9 ± 0.01	2.0 ± 0.02	2.5 ± 0.02	3.0 ± 0.03	3.4 ± 0.02	4.0 ± 0.04
density ρ_p [kg/m^3]	894 ± 3.1	882 ± 2.1	872 ± 0.8	863 ± 4.6	864 ± 3.5	884 ± 1.5

Table 3.2: Particle size and density properties of pp-spheres for mono-dispersed swarms

diameter d_p [mm]	3.0 ± 0.06	3.5 ± 0.04	4.0 ± 0.04
density ρ_p [kg/m^3]	875 ± 4.0	888 ± 5.2	890 ± 4.6

3.2 Toluene/Acetone/Water and Butyl Acetate/Acetone/Water

Investigations with liquid/liquid-systems were carried out to clarify the influence of physical properties and the influence of surface mobility of single drops on characteristic velocities, breakage mechanisms and mass transfer rates. Furthermore, experiments with poly-dispersed drop swarms were performed. The aim of these investigations was to determine whether or not the developed correlations for swarms of rigid particles can be transferred to liquid/liquid-systems. Two standard systems recommended by the European Federation of Chemical Engineering, see *EFCE 1984*, were used: toluene/acetone/water and butyl acetate/acetone/water. Physical properties are listed in the following tables while information about the phase equilibria of both systems can be found in the appendix, see *chapter A*.

Table 3.3: Physical properties of mutually saturated liquid/liquid-systems toluene/acetone/water "t/a/w" and butyl acetate/acetone/water "bu-ac/a/w" at 20°C according to EFCE 1984; x_a= denotes for the weight fraction of acetone in the aqueous phase; index a = aqueous phase, index o = organic phase

physical property	unit	t/w	t/a/w x_a= 0.05	bu-ac/w	bu-ac/a/w x_a= 0.05
density ρ_a	[kg/m^3]	998.8	992.0	996.4	990.9
density ρ_o	[kg/m^3]	867.5	863.3	881.3	877.5
viscosity η_a	[10^{-3} Pa · s]	1.029	1.134	1.022	1.163
viscosity η_o	[10^{-3} Pa · s]	0.596	0.566	0.738	0.709
interfacial tension σ	[10^{-3} N · m]	34.31	24.41	13.97	10.96
distribution coefficient *m*	[kg/kg]	–	0.843	–	0.933

Table 3.4: Binary diffusion coefficients of acetone for different acetone concentrations in both the aqueous and organic phase of toluene/acetone/water at 20°C according to EFCE 1984

weight fraction of acetone [kg / kg]	diffusion coefficient of acetone in aqueous phase D_a [10^{-9}m^2/s]	diffusion coefficient of acetone in toluene phase D_o [10^{-9}m^2/s]
0.03	1.155	2.789
0.05	1.152	2.788

Table 3.5: Binary diffusion coefficients of acetone for different acetone concentrations in both the aqueous and organic phase of butyl acetate/acetone/water at 20°C according to EFCE 1984

weight fraction of acetone [kg / kg]	diffusion coefficient of acetone in aqueous phase D_a [10^{-9}m^2/s]	diffusion coefficient of acetone in butyl acetate phase D_o [10^{-9}m^2/s]
0.03	1.093	2.200
0.05	1.092	2.199

The results of the investigation of the phase equilibrium and the distribution coefficient *m* reveal deviations between the experimental data and calculated values from equations proposed by *EFCE 1984*. In particular, the distribution coefficient for acetone in the toluene/acetone/water system shows relatively large deviations, see *figure (3.1)*. Similar differences for *m* were found by *Henschke 2003*. His empirical correlation agrees very well with the experimental data of this work. The comparison of the distribution coefficient for butyl acetate/acetone/water reveals that

the experimental data can be predicted in close agreement with the correlation of *Reissinger 1985*, while small deviations occur compared to the equation given in *EFCE 1984*.

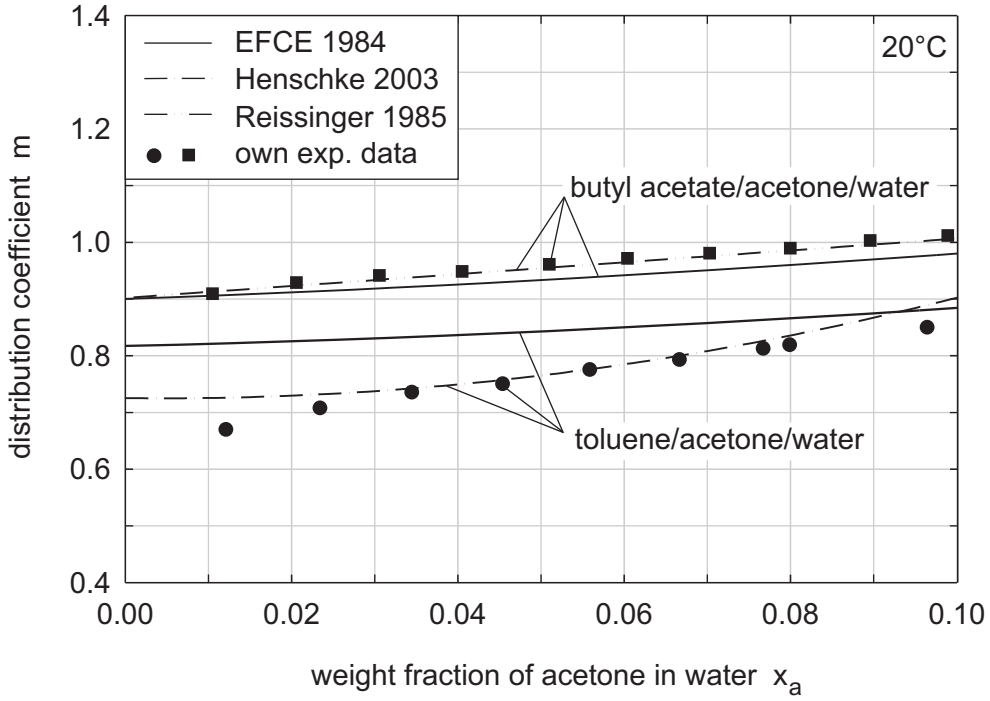

Figure 3.1: Distribution coefficient m for both liquid/liquid-systems and comparison of experimental data to different correlations in the literature

Despite these deviations, all other experimentally evaluated physical properties are predicted very well by the correlations of the *EFCE 1984*. For this reason, these correlations were used for all calculations.

Deionised water was used for the aqueous continuous phase. The quality of the water was controlled by continuously monitoring its conductivity. The conductivity measurements for the deionised water showed the same values as for bi-distilled water, which is in the range of $\kappa_{bdw} = 0.5 - 1.0\ \mu S/cm$, see *Wagner 2003*. As an example, the results of conductivity measurements for the deionised water used are shown in *figure (3.2)*. It is obvious that the deionised water had a very low conductivity of about $\kappa_{dw} = 0.63\ \mu S/cm$ for a temperature of $20°C$. From this result it can be concluded that the deionised water used was very pure and contained only small amounts of electrolytes.

Experiments with single drops were performed with organic liquids of the quality *pro analysis (p. a.)*. During the experiments the settling time of the liquid/liquid-systems was continuously checked to see whether coalescence behaviour had changed. If differences in the settling time

were detected or if the stationary continuous phase was in the laboratory scale columns for three weeks, the liquid/liquid-system was replaced and disposed of. In contrast, experiments with swarms of drops in different pilot plant extractors were conducted with toluene and butyl acetate of the quality *technically pure*. Constant liquid purity was provided for the pilot plant experiments with swarms of drops through the regeneration of the process liquids in a distillation column.

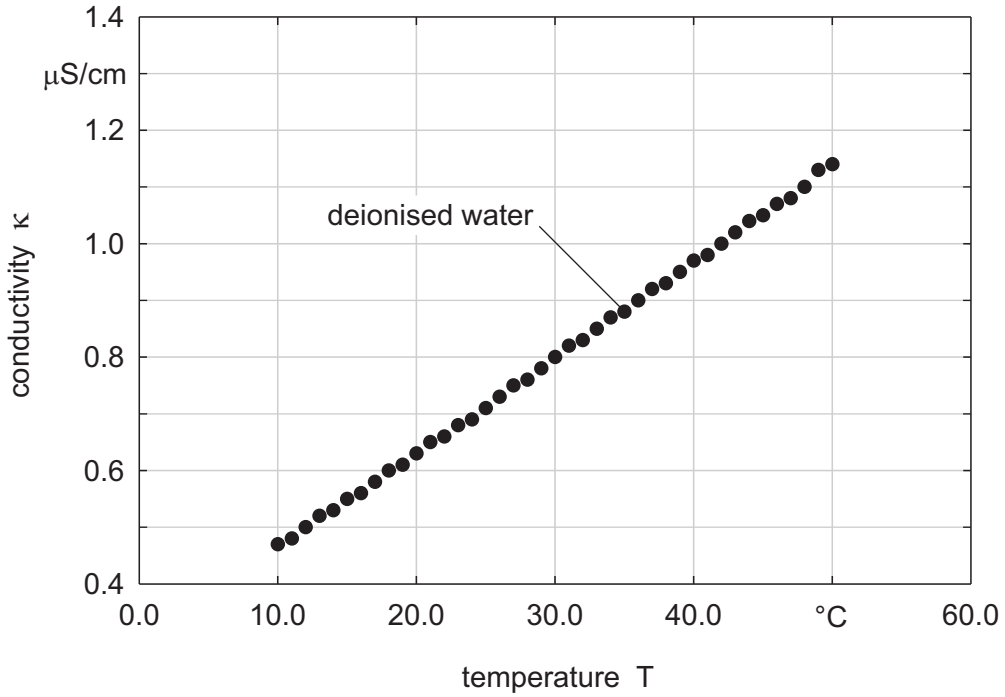

Figure 3.2: Representative plot of the conductivity of the deionised water used for the experimental investigations

Finally, it should be mentioned that in all fluiddynamic investigations the phases were mutually saturated. When both fluiddynamics and mass transfer rates were investigated, the water and the solvent were mutually saturated before acetone was admixed to the aqueous phase. This allowed the experiments for the mass transfer of the solute to be performed in absence of any superimposed mass transfer currents.

4 Experimental Devices, Internals and Measuring Technique

The experimental investigations of single rigid spheres and drops as well as of swarms of rigid spheres and drops were conducted in several columns. Experiments with rigid spheres were carried out to investigate the fluiddynamic behaviour in different extractors while experiments with single drops and swarms of drops were performed to obtain information about fluiddynamics and mass transfer in liquid/liquid-systems.

4.1 Single Rigid Sphere Mini Plant

The terminal velocity and characteristic velocity of single rigid spheres were determined in a mini plant that consisted of a laboratory scale pulsed and agitated column. In both columns the inner diameter of the active part was 80 mm, the total height was 1000 mm and each column had a total volume of approximately 10 litres, see *figure (4.1)*. The temperature of the continuous water phase in both columns was maintained at 20°C with an external cooling unit and was monitored underneath and above the active part of the column. The cooling double wall consisted of a rectangular PVC shell which was filled with water. The rectangular shape of the double wall prevented refraction, which normally exists in a cylindrical glass column.

The single rigid spheres were pumped to the bottom section of the columns with a hose pump. After rising through the column, the spheres were sucked from the top section through a glass funnel. In this way, infiltration and adhesion of small air bubbles into the column and onto the pp-spheres was prevented. As the rigid spheres rose through the column the pump was switched off to ensure that the water phase was stationary. There existed no co-current flow or counter-current flow of the rigid spheres and the continuous water phase. The velocities of the rigid spheres were measured in a 300 mm long column section with a digital camcorder and a PC. The frame rate of the camcorder was 25 frames/sec, reducing time measurement deviations to a minimum of $\Delta t = \pm 0.04\ sec.$ The velocity of a rigid sphere in the mini plant was determined as the average of at least 50 single measurements to eliminate stochastic effects.

A pulsator was installed at the bottom of the pulsed column which caused the liquids to oscillate. The pulsation amplitude in all experiments was 8 mm. Note that the amplitude characterises the total liquid stroke in the column and not the amplitude of the pulsator. For the agitated column the rotational speed could be continuously varied in a wide range (n_R = 0 - 2000 1/min).

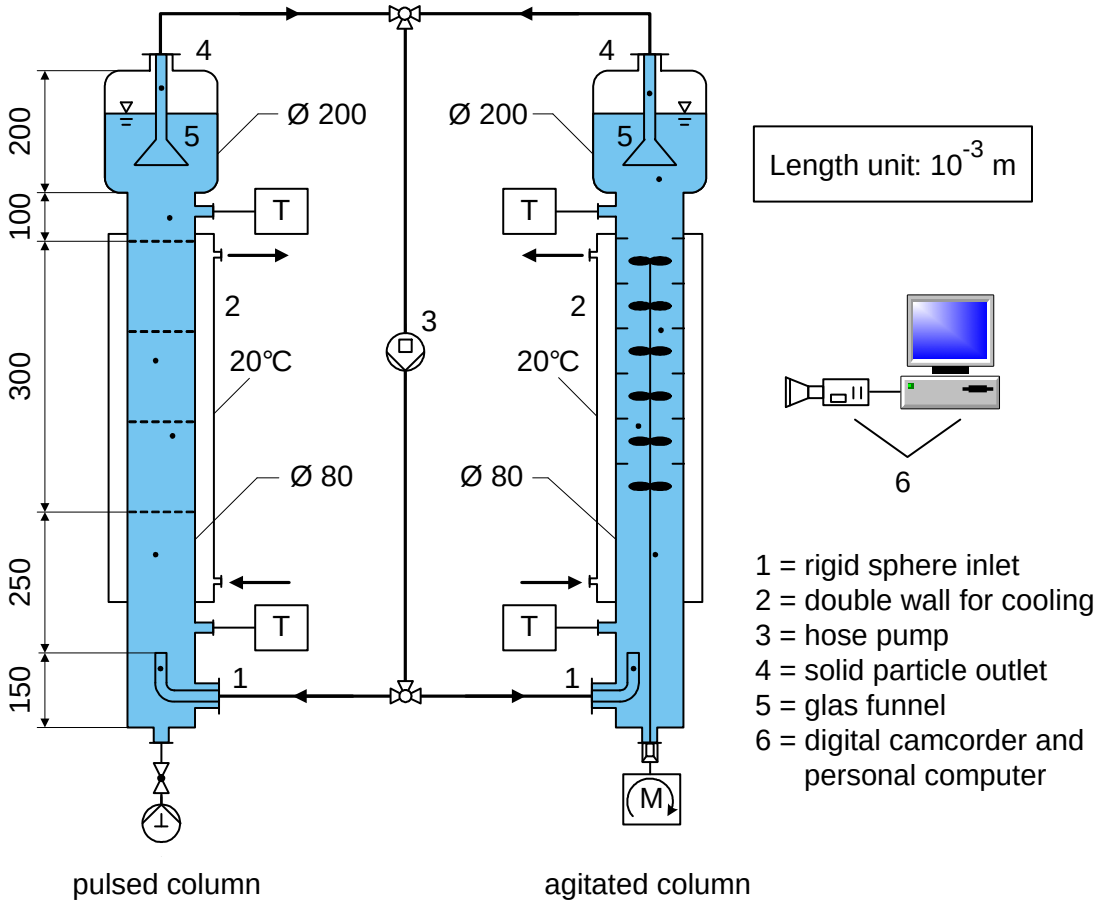

Figure 4.1: Single rigid sphere mini plant: pulsed and agitated column configuration and measuring technique

4.2 Single Drop Mini Plant

The experimental set-up of the single drop mini plant was very similar to the configuration of the single rigid sphere mini plant. Single drops were generated by a syringe system and small stainless steel capillaries and then dispersed in one of the two columns by the use of an eight-way valve, see *figure (4.2)*. Using this syringe system, drops with a diameter within 1 % deviation from the nominal diameter were generated by an impulse-type movement of the syringe plunger.

The investigation of single drops was carried out in a stationary water column maintained at 20°C. Several internals of the one type were installed inside the columns when the velocity of single drops was determined. The drop velocity was evaluated with a digital camcorder by averaging at least 50 single measurements for each drop size and operating mode.

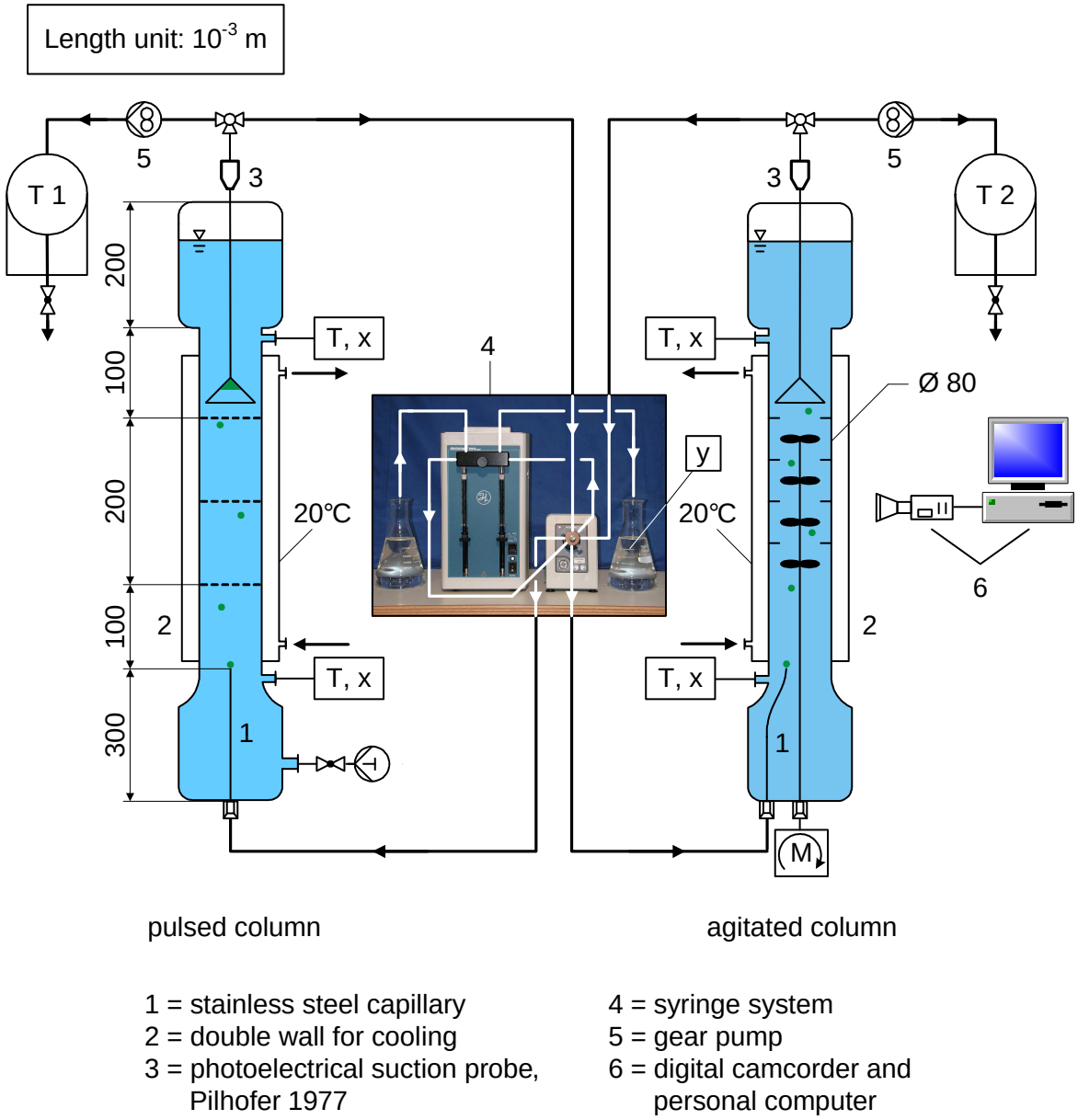

Figure 4.2: Single drop mini plant: pulsed and agitated column configuration; syringe system for the generation of single drops and measuring technique

In contrast, the investigation of single drop breakage was carried out in columns with only a single sieve tray, a single structured packing and either one or two agitators. The number of daughter drops produced was determined visually with or without the help of a digital camcorder. The size and size distribution of the daughter drops was measured by a photoelectrical suction probe developed by *Pilhofer 1977*. A schematic of a photoelectrical suction probe, which consists of a cylindrical glass capillary and a measuring device, is plotted in *figure (4.3)*. The measuring device consists of two lamps and two photo transistors. Drops are deformed into cylinders in the glass capillary. The length of the cylindrically deformed drops

l_d and their velocity is determined by the measuring device due to the different refractive indexes of organic and aqueous liquids. From knowledge of the diameter of the glass capillary d_{cap} and the length of a cylindrically deformed drop l_d, the diameter of a volumetric equivalent spherical drop can be determined.

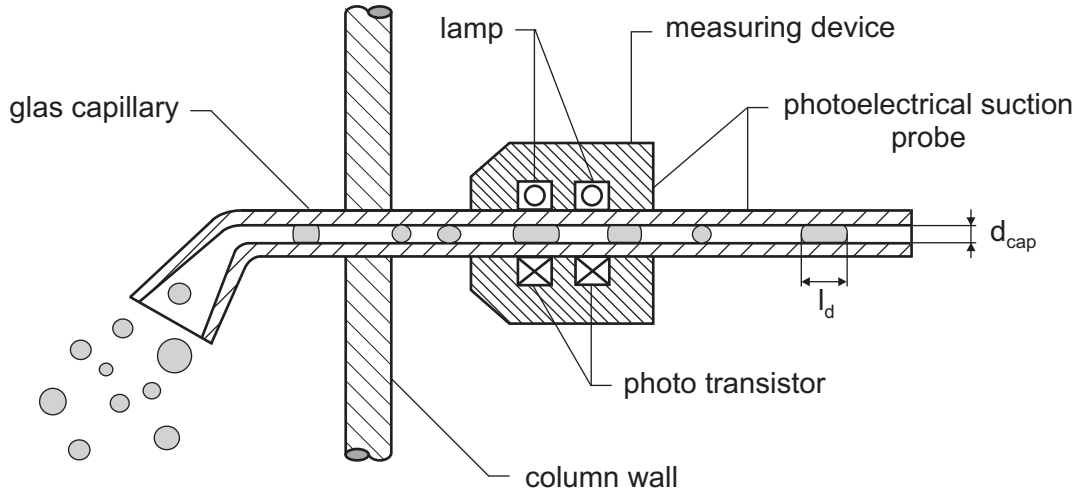

Figure 4.3: Photoelectrical suction probe to determine drop size distributions

For each experiment, the size of 1000 drops was measured to gain reliable results for drop size distribution and average daughter drop size. Furthermore, to obtain precise results for the drop size distribution, it was necessary to suck the two-phase mixture through the glass capillary at a constant flow rate. This was achieved by the use of a gear pump, see *figure (4.2)*.

Mass transfer rates of single drops were determined by evaluating the overall dispersed phase mass transfer coefficient β_{od}. For this purpose, the same measuring technique and the same set-up was used as by *Qi 1992*, see *chapter 2.3*. Mass transfer coefficients were determined by measuring the change of the drop concentration within a measuring section. The drop concentration at the start of the measuring section, which was 100 mm above the tip of the stainless steel capillary, was measured for each drop size before internals were installed inside the columns, see also *Wagner 1999*. Afterwards, the concentration of the drops was measured at the end of the measuring section with or without internals, which was 200 mm above the starting point, see *figure (4.2)*. The concentration of the continuous phase was continuously measured by two sample probes connected at a lower and an upper column section.

To correctly determine the drop concentration, it is important that the height of the coalesced drops in the glass funnel is as small as possible. The coalescence height was minimised by ensuring that the drops coalesced rapidly. For this purpose, a funnel was built that significantly

reduced the coalescence time by the use of a porous teflon filter. A technical sketch of the funnel is shown in *figure (4.4)*. After coalescence, the organic phase was evenly distributed along the teflon filter and built a thin liquid layer on the filter. A constant film thickness of the organic phase in the funnel was maintained during the experiments by continuously withdrawing the liquid film by the syringe system. After a sufficient number of drops was collected by the syringe system the concentration of the drops was analysed.

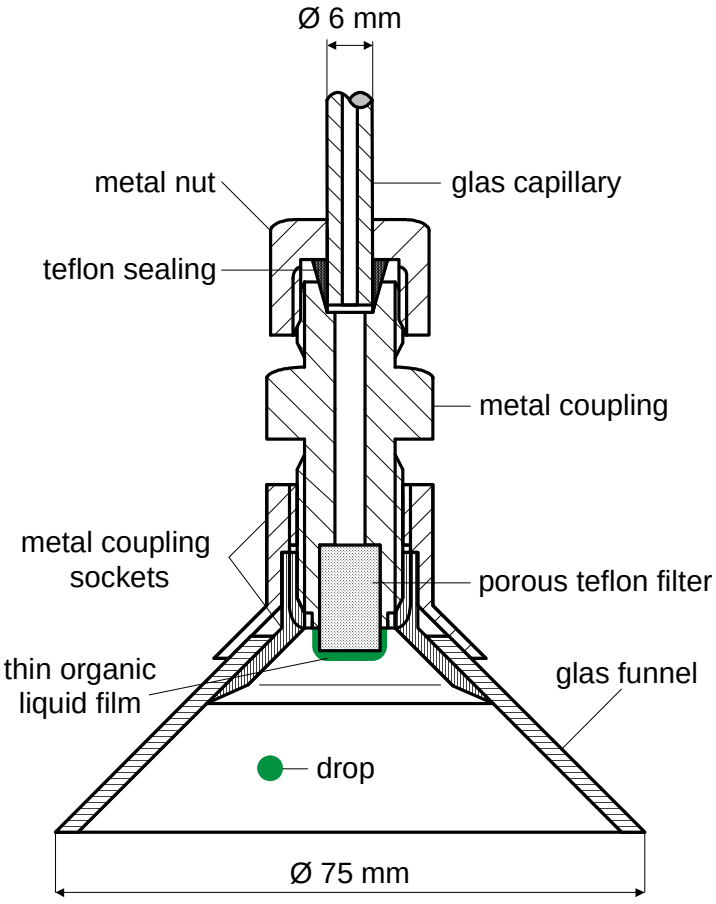

Figure 4.4: Scheme of the funnel for the extraction of single-phase drop samples (as material for the metal nut, the coupling and the coupling sockets stainless steel was used)

4.3 Rigid Sphere Swarm Extractor

The investigation of the influence of the particle concentration on the velocity of rigid spheres was carried out in an extraction column with a total height of 3.65 m and a diameter of 80 mm, see *figure (4.5)*. PP-spheres, see $\dot{V}_p$ in *figure (4.5)*, were transported from a particle/water-tank into the column by an eccentric screw pump. To prevent infiltration of air into the column the particle/water-tank was mixed by a stirrer and the two-phase mixture was withdrawn from the

tank beneath the water surface. The water $\dot{V}_{we}$ fed to the column via the screw pump exited the column immediately and did not flow co-currently upwards with the pp-spheres. This was proven by colour tracer experiments, which showed that the water stream $\dot{V}_{we}$ was carried out at the bottom of the column and did not flow into the active part of the column. The pp-spheres flowed up through the column due to their lower density. The rigid spheres were removed at the top of the column with a small water flux $\dot{V}_{wb}$ and then returned to the particle/water-tank.

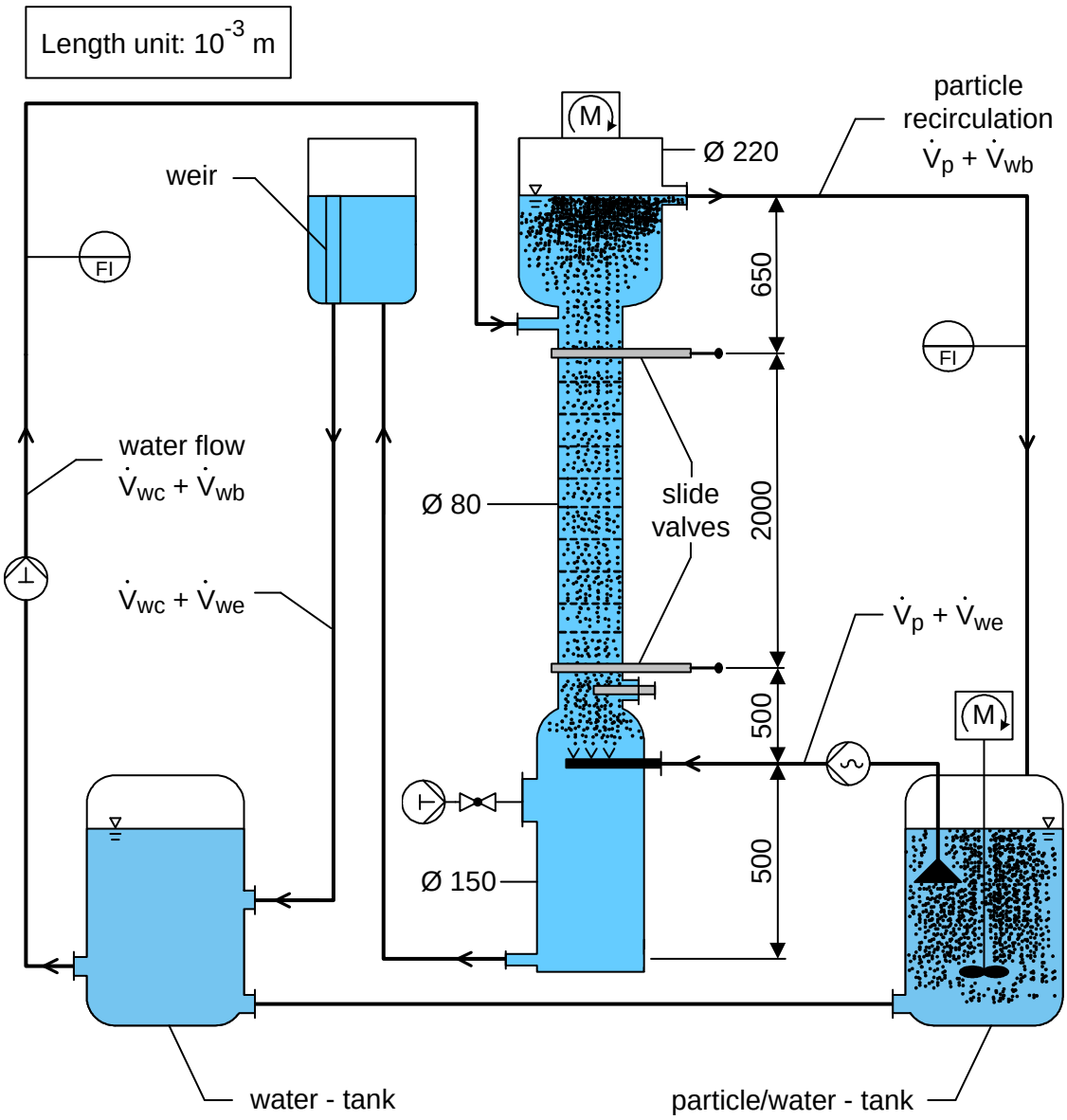

Figure 4.5: Pilot plant for the investigation of swarms of rigid spheres to determine the influence of particle concentration on fluiddynamics in different extractor types

The water that flowed counter currently to the particle phase in the column was pumped to the inlet above the active part of the column with a piston pump. A small portion $\dot{V}_{wb}$ of the total water pumped to the water inlet was used for removing the rigid spheres, while the main portion $\dot{V}_{wc}$ flowed downwards in the column, see *figure (4.5)*. Both liquid and particle flow rates $\dot{V}_{wc}$, $\dot{V}_{wb}$, $\dot{V}_{we}$ and $\dot{V}_p$ were continuously measured. This was achieved by temporarily diverting the flows to beakers and measuring the weight and volume collected in a certain time interval. Steady state conditions were reached when all volume flows remained constant for an hour. The liquid level in the column was controlled by a weir.

The hold-up of rigid spheres within the active part of the column was determined using two slide valves. The slide valves were pneumatically opened and closed. After both valves were closed, the spheres accumulated beneath the upper valve. By determining the height of the particle bed beneath the upper valve H_{pb}, the hold-up h_d within the active part of the column was calculated by:

$$h_d = \frac{H_{pb} \cdot h_{pb}}{H_{ac}} \quad \text{where} \quad H_{ac} = 2000\ mm \tag{4.1}$$

Here, H_{ac} is the active height of the column and h_{pb} is the volume fraction of the spheres within the densely packed bed, which is known from preliminary tests. The special design of the closing plates inside the valves allowed the rigid pp-spheres to be held back but not the water phase. Thereby, the entire quantity of particles within the active column section could be transported under the upper slide valve with the help of a pulsator or agitators. *Figure (A.4)* in the appendix illustrates the various closing plates used to determine the hold-up, see *chapter A*. Although PVC, aluminium and silicon were used as construction materials, only chemically resistant materials were used for all other column elements. For the single drop mini plant and the drop swarm extractor, which will be introduced in the following section, only teflon, glass and stainless steel were used for all column parts which contacted the liquids.

4.4 Drop Swarm Extractor

The influence of hold-up on fluiddynamics and mass transfer of drop swarms was investigated in the extractor illustrated in *figure (4.6)*. A scheme of the entire extraction plant including the distillation column for the regeneration of the solvent is given in the appendix, see *chapter A*. Pulsed and agitated experiments were carried out in the extractor with different types of column

internals such as sieve trays, structured packings and different types of agitators. In all experiments the organic phase was dispersed beneath the active part of the column with a cylindrical finger distributor (4 rows each with 12 holes, hole diameter = 1 mm). The dispersed phase left the column at the top after the drops coalesced at the principal interface in the upper settling zone. The water phase flowed counter currently downwards. The flow rates of both liquid phases were determined with pump calibration curves and controlled by flow meters. Both phases were cooled to a temperature of 20°C before entering the column. To control the temperature of the liquids, the temperature of the inlet and outlet of each phase as well as the temperature profile within the column was recorded.

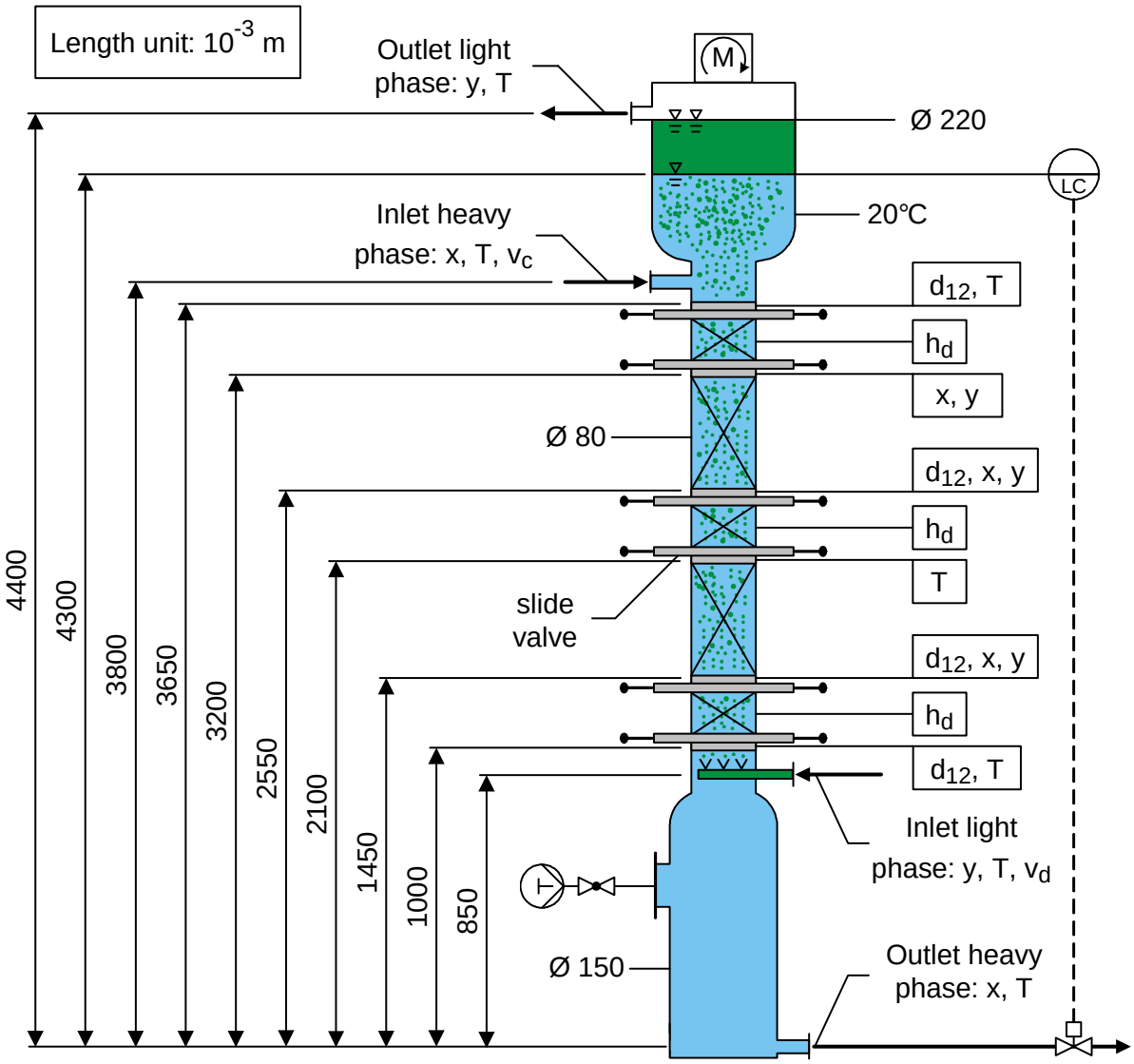

Figure 4.6: Pilot plant extractor for the investigation of drop swarms to evaluate the influence of drop concentration on fluiddynamics and mass transfer rates

The size distribution of the drops was measured immediately above the inlet of the dispersed phase and at three positions within the active part of the column by photoelectrical suction probes. Each photoelectrical suction probe performed at least 1000 single drop measurements to determine the size distribution, see *chapter 4.2*. The hold-up was determined by a similar procedure as in the rigid sphere swarm extractor, using three pairs of stainless steel slide valves and teflon closing plates inside the valves. The use of pneumatic double stroke cylinders permitted the simultaneous measuring of the hold-up in three different column sections, each with a length of 300 mm. Photos of the teflon closing plates can be found in the appendix, see *chapter A.*

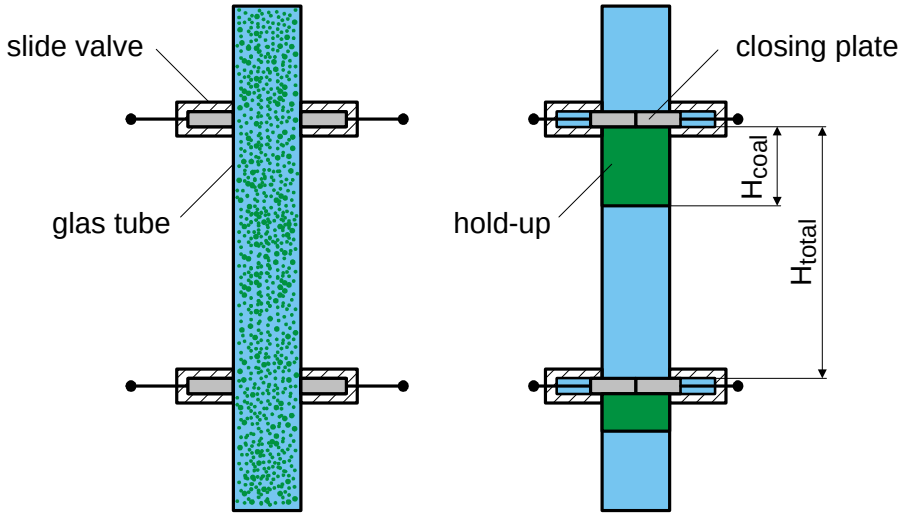

Figure 4.7: Slide valves for the determination of the hold-up within a measuring section of $H_{total} = 300\ mm$

After simultaneously closing all valves, the rising drops coalesce underneath the upper valve. Measuring the height of coalescence H_{coal} allows the determination of the hold-up, see *figure (4.7)*. The hold-up within a certain column section is then given by:

$$h_d = \frac{H_{coal}}{H_{total}} \quad \text{where} \quad H_{total} = 300\ mm \tag{4.2}$$

The advantage of this measuring technique is that no time-consuming calibration of the measuring system is necessary. In addition, this technique provides very accurate results for both pulsed and agitated extractors. A disadvantage of this technique is that all phase inlets have to be shut after the valves are closed. Thus, experiments have to be interrupted until the column once again reaches steady state conditions. Preliminary tests revealed that a steady state was

reached for all types of column configurations after a minimum of five column volumes was replaced.

The concentration of the solute in the continuous and the dispersed phase was determined at the phase inlets and outlets as well as at three positions within the column. To obtain single-phase samples from the two-phase mixture, measuring probes with cylindrical porous filter elements were used, see *figure (4.8)*. Due to the different wettability of teflon and stainless steel, single-phase samples could be obtained by adjusting the filter element material and by low suction flow rates. The advantage of the cylindrical form is that the whole filter is always wetted with one liquid (organic or aqueous) independent of the type of column and operating mode. In this way, single-phase samples are obtained in columns even at high levels of energy input, for instance, in Kühni-extractors with high rotational speeds.

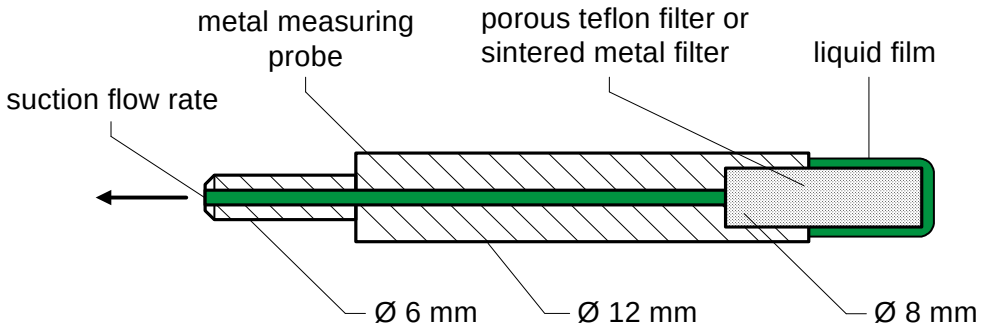

Figure 4.8: Measuring probe for different porous filter elements to obtain single-phase concentration samples within the two-phase flow (porous teflon filter elements are preferentially wetted by organic liquids while sintered stainless steel filter elements are preferentially wetted by water)

4.5 Internals

In the mini plants and the swarm extractors, four different types of internals were installed. For pulsed experiments, different types of sieve trays and a structured packing (Montz-Pak B1-350) were used. The investigations in agitated columns were carried out with two different types of agitators: rotating discs and Kühni blade agitators. The agitated compartments (height = 50 mm, relative free cross-sectional stator area = 40 %) were the same for both types of agitators. *Figure (4.9)* illustrates the compartments that were installed inside the columns. Geometric data of the internals are listed in *table (A.1)* in the appendix, see *chapter A*.

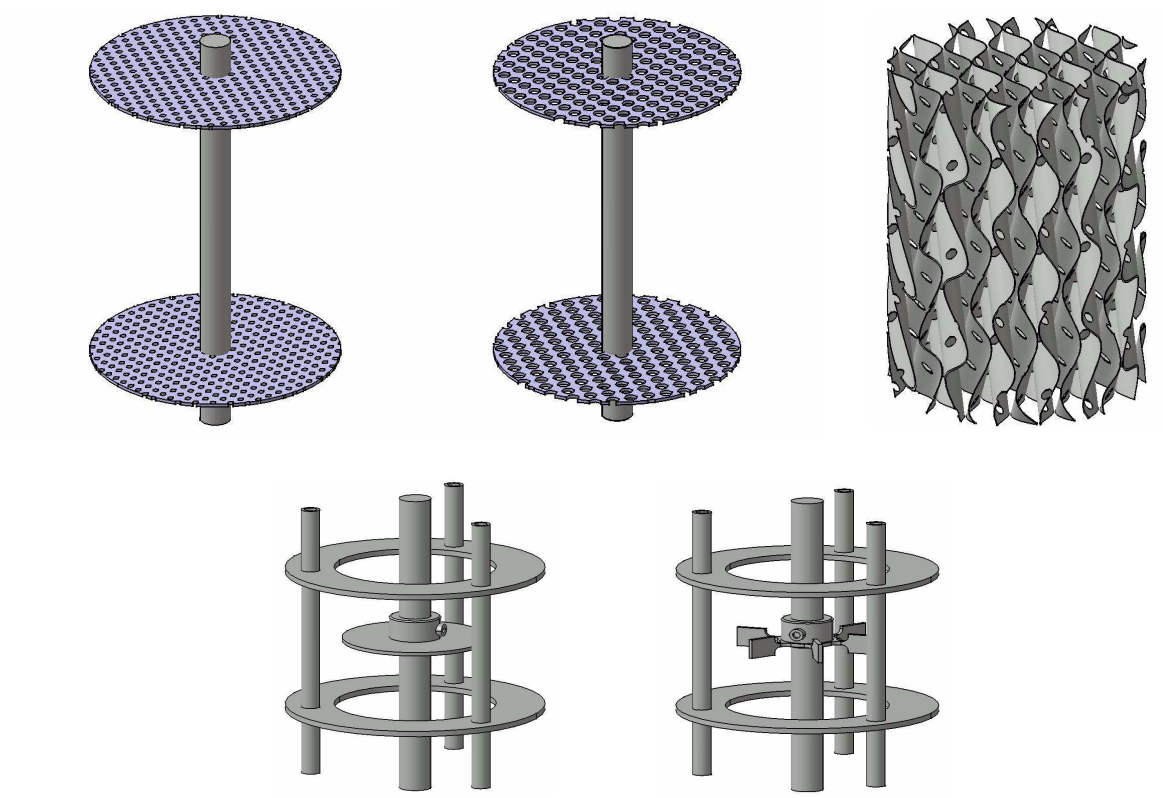

Figure 4.9: Various compartments that were installed inside the columns; top row (from left to right): sieve tray - d_h = 2 mm, sieve tray - d_h = 4 mm, Montz-Pak B1-350, second row (from left to right): RDC-compartment, Kühni-compartment

4.6 Determination of Phase Concentrations

The analysis of the composition of both liquid phases was carried out by three different methods. While only refraction and titration methods were used to control the acetone concentration of the feed mixtures for the experiments, gas chromatography was applied for determining the concentration of all components in the experimental samples.

- *Gas chromatography*

In all runs the samples were analysed in a gas chromatograph (Hewlett-Packard gas chromatograph of the type 6890 in combination with a Pora-Plot-Q capillary column). The capillary column had a length of 25 m, an inner diameter of 0.32 mm, an outer diameter of 0.45 mm and a coated film thickness of 10 µm. A thermal conductivity detector (TCD) and helium as the carrier gas were used. For calibration, samples with known compositions were prepared. Furthermore, quality of the calibration curve was checked by three control samples.

Each experimental sample was analysed three times and the results were only accepted if all measurements did not significantly differ. For a certain operating condition during single drop experiments, three samples with a total volume of 1 ml per sample were taken to determine the drop concentration. For example, for a drop with a diameter of 2 mm, the average concentration of approximately 230 drops per sample was measured since the volume of a 2 mm drop is 4.2 µl. Thus, 690 drops ($3\ samples \times 230\ drops$) per experiment were analysed. The concentration of the dispersed and continuous phase in the drop swarm extractor was evaluated with two samples at each measuring point, which were successively extracted in a short time interval. There were three measuring points for each phase within the active part of the column and one measuring point at the inlets and outlets of both phases. Thus, 10×2 samples were taken in each experimental run.

The advantage of gas chromatography is that all substances in a multi-component mixture can be detected with a very high degree of accuracy. The disadvantage is that the calibration and the measurements are time-consuming.

- *Titration*

Due to the long time required for the analysis by gas chromatography, other measuring techniques were used to determine the concentration of acetone in the feed mixtures. The analysis of the aqueous feed mixtures was carried out by titration (Mettler Toledo titrator of the type DL 20). Acetone was converted with hydroxyl ammonium chloride into an oxime and equivalently converted into hydrochloric acid. The hydrochloric acid was subsequently titrated with 0.1 N NaOH. Through neutralisation of the hydrochloric acid, the concentration of acetone was found from the quantity of 0.1 N NaOH consumed.

- *Refractometry*

The concentration of acetone in the organic and aqueous feed mixtures was additionally assessed by refractometry. A digital refractometer (Mettler Toledo refractometer of the type RE 40) was used with a refractive index metering range from n_D = 1.32 to 1.70. The wave length of the light source was $\lambda_{ls} = 635 \cdot 10^{-9} m$ and the required minimum volume of a sample was $V_{sv} = 0.25\ ml$. The probe chamber could be sealed to prevent any change of the composition by evaporation of the volatile components. The temperature inside the chamber

could be controlled with a precision of $\Delta T = \pm 0.1\,°C$ while the deviation of the refractive index was given by $\Delta n_D = \pm 1 \cdot 10^{-4}$. The advantage of this method is that only small amounts of liquids are necessary and results are obtained quickly. The disadvantage of this method is that reliable results are only obtained for binary mixtures. Because the liquid/liquid-systems used for the experiments have a wide miscibility gap, especially for a weight concentration of acetone from 0 to 6 %, mixtures could be treated as binary mixtures. Thus, the acetone concentration was determined using the refractive index and calibration curves for both liquid/liquid-systems.

It should be emphasised that the exact determination of component concentrations was always carried out by gas chromatography. Only the acetone concentration in the feed mixtures was controlled by titration and refractometry.

5 Terminal and Characteristic Velocities of Single Particles

Knowledge of the velocity of single particles plays a decisive role in modelling the fluiddynamics and mass transfer rates of extractors, particularly by the use of drop population balance models. The evaluation of the velocity of single particles is the basis for determining the relative swarm velocity and the effective phase velocity. Consequently, it allows the prediction of the hold-up, the residence time of both phases and the mass transfer rates.

5.1 Terminal Velocity

While the velocity of single rigid spheres in columns without internals, which means the terminal velocity, is well known, the prediction of the terminal velocity of drops is still associated with some uncertainties. This is due to the fact that the influence of the mobility of the drop surface and the influence of the mass transfer are only qualitatively understood. Investigations with single rigid polypropylene-spheres (pp-spheres), toluene drops and butyl acetate drops were conducted to determine the effect of circulations within a drop on terminal velocities. In addition, the behaviour of drops with oscillations and deformations was experimentally examined.[1]

The experimental results for the terminal velocity of rigid spheres and drops are illustrated in *figure (5.1)* in dimensionless form. It is obvious that toluene and butyl acetate drops move faster than pp-spheres within a wide range of particle sizes. This difference must be related to the mobility of the drop surface, which causes a lower flow resistance. Furthermore, it can be seen that butyl acetate drops have higher terminal velocities than toluene drops in the range of the dimensionless diameter from $\pi_d = 16$ *to* 40. This must be due to the higher degree of circulations within the butyl acetate drops. Obviously, the formation of circulations within a drop is influenced by the interfacial tension, which is significantly lower for butyl acetate (d)/ water than for toluene (d)/water.

As an additional effect of the lower interfacial tension of the butyl acetate (d)/water system, butyl acetate drops lose their form stability at smaller drop sizes than toluene drops. Thus, butyl acetate drops reach their maximum terminal velocity at a drop size of $\pi_d = 36$ *(i. e.* d = 3.5 mm)

1. It should be noted that the symbols in the figures in this chapter as well as in the following chapters present own experimental data. Whenever data from the literature is used, this is explicitly stated.

while toluene drops reach their maximum terminal velocity at a drop size of $\pi_d = 64$ *(i. e.* d = 6.0 mm), see *figure (5.1)*.[2]

Although the prediction of the terminal velocity with published correlations is associated with deviations, particularly for butyl acetate drops, the model of *Henschke 2003* (see *chapter 2.2*) shows a good agreement with the own experimental data. Moreover, the model accurately describes the change from rigid to circulating drop behaviour and from circulating to oscillating drop behaviour, see *figure (5.1)*.

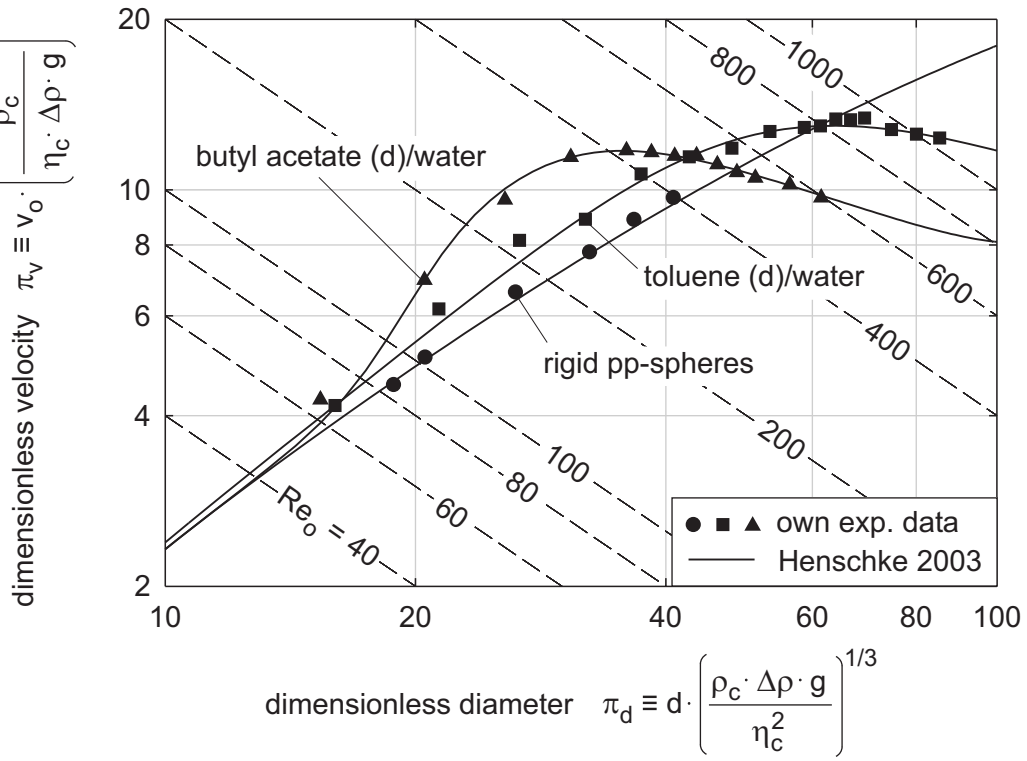

Figure 5.1: Terminal velocity of single rigid pp-spheres, toluene and butyl acetate drops

In addition to the mobility of the drop surface, the mass transfer influences the terminal velocities of single drops. During mass transfer, Marangoni convections and eruptions are generally produced at the drop surface. Due to these eruptions, the circulations within the drops are suppressed so that they move slower than without mass transfer. In the experiments, the influence of mass transfer on the motion of both single toluene and butyl acetate drops was observed. The Marangoni convections caused a distinct reduction of the terminal velocity of

2. It should be noted that also the dynamic viscosity of the drops influences the terminal velocities. The higher the dynamic viscosity is the more the drops behave like rigid spheres due to the suppression of circulations within the drops. Since the liquid/liquid-systems used have a similar dynamic viscosity, the influence on terminal velocities could not be determined. Information about the influence of the dynamic viscosity on the terminal velocity can be found in *Brauer 1971*, *Clift et al. 1978* and *Wagner 1999*.

toluene drops, see *figure (5.2)*. For mass transfer from the continuous to the dispersed phase (c to d) and for the reverse direction (d to c) a maximum reduction of 3 cm/s was found for a drop diameter of 4 mm. Furthermore, it could be observed that the direction of mass transfer did not influence the terminal velocities of toluene drops.

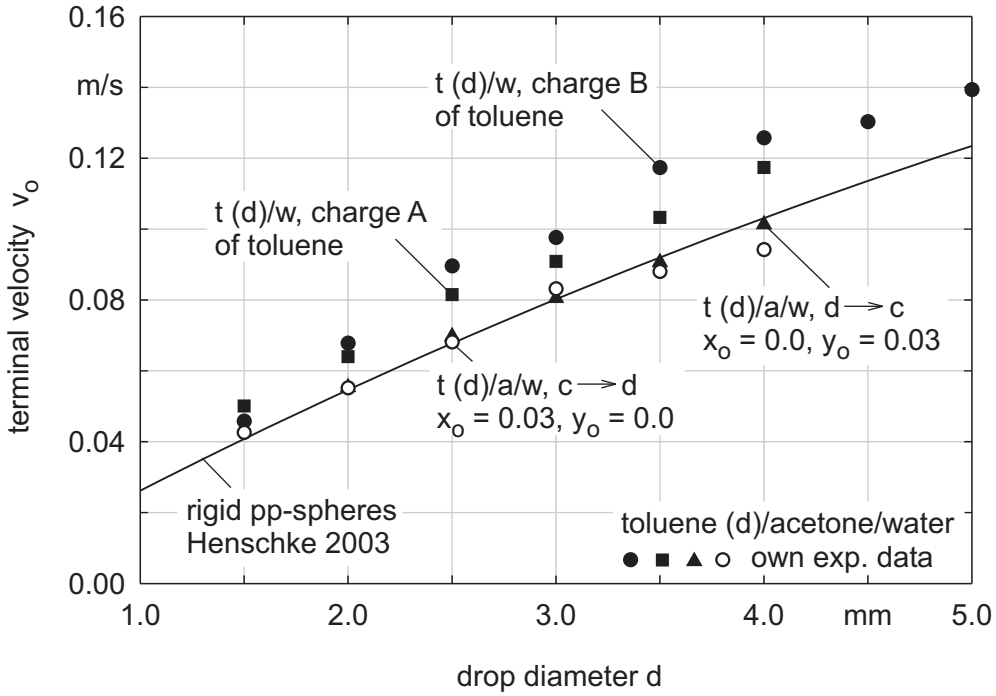

Figure 5.2: Influence of mass transfer on the terminal velocity of single toluene drops and comparison of their velocities with rigid pp-spheres (see figure (5.1)); mass transfer of toluene drops was always studied with toluene of charge A

In contrast, the terminal velocities of butyl acetate drops were lower for mass transfer from "*d to c*" than for the reverse direction "*c to d*" for the same initial concentration difference, see *figure (5.3)*. Only an increase of the initial concentration difference to $x_o - y_o = 6$ *wt.-%* for mass transfer from "*c to d*" resulted in terminal velocities similar to that for an initial concentration difference of $y_o - x_o = 3$ *wt.-%* for the reverse direction "*d to c*". Thus, the effects of Marangoni convections and eruptions at the interface on the terminal velocities do not only depend on the physical properties of the system and the concentration difference. Additionally, they depend on the mass transfer direction. This is confirmed by the results of *Wolf 1999*, who investigated the generation of Marangoni convections for several liquid/liquid-systems.

Although experimental results of different groups (*Thorsen et al. 1968, Hoting 1996, Henschke 2003, etc.*) prove that mass transfer reduces the terminal velocity, a quantitative prediction of this influence is not yet possible. Therefore, further investigations must be carried out to clarify the influence of mass transfer on the terminal velocities of single drops.

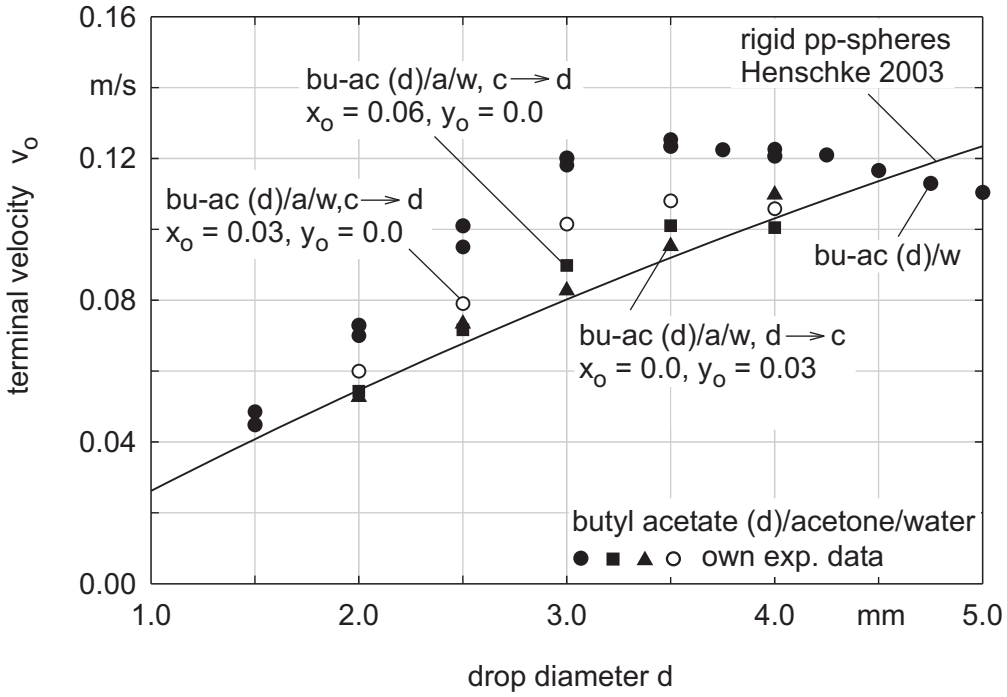

Figure 5.3: Influence of mass transfer and mass transfer direction on the terminal velocity of single butyl acetate drops

A further interesting result is that different terminal velocities were found for toluene drops for two different charges of toluene (charge A and B). For both experimental runs, toluene of the same quality (quality: *pro analysis*) but from different companies was used. Although no difference in the physical properties could be detected in the laboratory or by settling time measurements for the liquid/liquid-systems, drops of charge A had lower terminal velocities than drops of charge B, see *figure (5.2)*. This effect may be attributed to small amounts of impurities in charge A, which affected the development of circulations within the toluene drops. Experiments with different charges of butyl acetate did not show any notable deviations of terminal velocities, as can be seen in *figure (5.3)*.

- *Single particle velocity in pulsed columns without internals*

The velocity of a single rigid sphere or drop in a pulsed column without internals is lower than the terminal velocity. This reduction is attributed to the steady change of flow around the particle. The permanent acceleration and deceleration of the particle is associated with a higher flow resistance than in a column without pulsation. Thus, increased pulsation intensity results in higher transfer of shearing stresses and friction forces at the particle interface. This effect was

studied in detail by *Molinier 1976* and *Haverland 1988*. According to Haverland the velocity of a drop is reduced to 95 % of the terminal velocity for a drop diameter of d = 3 mm for pulsation intensities in the range of $a \cdot f = 0 - 2.5$ *cm/s*. The ratio of the velocity of a single drop in a pulsed liquid $v_{o,\,pulsed}$ to its terminal velocity v_o is well described by Haverland's correlation:

$$\frac{v_{o,\,pulsed}}{v_o} = 1 - 59.9 \cdot a^{0.91} \cdot f^{1.90} \cdot d^{0.85} \qquad (5.1)$$

The own experiments confirm this correlation, see *figure (5.4)*. Furthermore, it can be seen that the influence of the pulsation intensity is slightly larger on drops than on rigid pp-spheres. The larger impact of the pulsation intensity on the drop velocities seems to be a consequence of the disturbance and suppression of circulations within the drops.

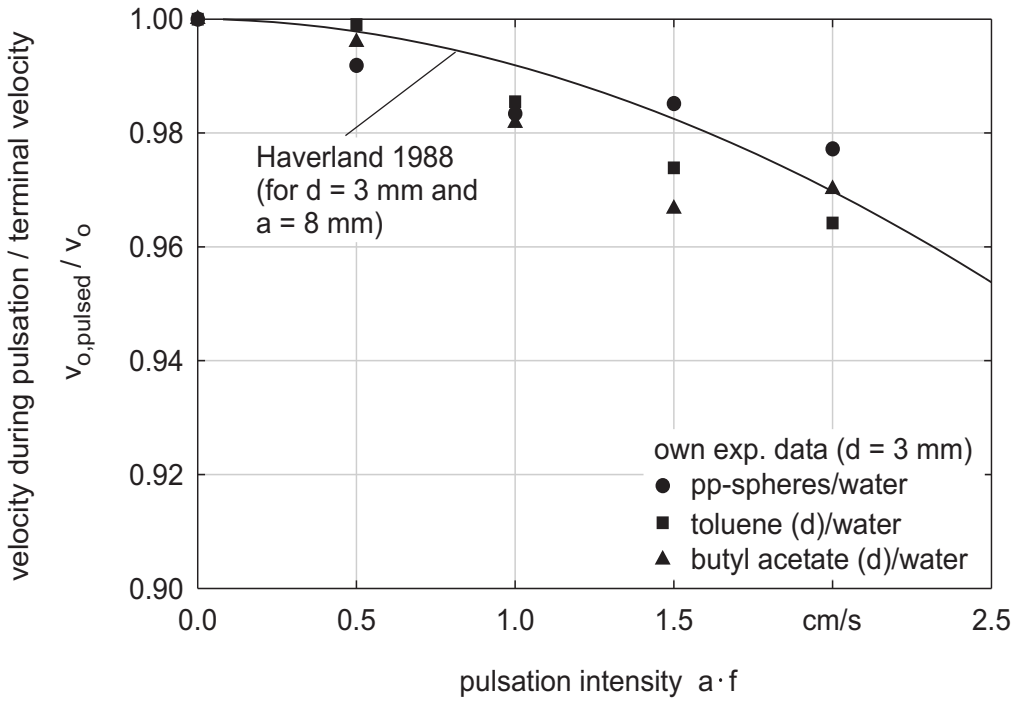

Figure 5.4: Effect of pulsation intensity on the velocities of rigid spheres and drops in columns without internals; comparison of own experiments with Haverland's correlation

5.2 Characteristic Velocity in Pulsed Columns with Sieve Trays

While the influence of the pulsation intensity on the particle velocity in columns without internals is relatively small, internals in pulsed and agitated columns strongly influence the single particle velocities, i. e. the characteristic velocities. The characteristic velocities in columns with different internals was studied with and without superimposed mass transfer. In absence of mass transfer, four sieve trays, three structured packings or six agitated compartments were installed inside the laboratory scale columns. In presence of mass transfer, three sieve trays, two structured packings or four agitated compartments were used.

Single particles in pulsed sieve tray columns show significantly lower velocities than in columns without internals. This is due to the steady collisions of the particles with the sieve trays. Thus, the characteristic velocities of toluene drops with a diameter from 1.5 to 4.0 mm reach values from 4.2 to 7.8 cm/s, which are significantly lower than the values of their terminal velocities, compare *figure (5.5)* with *figure (5.2)*.

An important parameter for the characteristic velocities in sieve tray compartments is the diameter of the drops. However, a change of the pulsation intensity from $a \cdot f$ = 0.5 to 2.0 cm/s has no significant effect. This is also proven by the results with rigid pp-spheres, see *figure (5.5)*.

Rigid pp-spheres have lower characteristic velocities than toluene drops. This is due to the lower velocities of the single pp-spheres in the free sections between the sieve trays. For this reason, the differences of the characteristic velocities between single toluene drops and single rigid spheres are similar to the differences of their terminal velocities.

Figure (5.6) shows the influence of the particle diameter on the ratio of the characteristic velocity of a single particle in pulsed sieve tray compartments to its terminal velocity $v_{char,o} / v_o$. Although the absolute values of the characteristic velocities of rigid pp-spheres, toluene drops and butyl acetate drops differ, the influence of the sieve trays on the velocity ratio $v_{char,o} / v_o$ is almost the same. For all binary test systems the velocity ratio is reduced to a value of 0.6 for particle diameters from 1.5 to 4.0 mm.

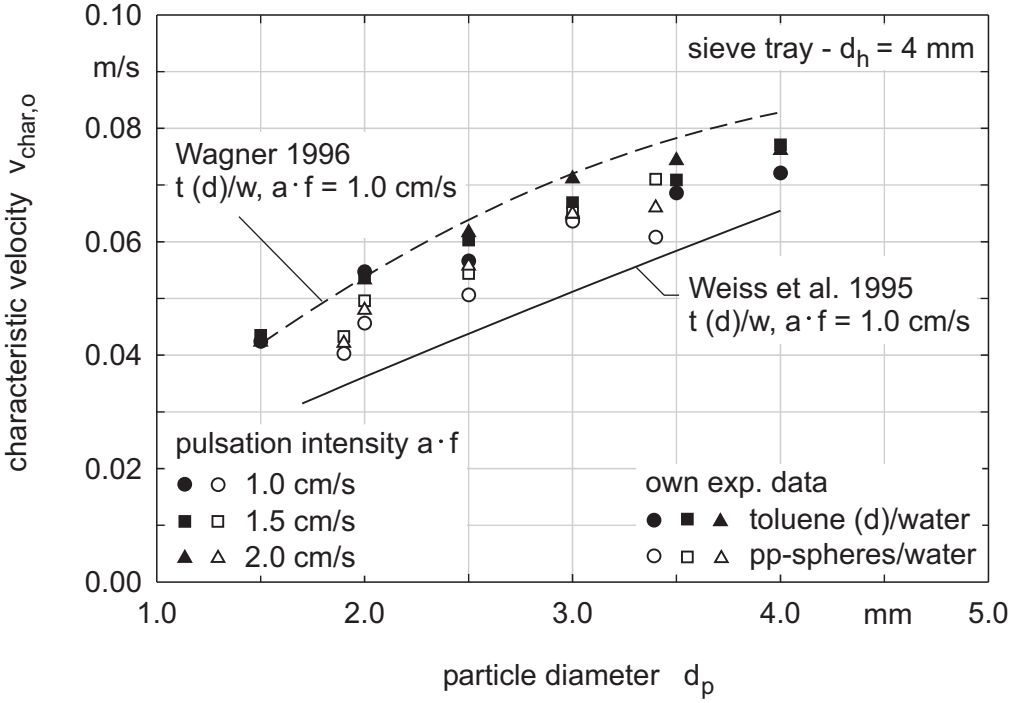

Figure 5.5: Characteristic velocities of single pp-spheres and single toluene drops in pulsed sieve tray compartments; comparison of the characteristic velocities of toluene drops with correlations from the literature

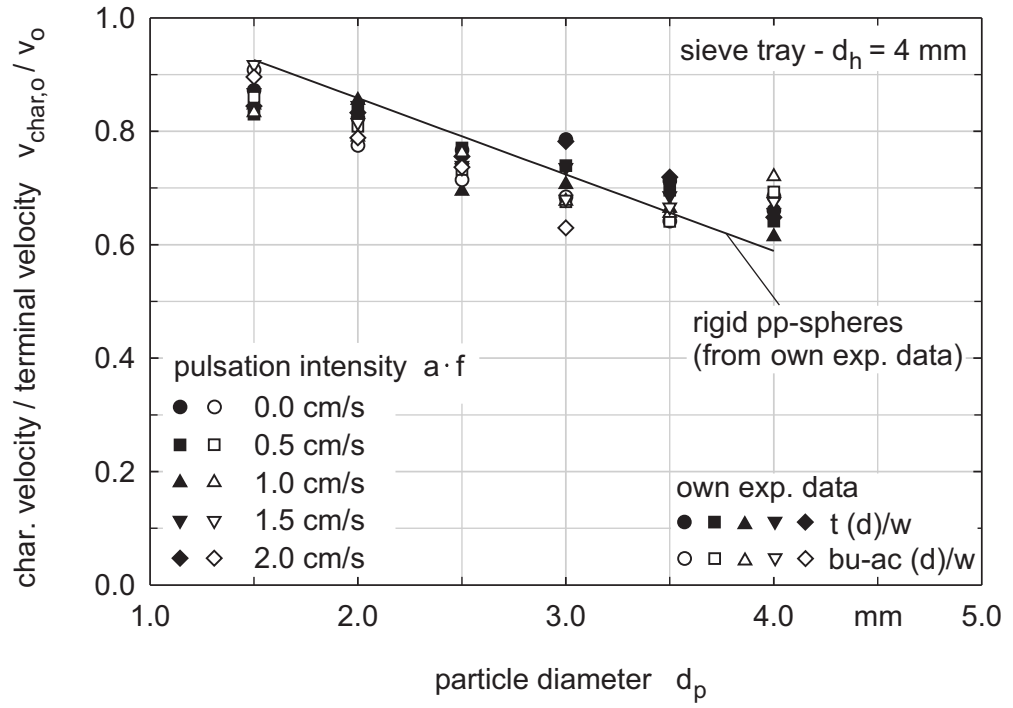

Figure 5.6: Influence of physical properties of the test systems on the reduction of the characteristic velocity of single particles in pulsed sieve tray compartments in reference to their terminal velocity

The characteristic velocities in pulsed compartments with different types of sieve trays reveal that the velocity ratio $v_{char,o}/v_o$ is not only determined by the particle diameter, but also by the ratio of the particle diameter to the hole diameter of the sieve trays d/d_h. To illustrate this, the experimental results for sieve trays with a hole diameter of 2 mm and 4 mm are depicted in *figure (5.7)* for a pulsation intensity of 1.0 cm/s. The ratio $v_{char,o}/v_o$ shows a continuous decrease for an increasing diameter ratio d/d_h. The strong influence of the diameter ratio d/d_h on the characteristic velocity is affirmed by the results of *Wagner 1999*, see also *table (2.1)*.

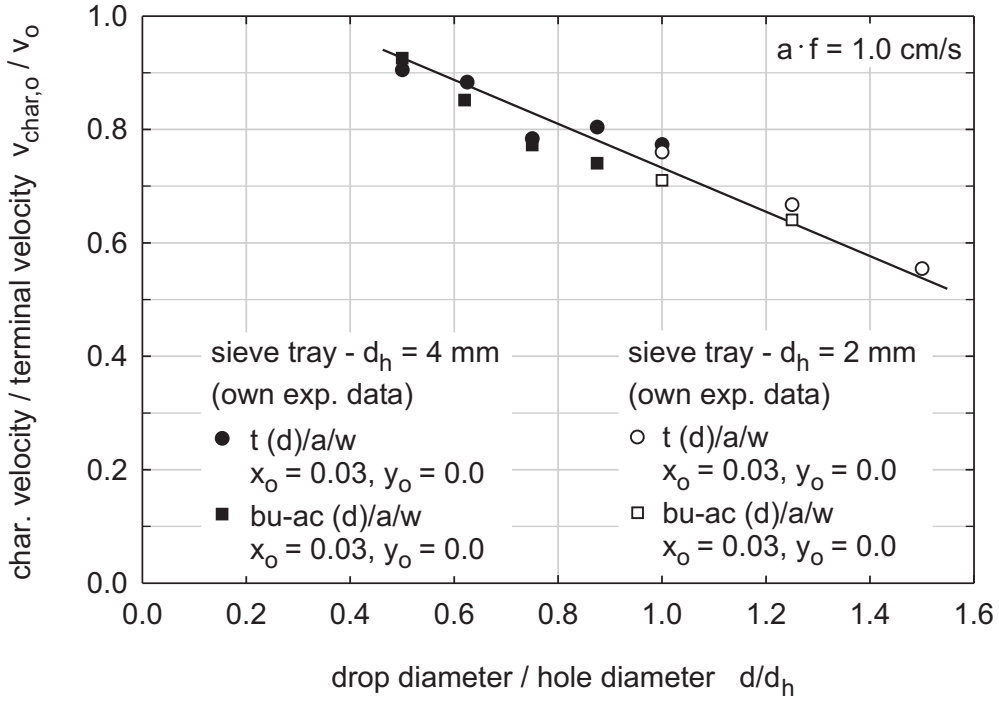

Figure 5.7: Influence of the diameter ratio d/d_h on the velocity ratio $v_{char,o}/v_o$ of single drops in compartments with different sieve trays

The influence of sieve trays on the characteristic velocity $v_{char,o}$ is very similar for all test systems. Same characteristic velocities are determined for drops with and without superimposed mass transfer. However, since the terminal velocity v_o is lower in presence of mass transfer, some deviations of the ratio $v_{char,o}/v_o$ are seen. Higher values of the ratio $v_{char,o}/v_o$ result for mass transfer than without mass transfer, see *figure (5.8)*. An accurate model to predict the velocity ratio $v_{char,o}/v_o$ has to take this interrelationship into account.

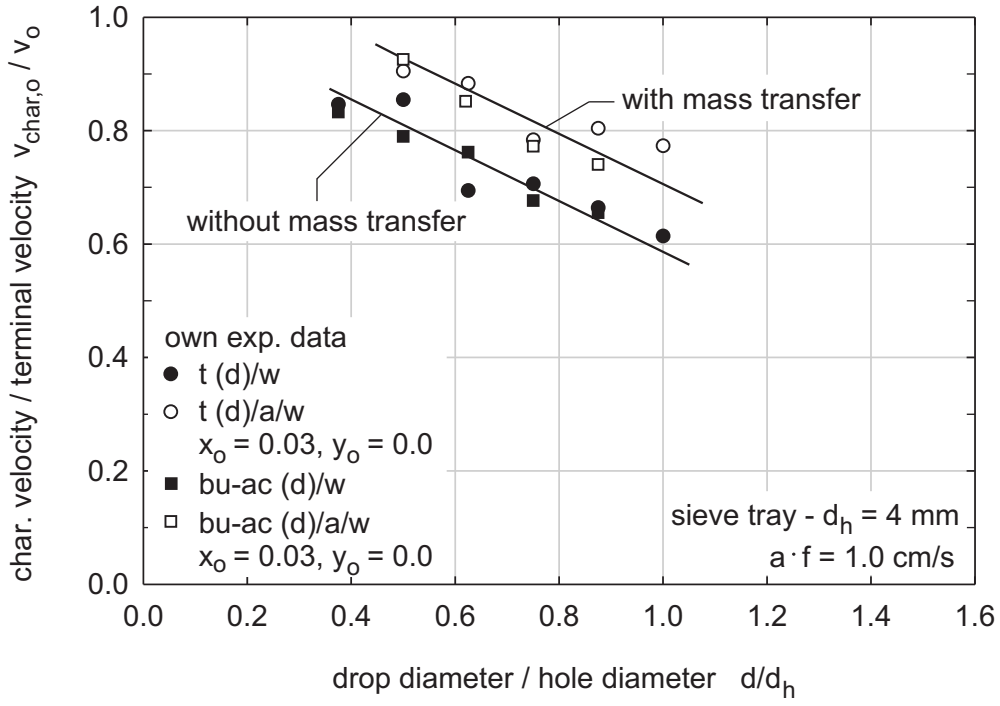

Figure 5.8: Influence of mass transfer on the velocity ratio $v_{char,o} / v_o$ of toluene and butyl acetate drops in pulsed sieve tray compartments

The characteristic velocities of single drops in pulsed sieve tray columns are often evaluated with correlations that do not account for all relevant parameters. For instance, the correlation of *Weiss et. al 1995* includes neither the ratio of the diameters d/d_h nor other geometrical parameters of the sieve trays, see *chapter 2.2*. Consequently, it predicts characteristic velocities which significantly differ from the experimental values, see *figure (5.5)*. The equation of *Wagner 1999*, see also *chapter 2.2*, takes the influence of the diameter ratio d/d_h into account. However, in this equation the characteristic velocities of the drops are determined independently of the relative free cross-sectional area of the plates. Thus, Wagner's equation predicts values of the characteristic velocity that are too high, particularly for larger drop sizes. The influence of mass transfer on the velocity in pulsed sieve tray compartments is not taken into account by either correlation.

Based on the analysis of experimental results, a new correlation was developed which includes the diameter ratio d/d_h, the relative free cross-sectional area φ_{st} and a modified dimensionless liquid number. The ratio of the velocities $v_{char,o}/v_o$ is given by:

$$\frac{v_{char,o}}{v_o} = 1.406 \cdot \varphi_{st}^{0.145} \cdot \pi_\sigma^{-0.028} \cdot exp\left[-0.129 \cdot \left(\frac{d}{d_h}\right)^{1.134} \cdot (1-\varphi_{st})^{-2.161}\right] \qquad (5.2)$$

where π_σ is the dimensionless interfacial tension: $\pi_\sigma = \sigma \cdot \left(\frac{\rho_c^2}{\eta_c^4 \cdot \Delta\rho \cdot g} \right)^{1/3}$

The correspondence between own experiments and experimental data from *Qi 1992* and *Wagner 1999* with the new correlation is shown in *figure (5.9)*. The new correlation agrees very well with the experimental data for different liquid/liquid-systems, sieve trays, mass transfer conditions and a wide range of pulsation intensities and drop sizes. The comparison of *equation (5.2)* with 152 data points results in a relative error of 5.8 %.

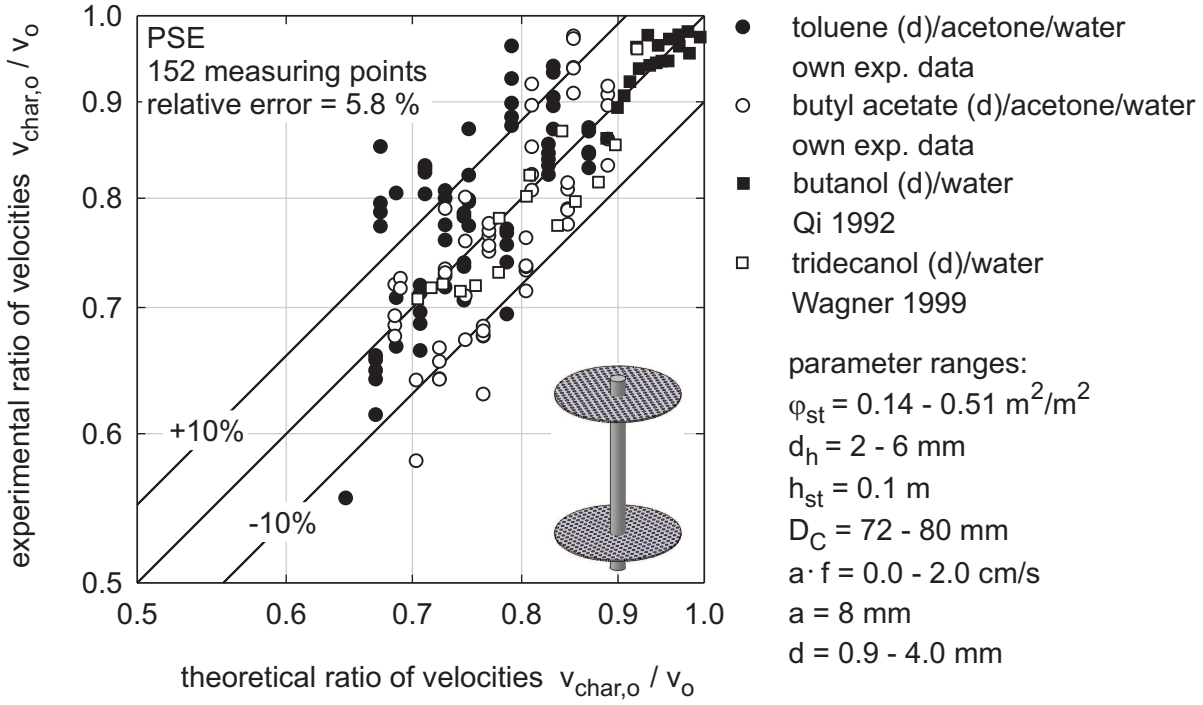

Figure 5.9: Comparison of the predicted velocity ratio from equation (5.2) with experimental values for the velocity ratio $v_{char,o} / v_o$ of single drops in pulsed sieve tray compartments

Despite the good correspondence with experimental data it was not possible to determine the influence of the compartment height h_{st}. This was due to the fact that no experimental data was found in the literature for the same sieve tray geometry and different compartment heights. Smaller compartment heights are associated with lower characteristic velocities due to increased hindrance of the drops. Investigations with different compartment heights are recommended to develop a correlation which is even more generally applicable than *equation (5.2)*.

5.3 Characteristic Velocity in Pulsed Columns with Structured Packings

The characteristic velocities of single particles in pulsed extractors with structured packings are lower than the terminal velocities due to the steady collisions of the drops with the packings. In addition, the increased length of the path due to the inclined channels of the packings causes a significant velocity reduction. The results of the investigations of the characteristic velocities in pulsed compartments with structured packings show that particles move much slower than in columns without internals. It is also obvious that the characteristic velocity of single particles is nearly independent of the particle diameter, see *figure (5.10)*. This means that compared to their terminal velocities, particles are increasingly slowed down by the packings with increasing diameter, see also *figure (5.2)*.

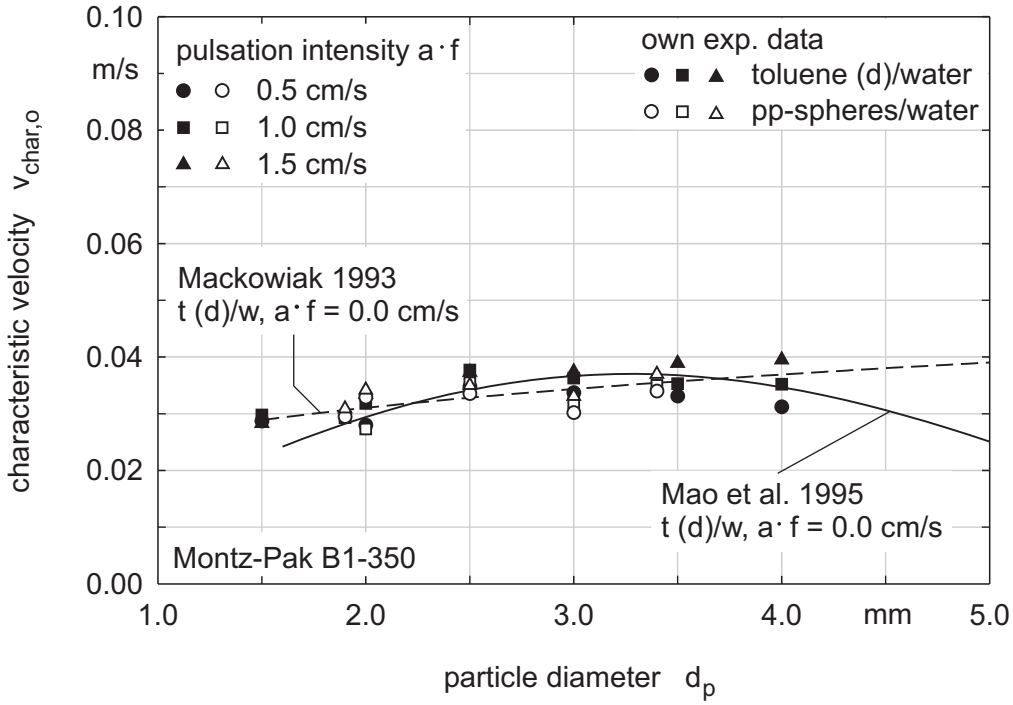

Figure 5.10: Characteristic velocities of single rigid pp-spheres and single toluene drops in pulsed compartments with structured packings; comparison of the obtained characteristic velocities with correlations from the literature

The pulsation intensity in packed compartments slightly influences the characteristic velocity. The characteristic velocity of pp-spheres and toluene drops as well as butyl acetate drops is generally higher for higher pulsation intensities, see *figure (5.11)*. This is explained by the fact that higher pulsation intensities push the particles faster through the packing channels.

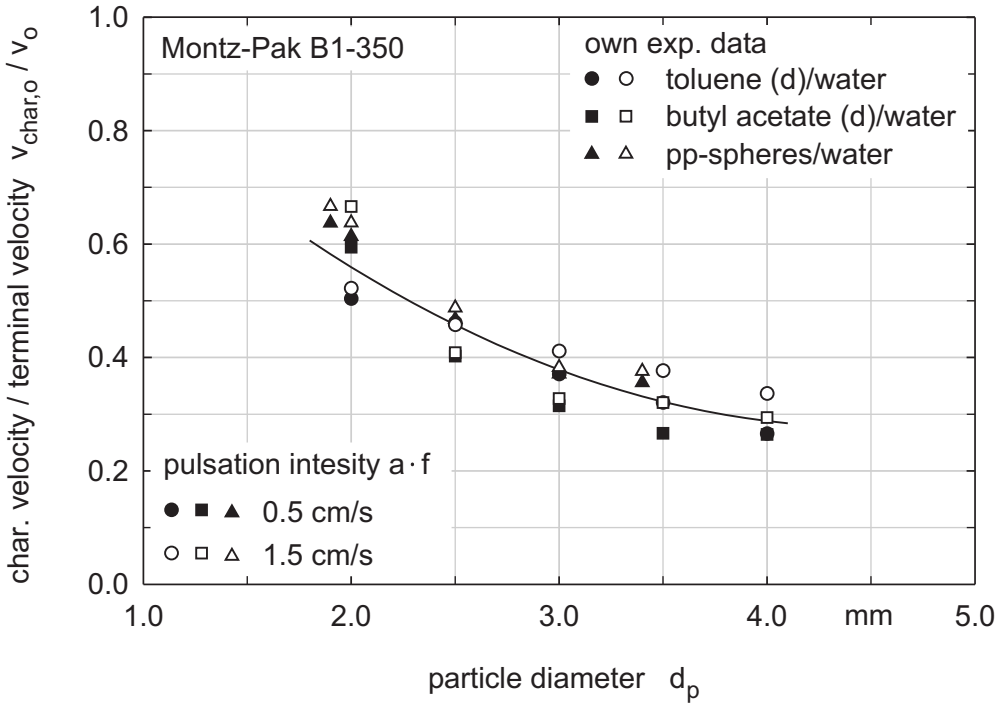

Figure 5.11: Comparison of the velocity ratio $v_{char,o} / v_o$ of single particles in pulsed compartments with structured packings; binary test systems

In comparison to pulsed sieve tray columns, the values for the velocity ratio $v_{char,o}/v_o$ are notably smaller and reach values down to 0.3 for particles with a diameter of 4 mm, see *figure (5.11)* and *figure (5.6)*. Similar to pulsed sieve tray compartments, the velocity ratio $v_{char,o}/v_o$ of pulsed packed compartments is higher when mass transfer is present, see *figure (5.12)*. Because the characteristic velocities of toluene and butyl acetate drops are almost the same in pulsed packed compartments with and without mass transfer, this effect must be related to the different terminal velocities of the drops.

The comparison of the correlations of *Mackowiak 1993* and *Mao et al. 1995* with own experimental data reveals that both correlations deliver good results for the characteristic velocities, see *figure (5.10)*. However, the correlation of Mackowiak was fitted to the experimental data by a regression analysis. Thereby, a drag coefficient of $\Psi_m = 8.54$ was found which is significantly higher than the values of Mackowiak (e. g. for a structured packing of the type "Montz-Pak B1-300" a drag coefficient of $\Psi_m = 0.81$ is given in the literature). The correlation of *Mao et al. 1995* is in good agreement with the experimental data for a range of the drop diameter from d = 1.5 to 4.0 mm. This correlation was evaluated with *n = 54* and *C = 0.5*, where *n* is the number of channels per cross-sectional area of the packing and *C* is a constant parameter that can be fitted to the experimental data, see *chapter 2.2*. The disadvantage

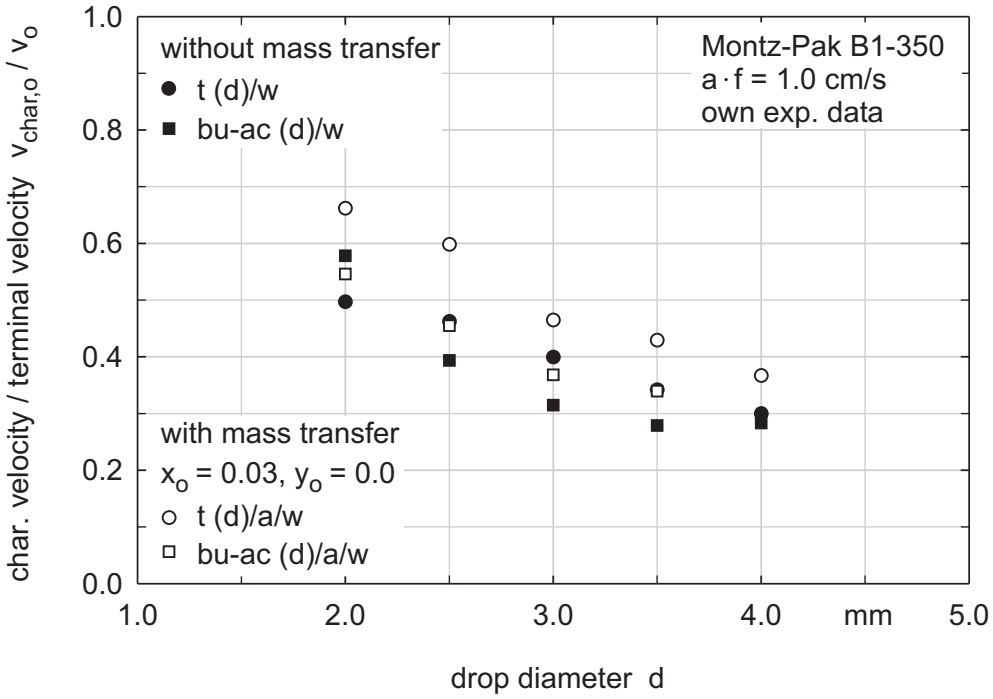

Figure 5.12: Influence of mass transfer on the velocity ratio $v_{char,o} / v_o$ of single drops in compartments with structured packings

of this correlation is that it shows a strong decrease of the characteristic velocity for drop sizes larger than d = 4.0 mm. This disagrees with experimental data from the literature, see *Leu 1995*. In addition, both correlations do not account for the influence of the packing height. Each single packing is positioned with a difference of 90° in its horizontal orientation to the next packing. An increase of the number of packings produces lower characteristic velocities because the drops are abruptly decelerated by the change of their moving direction between two adjacent elements, see also *Leu 1995*.

A more sophisticated model for the ratio $v_{char,o} / v_o$ should also include the height and the volumetric surface of a packing. Drops are increasingly hindered in their motion through packings with higher volumetric surface areas. Thus, the characteristic ratio of the velocities $v_{char,o} / v_o$ was correlated by:

$$\frac{v_{char,o}}{v_o} = 0.077 \cdot \pi_{H_P}^{0.138} \cdot \pi_{a_P}^{-0.566} \cdot \pi_d^{-0.769} \cdot \pi_\sigma^{0.184} \cdot (1 + \pi_{af})^{0.08} \tag{5.3}$$

The dimensionless numbers in *equation (5.3)* were derived by a dimensional analysis of the main characteristic parameters:

$$\pi_{h_P} = h_P \cdot \left[\frac{\rho_c \cdot \Delta\rho \cdot g}{\eta_c^2} \right]^{1/3}, \quad \pi_{a_P} = a_P \cdot \left[\frac{\eta_c^2}{\rho_c \cdot \Delta\rho \cdot g} \right]^{1/3}, \quad \pi_d = d \cdot \left[\frac{\rho_c \cdot \Delta\rho \cdot g}{\eta_c^2} \right]^{1/3}$$

$$\pi_\sigma = \sigma \cdot \left[\frac{\rho_c^2}{\eta_c^4 \cdot \Delta\rho \cdot g} \right]^{1/3}, \quad \pi_{af} = a \cdot f \cdot \left[\frac{\rho_c^2}{\eta_c \cdot \Delta\rho \cdot g} \right]^{1/3}$$

Figure (5.13) shows that *equation (5.3)* correlates well own experimental data and data from the literature. This is remarkable because the experiments of *Leu 1995* were carried out in columns with different types of packings. In addition, *Hoting 1996* carried out experiments in presence of mass transfer.

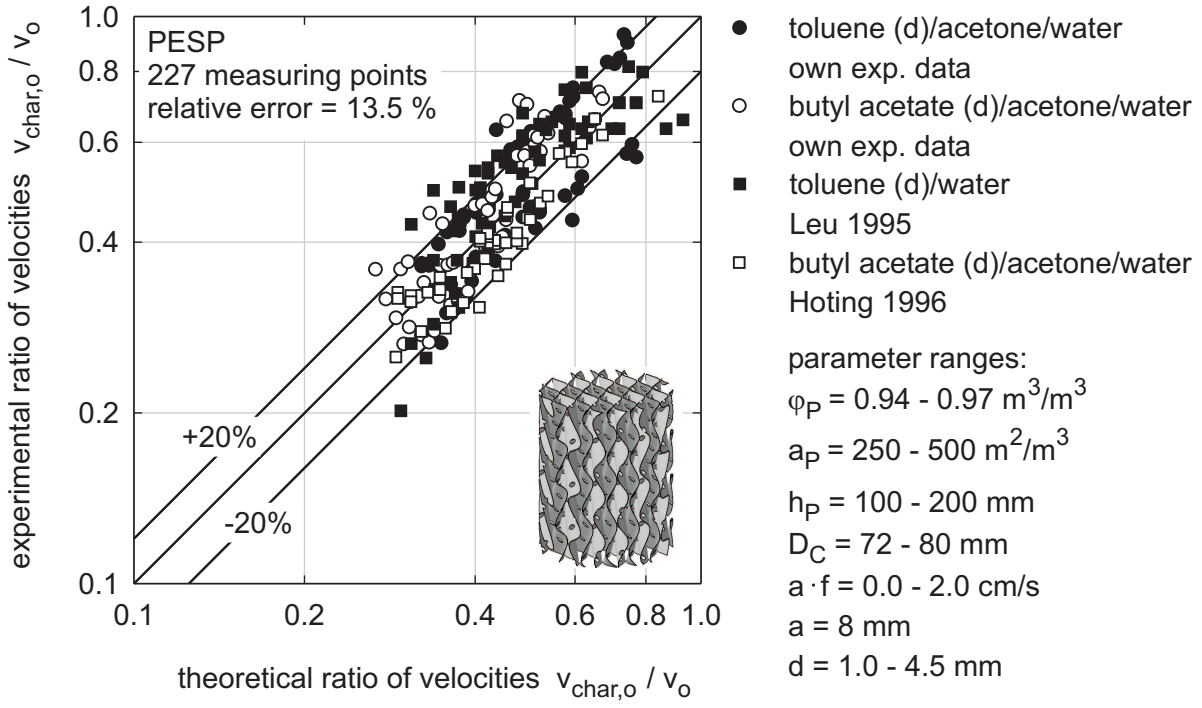

Figure 5.13: Comparison of measured velocity ratios $v_{char,o} / v_o$ of single drops with predicted values from equation (5.3) for compartments with different structured packings

5.4 Characteristic Velocity in Agitated Columns with Rotating Discs

The characteristic velocities of single particles in agitated columns are controlled by the size of the particles and the energy input. Compared to blade agitators, rotating discs are characterised by a significantly lower energy input for same rotational speeds and agitator sizes. This is proven by the small decrease of the characteristic velocities of single toluene drops with increasing rotational speeds in the RDC-compartments, see *figure (5.14)*.

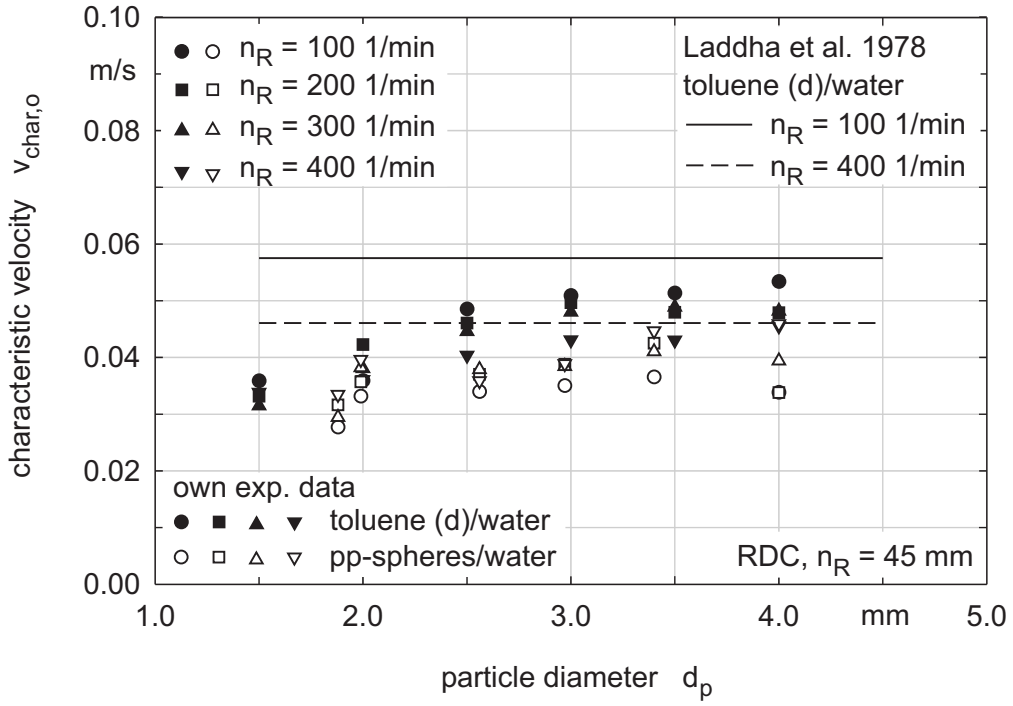

Figure 5.14: Characteristic velocity of single particles in RDC-compartments; comparison of experimentally obtained characteristic velocities with the correlation of Laddha et al. 1978

Figure (5.14) also shows that rigid pp-spheres move slightly slower through RDC-compartments than toluene drops of same size. As long as the rotational speed is relatively low (which is approximately up to n_R = 600 1/min) and the particles do not circulate within the compartments, the characteristic velocities differ similarly to the terminal velocities. The influence of rotating discs on the velocity ratio $v_{char,o}/v_o$ is thus independent of the test systems. In addition, almost the same velocity ratios are determined regardless of whether mass transfer is present or not. To illustrate this point, characteristic velocities for rotational speeds from n_R = 100 to 400 1/min were averaged for each particle size and test system. The ratio of the averaged characteristic velocity to the terminal velocity of the particles is depicted in *figure (5.15)*. For all test systems the evaluated velocity ratios $v_{char,o}/v_o$ have similar values from 0.73 to 0.38 for the range of particle sizes.

The characteristic velocity in RDC-compartments can be modelled by only considering the size of the particles, the geometry of the agitators and stators, and the energy input. The correlation of *Laddha et al. 1978*, see *chapter 2.2*, includes most of these parameters. However, it does not contain the diameter of the particles even though experimental data show a significant influence for smaller particle sizes, see *figure (5.14)*. Furthermore, this correlation predicts too high

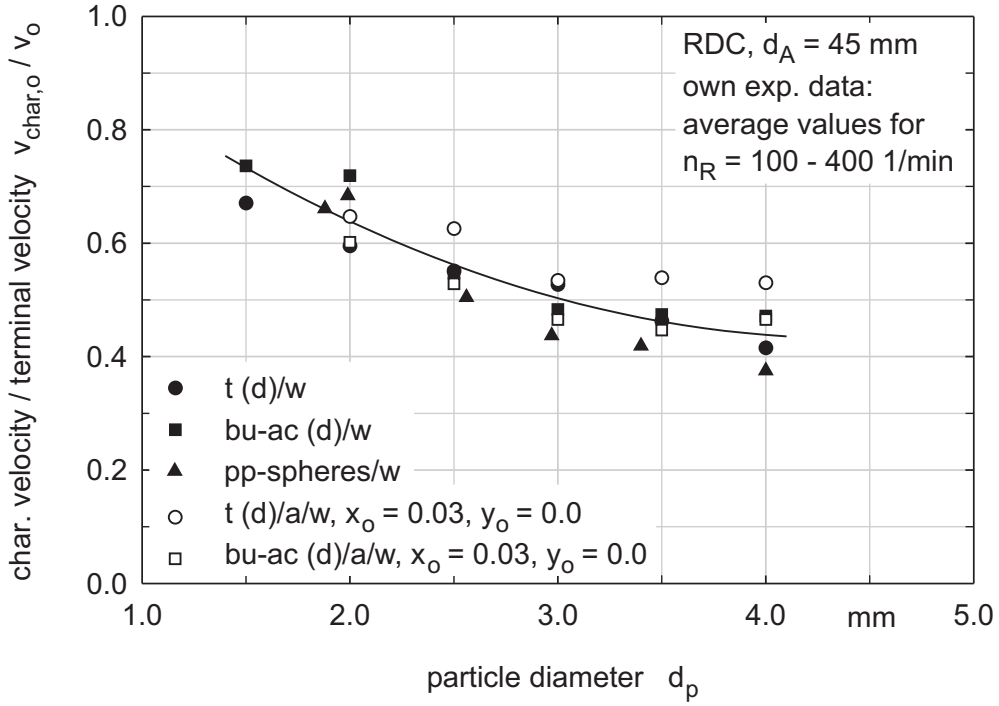

Figure 5.15: Influence of physical properties and mass transfer on the velocity ratio $v_{char,o} / v_o$ in RDC-compartments; averaged characteristic velocities for rotational speeds from 100 to 400 1/min were used to determine $v_{char,o} / v_o$ for each particle size

values of the characteristic velocities, particularly for a rotational speed of n_R = 100 1/min. Contrary to the correlation of *Laddha et al. 1978*, the correlation of *Modes 1999* predicts unrealistically high values of the characteristic velocities.

However, Modes' correlation describes the ratio $v_{char,o} / v_o$ very well for smaller compartment dimensions than were used in this work. Thus, this correlation was chosen to develop a more general and efficient correlation. Firstly, the improvement of Modes' correlation was carried out by using only dimensionless groups and considering the dimensionless power number N_P given by *Kumar and Hartland 1996*:

$$N_P = \frac{109.36}{Re_R} + 0.74 \cdot \left[\frac{1000 + 1.2 \cdot Re_R^{0.72}}{1000 + 3.2 \cdot Re_R^{0.72}} \right]^{3.30} \quad \text{where} \quad Re_R = \frac{n_R \cdot d_A^2 \cdot \rho_c}{\eta_c} \qquad (5.4)$$

Secondly, the correlation of Modes was extended to different compartment geometries by a regression analysis of own experimental data and data from Modes and *Fan et al. 1987*. The analysis of the characteristic velocities in RDC-compartments yielded the following correlation:

$$\frac{v_{char,\,o}}{v_o} = 1 + 0.512 \cdot N_P^{0.362} - 0.507 \cdot \left(\frac{d}{d_s - d_A}\right)^{1.035} - 0.341 \cdot \left(\frac{h_c}{D_C}\right)^{-0.565} \qquad (5.5)$$

As can be seen in *figure (5.16)*, the compartment height h_c has a large impact on the characteristic velocities in RDC-columns. Fan et al. determined the characteristic velocities in RDC-compartments with a height of 70 mm. In contrast, Modes used RDC-compartments with a height of 30 mm. The velocity ratios $v_{char,o}/v_o$ of Modes show significantly lower values than of Fan et al. This is due to the increased deflection of the drops from the vertical path by the increased number of agitators and stators for lower compartment heights. *Equation (5.5)* correlates the velocity ratio $v_{char,o}/v_o$ for all compartment heights, large, medium and small, very well. A good agreement for many experiments with different compartment dimensions, rotational speeds and liquid/liquid-systems is shown in *figure (5.16)*.

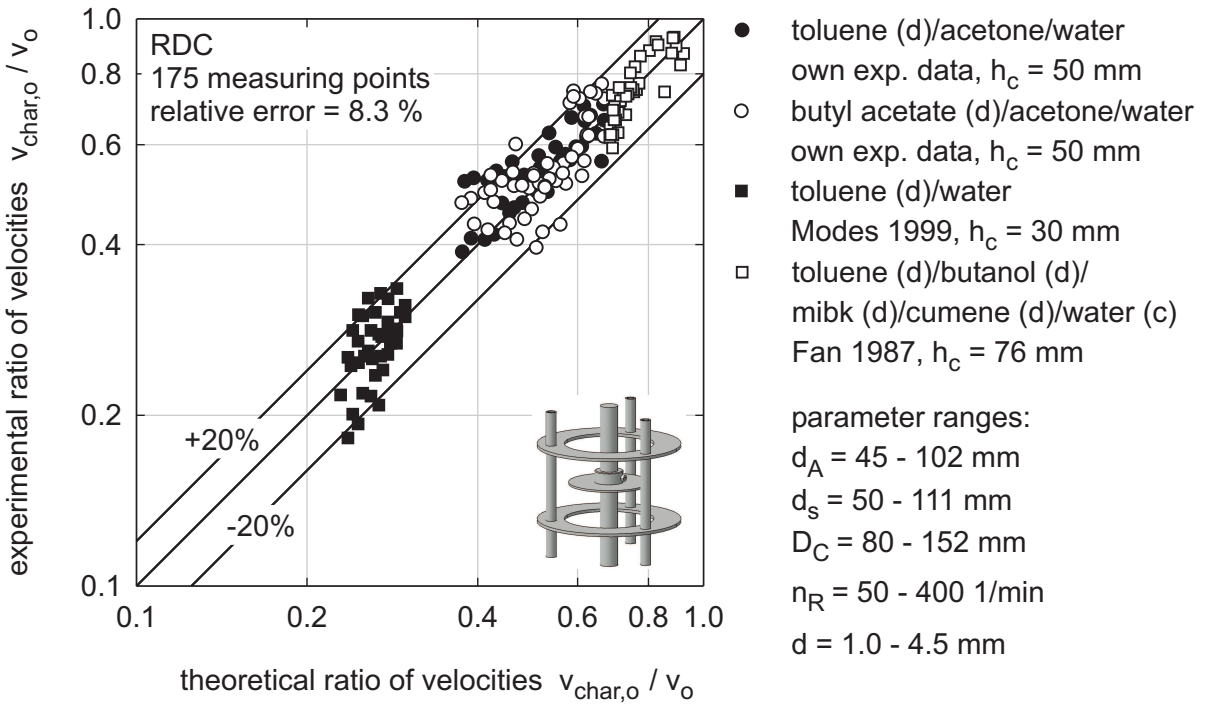

Figure 5.16: Verification of equation (5.5) for the prediction of the velocity ratio $v_{char,o}/v_o$ for RDC-compartments with different dimensions

5.5 Characteristic Velocity in Agitated Columns with Kühni Blade Agitators

The energy input of Kühni blade agitators is much higher than of rotating discs. Even for low rotational speeds from n_R = 100 - 200 1/min rotational flow patterns and circulating cells within the single compartments are generated, compare *figure (5.17)*. The residence time of the

particles within the compartments is increased at higher rotational speeds, since the particles circulate more intensely.

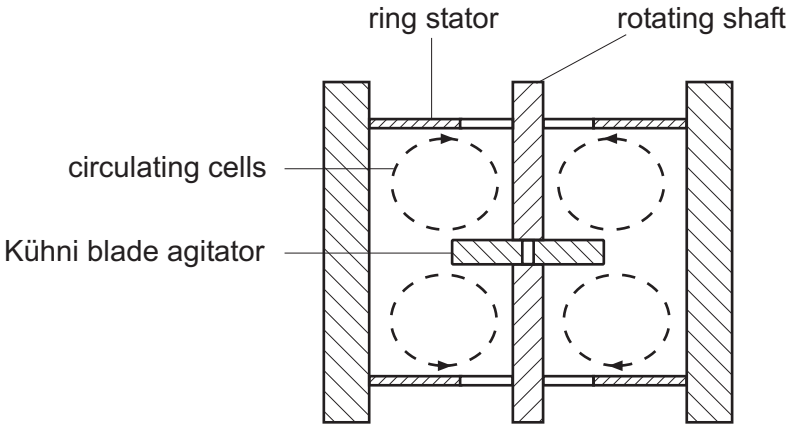

Figure 5.17: Symmetrical circulating cells in a Kühni-compartment

The quantitative influence of the rotational speed on the characteristic velocities of toluene drops is illustrated in *figure (5.18)*. An increase of the rotational speed leads to a decrease of the characteristic velocity. This is also proven by the characteristic velocities of butyl acetate drops which show a very similar behaviour, see *figure (5.19)*. Furthermore, it is observed that for all test systems the velocity ratios $v_{char,o}/v_o$ are similarly reduced. No significant impact of the mass transfer in either of the liquid/liquid-systems is detected for the range of drop diameters and rotational speeds investigated.

To predict the characteristic velocity in Kühni-columns the geometry of the compartments has to be considered, i. e. the dimensions of the agitators, the relative free cross-sectional area of the stators and the height of the compartments. Furthermore, the drop diameter and the energy input have to be taken into account. It is thus recommended not to use the correlation of *Weiss et. al 1995* because it does not include any geometrical parameter, see *chapter 2.2*. The application of this correlation to compartment sizes different from the one used by Weiss et al. results in values for the characteristic velocities that are too low, see *figure (5.18)*. The correlation of *Fang et al. 1995* accounts for the influence of the relative free cross-sectional area of the stators and the dimensions of the agitators. However, it disregards the influence of the drop diameter, which is in contrast to the experimental data, see *figure (5.18)* and *figure (5.19)*.

The characteristic velocities are thus correlated similarly to RDC-columns. The velocity ratio $v_{char,o}/v_o$ in Kühni-columns is given by:

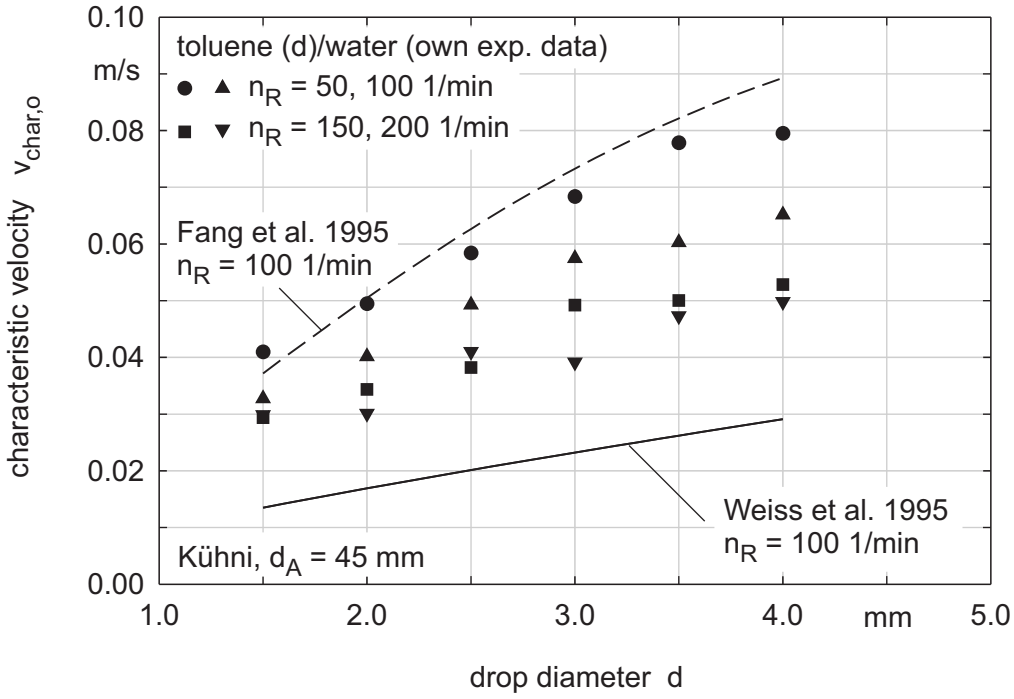

Figure 5.18: Influence of the rotational speed and drop size on the characteristic velocity in Kühni-compartments

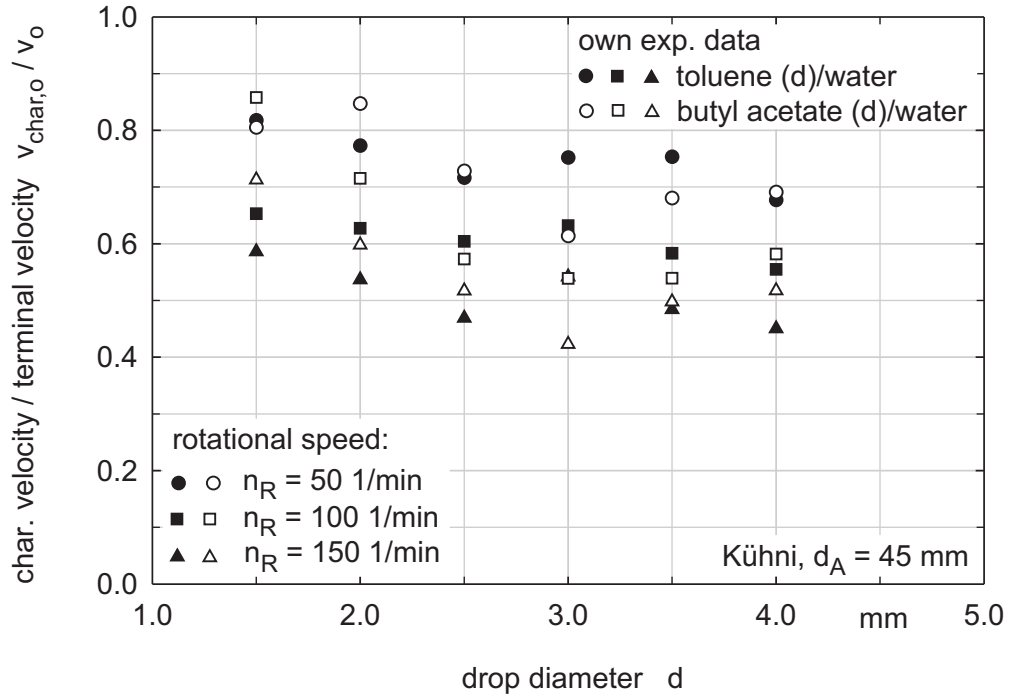

Figure 5.19: Velocity reduction in Kühni-compartments for single toluene and butyl acetate drops compared to their terminal velocities

$$\frac{v_{char,\,o}}{v_o} = 1 - 1.669 \cdot N_P^{-3.945} - 2.807 \cdot \left(\frac{d}{D_C - d_A} \right)^{1.336} - 1.159 \cdot \left(\frac{h_c}{D_C} \right)^{2.049} + 2.1 \cdot \varphi_s^{1.032} \tag{5.6}$$

where the dimensionless power number N_P is given by *Kumar and Hartland 1996*:

$$N_P = 1.08 + \frac{10.94}{Re_R^{0.5}} + \frac{257.37}{Re_R^{1.5}} \tag{5.7}$$

The ratio of the velocities $v_{char,o} / v_o$ is determined very accurately with *equation (5.6)*. This equation describes the experimental velocities for different liquid/liquid-systems and different compartment dimensions qualitatively and quantitatively very well, see *figure (5.20)*. Only small deviations between calculated velocities and data from own experiments and from the literature are seen.

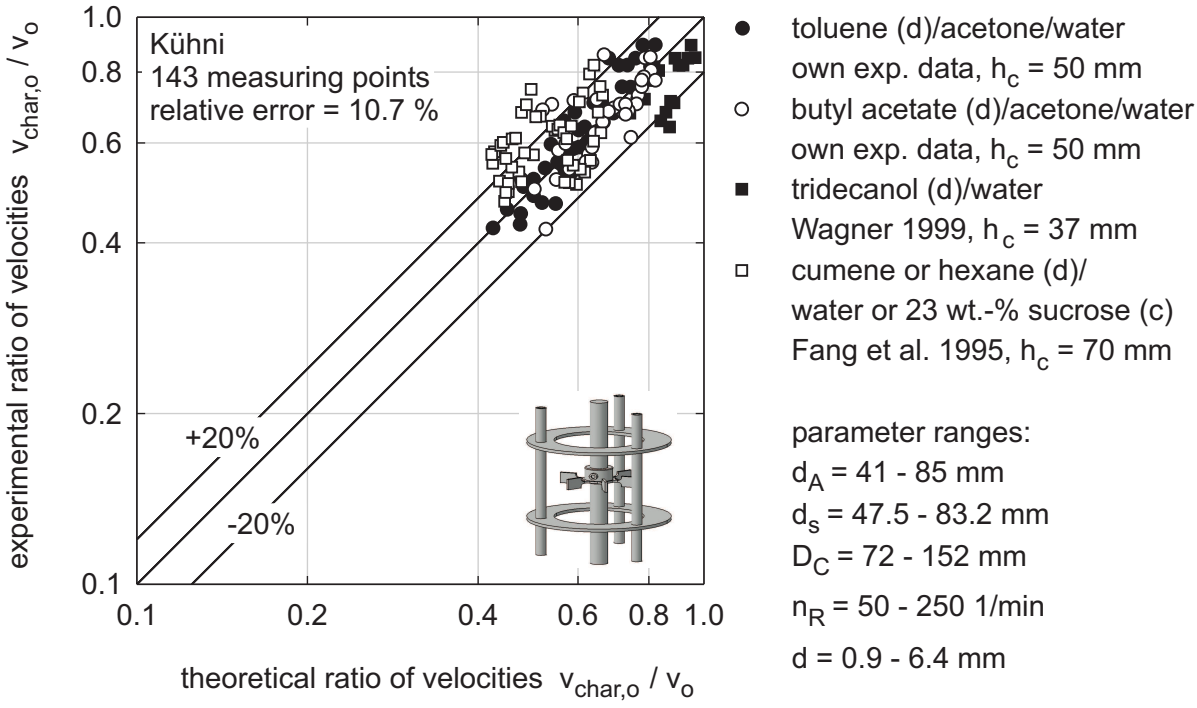

Figure 5.20: Comparison of the experimental velocity ratios $v_{char,o} / v_o$ with calculated values from equation (5.6) for Kühni-compartments

The analysis of all available data makes clear that the influence of the compartment height is lower in Kühni-columns than in RDC-columns. However, this statement has to be put into perspective. Fang et al. used Kühni-compartments with a height of 70 mm. In contrast, Wagner used compartments with a height of 37 mm. But not only the compartment height was different. Fang et al. worked with perforated stators and not with ring stators as used by Wagner and in

own experiments. Since the compartment height and the stator design differ, no exact conclusion can be drawn about the influence of the compartment height on the characteristic velocity. For this reason, the influence of compartment height in Kühni-columns should be investigated. In addition, it would be of interest to investigate the effect of the stator design (perforated or ring shape) for a given relative free cross-sectional area.

5.6 Comparison of Characteristic Velocities in Different Columns

A comparison of the characteristic velocity ratio $v_{char,o}/v_o$ for agitated and pulsed columns is given in *figure (5.21)*. It is obvious that the motion of single drops in sieve tray columns is hindered in a small degree only. In contrast, in RDC-columns the velocity ratio $v_{char,o}/v_o$ reaches lower values. Lower characteristic velocities also exist in pulsed columns with structured packings. For these columns the characteristic velocity ratio $v_{char,o}/v_o$ decreases from 0.6 down to 0.3 if the drop diameter is increased from 1.5 to 4.0 mm. For rotational speeds from 50 to 200 1/min in Kühni-columns, values for $v_{char,o}/v_o$ from 0.8 to 0.3 are observed. Thus, the characteristic velocities in Kühni-columns cover the whole range of characteristic velocities for all other investigated types of columns.

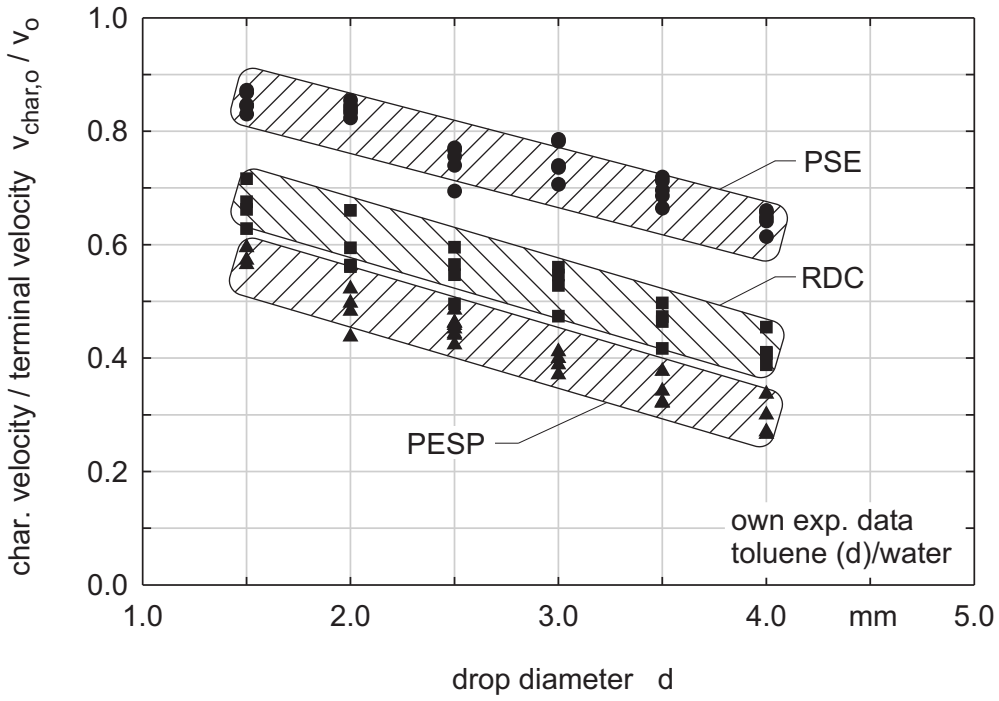

Figure 5.21: Velocity ratio $v_{char,o}/v_o$ of single toluene drops for different types of extractors: PSE = pulsed sieve tray extractor (sieve tray d_h=4 mm), RDC = rotating disc contactor, PESP = pulsed extractor with structured packings

6 Single Drop Breakage

The drop size is one of the most important parameter for the performance of an extractor because it determines the velocity and the mass transfer rate of drops in a swarm. Breakage and coalescence control the drop size and the drop size distribution in a column. Because coalescence is normally reduced by the choice of the mass transfer direction, breakage mainly affects the drop size profiles. To determine drop size profiles along the column height by DPBMs, it is necessary to quantitatively describe the drop breakage with parameters such as the breakage probability of single mother drops and the volumetric density distribution of daughter drops.

The breakage probability p_B of single drops can be experimentally determined by the number of breaking mother drops N_{BM} from a number of investigated mother drops N_{IM}: $p_B = N_{BM}/N_{IM}$. Numerous experiments were conducted to determine the influence of mother drop size and of energy input on the breakage probability. These experiments were carried out in columns with only a single sieve tray, a single structured packing and a single agitated compartment. Two binary systems (toluene (d)/water and butyl acetate (d)/water) and two ternary systems (toluene (d)/acetone/water and butyl acetate (d)/acetone/water) were used. All systems were mutually saturated. No mass transfer occurred during the tests. For the ternary systems the acetone concentration of the continuous aqueous phases was always 5 wt.-% and the acetone concentration of the organic dispersed phases was the equilibrium concentration. The use of different liquid/liquid-systems reveals how the interfacial tension affects the drop breakage.

The acetone concentrations and the interfacial tensions of the test systems, which can be predicted by the correlations of the European Federation of Chemical Engineering (*EFCE 1984*), are listed in *table (6.1)*. In this chapter the different test systems are denoted by the nomenclature given in this table.

Table 6.1: Weight concentrations of acetone and interfacial tensions of the mutually saturated liquid/liquid-systems according to EFCE 1984; x = weight concentration of acetone in the continuous phase; y = weight concentration of acetone in the dispersed phase at equilibrium; σ = interfacial tension of the test system*

Nomenclature	x [kg/kg]	y* [kg/kg]	σ [N/m]
toluene (d)/water or t (d)/w	-	-	0.034
toluene (d)/acetone/water or t (d)/a/w	0.050	0.042	0.024
butyl acetate (d)/water or bu-ac (d)/w	-	-	0.014
butyl acetate (d)/acetone/water or bu-ac (d)/a/w	0.050	0.047	0.011

6.1 Breakage Probability of Single Drops in Pulsed Columns

The breakage of single drops in pulsed extraction columns depends on the geometry of the internals and the energy input. In pulsed sieve tray columns drop breakage is basically governed by the size of the sieve tray holes and the pulsation intensity, see *Haverland 1988* and *Wagner and Blaß 1999*.

- *Breakage probabilities in pulsed sieve tray columns*

In pulsed sieve tray columns drops generally break during their passage through the sieve tray holes. Large shear stresses act on the drops during their passage which mainly result from the pulsation of the liquids in the columns. In addition, drops with a diameter larger than the hole diameter are deformed during their passage through the sieve trays. If the stabilising drop forces are not sufficient to withstand the deformation, the drop will be split into several smaller drops. Because larger drops are less stable, breakage probabilities of large drops are higher than of small drops. This is proven by the investigations in the pulsed column, where drops with a diameter d_M larger than the hole diameter d_h showed significantly higher breakage probabilities, see *figure (6.1)* and *figure (6.2)*.

The experiments make clear that in pulsed sieve tray columns the breakage probability p_B continuously increases with increasing mother drop diameter, see *figure (6.1)* and *figure (6.2)*. In addition, the pulsation intensity has a large impact on the drop breakage. An increase of the pulsation intensity results in a significant increase of the breakage probability. This is due to enlargement of destructive forces which act upon the drops at higher pulsation intensities.

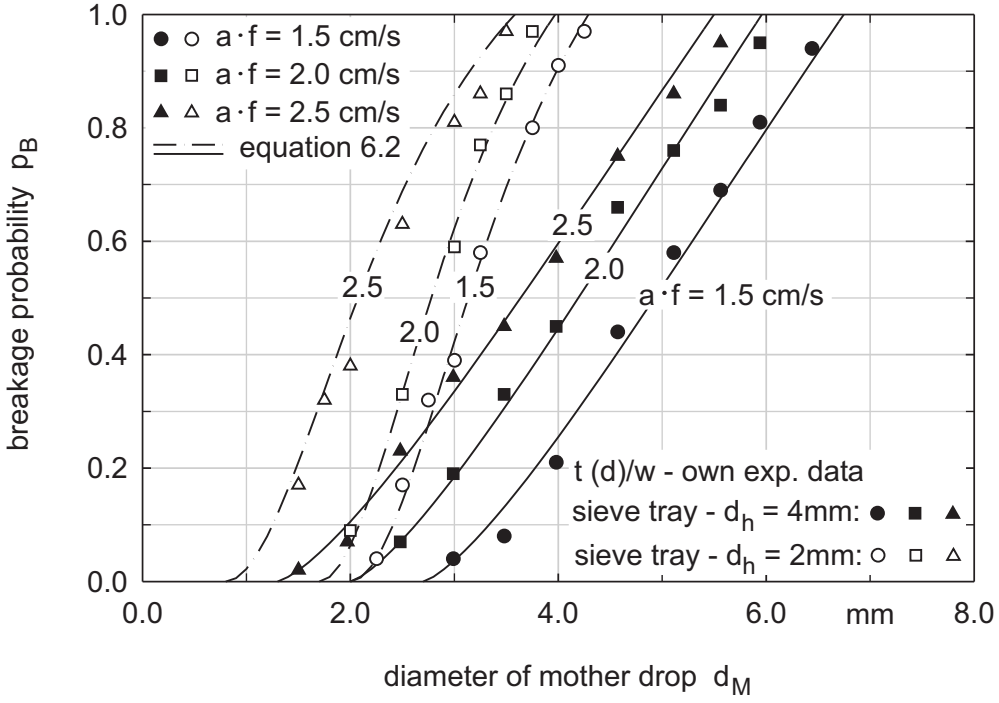

Figure 6.1: Toluene (d)/water: Breakage probability of single toluene drops in single sieve tray compartments; comparison of the experimental data and equation (6.2)

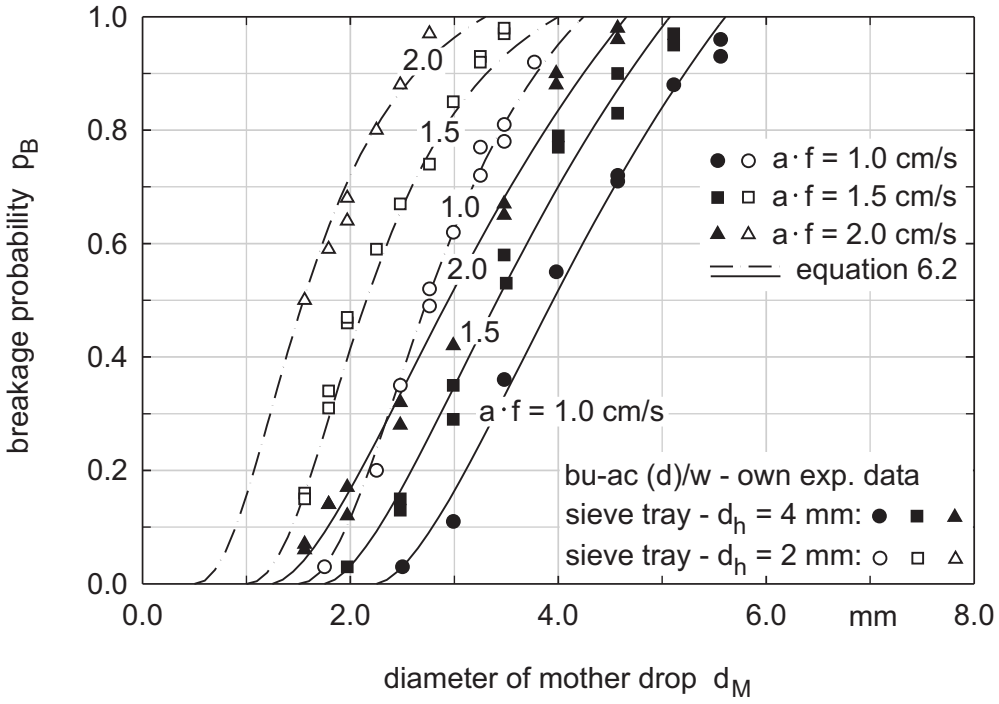

Figure 6.2: Butyl acetate(d)/water: Breakage probability of single butyl acetate drops in single sieve tray compartments; comparison of the experimental data and equation (6.2)

The use of sieve trays with small holes results in significantly higher breakage rates than the use of sieve trays with large holes. Moreover, sieve trays with smaller holes cause drops to split which do not break in compartments with sieve trays with larger holes. The experiments with a single sieve tray with 2 mm hole diameter and with a single sieve tray with 4 mm hole diameter confirm these statements, see *figure (6.1)* and *figure (6.2)*. For this reason, the use of sieve trays with 2 mm holes in an extractor results in a good mass transfer efficiency since this type of sieve tray produces smaller drops and, in turn, a large mass transfer area, see also *Wagner 1999*.

The interfacial tension of the toluene (d)/acetone/water system with an acetone weight concentration of 5.0 % in the aqueous phase is almost 30 % lower than of the acetone free system. For the same acetone concentration in the aqueous phase the interfacial tension of the butyl acetate (d)/acetone/water system is only 20 % lower than of the corresponding acetone free system. The influence of the interfacial tension on the breakage probability is shown in *figure (6.3)* and *figure (6.4)*. As expected, the breakage probability increases with decreasing interfacial tension. Subsequently, the breakage probability is higher in the ternary toluene and butyl acetate systems than in the binary systems.

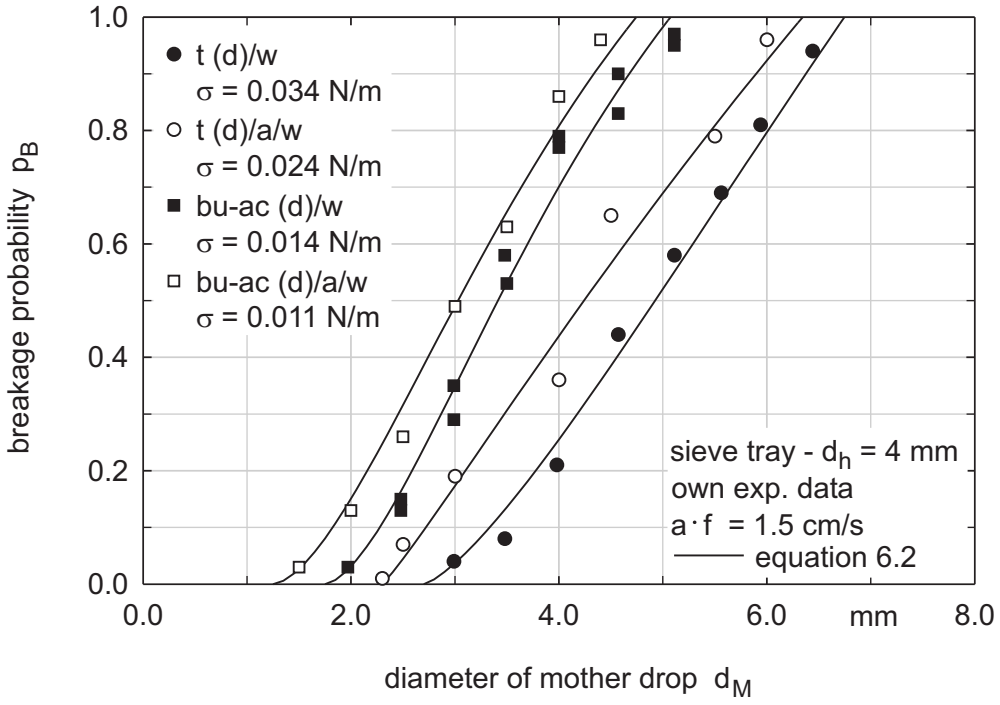

Figure 6.3: Influence of the interfacial tension σ on the breakage probability in a pulsed compartment with a sieve tray with 4 mm hole diameter

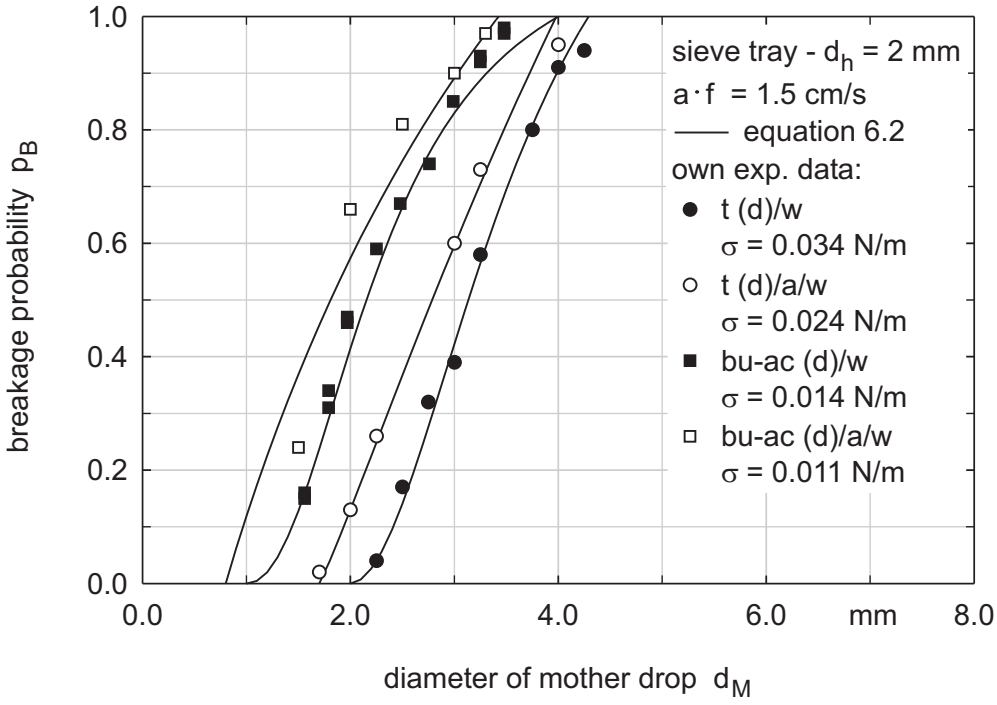

Figure 6.4: Influence of the interfacial tension σ on the breakage probability in a pulsed compartment with a sieve tray with 2 mm hole diameter

The results of all experiments in pulsed compartments with sieve trays reveal that increasing the mother drop diameter and the pulsation intensity leads to higher breakage probabilities. In addition, higher breakage probabilities result for smaller sieve tray holes and lower interfacial tensions.

The breakage probability in pulsed sieve tray compartments can be predicted by a simple correlation introduced by *Haverland 1988*:

$$p_B(d_M) = [(d_M - d_{stab})/(d_{100} - d_{stab})]^C \tag{6.1}$$

Here, d_{stab} and d_{100} are the characteristic drop diameters (see *chapter 2.2*) and *C* depends on the pulsation intensity. The disadvantage of this correlation is that the exponent *C* has to be determined for each individual pulsation intensity and that extrapolation to other pulsation intensities is difficult. Against this background, a new correlation based on *equation (6.1)* was developed:

$$p_B(d_M) = C_1 \cdot \pi_{af}^{C_2} \cdot \frac{[(d_M - d_{stab})/(d_{100} - d_{stab})]^{C_3}}{C_4 + [(d_M - d_{stab})/(d_{100} - d_{stab})]^{C_3}} \tag{6.2}$$

The dimensionless number π_{af} considers the influence of the pulsation intensity on the breakage probability: $\pi_{af} = a \cdot f \cdot (\rho_c^2/(\eta_c \cdot \Delta\rho \cdot g))^{1/3}$. The new correlation describes the breakage in a sieve tray compartment for a wide range of pulsation intensities with only one set of constant factors C_i for a liquid/liquid-system. The constant factors in *equation (6.2)* are listed in *table (6.2)* for both types of sieve trays.

Table 6.2: Constant factors C_i of equation (6.2) for determining the breakage probability in sieve tray compartments

Type of sieve tray	Liquid/liquid-system	C_1	C_2	C_3	C_4
sieve tray - d_h = 2 mm	toluene (d)/water	1.64	-0.18	1.91	0.55
sieve tray - d_h = 2 mm	toluene (d)/acetone/water	3.81	0.61	1.11	3.47
sieve tray - d_h = 2 mm	butyl acetate (d)/water	1.33	0.03	2.03	0.42
sieve tray - d_h = 2 mm	butyl acetate (d)/acetone/water	2.49	0.27	0.95	1.77
sieve tray - d_h = 4 mm	toluene (d)/water	4.80	0.27	1.35	4.31
sieve tray - d_h = 4 mm	toluene (d)/acetone/water	4.75	0.14	1.11	4.35
sieve tray - d_h = 4 mm	butyl acetate (d)/water	2.00	-0.07	1.61	0.95
sieve tray - d_h = 4 mm	butyl acetate (d)/acetone/water	2.18	-0.33	1.61	1.15

To predict the breakage probability in sieve tray compartments with *equation (6.2)*, the characteristic drop diameters d_{stab} and d_{100} have to be experimentally determined for each pulsation intensity. According to the definition, d_{stab} is determined by a drop with a breakage probability somewhere between $0 < p_B \leq 0.03$ and the diameter d_{100} is given by a drop with a breakage probability somewhere between $0.97 \leq p_B < 1$. The data for the characteristic drop diameters for both types of sieve trays investigated are listed in *table (A.8)* in the appendix, see *chapter A.*[3] The breakage probabilities calculated from *equation (6.2)* are plotted as dashed and solid lines in the figures previously discussed. These figures show that the new correlation is applicable to determine the breakage probability in pulsed sieve tray compartments. In addition, it can be extrapolated to other pulsation intensities just from knowledge of the characteristic drop diameters.

3. For a few operating conditions the characteristic drop diameters d_{stab} and d_{100} could not be determined during the experiments. This was due to the fact that for high pulsation intensities ($a \cdot f \geq 2.0\ cm/s$) the stable drop diameter d_{stab} was too small to be generated by the experimental equipment that was available. The determination of the drop diameter d_{100} was difficult for low pulsation intensities since large drops adhered to the bottom side of the sieve trays and were not pushed through. In these few cases the characteristic drop diameters were determined by an extrapolation of the measured breakage probability values.

• *Breakage probabilities in pulsed columns with structured packings*

Breakage of single drops in a pulsed column with structured packings was investigated in detail by *Leu 1995*. Leu identified the bottom line of the corrugated sheets and the crosspoints of adjacent corrugated sheets as possible places where breakage occurs. Accordingly, packings with a high volumetric surface area possess more breakage places and result in a higher breakage performance. In addition, perforation of the corrugated sheets leads to significantly higher levels of drop breakage. The "Montz-Pak B1-350" packing has perforated corrugated sheets and a high volumetric surface area of a_P = 350 m^2/m^3. The level of breakage of single mother drops is thus very high in both binary systems, see *figure (6.5)* and *figure (6.6)*.

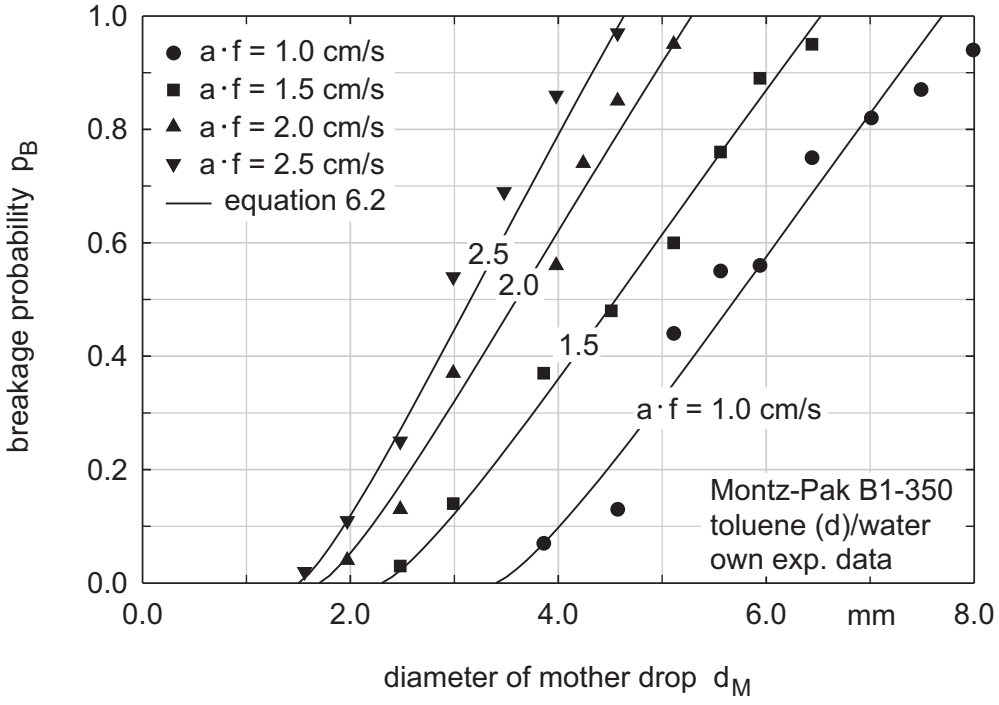

Figure 6.5: Toluene (d)/water: Influence of drop size and energy input on the breakage of single drops in a pulsed packed compartment; comparison of the experimental data and equation (6.2)

Again, increasing the mother drop diameter and the pulsation intensity causes an increase of the breakage probability. Comparing the results for both binary systems, the large influence of the interfacial tension on the drop breakage is obvious. The large difference in the breakage probabilities for same operating conditions is explained by the significantly lower interfacial tension of the butyl acetate (d)/water system. The strong impact of the interfacial tension is also proven by the results of both ternary test systems. Generally, the lower the interfacial tension, the higher the breakage probability, see *figure (6.7)*.

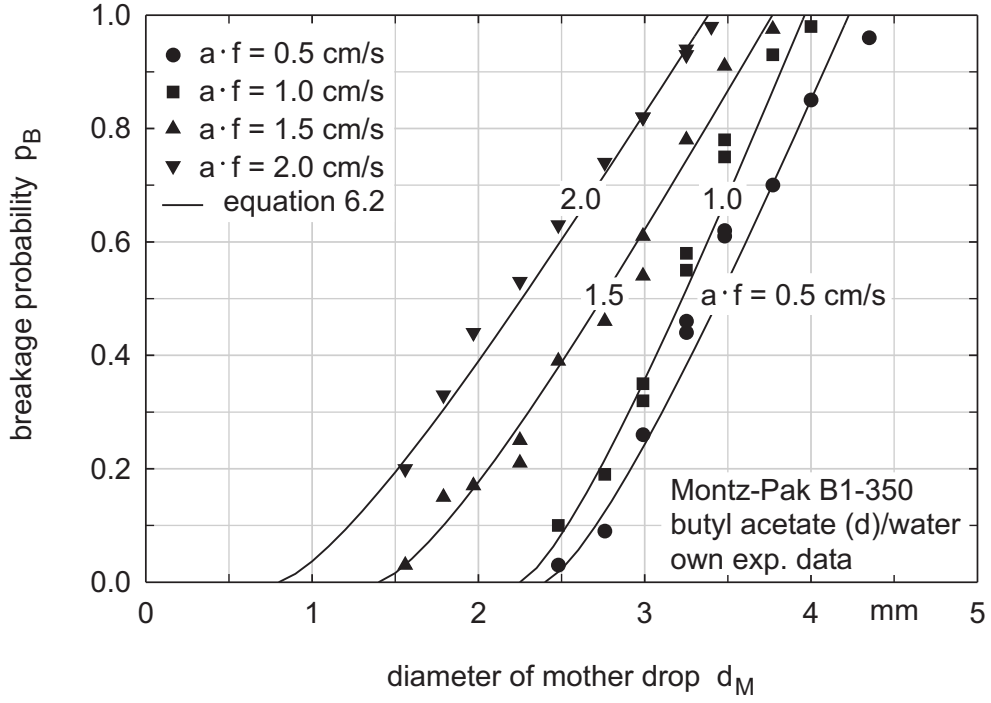

Figure 6.6: Butyl acetate (d)/water: Influence of drop size and energy input on the breakage of single drops in a pulsed packed compartment; comparison of the experimental data and equation (6.2)

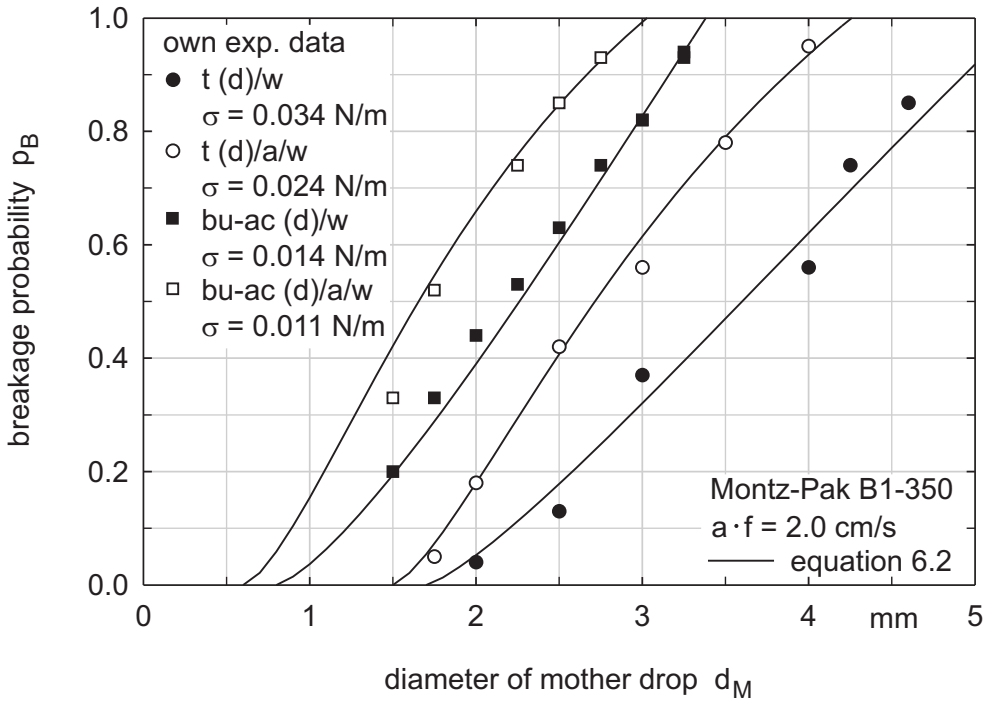

Figure 6.7: Influence of the interfacial tension σ on the breakage of single drops in a structured packing

The interfacial tension of the system together with the diameter of the mother drops and the pulsation intensity determine the breakage in structured packings. For this reason, these parameters have to be considered in modelling the breakage probability. The characteristic diameters d_{stab} and d_{100} account for the influence of the physical properties of the system and the energy input. Thus, *equation (6.2)* can also be successfully applied to determine the breakage probability in pulsed packings. The constant parameters C_i in *equation (6.2)* are listed in *table (6.3)* for the Montz packing. The characteristic diameters d_{stab} and d_{100} can be found in *table (A.8)* in the appendix, see *chapter A*. The comparison of *equation (6.2)* with the experimental data shows a good agreement, see *figure (6.5)*, *figure (6.6)* and *figure (6.7)*.

Due to the complex mechanisms that influence the breakage of single drops in pulsed compartments, no general model could be developed to predict the characteristic drop diameters d_{stab} and d_{100} together with the breakage probability p_B. However, the new correlation allows the determination of the breakage probability in a wide range of pulsation intensities just from knowledge of the characteristic diameters. Therefore, the new correlation leads to a significant reduction of the experimental effort.

Table 6.3: Constant factors C_i of equation (6.2) for determining the breakage probability of single drops in the Montz packing

Type of internal	Liquid/liquid-system	C_1	C_2	C_3	C_4
Montz-Pak B1-350	toluene (d)/water	5.81	-0.17	1.27	3.95
Montz-Pak B1-350	toluene (d)/acetone/water	1.98	-0.08	1.39	0.80
Montz-Pak B1-350	butyl acetate (d)/water	8.87	-0.15	1.37	6.89
Montz-Pak B1-350	butyl acetate (d)/acetone/water	1.06	-0.07	2.99	0.13

6.2 Breakage Probability of Single Drops in Agitated Columns

Drop breakage in agitated columns results from the shear stresses caused by the velocity gradients in the compartments. These stresses have their highest values at the outer edges of the agitators. Furthermore, the collisions of the drops with the rotating elements influence the breakage of single drops.

- *Breakage probabilities in agitated columns with rotating discs*

The shear stresses caused by a rotational flow in the compartments and the effect of drop collisions with the agitators depend on the rotator geometry and its dimensions. Rotating discs have a low energy input. In RDC-compartments drops start to break at much higher rotational speeds than in compartments with Kühni blade agitators. For this reason, the investigation of the single drop breakage in a single RDC-compartment has to be carried out with relatively high rotational speeds (n_R = 300 - 1200 1/min). The strong dependence of the breakage probability on the rotational speed and the diameter of the mother drops is shown in *figure (6.8)* and *figure (6.9).*

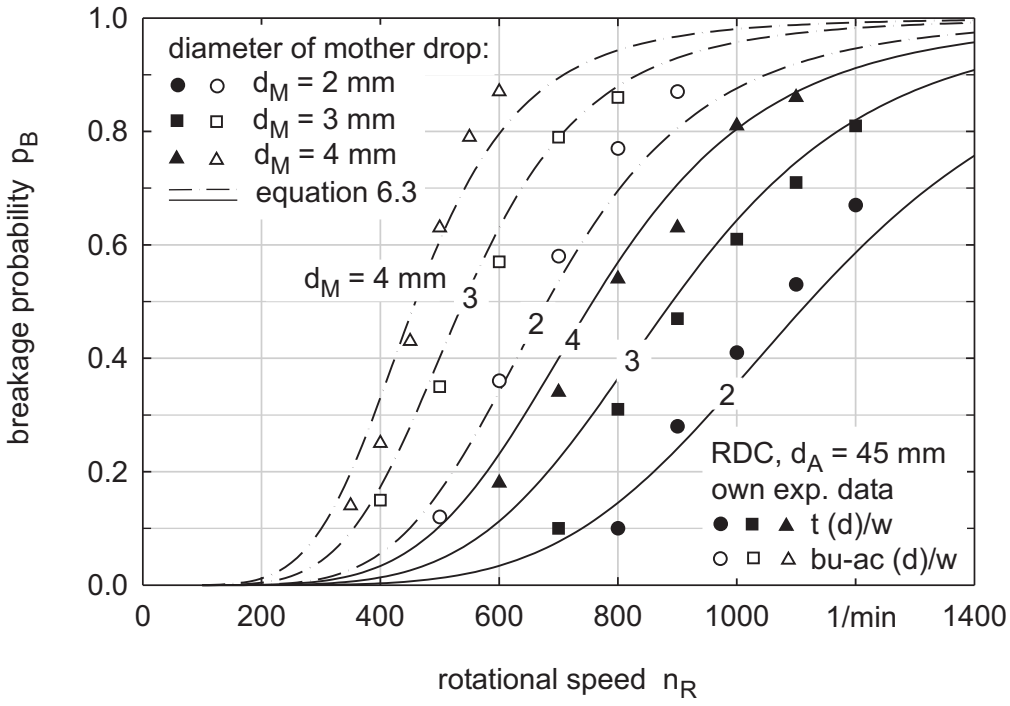

Figure 6.8: Influence of the mother drop size and rotational speed on the breakage probability of single toluene (d) and butyl acetate (d) drops in an agitated RDC-compartment; t (d)/w = toluene (d)/water, bu-ac (d)/w = butyl acetate (d)/water

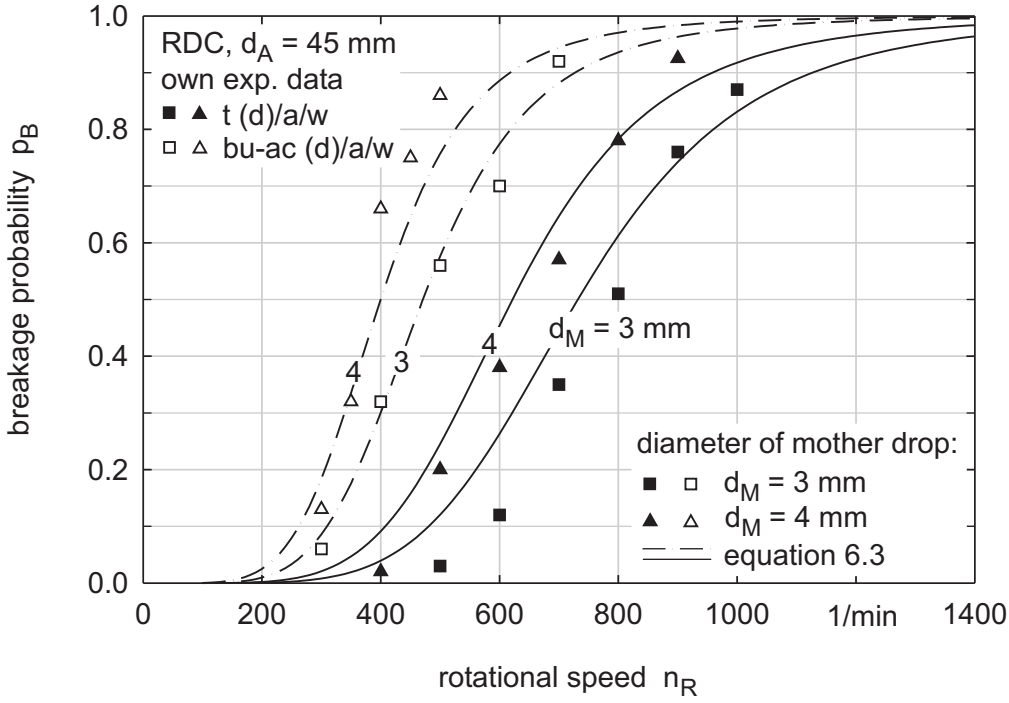

Figure 6.9: Influence of the mother drop size and rotational speed on the breakage probability for the ternary test systems: t (d)/a/w = toluene (d)/acetone/water and bu-ac (d)/a/w = butyl acetate (d)/acetone/water

At constant mother drop size, an increase of the rotational speed causes a strong increase of the breakage probability. Analogously, an increase of the mother drop diameter at a constant rotational speed leads to an increase of the breakage probability. As in pulsed compartments, the interfacial tension significantly influences the drop breakage in agitated RDC-compartments. The lower the interfacial tension, the higher the values of the breakage probability, see *figure (6.10)*.

The breakage probability in a RDC-compartment can be determined by a correlation which was developed by *Schmidt 2004*.[4] Based on the results of *Bahmanyar and Slater 1991*, *Cauwenberg 1995* and *Modes 1999*, the following correlation holds:

$$\frac{p_B}{1-p_B} = C_1 \cdot \left(\frac{We_{mod}}{1 + C_2 \cdot \eta_d \cdot [We_{mod}/(\sigma \cdot d_M \cdot \rho_d)]^{0.5}} \right)^{C_3} \tag{6.3}$$

4. Schmidt, S.: Member of the Institute of Chemical Engineering at the University of Kaiserslautern (Germany) and project partner during the work on the industrial funded research project previously mentioned.

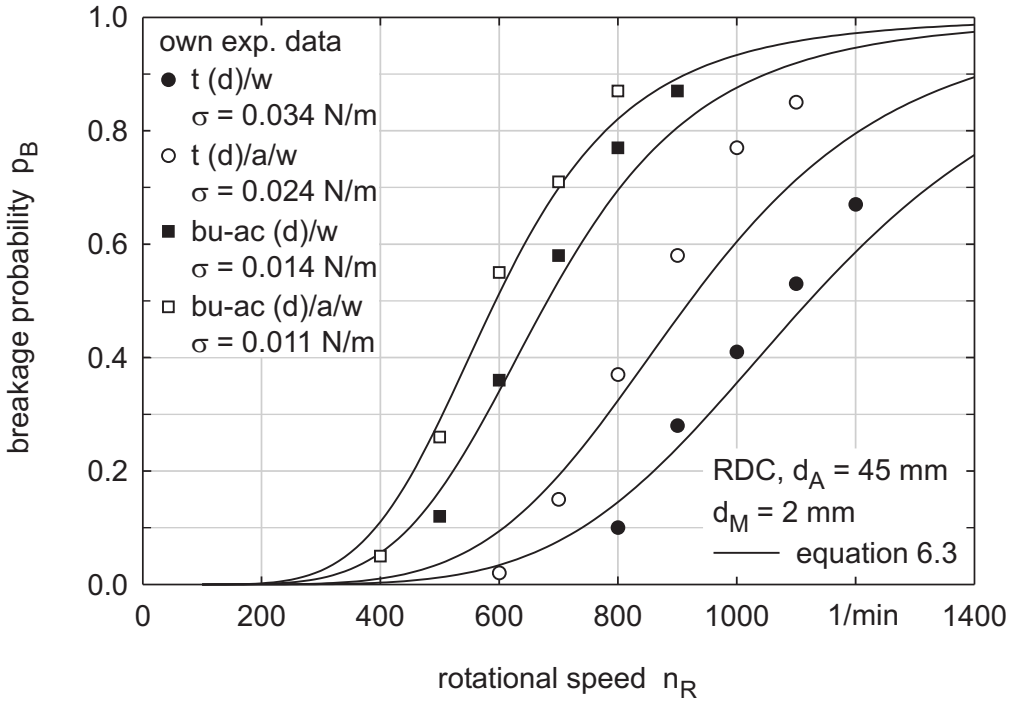

Figure 6.10: Impact of the interfacial tension σ on the single drop breakage in a compartment with a rotating disc

The parameter We_{mod} in *equation (6.3)* is a modified Weber number given by:

$$We_{mod} = \frac{\rho_c^{0.8} \cdot \eta_c^{0.2} \cdot d_M \cdot d_A^{1.6} \cdot [(2 \cdot \pi \cdot n_R)^{1.8} - (2 \cdot \pi \cdot n_{R,\,crit.})^{1.8}]}{\sigma} \tag{6.4}$$

The Weber number describes the ratio of the destructive forces of the flow in the compartment to the stabilising forces from the interfacial tension. The critical rotational speed $n_{R,\,crit.}$ characterises that rotational speed at which a mother drop with a certain size first splits. It is given by:

$$n_{R,\,crit.} = C_4 \cdot \frac{d_A^{-2/3} \cdot \eta_d \cdot d_M^{-4/3}}{2 \cdot (\rho_c \cdot \rho_d)^{0.5}} + \left[\left(C_4 \cdot \frac{d_A^{-2/3} \cdot \eta_d \cdot d_M^{-4/3}}{2 \cdot (\rho_c \cdot \rho_d)^{0.5}} \right)^2 + C_5 \cdot \frac{\sigma}{\rho_c \cdot d_A^{4/3} \cdot d_M^{5/3}} \right]^{0.5} \tag{6.5}$$

The constant factors C_i in *equation (6.3)* and *equation (6.5)* were determined by analysing the experiments of several groups, see also *Final Report AiF 40 ZN 2004*. The constant parameters C_i for RDC-compartments are listed in *table (6.4)*.

Table 6.4: Constant factors C_i of equation (6.3) and equation (6.5) for determining the breakage probability in agitated compartments

Type of internal	C_1	C_2	C_3	C_4	C_5
Rotating disc	$1.29 \cdot 10^{-6}$	0.33	2.78	0.02	0.13
Kühni - blade agitator	$1.63 \cdot 10^{-3}$	0.48	3.05	0.13	$1.21 \cdot 10^{-2}$

The breakage probabilities calculated from *equation (6.3)* are shown in *figure (6.8)*, *figure (6.9)* and *figure (6.10)* by dashed and solid lines. These figures and the investigations of Schmidt prove that *equation (6.3)* represents a good correlation to determine the breakage probability in different RDC-compartments for a wide range of operating conditions.

- *Breakage probabilities in agitated columns with Kühni blade agitators*

Kühni blade agitators accelerate the liquid in radial direction, producing a characteristic flow pattern within the compartments, see *chapter 5.5*. Due to the large shear stresses, even small drops are split at low rotational speeds. For this reason, the breakage of drops in a Kühni-compartment was investigated with rotational speeds as low as 50 to 250 1/min. Experiments with higher rotational speeds were difficult to carry out because many drops remained in the Kühni-compartment for a long time. In addition, drops were often pulled back into the compartment after passing the measuring section. However, rotational speeds higher than 250 1/min are generally of no practical interest. The breakage of single drops for rotational speeds higher than 250 1/min was therefore not investigated.

Similar to the RDC-compartment, the breakage probability in the Kühni-compartment increases with increasing rotational speed and mother drop size. The breakage probability of the butyl acetate system is noticeably higher than of the toluene system, see *figure (6.11)*. Furthermore, addition of some acetone to the binary mixtures results in a significant increase of the breakage events due to the reduction of the interfacial tension, see *figure (6.12)*.

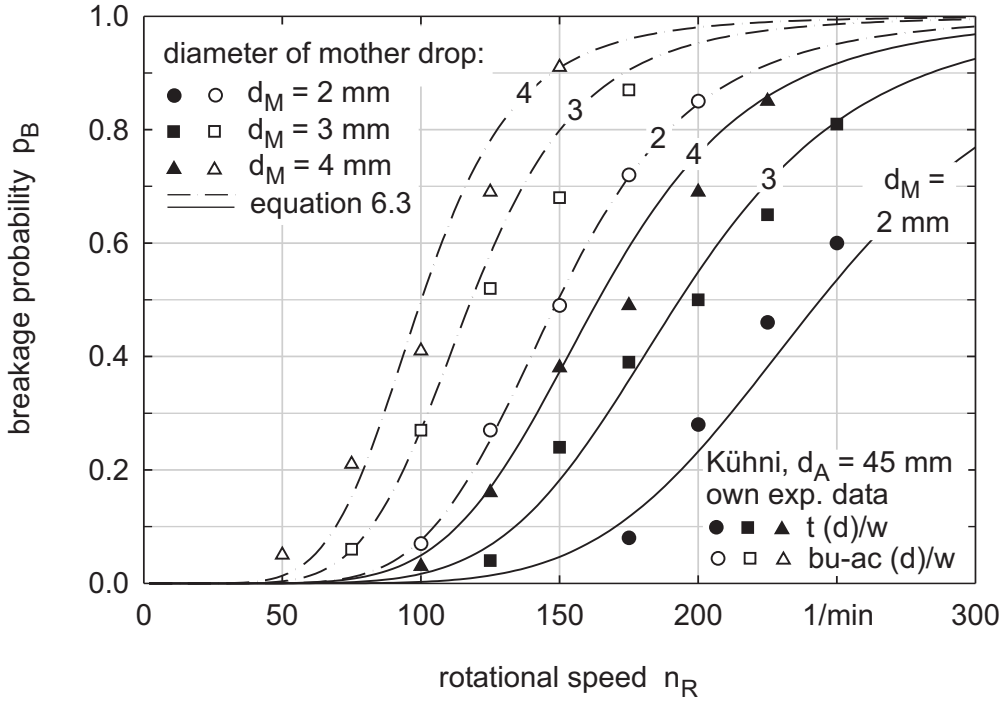

Figure 6.11: Breakage probability of single toluene and butyl acetate drops in an agitated Kühni-compartment; influence of drop size, energy input and interfacial tension

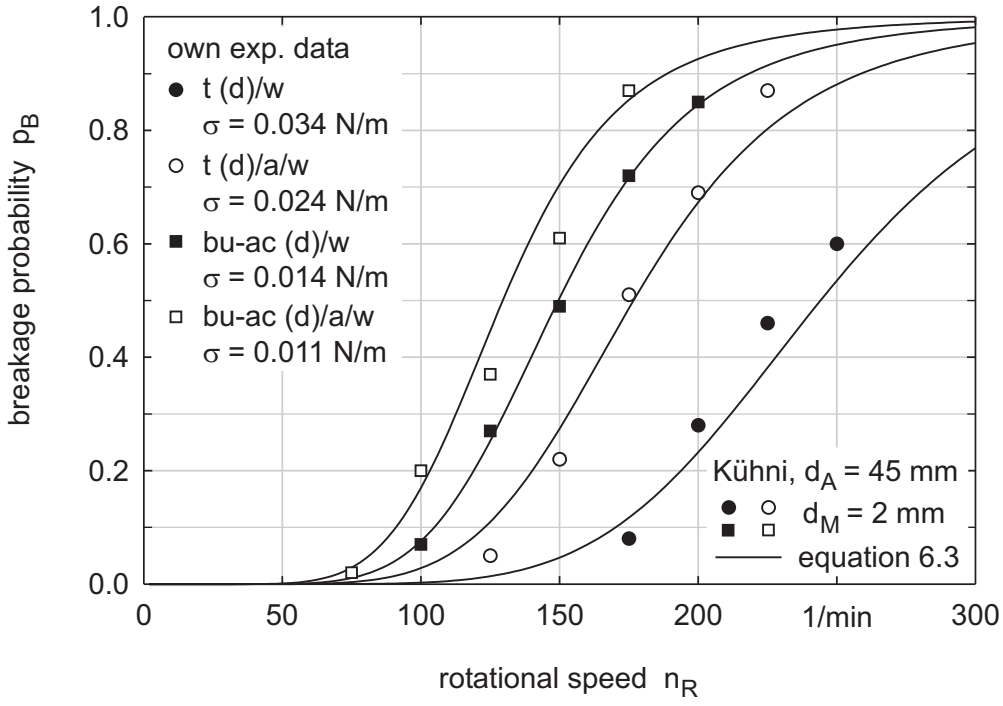

Figure 6.12: Reduction of the interfacial tension σ in liquid/liquid-systems and its effect on the breakage mechanisms in an agitated Kühni-compartment

Almost the same correlation as for RDC-compartments can be used to predict the breakage probability in Kühni-compartments. The parameters C_i in *equation (6.3)*, which were determined by a rigorous regression analysis, are listed in *table (6.4)*. For all test systems a satisfactory agreement between the calculated and measured values was found, see *figure (6.11)* and *figure (6.12)*. Hence, the breakage probability in agitated RDC- and Kühni-compartments can be determined with only one correlation and two sets of parameters. This leads to a simplification if the new correlation is used to determine drop size profiles in extraction columns by DPBMs.

• *Comparison of the breakage probability in columns with different internals*

The breakage probabilities of butyl acetate drops in pulsed compartments for a pulsation intensity of 2.0 cm/s are shown in *figure (6.13)*. The comparison of the breakage probabilities of both investigated types of sieve trays reveals that breakage is significantly higher for sieve trays with smaller holes. The structured packing demonstrates a significantly higher breakage performance than the sieve tray with 4 mm holes but results in lower breakage probabilities than the sieve tray with 2 mm holes.

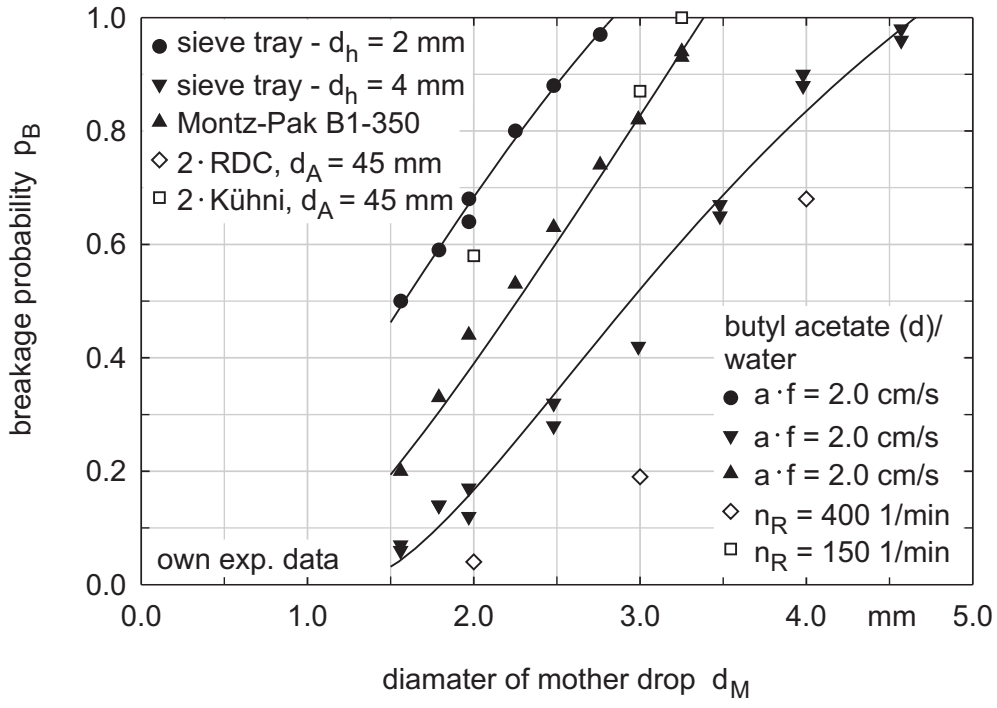

Figure 6.13: Comparison of the breakage probability in compartments with different internals but same compartment height (a single sieve tray, a single packing and two agitators were installed inside the columns)

The influence of the agitator geometry on the breakage rates was previously discussed. Kühni blade agitators have a high energy input and thus drop breakage occurs for much lower rotational speeds than for rotating discs, see *figure (6.14)*. While in the Kühni-compartment breakage probabilities of about 90 % are recorded at a rotational speed of 175 1/min, breakage of single drops in the RDC-compartment begins at a rotational speed of 300 1/min.

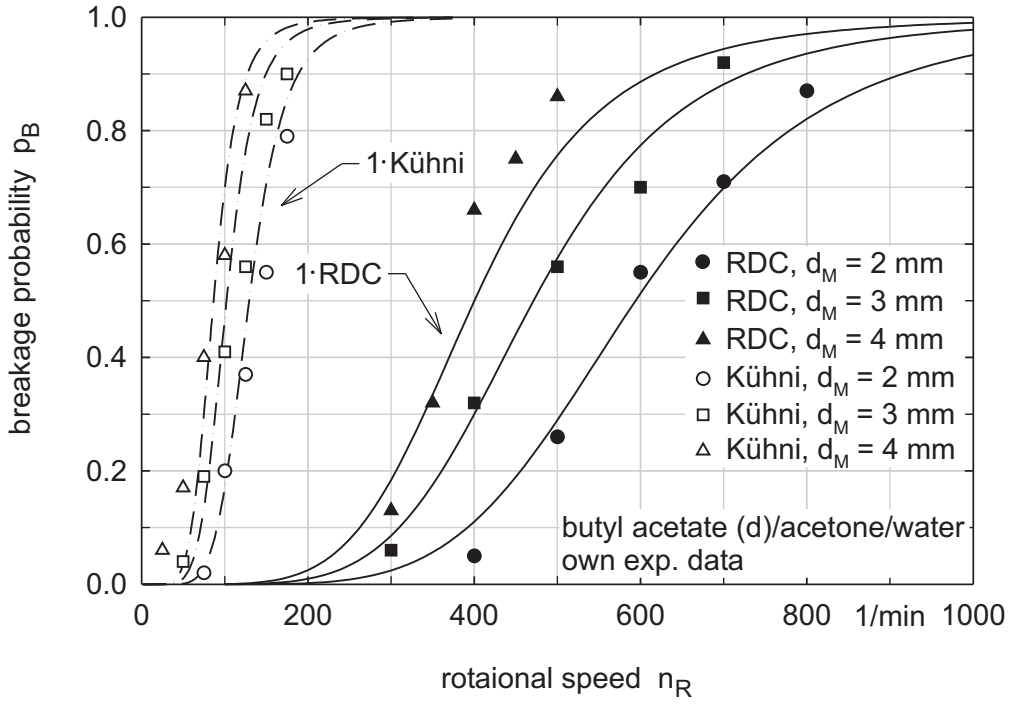

Figure 6.14: Comparison of the influence of the geometry of a rotating disc and a Kühni blade agitator on the breakage probability of single drops (a single rotating disc and a single Kühni blade agitator were installed inside the agitated column)

To compare the breakage rates of all internals used in the experiments, additional tests were carried out with two rotating elements of the same type. The set-up with two agitated compartments, each with a height of 50 mm, had the same overall compartment height of 100 mm as the sieve tray and the structured packing. The results of these experiments are shown in *figure (6.13)*. The use of two rotating discs yields very low breakage probabilities for rotational speeds as high as 400 1/min. The use of two Kühni blade agitators results in high breakage probabilities for rotational speeds as low as 150 1/min. The breakage in the Kühni-compartments is slightly higher than in the pulsed packed compartment and somewhat lower than in the compartment with a sieve tray with 2 mm holes.

6.3 Number of Daughter Drops Produced by the Breakage of a Mother Drop

During the breakage of a single mother drop more than two daughter drops are often produced. Particularly at relative high energy inputs, large drops break into several daughter drops with a relatively wide size distribution. The data of the number of produced daughter drops in this chapter represent averaged values from at least 100 measurements.

- *Number of daughter drops produced in pulsed columns*

In pulsed columns the number of daughter drops steadily increases with increasing mother drop diameter and pulsation intensity. As a typical example for pulsed columns, the number of daughter drops produced in a compartment with a sieve tray with 4 mm diameter holes is shown in *figure (6.15)*. At a pulsation intensity of 2.0 cm/s, a single butyl acetate mother drop splits into up to six daughter drops.

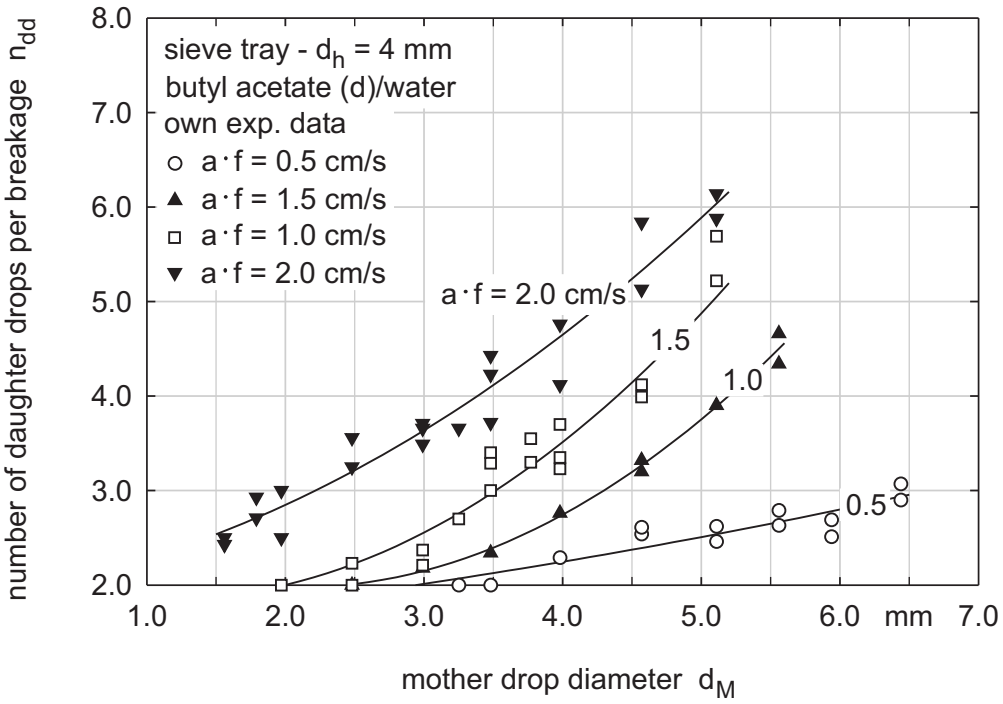

Figure 6.15: Number of daughter drops as a function of mother drop size and pulsation intensity in a sieve tray compartment

The experiments in the pulsed sieve tray compartments also reveal that, regardless of the test system, similar numbers of daughter drops are produced for same ratios of the mother drop diameter to the stable diameter d_M/d_{stab}. An increase of this ratio leads to a similar increase

in the number of daughter drops produced, see *figure (6.16)*. Since the experimental results with sieve trays with smaller and with larger holes show the same dependence on d_M/d_{stab}, *figure (6.16)* represents a characteristic plot for both types of sieve trays.

The averaged number of daughter drops per breakage in pulsed compartments can thus be described by a correlation developed by *Hancil and Rod 1988*:

$$n_{dd} = 2 + C_1 \cdot \left[\left(\frac{d_M}{d_{stab}} \right) - 1 \right]^{C_2} \tag{6.6}$$

The parameters C_i of this equation (determined from own experiments) are listed in *table (6.5)*. *Figure (6.16)* proves that *equation (6.6)* correlates the number of daughter drops in pulsed sieve tray compartments for all test systems very well.

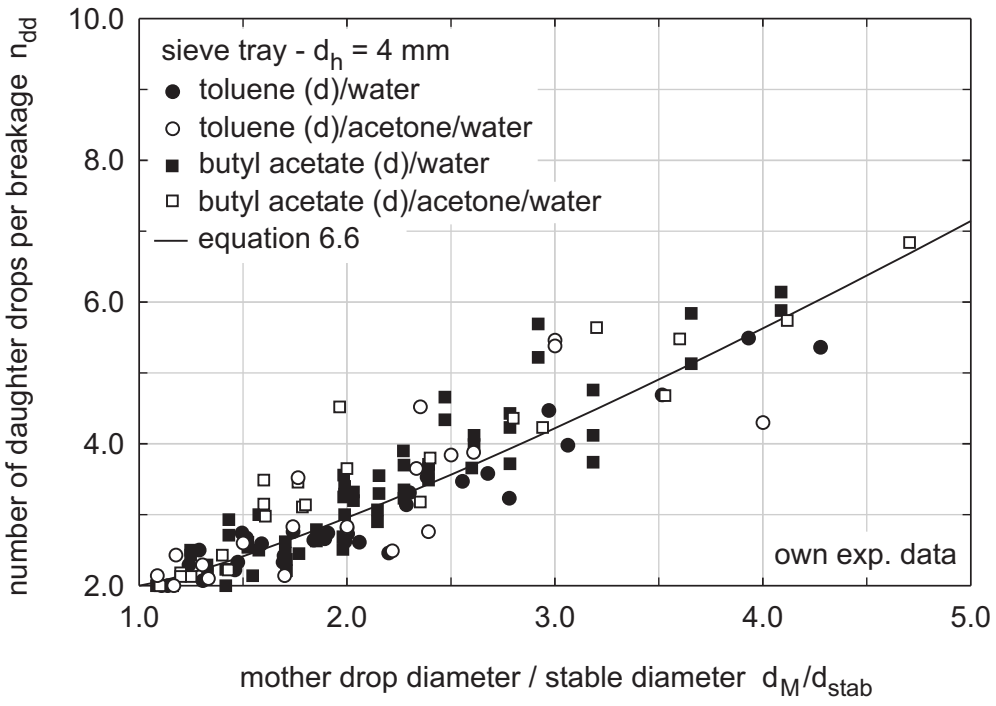

Figure 6.16: Influence of the characteristic ratio of the drop diameters d_M/d_{stab} on the production of daughter drops in pulsed sieve tray compartments

Table 6.5: Parameters C_i of equation (6.6) for the prediction of the averaged daughter drop number produced during the breakage of a mother drop in different compartments

Type of internal	C_1	C_2
Sieve tray - d_h = 2 mm	0.96	1.21
Sieve tray - d_h = 4 mm	0.96	1.21
Montz-Pak B1-350	0.34	1.96
Rotating disc	$1.44 \cdot 10^{-3}$	2.93
Kühni - blade agitator	0.03	2.45

The number of daughter drops produced in the structured packing can also be determined by *equation (6.6)*. However, the investigations in the pulsed packed compartment reveal that the breakage of mother drops results in lower numbers of daughter drops than in the sieve tray compartments, see *figure (6.17)*. Hence, the prediction of the number of daughter drops with *equation (6.6)* has to be carried out with different parameters C_i which are listed in *table (6.5)*.

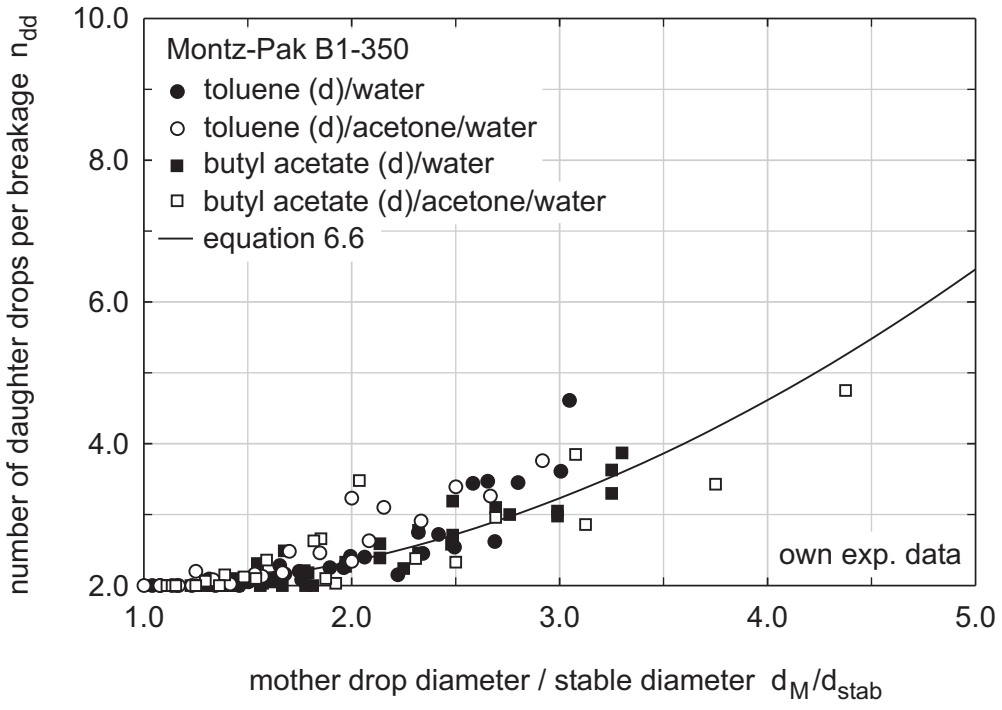

Figure 6.17: Influence of the characteristic ratio of the drop diameters d_M/d_{stab} on the averaged number of daughter drops in a pulsed packed compartment

- *Number of daughter drops produced in agitated columns*

The breakage behaviour and the number of daughter drops produced in agitated columns depends on the same parameters as in pulsed columns. An increase of mother drop size and of energy input always results in higher numbers of daughter drops. In particular, for systems with a low interfacial tension more daughter drops are produced by the shear stresses in the flow fields.

The results of the investigations in the RDC-compartment with single toluene drops are shown in *figure (6.18)*. Generally more than two drops are produced. Almost the same numbers of daughter drops are produced by the Kühni blade agitator. However, drop breakage occurs at significantly lower rotational speeds.

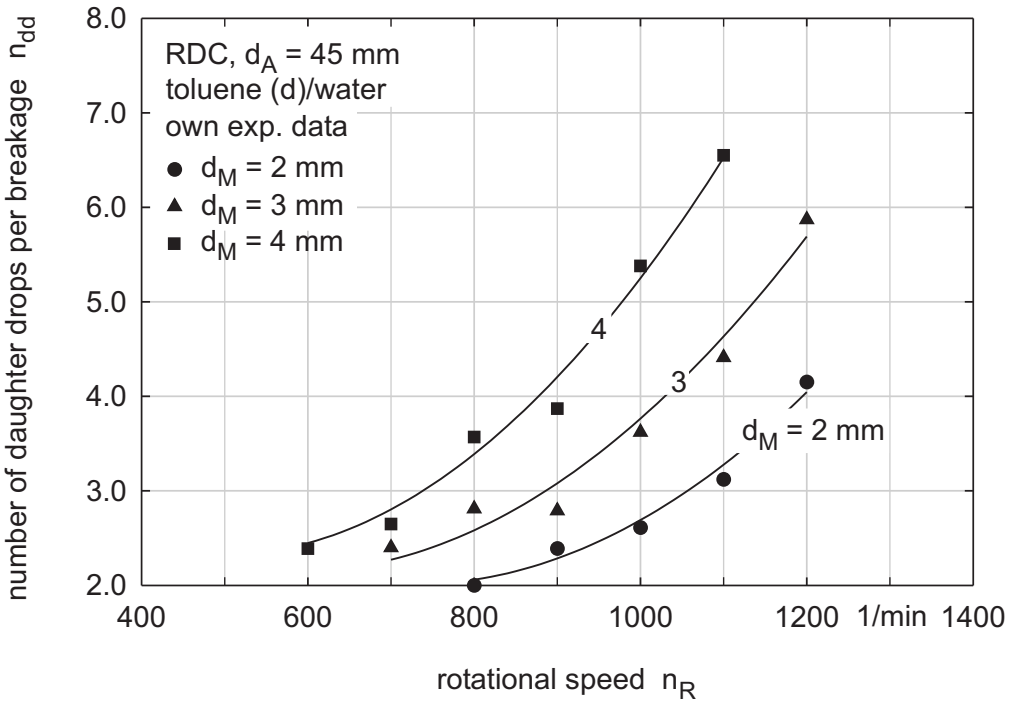

Figure 6.18: Impact of the mother drop size and the rotational speed on the averaged number of daughter drops produced during breakage in the RDC-compartment

An increase of the characteristic ratio d_M/d_{stab} causes an increase of the number of daughter drops in both the RDC-compartment and the Kühni-compartment, see *figure (6.19)*. The number of daughter drops in agitated compartments can thus be predicted by *equation (6.6)*. The stable diameter required is found with *equation (6.5)*. For this purpose, the parameter d_M has to be replaced with d_{stab}.

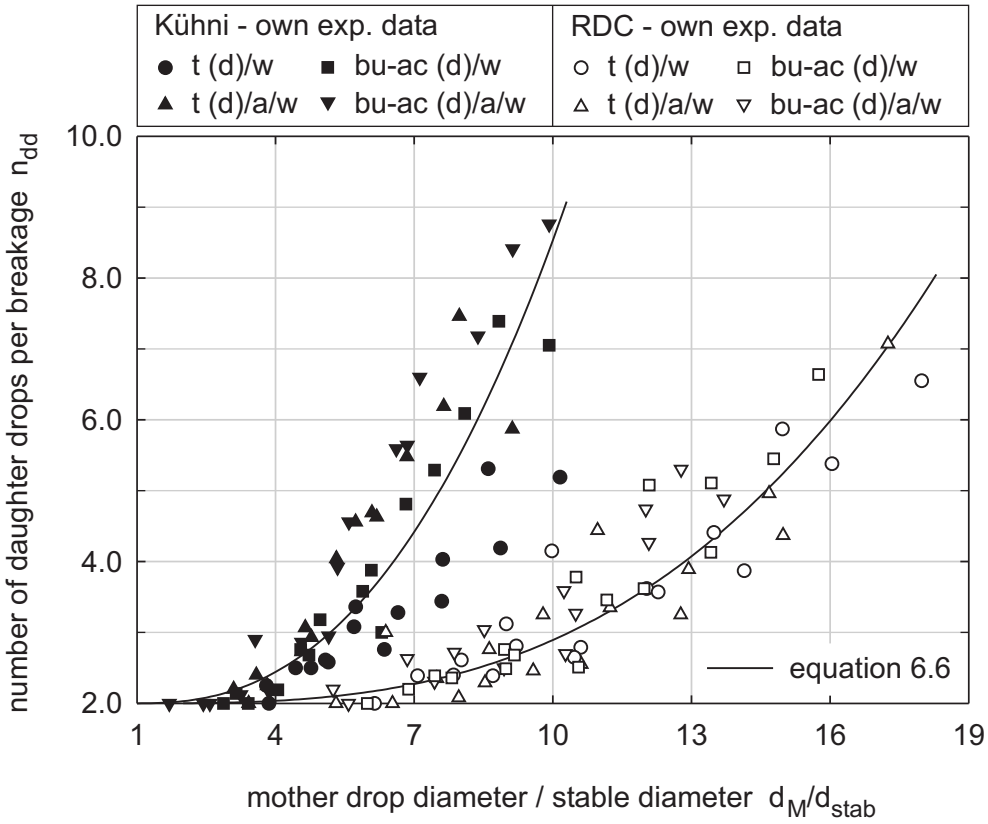

Figure 6.19: Effect of an increase of the characteristic ratio d_M/d_{stab} on the daughter drop production in an agitated RDC-compartment or Kühni-compartment

It has to be mentioned that *equation (6.5)* was developed for predicting the breakage probability and not for predicting the stable drop diameter. For this reason, *equation (6.5)* results in relatively low values of the characteristic diameter d_{stab}[5] and hence in high values of the ratio d_M/d_{stab}. Apart from this deviation, the combination of *equation (6.5)* with *equation (6.6)* results in satisfactory agreement with the measured numbers of daughter drops in the RDC-compartment and in the Kühni-compartment, see *figure (6.19)*. The parameters that are necessary to determine the number of daughter drops in agitated compartments are listed in *table (6.5)*.

5. In the literature d_{stab} is also often called the critical drop diameter d_{crit}. For better understanding and to prevent confusion, the term d_{stab} is always used in this chapter.

6.4 Volumetric Density Distribution of Produced Daughter Drops

The volumetric density distribution of the produced daughter drops has to be known for predicting the drop breakage in extraction columns by DPBMs. As previously mentioned, there are numerous correlations in the literature for the volumetric density distribution of daughter drops. One method which proved its worth during this work is given by *Bahmanyar and Slater 1991*. According to these authors, the volumetric density distribution q_3 of the daughter drops is determined as a function of the number of daughter drops n_{dd} by the following correlation:

$$q_3(d_M, d_{dd}) = 3 \cdot n_{dd} \cdot (n_{dd} - 1) \cdot \left[1 - \left(\frac{d_{dd}}{d_M}\right)^3\right]^{(n_{dd}-2)} \cdot \frac{d_{dd}^5}{d_M^6} \tag{6.7}$$

The comparison of this correlation with data obtained in the own experiments in pulsed and agitated compartments is shown in the diagrams of *figure (6.20)*. The diagrams reveal that *equation (6.7)* is suitable for determining the volumetric density distribution of daughter drops for different systems, different sizes of mother drops and different energy inputs.

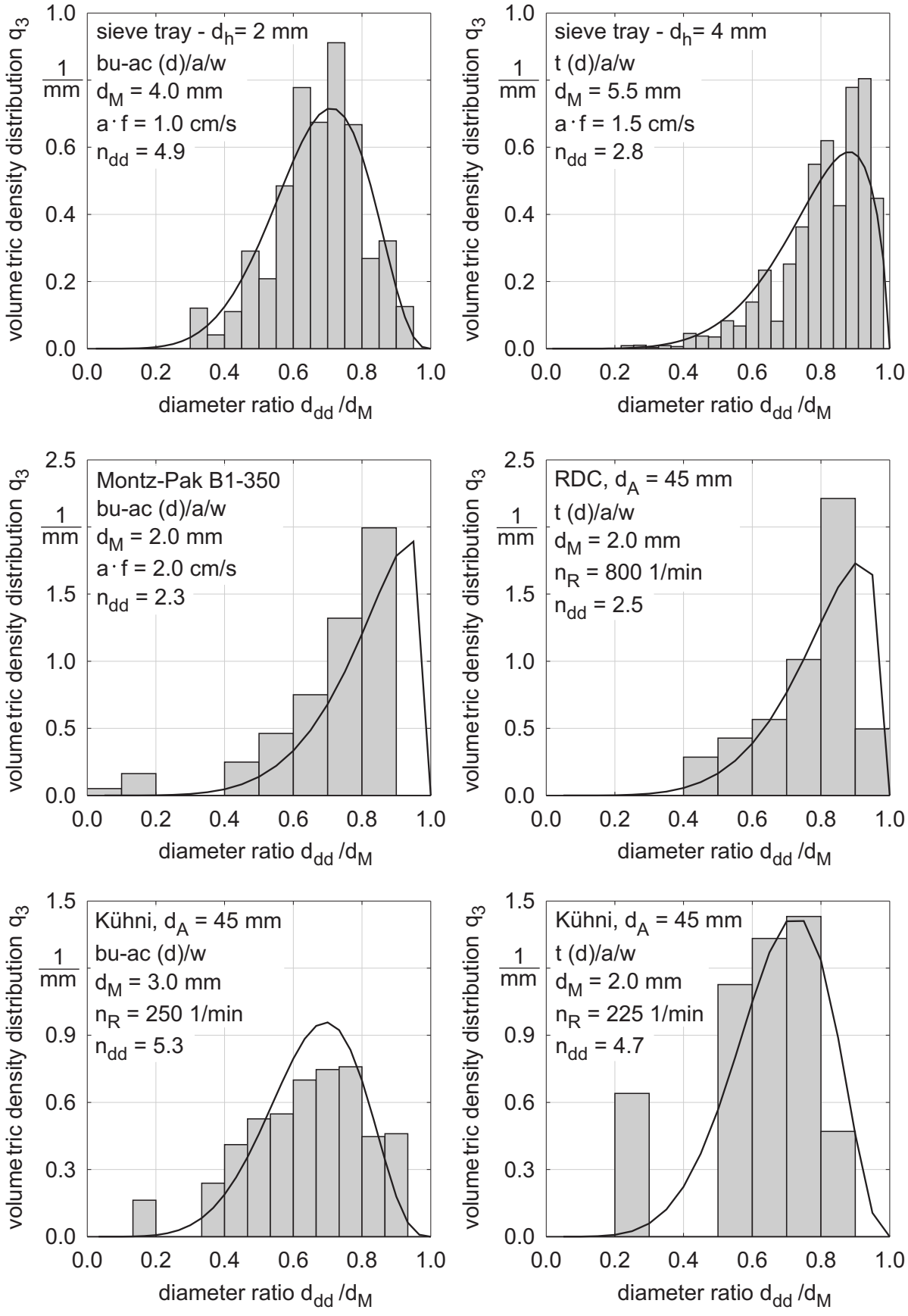

Figure 6.20: Comparison of equation (6.7) with volumetric density distributions of daughter drops measured in compartments with different internals (own exp. data)

7 Mass Transfer In and Out of Single Drops

Although the phenomena that influence mass transfer in and out of single drops are well known, a general model has not been developed yet for accurately predicting mass transfer rates, see *Wagner 1999*. Uncertainties exist in quantitatively determining the effects of circulations within a drop, of Marangoni convections as well as of wakes and eddies around the drop, see also *Brandner and Brauer 1993*. An unsolved problem is also the prediction of the influence of surfactants and electrolytes on mass transfer behaviour of single drops.

Against this background, it is still necessary to perform experiments with single drops to obtain accurate information about mass transfer rates. Mass transfer investigations in laboratory scale columns with and without internals allow the determination of overall mass transfer coefficients β_{od} of single drops. For this purpose, mass transfer experiments were carried out using the same approach as *Qi 1992*, *Hoting 1996* and *Wagner 1999*, see *chapter 2.3*. The overall mass transfer coefficients were calculated by

$$\beta_{od} = \frac{d}{6 \cdot \Delta t} \cdot ln\left(\frac{y^* - y_1}{y^* - y_2}\right) \tag{7.1}$$

7.1 Mass Transfer in Columns Without Internals

Experiments with both liquid/liquid-systems in columns without internals show that the overall mass transfer coefficient β_{od} is considerably increased by an increase of the drop size, see *figure (7.1)* and *figure (7.2)*. Overall mass transfer coefficients of drops with a diameter of 4 mm are approximately twice as high as of drops with a diameter of 2 mm. Furthermore, overall mass transfer coefficients of butyl acetate drops are significantly higher than of toluene drops. This is particularly seen for a transfer direction from the continuous phase to the dispersed phase “c to d“ with an initial concentration difference of x_o -y_o = 0.03 kg/kg. The higher mass transfer rates of butyl acetate drops result from the higher surface mobility of these drops. High surface mobility promotes the generation of circulations within a drop. This causes better mixing of the drop interior and hence higher mass transfer rates than for toluene drops.

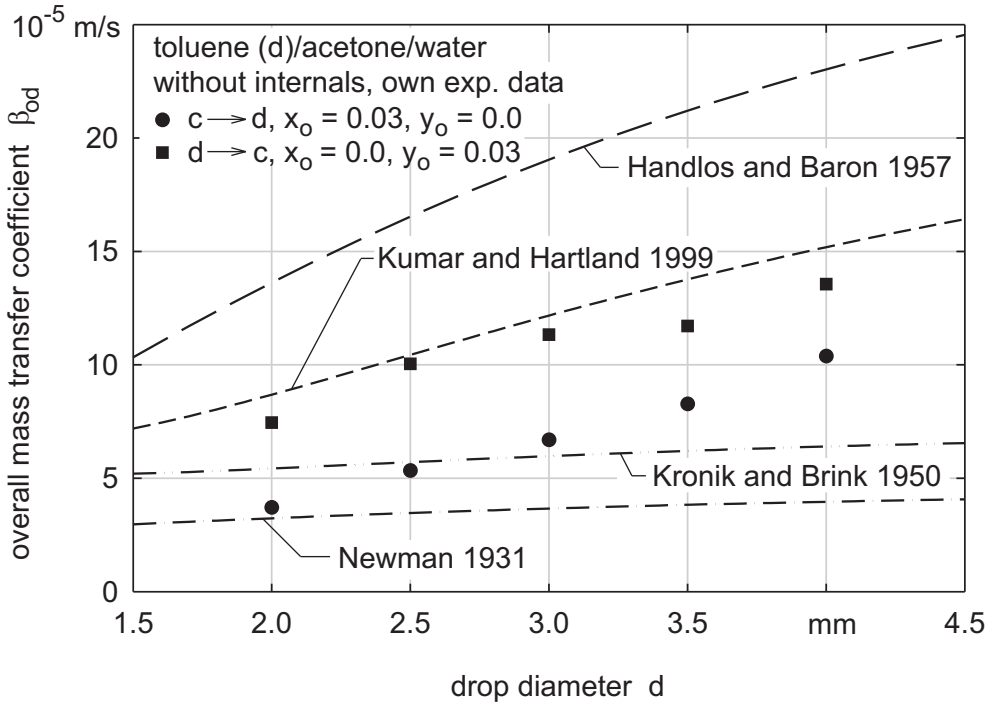

Figure 7.1: Overall mass transfer coefficients of single toluene drops in a column without internals and comparison with models from the literature (see also chapter 2.3)

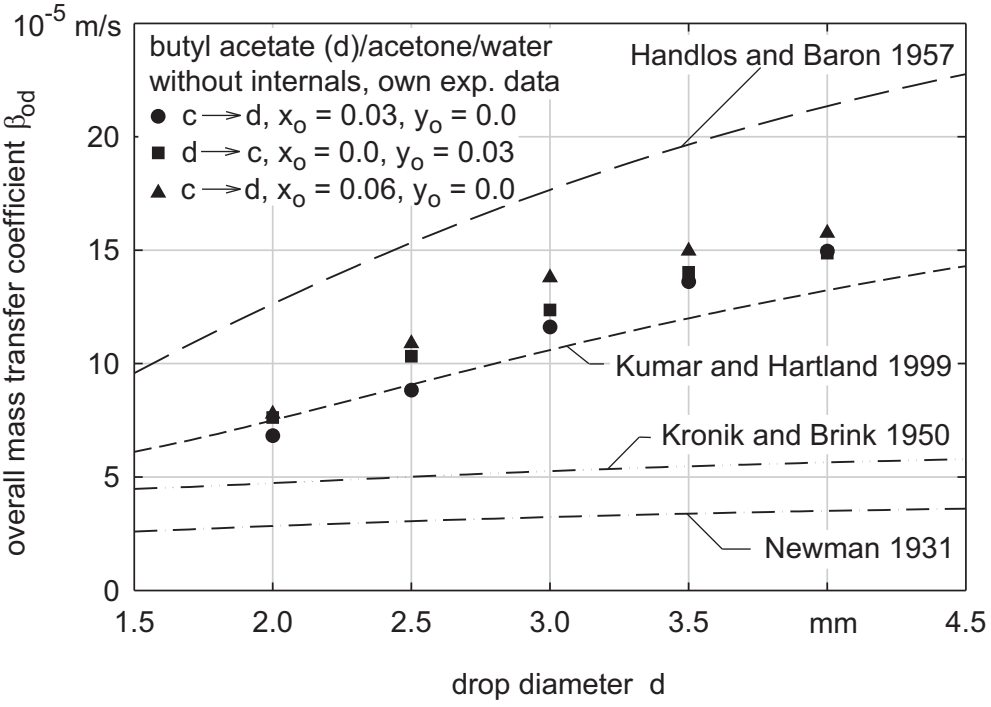

Figure 7.2: Overall mass transfer coefficients of single butyl acetate drops in a column without internals and comparison with models of the literature (see also chapter 2.3)

The influence of the initial concentration difference on mass transfer rates was investigated with butyl acetate drops, see *figure (7.2)*. As expected, higher overall mass transfer coefficients are observed for a higher concentration difference x_o - y_o for the same transfer direction. This is due to the development of Marangoni convections which rise with increasing concentration difference at the interface and which cause turbulent currents inside and outside of a drop. The dependence of Marangoni convections on the concentration difference is also shown by *Wolf 1999* and *Tourneau 2004* for several liquid/liquid-systems.

The results of the investigations for both mass transfer directions ("c to d" and "d to c") are shown in *figure (7.1)* and *figure (7.2)*. For an initial concentration difference of x_o - y_o = 0.03 kg/kg, the mass transfer rates for a transfer direction from "d to c" are higher than for "c to d". The influence of the transfer direction is particularly seen for toluene drops. *Qi 1992* also found a strong increase of the overall mass transfer coefficients of toluene drops for a mass transfer direction from "d to c" compared to the reverse direction.

Experiments with single drops prove that Marangoni convections almost always appear and eruptions are generated at the interface, see *Wolf 1999*. Such eruptions are normally directed into the drops as well as into the bulk of the continuous phase. According to *Qi 1992*, stronger eruptions are produced in that phase to which the solute is transferred. Thus, for a mass transfer direction from "c to d" stronger eruptions are produced in the drops than for the opposite mass transfer direction. For a mass transfer direction from "d to c", stronger eruptions occur in the continuous phase than for the reverse transfer direction. These eruptions can reach deep into the continuous bulk phase. Therefore, the concentration at the interface of the continuous phase is significantly reduced by the constant delivery of "fresh" continuous phase with a low solute concentration. Assuming that this effect is dominant and is increased for a mass transfer direction from "d to c", higher overall mass transfer coefficients are obtained than for "c to d".

In order to compare overall mass transfer coefficients of single drops with models from the literature, it must be clarified whether the mass transfer resistance of only one phase or of both phases has to be taken into account. For this purpose, the dimensionless Brauer number can be used, see also *Henschke 2003*, which is given by:

$$Br = m \cdot \sqrt{\frac{D_d}{D_c}} \tag{7.2}$$

Here, m is the distribution coefficient, D_d is the diffusion coefficient in the dispersed phase and

D_c is the diffusion coefficient in the continuous phase. If the value of the Brauer number is close to zero ($Br \to 0$) the mass transfer resistance is definitely inside the drops. For very high values of the Brauer number ($Br \to \infty$) only the mass transfer resistance in the continuous phase has to be considered. Using the values for D_d, D_c and m proposed by the *EFCE 1984* for a concentration of x_o = 0.03 kg/kg and y_o = 0.03 kg/kg, the Brauer number reaches a value of *Br = 1.3* for both liquid/liquid-systems used.[6] Thus, the limiting mass transfer resistance is inside and not outside of the drops.

According to *Henschke 2003,* further information about the limiting mass transfer resistance is obtained when the mass transfer coefficients inside the drop β_d and outside the drop β_c are compared. For this purpose, the time required for β_d, which is time-dependent, to reach the same value as β_c, which is constant, is evaluated.

In the following sections, mass transfer of acetone from a continuous water phase (x_o = 0.03 kg/kg) to a toluene drop with a diameter of 4 mm (y_o = 0.0 kg/kg) is examined. Mass transfer coefficients β_c and β_d can be determined as follows: Applying *equation (2.74)* of *Steiner 1986* results in a mass transfer coefficient in the continuous phase of $\beta_c = 13.0 \cdot 10^{-5} m/s$.

Equation (2.62) in combination with the first derivatives of the approximate solutions to the Newman model, see *equations (2.61),* yields the following correlations for the mass transfer coefficient β_d for short and long contact times, respectively:

$$\beta_d = -\frac{y_o - y^*}{y(t) - y^*} \cdot \frac{2 \cdot D_d}{d} \cdot \left(1 - \sqrt{\frac{1}{\pi \cdot Fo_d}}\right) \qquad for \quad Fo_d < 0.1584 \qquad (7.3)$$

$$\beta_d = \frac{y_o - y^*}{y(t) - y^*} \cdot \frac{4 \cdot D_d}{d} \cdot exp(-\pi^2 \cdot Fo_d) \qquad for \quad Fo_d \geq 0.1584 \qquad (7.4)$$

Using *equations (2.61)* again to eliminate the concentration difference in the equations above permits the mass transfer coefficient β_d and the Sherwood number Sh_d to be correlated for very short and long contact times:

$$\beta_d = \sqrt{\frac{D_d}{\pi \cdot t}} \qquad \Rightarrow \qquad Sh_d = \frac{2}{\sqrt{\pi \cdot Fo_d}} \qquad for \quad Fo_d \to 0 \qquad (7.5)$$

$$\beta_d = \frac{2}{3} \cdot \frac{\pi^2 \cdot D_d}{d} \qquad \Rightarrow \qquad Sh_d = \frac{2}{3} \cdot \pi^2 \qquad for \quad Fo_d \geq 0.1584 \qquad (7.6)$$

6. For the given solute concentrations, the distribution coefficient *m* is 0.83 for the toluene system and 0.92 for the butyl acetate system. The diffusion coefficients are listed in *chapter 3.2*.

For short contact times the mass transfer coefficients β_c and β_d become equal at a time of t = 0.053 seconds. This is nearly the time a drop with a diameter of 4 mm needs to rise a distance which is identical to its own diameter. For long contact times the mass transfer coefficient β_d reaches a value of $\beta_d = 4.6 \cdot 10^{-6}\ m/s$, which is approximately 28 times lower than the mass transfer coefficient β_c. Even if the correlation of *Kronik and Brink 1950* is used, which leads to higher values of β_d than the model of Newman, the mass transfer coefficient β_c is still 11 times higher for long contact times.

Both mass transfer coefficients have the same values only for very short contact times. In addition, it is not certain whether the mass transfer coefficient β_c is actually constant or even higher for short times than for long contact times. It can thus be concluded that the whole mass transfer resistance lies inside the drop. Considerations of other drop sizes for both systems confirm this result. Thus, for all investigated drop sizes and systems it is assumed that the mass transfer resistance is mainly inside the drops. Therefore, the experimentally determined overall mass transfer coefficients β_{od} are compared with models from the literature for β_d.

To get time-averaged mass transfer coefficients from *Newman's* and *Kronik and Brink's* correlations the approximate solution of *Clift et al. 1978* for the time-averaged Sherwood number $\overline{Sh_d}$ is used:

$$\overline{Sh_d} = \frac{\overline{\beta_d} \cdot d}{D_d} = -\frac{2}{3 \cdot Fo_d} \cdot ln\left(\frac{y(t) - y^*}{y_o - y^*}\right) \tag{7.7}$$

The combination of *equation (7.7)* and *equations (2.61)* allows the determination of the time-averaged mass transfer coefficients from the model of Newman for rigid drops.

Kronik and Brink's model represents a further development of Newman's model for circulating drops. Thus, it can also be described by the same approximate solutions replacing the molecular diffusion coefficient D_d by an effective diffusivity $D_{d,\,eff}$ that is R times higher: $D_{d,\,eff} = R \cdot D_d$. The dimensionless number R can be interpreted as an enhancement factor that accounts for the effect of circulations within a drop on mass transfer, see *Clift et al. 1978*. Accordingly, the time-averaged Sherwood number $\overline{Sh_d}$ and the mass transfer coefficients $\overline{\beta_d}$ are predicted using the following equations for short and long contact times for both models:

$$\overline{Sh_d} = -\frac{2}{3 \cdot Fo_d} \cdot ln\left[1 - \left(\frac{6}{\sqrt{\pi}} \cdot \sqrt{R \cdot Fo_d}\right) + 3 \cdot R \cdot Fo_d\right] \qquad for \quad Fo_d < 0.1584 \qquad (7.8)$$

$$\overline{Sh_d} = -\frac{2}{3 \cdot Fo_d} \cdot ln\left[\frac{6}{\pi^2} \cdot exp(-\pi^2 \cdot R \cdot Fo_d)\right] \qquad for \quad Fo_d \geq 0.1584 \qquad (7.9)$$

where $R = 1$ for the model of *Newman* and $R = 2.5$ for the model of *Kronik and Brink*.

The comparison of the experimental overall mass transfer coefficients with the models discussed above as well as with the models of *Handlos and Baron 1957* and *Kumar and Hartland 1999* is illustrated in *figure (7.1)* and *figure (7.2)*.

Small toluene drops show a behaviour similar to rigid drops for a mass transfer direction from "c to d". At higher drop sizes the circulations within the drops increase the mass transfer. The mass transfer of toluene drops with a diameter of 2.5 to 3.0 mm is well described by the model of *Kronik and Brink*, see *figure (7.1)*. For larger toluene drops, higher overall mass transfer coefficients are experimentally determined than predicted by this model. The correlations of *Handlos and Baron* as well as *Kumar and Hartland* result in values of the mass transfer coefficients that are too high for a transfer direction from "c to d". However, a good agreement between *Kumar and Hartland's* correlation and the experimental data is given for the reverse transfer direction from "d to c".

The overall mass transfer coefficients of butyl acetate drops are higher than the values predicted by the models of *Newman* and *Kronik and Brink*. This must be related to the high degree of circulations inside the drops, see *figure (7.2)*. The model of *Kronik and Brink* predicts the same values as the experimentally values for an increase of the effective diffusivity only. A regression analysis for the dimensionless enhancement factor R yields values from 4.6 to 14.9 for the individual butyl acetate drop diameters. Similar enhancement factors were found by *Boyadzhiev et al. 1969* and *Steiner 1988* for several liquid/liquid-systems. The high values of the enhancement factors indicate the production of eruptions at the interface and turbulent mixing inside the butyl acetate drops. A very good agreement with the experimental data is given by the *Kumar and Hartland* model. Their model does not only properly predict the increase of the mass transfer coefficient with increasing drop diameter, but also predicts the same values as the measured ones. Again, the *Handlos and Baron* model shows large deviations from the experimental data.

7.2 Mass Transfer in Pulsed Columns with Different Internals

To determine the influence of internals on mass transfer rates of single drops, experiments were conducted in columns with different compartment types. Several internals of one type were always installed inside the laboratory scale columns resulting in an overall measuring section height of 200 mm. For example, three sieve trays with a distance of 100 mm from each other were assembled in the pulsed column. All experiments in columns with internals were carried out with a mass transfer direction from the continuous to the dispersed phase “c to d“ and an initial concentration difference of x_o - y_o = 0.03 kg/kg.

- *Mass transfer in pulsed columns with sieve trays*

The results of the investigations in the pulsed column with sieve tray compartments are shown in *figure (7.3)* and *figure (7.4)*. For both test systems mass transfer rates increase with increasing drop diameter. Furthermore, overall mass transfer coefficients β_{od} in the pulsed sieve tray column are higher than in columns without internals. Beside the influence of the drop diameter the effect of pulsation intensity on mass transfer rates is apparent. In general, an increase of the pulsation intensity causes increasing mass transfer rates. This is confirmed by the overall mass transfer coefficients for pulsation intensities of $a \cdot f$ = 1.5 cm/s and $a \cdot f$ = 2.0 cm/s which are higher than those for lower pulsation intensities.

Comparison of mass transfer coefficients of both liquid/liquid-systems reveals that mass transfer rates into butyl acetate drops are higher than into toluene drops. According to the results of *Qi 1992*, *Wagner 1999* and *Henschke 2003*, the mass transfer into a single drop in pulsed sieve tray compartments is enhanced by the turbulent currents close to the trays. These currents are primarily caused by the pulsation of liquid in the column. Furthermore, mass transfer improvement results from the deformations of the drops by their motion through the sieve trays. These deformations cause form oscillations of the drops and, thus, a high level of mixing of the drop interior. Because butyl acetate drops are less stable than toluene drops they show stronger form oscillations and subsequently higher mass transfer rates.

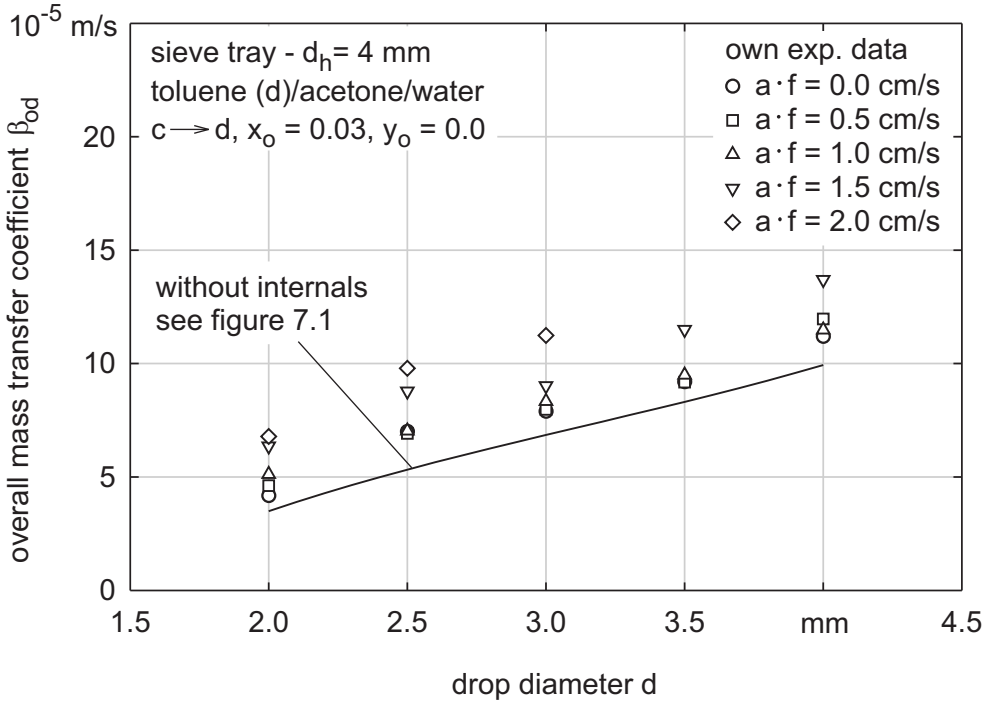

Figure 7.3: Overall mass transfer coefficients of toluene drops in pulsed compartments with sieve trays with a hole diameter of 4 mm

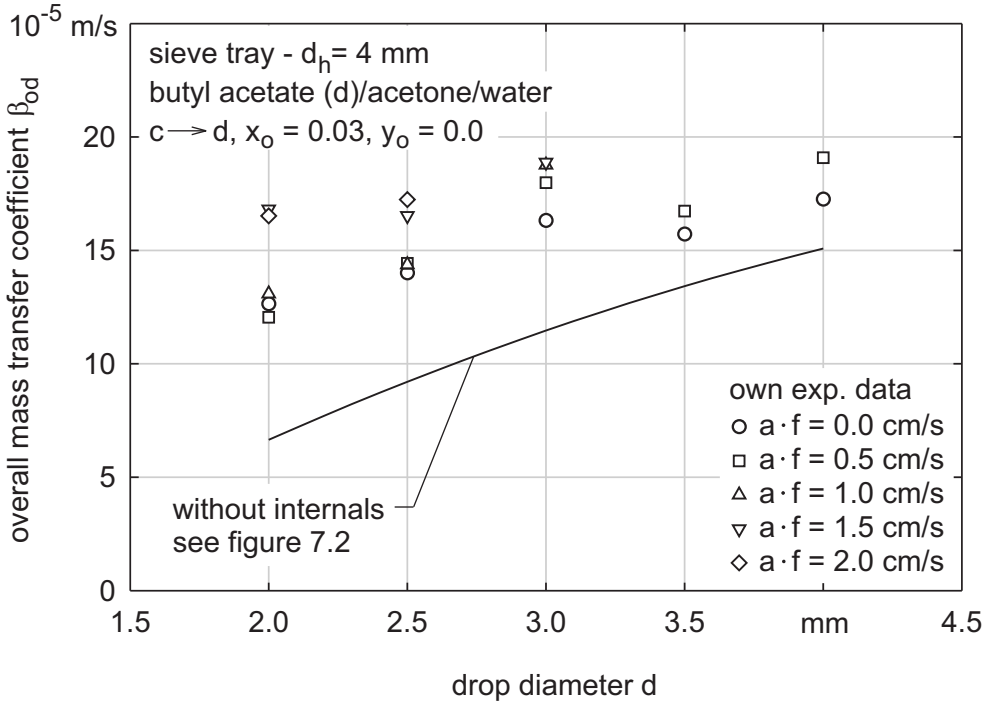

Figure 7.4: Overall mass transfer coefficients of butyl acetate drops in pulsed compartments with sieve trays with a hole diameter of 4 mm

Mass transfer of single drops in compartments with sieve trays with 2 mm holes is difficult to investigate since often too many breakage events occur. The determined overall mass transfer coefficient cannot be attributed to a certain drop size when several drops of different sizes are produced by breakage. For these reasons, only few experiments could be carried out with this type of sieve tray.[7]

Figure (7.5) shows that similar values for the overall mass transfer coefficients of toluene drops exist for both types of sieve trays. A very similar result was obtained in experiments with butyl acetate drops. However, the similar values of β_{od} do not mean that the same change of drop concentration is achieved for both types of sieve trays. Higher concentration changes are obtained in sieve trays with 2 mm holes than with 4 mm holes. Simultaneously, the velocities of single drops are lower in compartments with the sieve trays with the smaller holes. Since the overall mass transfer coefficients are determined as a function of both the drop concentration change and the drop velocity, similar mass transfer coefficients are calculated from *equation (7.1)*.

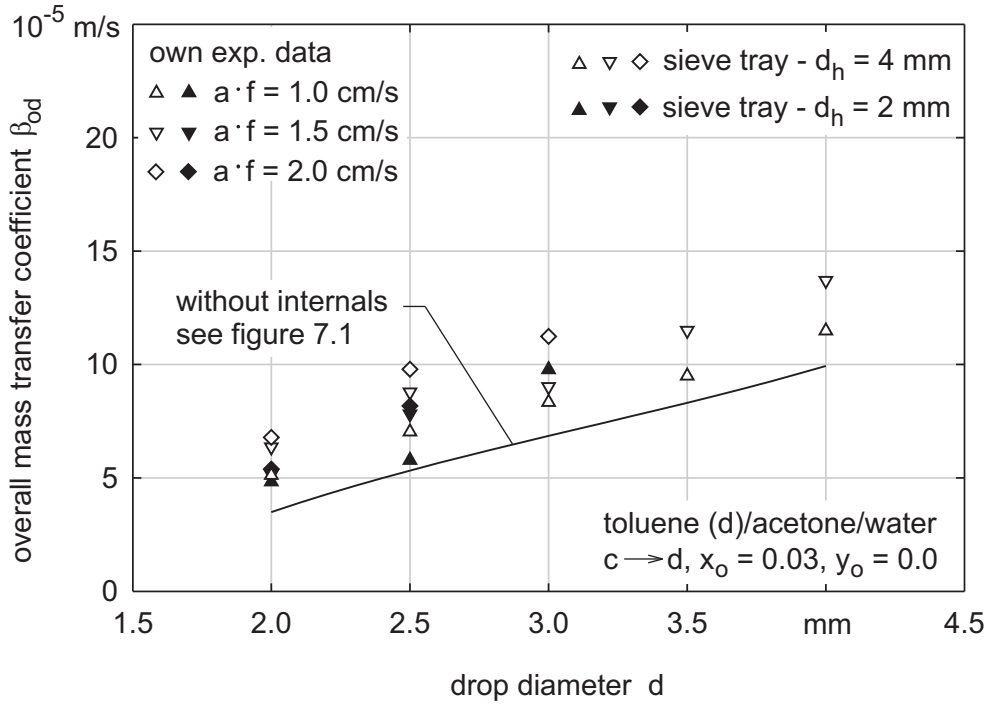

Figure 7.5: Influence of the hole diameter of the sieve trays on the mass transfer coefficients of toluene drops

7. There was a longer time interval between the investigations of mass transfer and of single drop breakage. The drops of the toluene and butyl acetate charges, which were used for these experiments, showed a slightly different breakage behaviour. Therefore, care was taken to insure that only mass transfer experiments where no breakage or where less than 10 of 100 drops were broken were used for analysis.

- *Mass transfer in pulsed columns with structured packings*

Mass transfer of single drops in pulsed columns with structured packings is generally improved by the steady collision of the drops with the packings, the abrupt changes of moving direction, and the steady deceleration and acceleration of the drops. These effects cause turbulent mixing of the drop interior and hence a higher degree of convective transport of the solute towards or away from the interface. Consequently, overall mass transfer coefficients in pulsed columns with structured packings are higher than in columns without internals. This is confirmed by the own experiments in the pulsed column with two structured packings, see *figure (7.6)* and *figure (7.7)*. The overall mass transfer coefficients in the pulsed packed compartments show almost the same increase with increasing pulsation intensity as in the pulsed sieve tray compartments, see also *figure (7.5)*.

In contrast to *Wagner 1999* and own results, *Hoting 1996* found a decrease of the overall mass transfer coefficients of single drops in a pulsed packed column compared to a column without internals. For his experiments, Hoting used structured packings of the same type as in this work. He suggested that the low characteristic drop velocities in pulsed packed compartments are responsible for the decrease of the overall mass transfer coefficients.

Hoting also carried out mass transfer experiments with swarms of drops in a pilot plant extractor with the same structured packings. Furthermore, he calculated concentration profiles by the use of a drop population balance model (DPBM) on the basis of his single drop mass transfer coefficients. Hoting found deviations between calculated and measured concentration profiles. The mass transfer efficiencies calculated by the DPBM were too low compared to the experiments. Since drop size profiles and hold-up profiles in the pilot plant column were correctly described by the DPBM, these deviations may be related to the low values of the mass transfer coefficients.

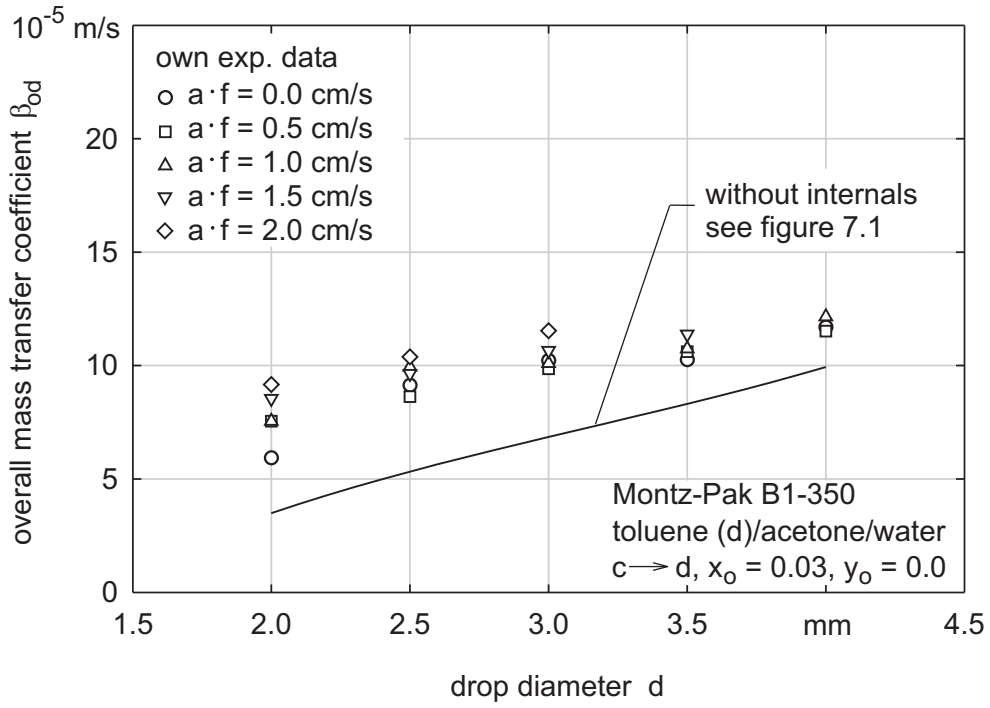

Figure 7.6: Effect of energy input in pulsed compartments with structured packings on the overall mass transfer coefficients of toluene drops

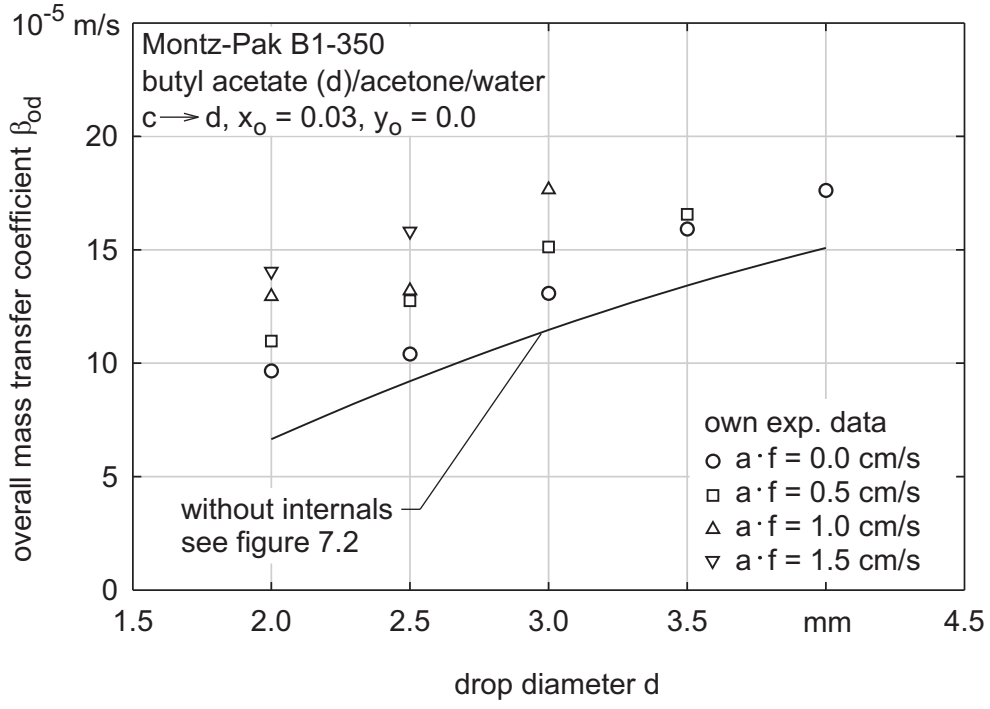

Figure 7.7: Effect of energy input in pulsed compartments with structured packings on the overall mass transfer coefficients of butyl acetate drops

7.3 Mass Transfer in Agitated Columns with Different Internals

The energy input in agitated columns increases the mass transfer by forced circulations of the drops in the compartments and by induced circulations within the drops. In particular, the increase of the circulations within the drops results in a significant increase of the mass transfer rates. Mass transfer of single drops in agitated columns was investigated using four RDC-compartments and four Kühni-compartments.

- *Mass transfer in agitated columns with rotating discs*

The investigations in the laboratory scale column with rotating discs confirm that mass transfer in agitated columns is significantly improved compared to columns without internals, see *figure (7.8)* and *figure (7.9)*. These figures show that drop size and rotational speed have a great influence on mass transfer into drops. While the characteristic velocity is relatively independent of the rotational speed, see *figure (5.14)*, a rising rotational speed is associated with increasing overall mass transfer coefficients. The influence of the rotational speed on mass transfer is larger for butyl acetate drops than for toluene drops. It is assumed that this is attributed to the higher degree of circulations within the butyl acetate drops and the stronger deformation of these drops when they collide with the agitators.

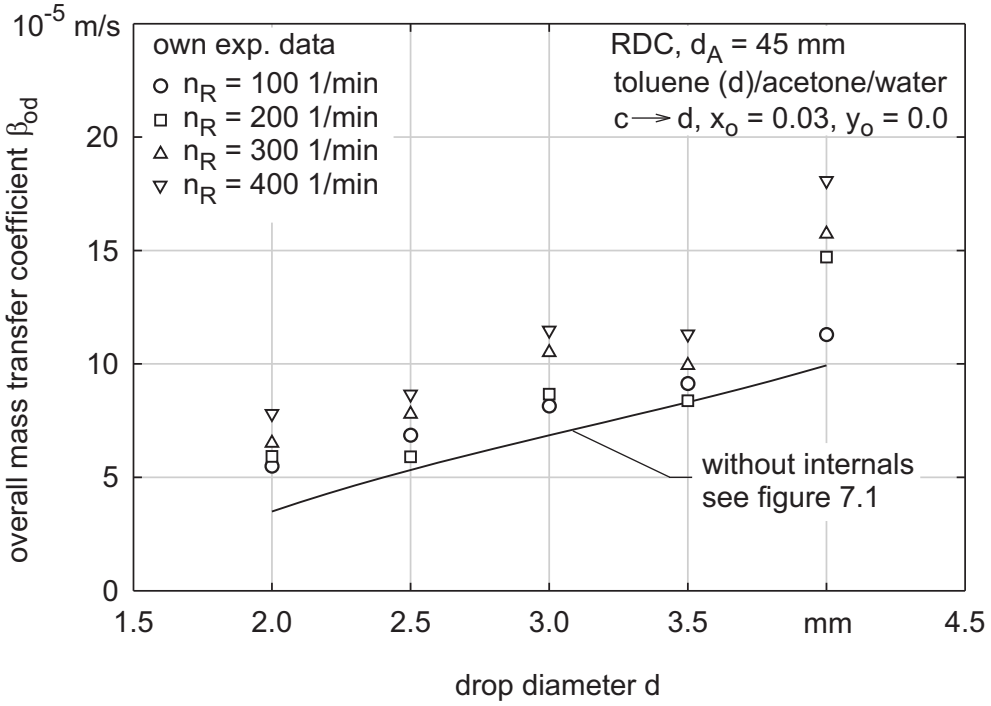

Figure 7.8: Influence of the rotational speed n_R in agitated compartments with rotating discs on the overall mass transfer coefficients of toluene drops

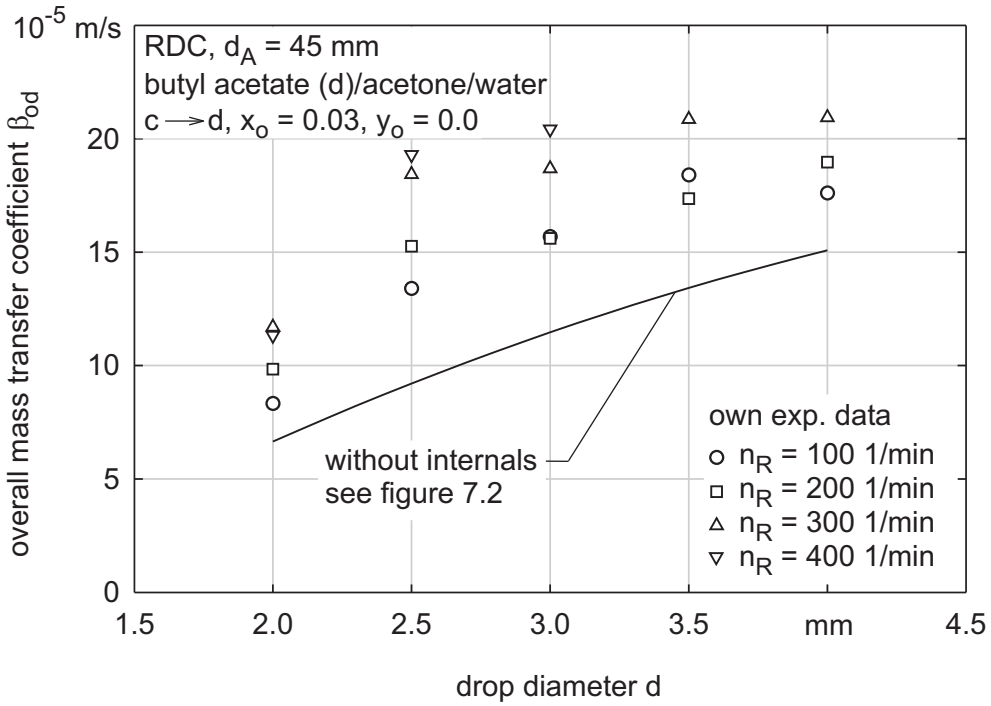

Figure 7.9: Influence of the rotational speed n_R in agitated compartments with rotating discs on the overall mass transfer coefficients of butyl acetate drops

- *Mass transfer in agitated columns with Kühni blade agitators*

Because of the high breakage rates in agitated Kühni-columns only a few experiments for rotational speeds lower than 150 1/min were carried out. The results of these mass transfer experiments show that higher rotational speeds result in higher mass transfer rates for both test systems, see *figure (7.10)*. The solute concentration in the drops is strongly increased by an increase of the rotational speed from n_R *= 50 to 100 1/min*. This is particularly confirmed by the changes in the extraction efficiency Q for higher rotational speeds. The extraction efficiency is defined as the achieved concentration change divided by the maximum possible concentration change of a single drop within the measuring section:

$$Q = \frac{y_2 - y_1}{y^* - y_1} \tag{7.10}$$

The extraction efficiency is significantly improved with increasing rotational speed in the Kühni-compartments. For instance, a butyl acetate drop with a diameter of 2.5 mm shows an extraction efficiency of $Q = 0.83$ for a rotational speed of 50 1/min. For a rotational speed of 100 1/min, the extraction efficiency increases to a value of $Q = 0.92$ for a drop of same size. For smaller butyl acetate drops even higher extraction efficiencies exist.

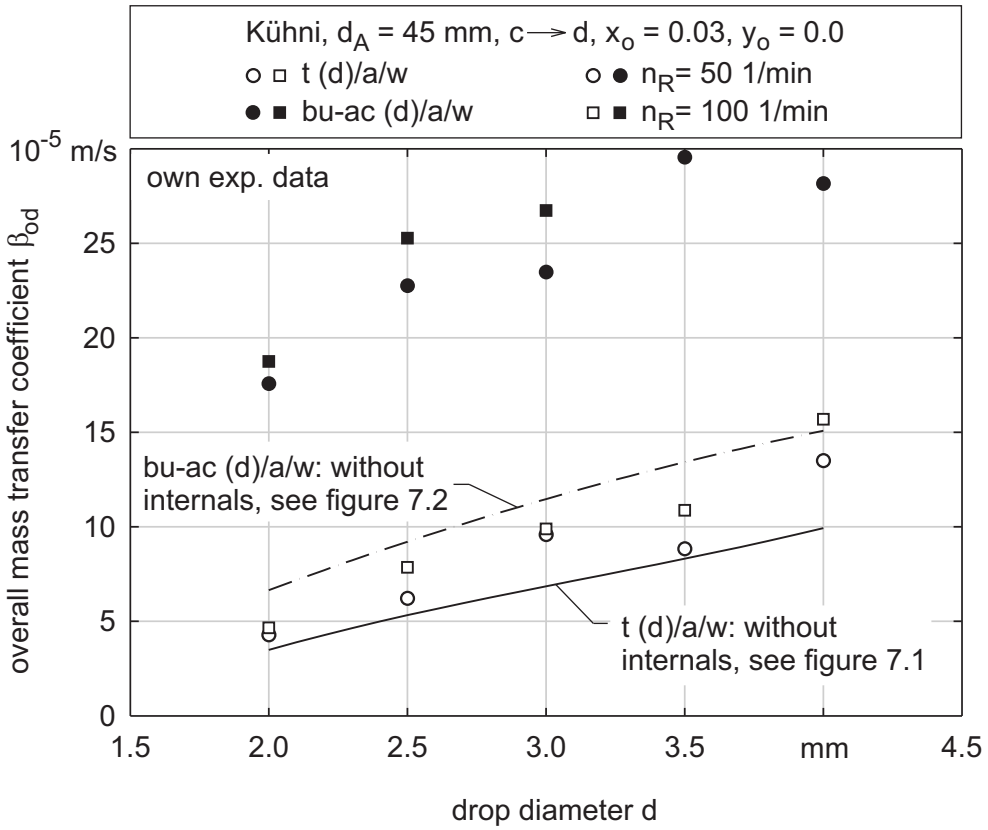

Figure 7.10: Impact of the rotational speed n_R on mass transfer rates of single drops in Kühni-compartments and comparison of the overall mass transfer coefficients of both investigated liquid/liquid-systems with the results for free rising drops

For this reason, an increase of the rotational speed considerably enhances the mass transfer in swarms of drops in columns with Kühni agitators, see also *Kumar 1985*. However, it also has to be mentioned that the column throughput is significantly reduced due to the strong decrease of the drop velocities, see also *figure (5.18)*.

• *General conclusion*

The own investigations of single drops reveal that mass transfer rates in different types of compartments are generally higher for butyl acetate drops than for toluene drops. In addition, for both test systems mass transfer rates are enhanced by an increase of drop size and energy input. As a consequence, the energy input in extraction columns should be as high as possible to improve the mass transfer performance. However, higher energy inputs are also associated with higher numbers of breakage events and, in turn, smaller drops. Such small drops can lead to flooding of the column even at low flow rates. The energy input in extraction columns is therefore limited.

8 Swarm Influence in Extraction Columns

The interaction of particles (rigid spheres or drops) within a swarm causes a significant reduction of the velocity of the swarm particles compared to the velocity of a single particle. For this reason, the influence of hold-up on the effective velocity of particles, which means the swarm influence, has to be considered. The effect of hold-up h_d on the effective particle velocity $v_{d,e}$ is often described by the following correlation:

$$v_{d,e} = \frac{v_s}{1-h_d} - \frac{v_c}{1-h_d} \tag{8.1}$$

According to *equation (8.1)*, the effective particle velocity $v_{d,e}$ is determined from the swarm velocity v_s, the superficial velocity of the continuous phase v_c and the hold-up h_d. A model for the prediction of the swarm velocity v_s that is often used is given by *Richardson and Zaki 1954*. As a result of many investigations with rigid spheres in columns without internals (fluidised beds), Richardson and Zaki derived the following correlation:

$$\frac{v_s}{v_o} = (1-h_d)^n \quad \textit{where} \quad n = f(Re_o) \tag{8.2}$$

The exponent *n* indicates the degree of swarm influence. Richardson and Zaki give several correlations for the so-called swarm exponent *n* in wide ranges of the Reynolds number, see *chapter 2.2*. However, this model is only validated for swarms of rigid spheres in columns without internals, which means for an unhindered flow of the particles. In contrast, in extraction columns a hindered flow of the particles exists because of the column internals. The validity of this model to drop swarms in extractors is thus questionable. In addition, the evaluation of the swarm exponent *n* according to Richardson and Zaki for swarms of drops is difficult. Extensive investigations must be carried out in pilot plant columns. Against this background, a new approach will be introduced to determine the swarm velocity v_s on the basis of single particle investigations only.

8.1 Modelling the Swarm Influence on the Basis of Single Particle Experiments

An elegant solution for describing the swarm influence in particle flows is achieved by the use of the model of *Stichlmair et al. 1989*, see also *chapter 2.2*. With this model, the influence of hold-up on the swarm velocity v_s is predicted from knowledge of the dependence of the drag

coefficient $c_{d,o}$ of a single particle on the Reynolds number *Re* only:

$$\frac{v_s}{v_o} = \sqrt{\frac{c_{d,o}(Re_o)}{c_{d,o}(Re_s)} \cdot (1-h_d)^{4.65}} \tag{8.3}$$

Since the Reynolds numbers of a single particle Re_o and a swarm of particles Re_s are different, the drag coefficient of a single particle has to be known in a wide range of Reynolds numbers. The relationship between the drag coefficient of a rigid sphere and the Reynolds number in an unhindered flow is well-known, see *Kaskas 1971, Bauer 1976, Clift et al. 1978, Henschke 2003, etc*. The use of one of these correlations in combination with the new swarm model (*equation 8.3*) allows the swarm exponent *n* to be determined according to Richardson and Zaki's model by:

$$n = \frac{1}{ln(1-h_d)} \cdot ln\sqrt{\frac{c_{d,o}(Re_o)}{c_{d,o}(Re_s)} \cdot (1-h_d)^{4.65}} \tag{8.4}$$

The comparison of Richardson and Zaki's model and *equation (8.4)*, which was presented in *chapter 2.2*, demonstrates the validity of the new swarm model for rigid spheres in an unhindered flow. To determine the swarm influence in drop systems in unhindered as well as in hindered flows, the terminal and characteristic velocities of single drops must be known. This leads to the desired relationship between the drag coefficient and the Reynolds number of the drops by:

$$c_{d,o}(Re) \equiv \frac{4}{3} \cdot \frac{Ar}{Re^2} \tag{8.5}$$

The dependence of the terminal velocity on the diameter of a single rigid sphere and a toluene drop is illustrated in the dimensionless diagram in *figure (8.1)*. Small toluene drops have slightly higher terminal velocities than rigid spheres of same size. In contrast, large toluene drops move significantly slower than rigid spheres due to the form instability of the drops and the subsequent increase of the drag coefficient. Thus, the drag coefficient[8] of small toluene drops shows values similar to those of rigid spheres for Reynolds numbers up to 800, see *figure (8.2)*. For higher Reynolds numbers the drag coefficient of the drops is significantly larger than for rigid spheres.

8. The model of *Henschke 2003* was fitted to the experimental terminal velocities of rigid pp-spheres and toluene drops, which can be seen by the lines in *figure (8.1)*. Afterwards the dependence of the drag coefficient on the Reynolds number in an unhindered flow was determined using *equation (8.5)*.

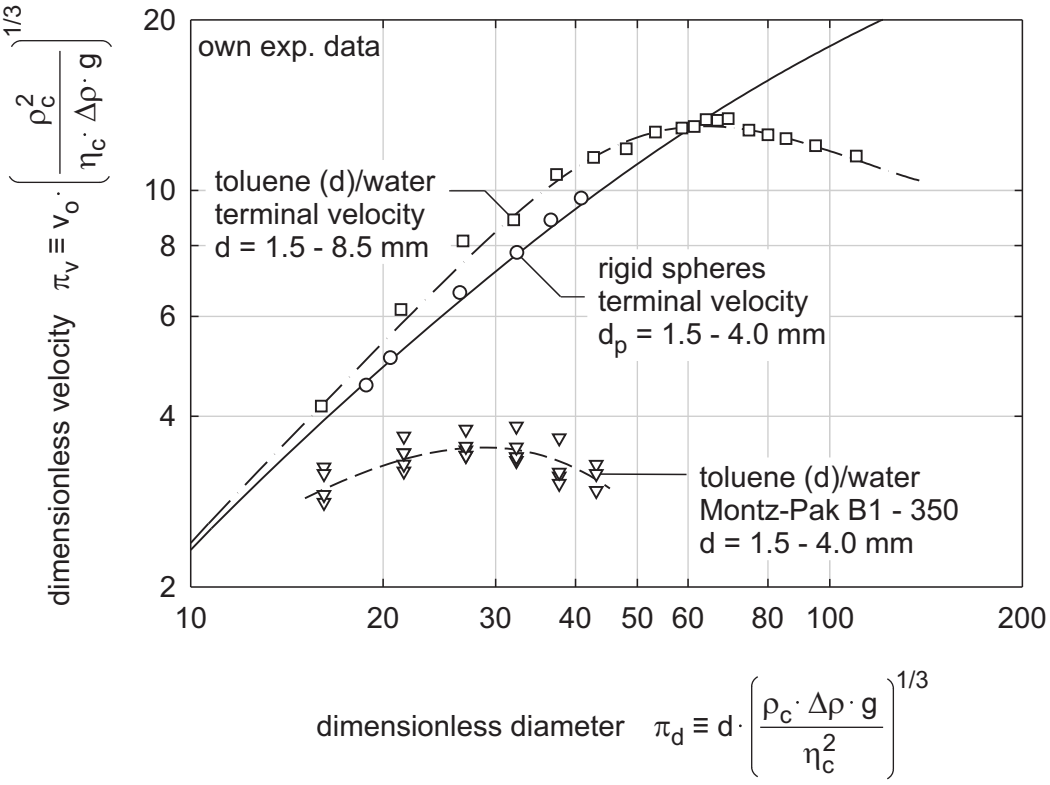

Figure 8.1: Terminal velocity (unhindered flow) of single particles and characteristic velocity (hindered flow) of single particles in structured packings

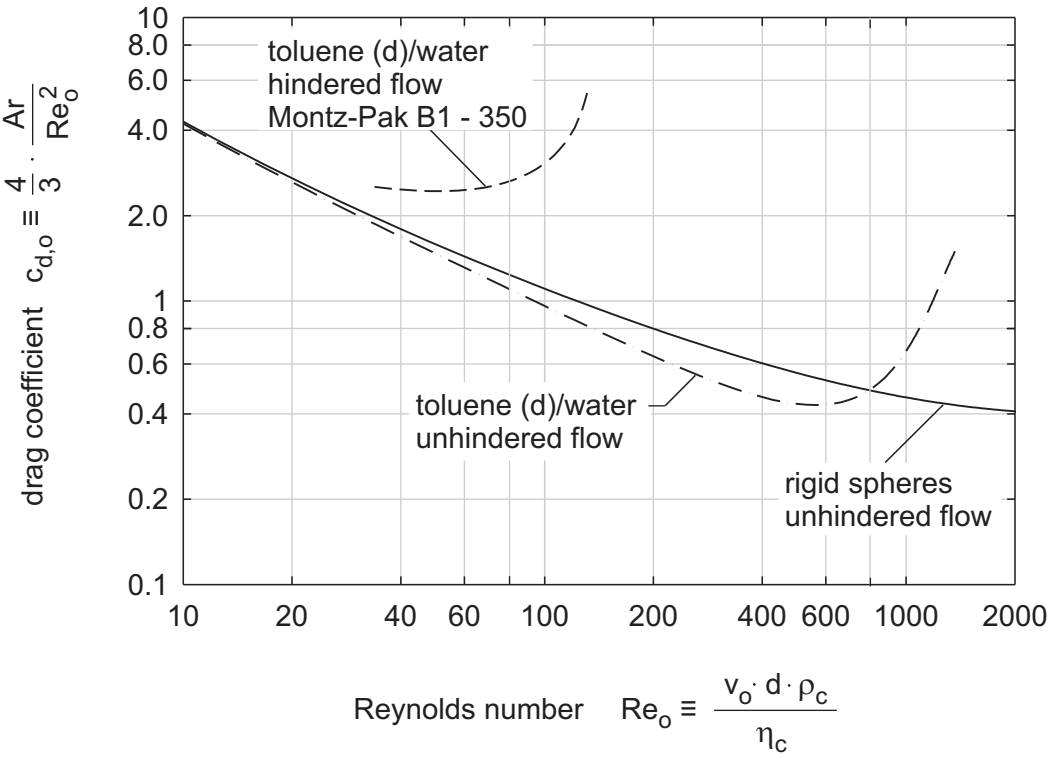

Figure 8.2: Drag coefficient of single rigid spheres and drops for an unhindered and hindered flow

Using *equation (8.4)* to determine the swarm exponent *n* results in slightly higher values for an unhindered flow of drop swarms than of rigid sphere swarms for Reynolds numbers from $Re_o \approx 60$ *to* 600, see *figure (8.3)*. In this region, the drag coefficient of toluene drops is lower than for rigid spheres, see *figure (8.2)*. In regions where the drag coefficient of drops is significantly larger than that of rigid spheres, the swarm exponent *n* falls to values significantly lower than the minimum value of 2.39 given by Richardson and Zaki.

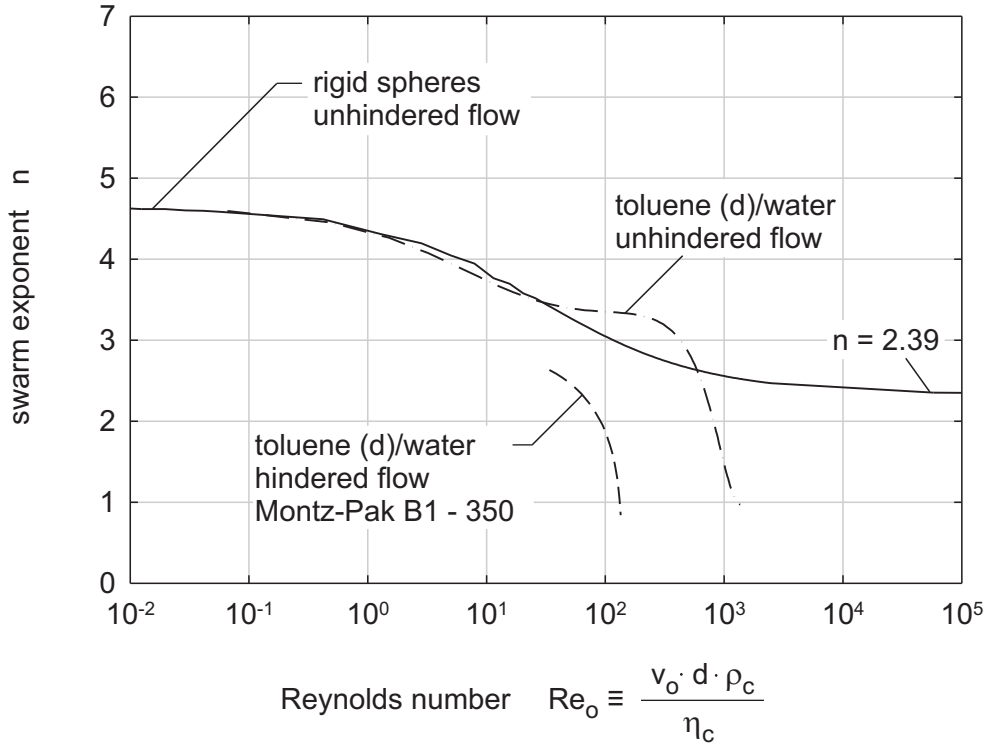

Figure 8.3: Comparison of the swarm exponent n of Richardson and Zaki (solid line) with the swarm exponents for drops in an unhindered and hindered flow calculated by equation (8.4)

Large deviations in the velocities, drag coefficients and swarm exponents between rigid spheres and drops in an unhindered flow exist for large and deformed drops only. In contrast, in a hindered flow, e. g. in a packed column, even small drops have lower velocities than rigid spheres in an unhindered flow, see *figure (8.1)*. Thus, the drag coefficients of single drops in packed columns are significantly higher than in columns without internals, see *figure (8.2)*.

Analogously to large drops in unhindered flow, the different drag coefficients of single drops in packed columns result in low values of the swarm exponent *n*, see *figure (8.3)*. The swarm exponents in columns with structured packings reach values between 0.95 and 2.8 and are much lower than the values for rigid spheres in an unhindered flow.

That the swarm exponents in columns with structured packings are actually lower than those of Richardson and Zaki and are within the range given above is confirmed by the investigations of *Mackowiak 1993* and *Hoting 1996*. *Figure (8.4)* shows a flooding diagram according to *Mersmann 1980* which includes the experimental results from Mackowiak and Hoting in columns with structured packings. The single parameter curves in this figure were determined by the use of Mersmann's approximate solution of *equation (2.48)*:

$$\frac{v_{d,f}}{v_o} = X \cdot (1-X)^{n-1} - \frac{v_{c,f}}{v_o} \cdot \frac{X}{1-X} \quad \text{where} \quad X = \frac{1}{n} \cdot \left[1 - \left(\frac{v_{c,f}}{v_o}\right)^{0.6}\right] \tag{8.6}$$

Figure (8.4) proves that flooding in packed columns is only correctly predicted by swarm exponents in the range of 1.0 to 3.0. The major part of the experimental data is only accurately described by swarm exponents that are significantly lower than the minimum value of Richardson and Zaki of 2.39. Many researchers observed that the swarm exponent and therefore the swarm influence in extraction columns is lower than predicted by Richardson and Zaki, see *Pilhofer 1978*, *Godfrey and Slater 1991*, *Mackowiak 1993*, *Wagner 1999*, *etc*. But for the first time, explanations for the deviations are given by the new swarm model.

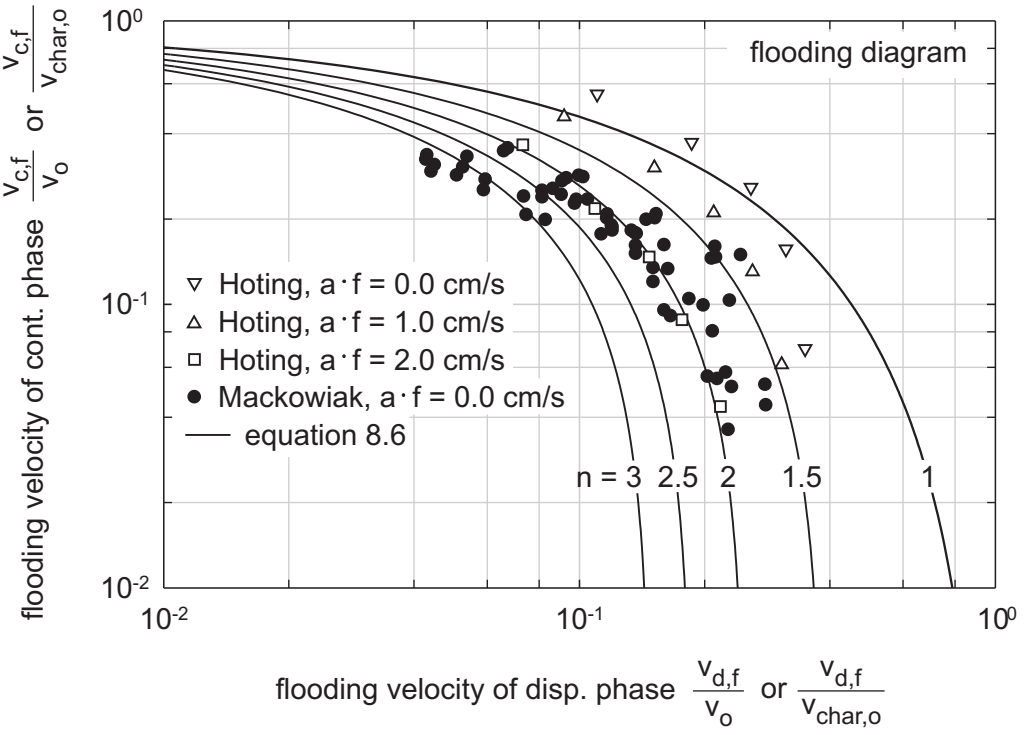

Figure 8.4: Flooding diagram according to Mersmann 1980 (Mackowiak 1993 presented flooding data for columns with structured packings and with random packings, but in the figure above only flooding data for columns with structured packings are depicted)

8.2 Simplification of the New Swarm Model

The prediction of the swarm influence plays a decisive role in the determination of the effective drop velocity $v_{d,e}$. It is also important in the determination of the hold-up in extractors by the following equation (see also *chapter 2.2*):

$$h_d = \frac{v_d}{v_s + v_d - v_c} \tag{8.7}$$

The new swarm model offers a good approach to predict the swarm velocity and the hold-up in extractors only through single drop investigations. However, its application is associated with a large computational effort. The procedure for the simultaneous determination of the swarm velocity and the hold-up with the new swarm model and *equation (8.7)* is depicted in *figure (8.5)*. First, the dependence of the drag coefficient on the Reynolds number has to be derived from the characteristic velocity data of single drops. Second, the hold-up in the extractor is estimated. Subsequently, the swarm velocity is determined by an iterative approach (see inner iteration circle). Finally, the hold-up is calculated by *equation (8.7)* and compared with the estimated value (see outer iteration circle).

Since the swarm velocity of each drop size in each height element has to be determined by the use of drop population balance models, a simplification of the previous procedure is desired. The following sections describe how the application of the new swarm model can be simplified to predict the swarm velocity of rigid spheres in columns without internals. The described procedure can be easily transferred to drop swarms in columns with internals if the correct characteristic velocities are used.

The velocity of a single particle depends on its drag coefficient:

$$v_o = \sqrt{\frac{4}{3} \cdot \frac{d \cdot \Delta\rho \cdot g}{c_{d,o}(Re_o) \cdot \rho_c}} \tag{8.8}$$

Using the model of *Stichlmair et al. 1989* to determine the drag coefficient of a swarm of particles ($c_{d,s}(Re_s) = c_{d,o}(Re_s) \cdot (1 - h_d)^{-4.65}$) results in the following correlation for the swarm velocity (see also *chapter 2.2*):

$$v_s = \sqrt{\frac{4}{3} \cdot \frac{d \cdot \Delta\rho \cdot g}{c_{d,o}(Re_s) \cdot \rho_c} \cdot (1 - h_d)^{4.65}} \tag{8.9}$$

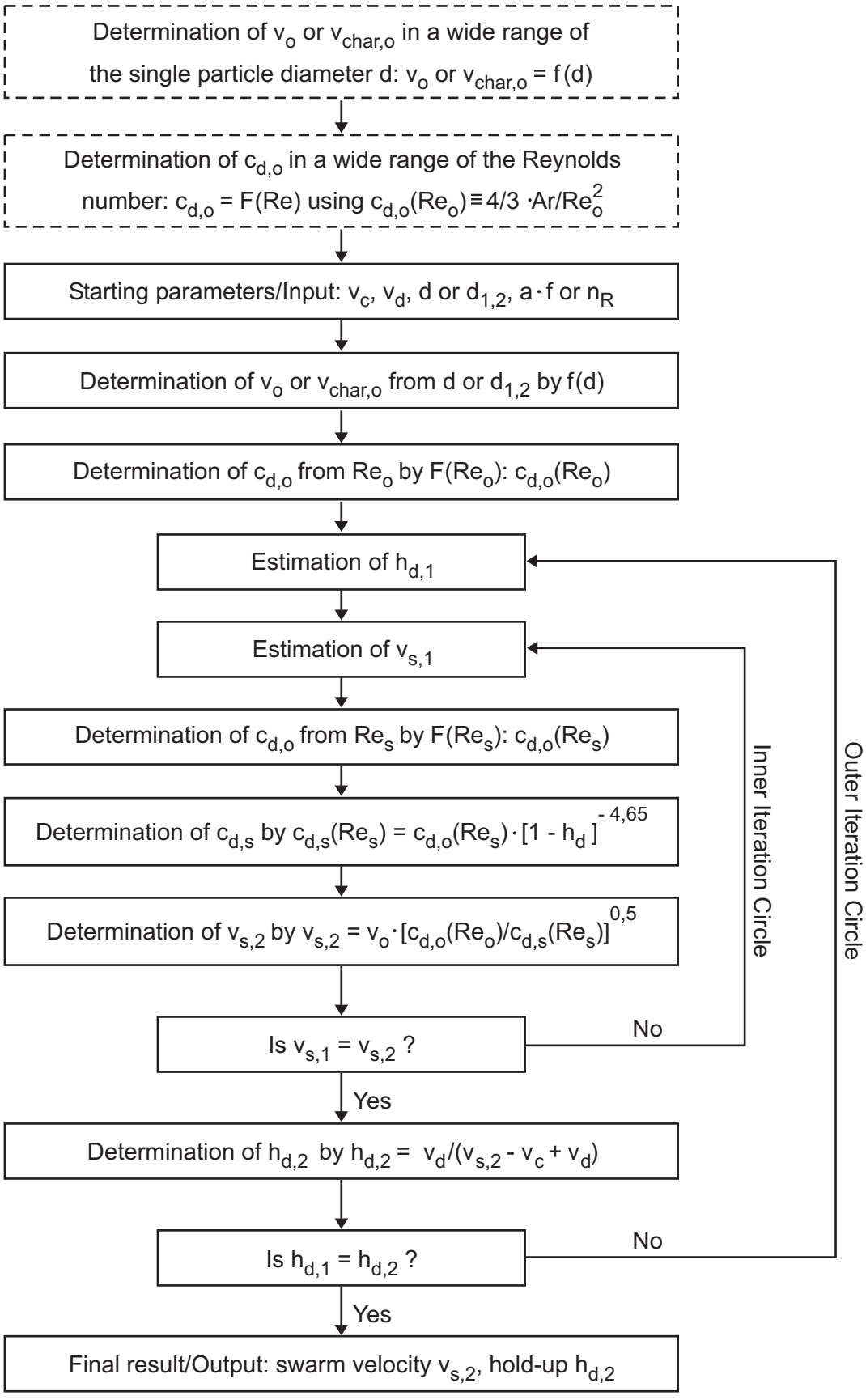

Figure 8.5: Schematic for the simultaneous determination of the swarm velocity and the hold-up using the new swarm model (equation 8.3) and equation (8.7)

Prediction of the swarm velocity can be simplified by determining the swarm velocity as a function of a single particle with diameter d_v which has the same Reynolds number as the swarm of particles:

$$Re_{o,v} = Re_s \Leftrightarrow \frac{v_{o,v} \cdot d_v \cdot \rho_c}{\eta_c} = \frac{v_s \cdot d \cdot \rho_c}{\eta_c} \tag{8.10}$$

Since the velocity of a single particle is different from the velocity of the particles in the swarm, the single particle which fulfils the Reynolds number condition of *equation (8.10)* must have a different size than the actual size of the particles in the swarm. The particle which is subjected to the Reynolds number condition is called a virtual single particle (d_v = diameter of the single virtual particle, $v_{o,v}$ = velocity of the single virtual particle).

Considering the swarm velocity for the actual particles with diameter *d* by *equation (8.9)* and the velocity of the virtual particle by *equation (8.8)* results in:

$$\frac{v_s}{v_{o,v}} = \sqrt{\frac{d}{d_v} \cdot (1 - h_d)^{4.65}} \tag{8.11}$$

Combination of *equation (8.10)* and *equation (8.11)* allows the diameter of the virtual particle d_v to be determined as a function of the particle diameter *d* and the hold-up h_d. In addition, the swarm velocity v_s can be evaluated from the velocity of the virtual particle $v_{o,v}$:

$$d_v = d \cdot (1 - h_d)^{4.65/3} \qquad \textit{as well as} \qquad v_s = v_{o,v} \cdot (1 - h_d)^{4.65/3} \tag{8.12}$$

Thus, starting from the known diameter of the particles in the swarm *d*, the diameter of the virtual particle d_v, the velocity of the virtual particle $v_{o,v}$ and finally the desired swarm velocity is determined for a certain value of hold-up. Without evaluating the dependence of the drag coefficient of a single particle on the Reynolds number and without any iterative calculations, the swarm velocity is derived in 3 steps. *Figure (8.6)* illustrates this simplified approach to determine the swarm velocity of rigid spheres for an unhindered flow. The three steps of the new approach are depicted by the thick solid lines. As can be seen, both calculation procedures give the same result (the direct way via an iteration is shown by the dashed line).

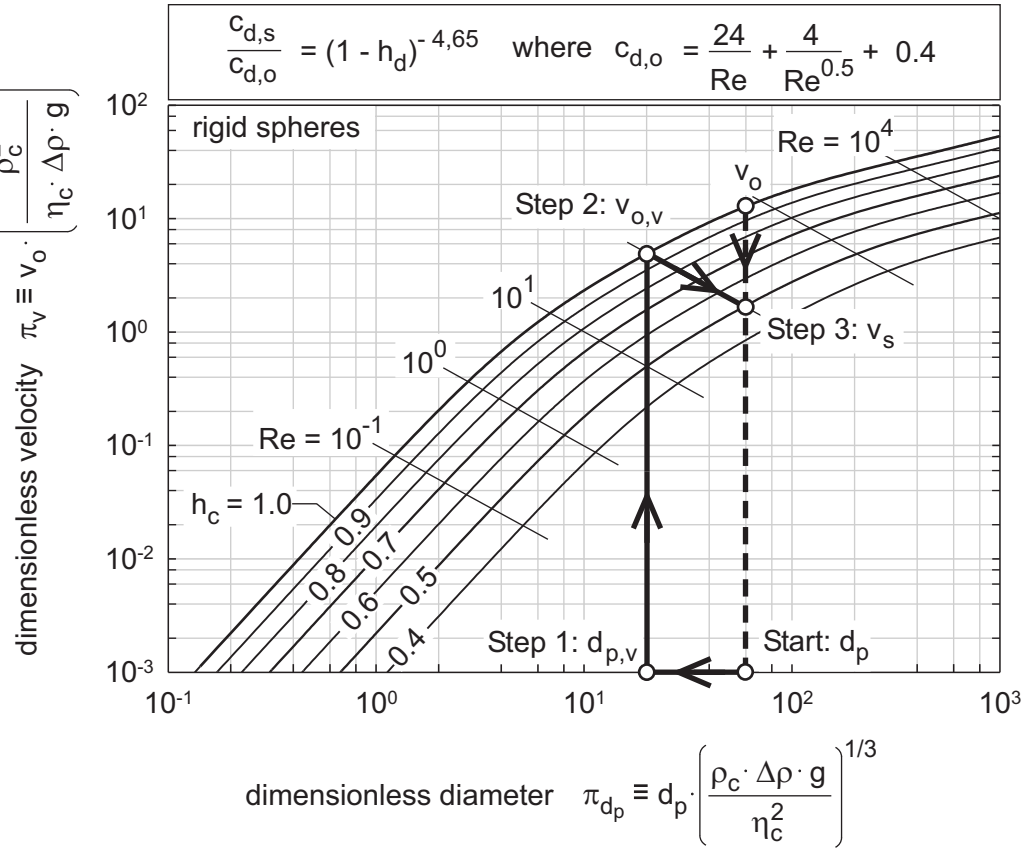

Figure 8.6: Illustration of the simplified procedure to determine the swarm velocity (thick solid lines) in contrast to the direct but complex procedure presented in chapter 8.1 (dashed line). The velocity of a single rigid sphere and the swarm velocity were determined using the correlation of Kaskas 1971 for the drag coefficient.

8.3 Validation of the New Swarm Model

As shown previously, the new swarm model predicts the swarm influence of rigid spheres in an unhindered flow very accurately. However, in extraction columns hindered flow exists because of the internals. For this reason, the validity of extending the new swarm model to rigid spheres in extraction columns with different internals was tested. The use of mono-dispersed swarms of rigid spheres permits experiments to be carried out in absence of breakage and coalescence.

- *Swarms of rigid polypropylene (pp)-spheres in extractors with different internals*

The hold-up in extraction columns can be determined with the help of the new swarm model and *equation (8.7)*. The comparison of the predicted and measured values of the hold-up provides confirmation of the accuracy of the new swarm model. Comparison of the theoretically

and experimentally derived hold-up data is advantageous since the hold-up is easier to measure than the swarm velocity of the particles. The hold-up in the rigid sphere swarm extractor was determined by measuring the height of the particle bed after closing the sliding valves, see *chapter 4.3*. To predict the swarm velocity and the hold-up, the measured terminal and characteristic velocities of single rigid pp-spheres presented in *chapter 5* were used in combination with the new swarm model.

The comparison of theoretical and experimental hold-up values reveals that the new swarm model predicts the hold-up of rigid spheres in extraction columns without internals very well, see *figure (8.7)*. The good agreement of predicted and measured hold-up values was expected since the new swarm model was derived for this purpose and already validated by the comparison with Richardson and Zaki's model, see also *chapter 2.2*.

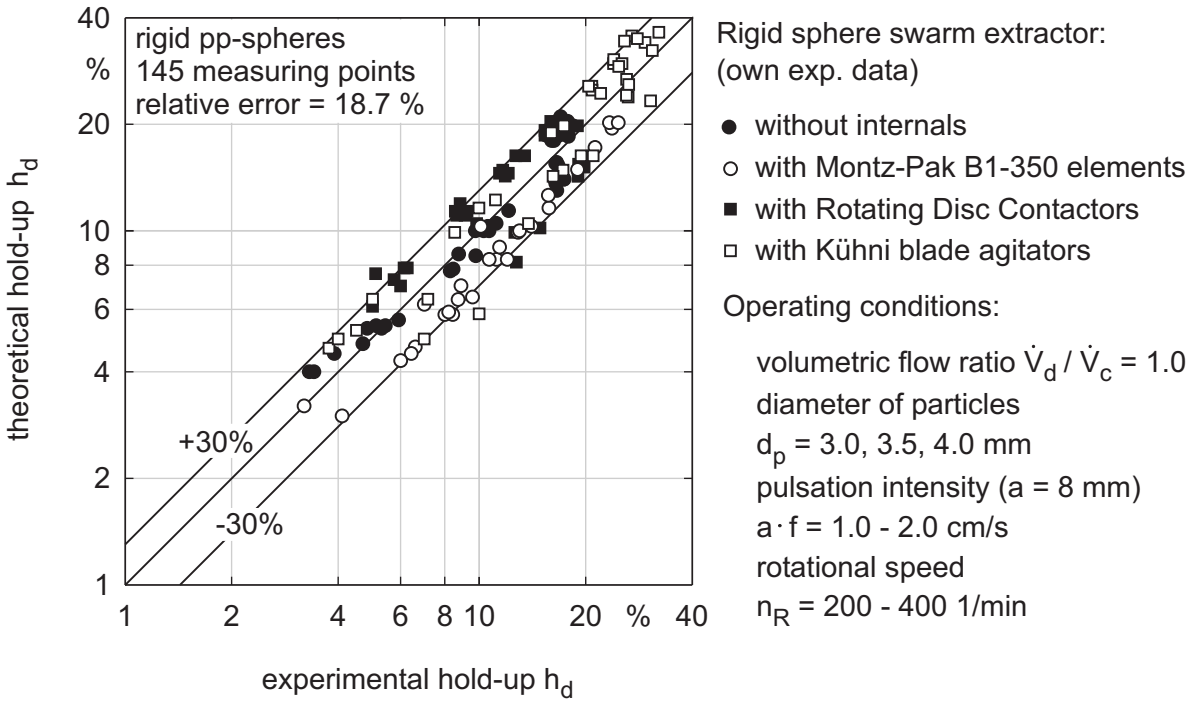

Figure 8.7: Comparison of the measured hold-up of swarms of pp-spheres and predicted values from the new swarm model, see equation (8.3), in different extractors

In addition, a good agreement of hold-up data in columns with different internals is seen in wide ranges of operating conditions such as the pulsation intensity and the rotational speed. It should be mentioned that experiments with sieve trays could not be carried out due to the large size of the rigid spheres. Even for very low throughputs and the use of sieve trays with larger holes (sieve tray - d_h = 4 mm) flooding occurred in the column.

- *Swarms of drops in extractors with different internals*

To test the validity of the new swarm model for predicting the swarm velocity and the hold-up of drops, numerous experiments under mass transfer conditions were carried out. For the experiments with toluene (d)/acetone/water and butyl acetate (d)/acetone/water the inlet concentration of acetone in the continuous aqueous phase was approximately 5 wt.-% while a solute-free solvent was used as the organic dispersed phase. Investigations were conducted for a constant phase ratio of $v_d/v_c = 1.2$ and a varying total throughput B ($B = v_d + v_c$). During the experiments, the sauter diameter and the hold-up were measured in three column sections, see *chapter 4.4*. Detailed information about the results of the experiments can be found in the appendix, see *chapter A*.

To predict the swarm velocity and the hold-up, the measured sauter diameters were averaged. These averaged sauter diameters were used to determine the terminal velocities of single drops and, in turn, the characteristic velocities of single drops with the correlations presented in *chapter 5*. Finally, the predicted hold-up values from the new swarm model were compared to the measured overall hold-up values.

In addition to own experimental data, data from the literature was used to check the validity of the new swarm model in large ranges of operating conditions in extractors. To compare hold-up data from the literature with values predicted from the new swarm model, single drop terminal velocities were evaluated with the correlations of *Qi 1992*. Qi's correlations were applied to determine the terminal velocities of single drops for systems with high, intermediate and low interfacial tensions. Furthermore, the required characteristic velocities of single drops were predicted by the correlations presented in *chapter 5*.

- *Swarm influence in pulsed sieve tray extractors*

For the own experiments in a pulsed sieve tray column only sieve trays with 2 mm holes were used and pulsation intensities of 1.0 and 2.0 cm/s were examined. The comparison of the predicted and measured values for the hold-up in the pulsed sieve tray column is shown in *figure (8.8)*. For both liquid/liquid-systems used, the predicted values of the hold-up match the measured values with only small deviations for most of all operating conditions.

Many results from the literature were consulted for further studies, see *figure (8.8)*. The hold-up is particularly well predicted for experimental data with a mass transfer direction from the

continuous to the dispersed phase “c to d“ and for experimental data without mass transfer. A good agreement with the experimental data is observed for varying column dimensions as well as for different phase ratios in a large range of total throughputs (B = 4 to 54 $m^3/(m^2 \cdot h)$).

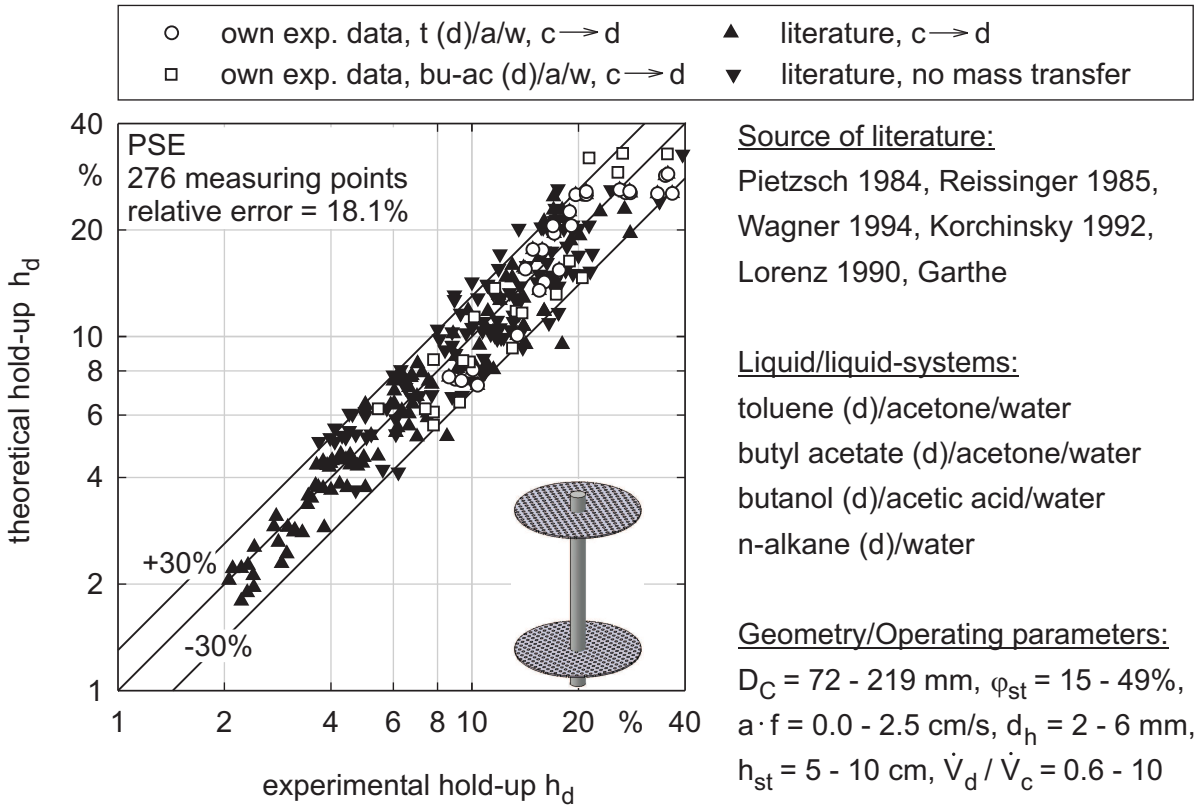

Figure 8.8: Analysis of the suitability of the new swarm model, see equation (8.3), for predicting the hold-up of drop swarms in pulsed sieve tray columns

In contrast, larger deviations between theoretical and experimental hold-up values were observed in experiments with a mass transfer from “d to c“. Due to the high number of coalescence events which are associated with this mass transfer direction, relatively large drops (d » 4 mm) are generated in the column. Such large drops have significantly different shapes compared to spherical drops. For this reason, they show a clearly different motion through the column and have other characteristic velocities. The characteristic velocity of such large drops is not accurately described by the correlations presented in *chapter 5*. This is the most significant reason for the deviations that occur in predicting the hold-up for this mass transfer direction. Because in technical processes coalescence is normally suppressed by the appropriate choice of the mass transfer direction, optimisation of the new swarm model for a mass transfer direction from “d to c“ was deemed unnecessary.

• *Swarm influence in pulsed extractors with structured packings*

The swarm influence in pulsed packed extractors is significantly lower than in columns without internals, as was demonstrated in *chapter 8.1*. For this reason, the application of Richardson and Zaki's model is not advised. In contrast, the use of the new swarm model turns out to be superior for predicting the swarm influence and the hold-up. This is confirmed by the analysis of the experiments with both liquid/liquid-systems used in this work. As in pulsed sieve tray extractors, the hold-up is satisfactorily predicted for pulsation intensities of 1.0 and 2.0 cm/s, see *figure (8.9)*.

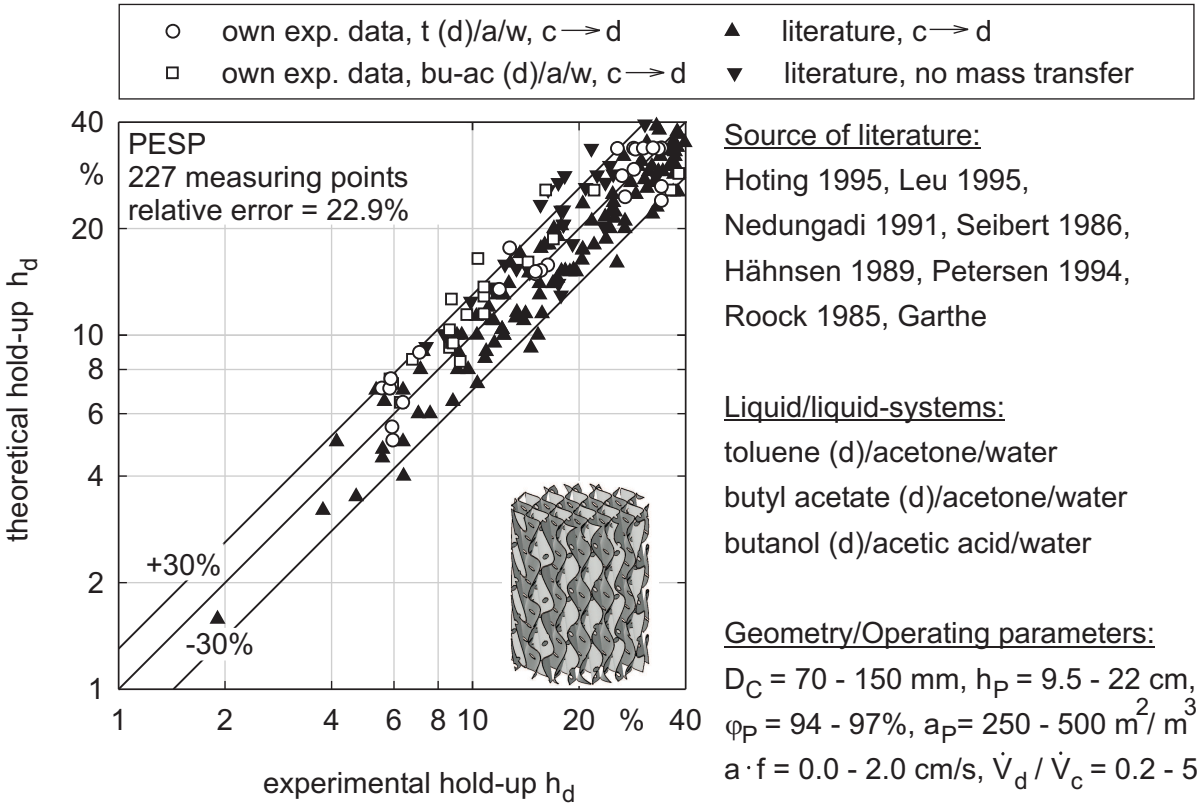

Figure 8.9: Control of the validity of equation (8.3) for predicting the hold-up in columns with structured packings

The analysis of data from the literature shows that for extractors with different structured packings the new swarm model results in good agreement with the experimental hold-up. For a wide range of operating parameters such as the pulsation intensity, the phase ratio and the total throughput ($B = 10 - 80\ m^3/(m^2 \cdot h)$), a good agreement is seen in *figure (8.9)*. In contrast, for a mass transfer direction from "d to c" significant deviations were found. This became apparent from the analysis of single measurements made by *Nedungadi 1991* and *Seibert 1986* who investigated both directions of mass transfer.

• *Swarm influence in extractors with rotating discs*

The swarm influence in agitated columns differs from the swarm influence in pulsed columns, see also *Godfrey and Slater 1991*, since the characteristic velocities of single drops are different. The new swarm model takes these differences into account by considering the characteristic velocity of a single drop. Thus, an accurate model for the characteristic velocity of single drops is required to correctly predict the swarm influence in agitated columns such as RDC-extractors.

The new swarm model was tested for RDC-extractors by comparing the hold-up in the own extractor for rotational speeds of n_R = 200 and 400 1/min for both test systems. In addition, data from the literature was used. The hold-up of these experiments is well predicted, see *figure (8.10)*. This is particularly confirmed by the experiments of *Zhang et al. 1985*. These authors investigated the performance of a RDC-extractor for relatively high rotational speeds of up to 900 1/min. Small deviations of the hold-up are observed for their experiments. This is remarkable because the correlation for the characteristic velocity of single drops is validated for a maximum rotational speed of 400 1/min only, see *chapter 5.4*.

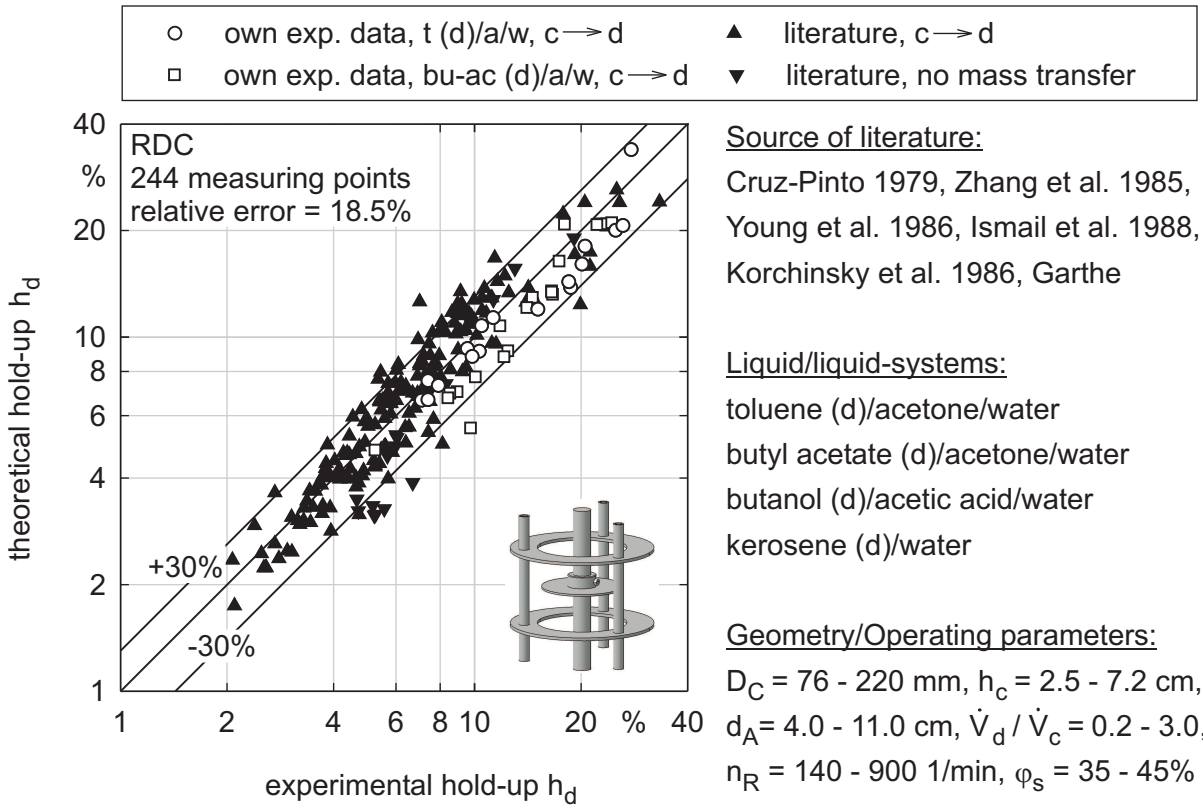

Figure 8.10: Applicability test of the new swarm model, see equation (8.3), to predict the hold-up in agitated rotating disc contactors

In general, for swarms of drops with a sauter diameter smaller than 4.5 mm, minor deviations between theoretical and experimental hold-up values of RDC-extractors are observed. For swarms of drops with larger sauter diameters, the hold-up cannot be satisfactorily predicted. This was confirmed by the investigations of *Al Aswad et al. 1985*, who extracted acetone from a dispersed organic phase to a continuous aqueous phase.

- *Swarm influence in extractors with Kühni blade agitators*

The comparison of predicted and measured hold-up in the own Kühni-extractor[9] is illustrated in *figure (8.11)*. In addition, the comparison with hold-up data from *Bailes et al. 1986* and *Goldmann 1986* is shown. The average relative deviations between predicted and measured hold-up values are 23.5 %. Larger deviations exist for a few experiments from Goldmann with a relative free cross-sectional stator area of 20 %. However, the experiments with larger relative free cross-sectional stator areas (including the ones of Goldmann) are satisfactorily predicted.

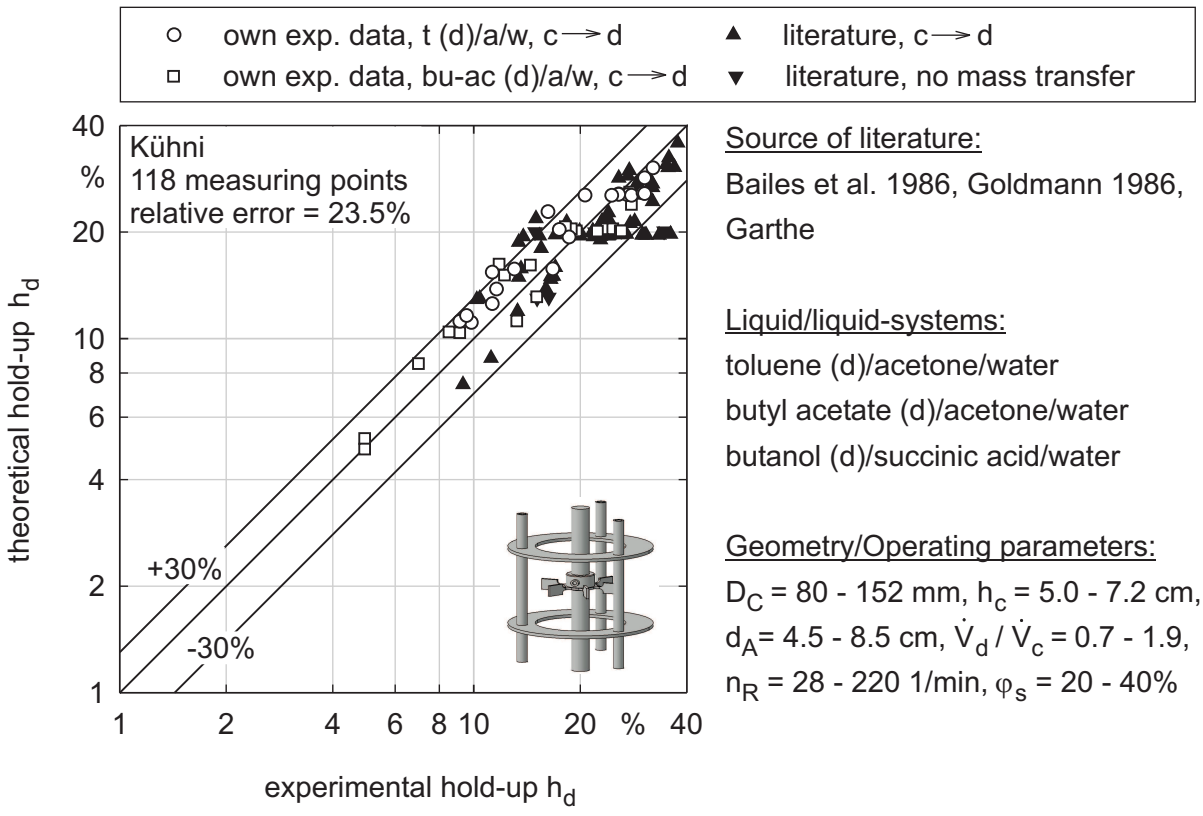

Figure 8.11: Comparison of the predicted hold-up using the new swarm model, see equation (8.3), and the experimental hold-up in agitated Kühni-extractors

9. Experiments with toluene (d)/acetone/water were conducted with rotational speeds of 150 and 200 1/min. Experiments with butyl acetate (d)/acetone/water were carried out with rotational speeds of 100 and 150 1/min, since for higher rotational speeds flooding of the Kühni-extractor appeared even for very low total throughputs.

• *General conclusion*

The comparison of hold-up data confirms that the new swarm model accurately predicts the hold-up in different extraction columns. The most important advantage of the new swarm model is that the swarm influence is determined from the velocity of single drops only. Consequently, the model can be easily applied to extraction columns with different internals.

• *Annotation*

The application of the new swarm model in combination with drop population balance models (DPBMs) was tested in the industrially financed cooperation project previously mentioned, see *Pfennig et al. 2005*. In the course of the project two DPBMs were developed by the project partners. The derived correlations for the characteristic velocities of single drops and swarms of drops were implemented in the DPBMs. Both DPBMs were successfully validated for predicting the fluiddynamics and mass transfer rates of extractors. Because the project partners developed the DPBMs, detailed information are found in the literature published by the project partners and in the *Final Report AiF 40 ZN 2004*.

9 Mass Transfer Performance of Extraction Columns

Mass transfer performance of extraction columns is controlled by several parameters such as physical properties of the liquid/liquid-system, drop size and velocities of the drops within a swarm. Previous investigations also reveal that an increase of the energy input significantly enhances the mass transfer rates. This is due to the generation of a larger interfacial area and the turbulent mixing of both phases. Numerous experiments in extractors with different internals were carried out to investigate the influence of energy input on mass transfer performance.

All investigations were conducted for a mass transfer direction from the continuous to the dispersed phase. The total throughput was increased in steps up to a value close to the flooding capacity of the column. During each experiment drop size distributions, hold-up distribution and concentration profiles of both phases were recorded. A detailed overview of the experimental data for a large number of experiments in the pulsed sieve tray column, in the pulsed packed column, in the agitated RDC-extractor and in the Kühni-extractor is given in the appendix, see *chapter A.*[10]

To evaluate the influence of total throughput and energy input on mass transfer rates, the number of equilibrium stages per active column height n_{th}/H_{ac} was determined by the following equations, see also *chapter 2.1*:

$$\frac{n_{th}}{H_{ac}} = \frac{1}{H_{ac} \cdot ln\lambda} \cdot ln\left[\left(\frac{X_{in} - Y_{in}/m}{X_{out} - Y_{in}/m}\right) \cdot \left(1 - \frac{1}{\lambda}\right) + \frac{1}{\lambda}\right] \qquad \text{when } \lambda \neq 1 \qquad (9.1)$$

$$\frac{n_{th}}{H_{ac}} = \left(\frac{X_{in} - Y_{in}/m}{X_{out} - Y_{in}/m} - 1\right) \cdot \frac{1}{H_{ac}} \qquad \text{when } \lambda = 1 \qquad (9.2)$$

$$\text{where} \quad \lambda = \frac{m}{\dot{M}_c/\dot{M}_d}$$

For high mass transfer rates, large numbers of equilibrium stages per active column height n_{th}/H_{ac} are calculated from the equations above. For low mass transfer rates, small numbers of n_{th}/H_{ac} are determined.

10. The appendix also includes examples for the initial drop size distribution immediately after the distributor.

9.1 Mass Transfer Performance of Pulsed Extractors

The pulsation intensity significantly improves the mass transfer rates in extractors. For example, an increase of the pulsation intensity in a sieve tray extractor leads to a large enhancement of drop breakage, as was already shown in *chapter 6.1*. The larger interfacial area and the longer residence time of small drops compared to large drops within the column are mainly responsible for the mass transfer improvement.

- *Mass transfer performance of pulsed sieve tray extractors (sieve tray - d_h = 2 mm)*

The investigations with both liquid/liquid-systems confirm that mass transfer rates in a pulsed sieve tray extractor increase with increasing pulsation intensity, see *figure (9.1)*. Comparison of the data reveals that mass transfer rates in the butyl acetate (d)/acetone/water system are significantly higher than in the toluene (d)/acetone/water system. The production of smaller drops due to the lower interfacial tension of the butyl acetate system and the higher overall mass transfer coefficients of single butyl acetate drops (see *chapter 7.2*) are responsible for the higher mass transfer performance.

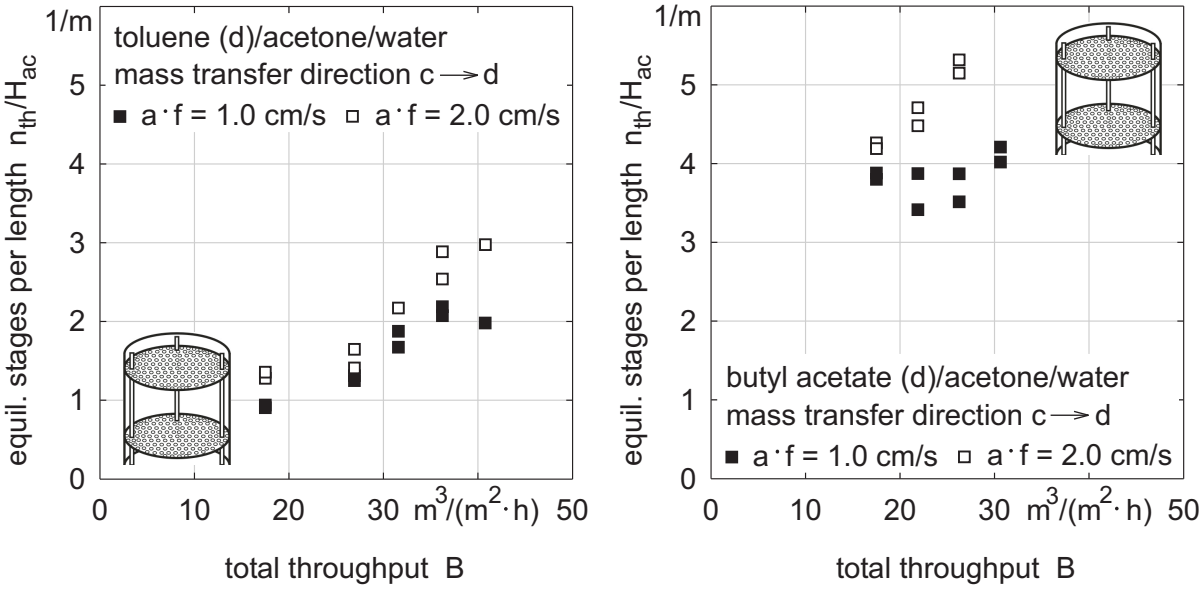

Figure 9.1: Number of equilibrium stages per active column height of a pulsed sieve tray extractor (sieve tray - d_h = 2 mm); comparison of own experiments with toluene (d)/acetone/water and butyl acetate (d)/acetone/water

A characteristic feature of the performance of a pulsed sieve tray extractor is that mass transfer rates increase with an increase of the total throughput up to the flooding capacity, see *figure (9.1)* and see also *Pietzsch 1984*, *Reissinger 1985* and *Bäcker et al. 1991*. Since the optimal throughput in a pulsed sieve tray column is near the flooding point, good knowledge of the flooding capacity is important.

- *Mass transfer performance of pulsed packed extractors (Montz-Pak B1-350)*

Pulsed extractors with structured packings prove to be very flexible and efficient due to their good mass transfer performance, see *Bäcker et al. 1991*. An advantage of this type of extractor in comparison to a pulsed sieve tray extractor is that high throughputs can be achieved even without pulsation. A further advantage of structured packings is the well-defined flow of both phases within the packing. This causes a large reduction of axial mixing and therefore makes the scale-up of such columns less difficult, see *Godfrey and Slater 1994*. In addition, pulsed packed columns show high and constant mass transfer rates in wide ranges of throughput (depending on pulsation intensity), see *Hähnsen 1989* and *Hoting 1996*. This simplifies the choice of the optimal operating conditions.

The experimental investigations confirm the good performance of pulsed packed columns, see *figure (9.2)*. For both test systems an increase of the mass transfer rates compared to the pulsed sieve tray extractor is seen. Almost constant and high numbers of equilibrium stages per active column height are determined in a wide range of throughput. This is particularly seen from the experiments with the butyl acetate system. Furthermore, the increase of mass transfer with an increase of pulsation intensity is more distinct for this system. This is attributed to the good breakage performance of the structured packings in combination with the low interfacial tension of the butyl acetate system.

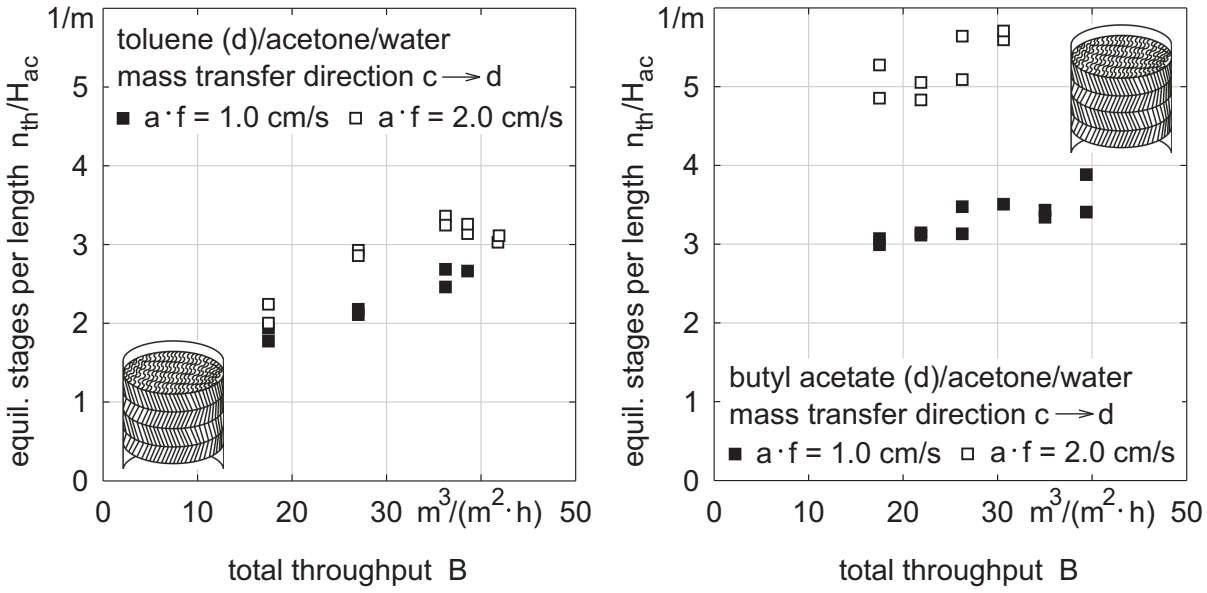

Figure 9.2: Influence of the pulsation intensity on the mass transfer rates in pulsed columns with structured packings (Montz-Pak B1-350); comparison of own experiments with toluene (d)/acetone/water and butyl acetate (d)/acetone/water

9.2 Mass Transfer Performance of Agitated Extractors

The performance of agitated extractors strongly depends on the geometry and dimensions of the rotators. Since the geometry of rotating discs significantly differs from that of blade agitators, mass transfer rates in RDC-extractors and in Kühni-extractors are different at similar rotational speeds.

- *Mass transfer performance of RDC-extractors*

Due to the low breakage rates in RDC-extractors, the initial drop size distribution is very important for the mass transfer performance of this type of extractor. Satisfactory mass transfer rates are achieved by the generation of small drops with a narrow drop size distribution at the dispersed phase inlet.

The results of the mass transfer investigations with both test systems in the own extractor with rotating discs for rotational speeds of 200 and 400 1/min are shown in *figure (9.3)*. Compared to other types of extractors, mass transfer rates of the RDC-extractor are very low, see also *figure (9.1)* and *figure (9.2)*. The main reason for this is the formation of liquid organic films under the stators caused by coalescence and low breakage of larger drops, as was seen during

the experiments. The production of large drops causes a strong reduction of the interfacial area and, in turn, low mass transfer rates. However, mass transfer rates in the RDC-extractor are relatively constant in a wide range of total throughput, see *figure (9.3)*.

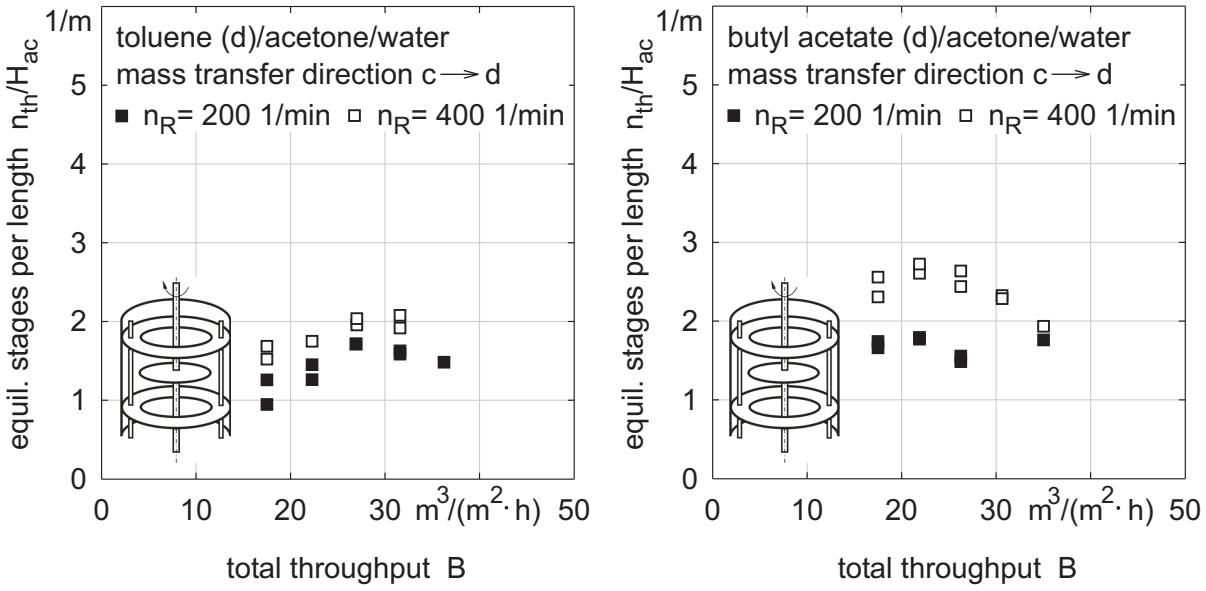

Figure 9.3: Mass transfer performance of an agitated RDC-extractor in dependence on the total throughput and rotational speed; comparison of own experiments with toluene (d)/acetone/water and butyl acetate (d)/acetone/water

- *Mass transfer performance of Kühni-extractors*

In a Kühni-extractor, the production of liquid films under the stators is prevented by the turbulent flow and the generation of circulating cells within the compartments even for low rotational speeds. The strong turbulence in the compartments, the relatively low axial mixing and the production of a large interfacial area result in a high mass transfer performance.

The investigations in the extractor with Kühni blade agitators show a strong influence of the rotational speed on mass transfer rates, see *figure (9.4)*. For instance, an increase of the rotational speed from 100 to 150 1/min causes an enhancement of the number of equilibrium stages per length n_{th}/H_{ac} for butyl acetate (d)/acetone/water of nearly 100 %.

For both test systems, mass transfer rates in the Kühni-extractor are higher than in all other investigated types of extractors, see *figure (9.4)*. However, mass transfer rates significantly decrease for a total throughput close to the flooding point. This is confirmed by the experiments with a rotational speed of 150 1/min. A further disadvantage of Kühni-extractors is the

relatively low maximum total throughput because of the production of relatively small drops and their low characteristic velocities. Thus, Kühni-extractors are associated with very high mass transfer efficiencies and low throughputs, see also *Kumar 1985*, *Goldmann and Blaß 1986* and *Goldmann 1986*.

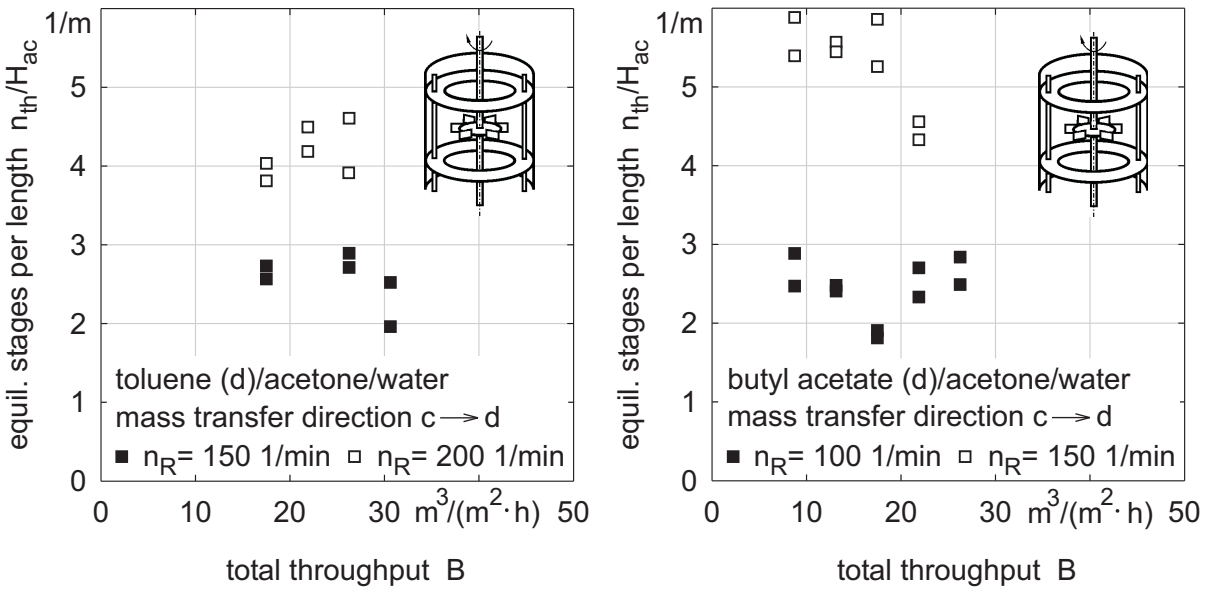

Figure 9.4: Influence of the rotational speed on the mass transfer rates of an agitated Kühni-extractor; comparison of own experiments with toluene (d)/acetone/water and butyl acetate (d)/acetone/water

9.3 Comparison of the Performance of Different Extractors

An overview of the maximum ranges of the total throughput and the number of equilibrium stages per active column height of all investigated extractors is given below for both test systems, see *figure (9.5)*. It should be mentioned that the conclusions from *figure (9.5)* are only valid for the examined test systems and operating conditions.

The pulsed extractor with structured packings (PESP) demonstrates a very good performance with respect to maximum throughput and mass transfer rates. This is shown from the experiments with toluene (d)/acetone/water (diagram A) as well as with butyl acetate (d)/ acetone/water (diagram B), see *figure (9.5)*. Compared to the pulsed extractor with sieve trays with 2 mm holes (PSE), higher throughputs and higher mass transfer rates are achieved in the pulsed packed extractor. The comparison of the investigations in both agitated columns reveals that mass transfer performance of the Kühni-extractor is significantly better than of the RDC-

extractor. This is also confirmed by the investigations of *Stichlmair 1980*. However, the higher mass transfer rates in the Kühni-extractor are associated with a reduction of the maximum throughput compared to the RDC-extractor.

The analysis of all experimental data shows that the mass transfer rates of the Kühni-extractor are highest while the mass transfer rates in the RDC-extractor are lowest. Beside these two types of extractors, the pulsed extractor with the structured Montz packings turns out to be very suitable. The maximum throughput is highest for this type of extractor while simultaneously very high mass transfer rates are realised, see *figure (9.5)*. Since high throughputs and high mass transfer rates are desired during the operation of an extractor, the application of pulsed extractors with structured packings is recommended.

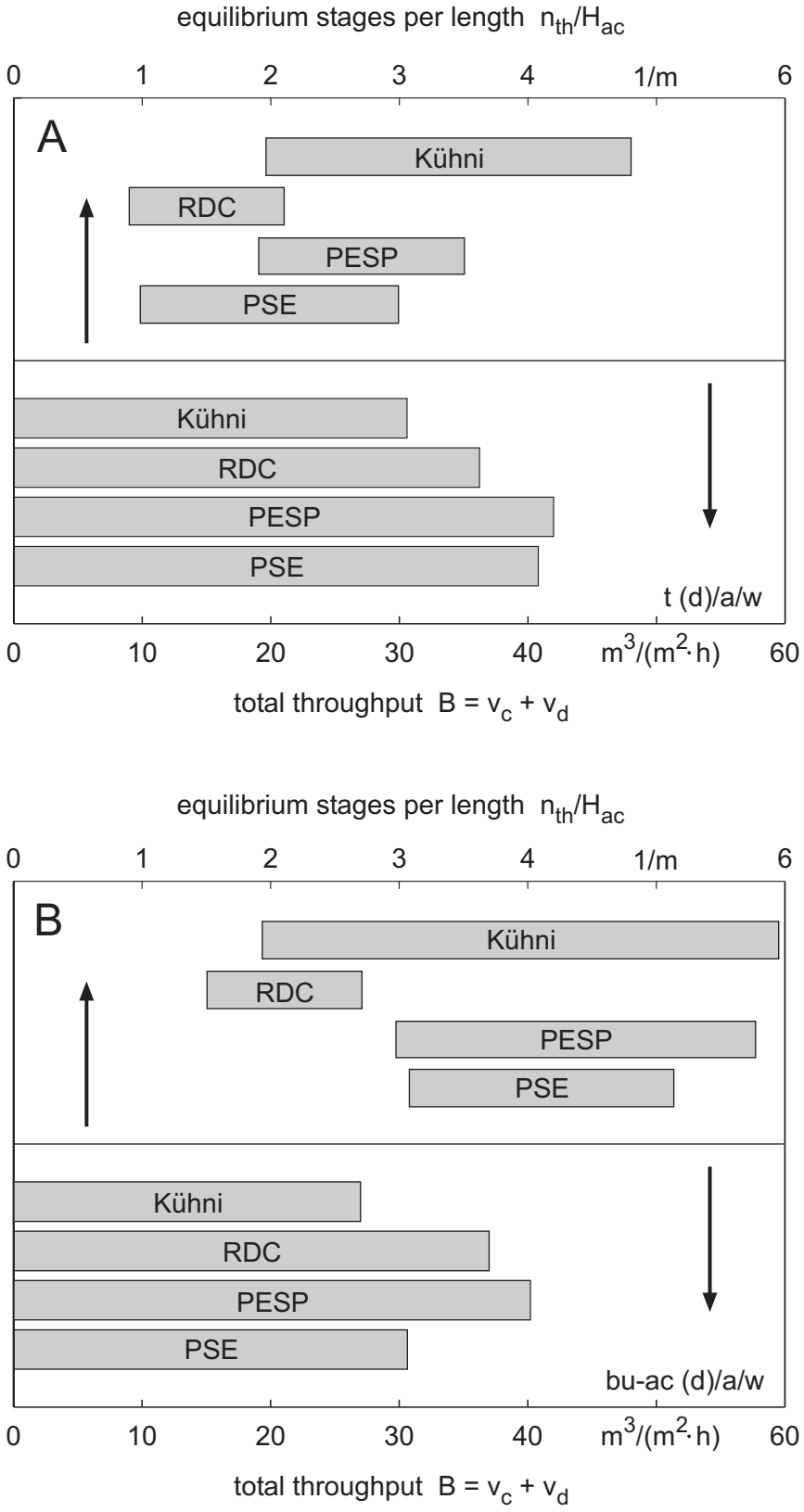

Figure 9.5: Maximum throughputs and equilibrium stages per active column height of the Kühni-extractor (Kühni), the RDC-extractor (RDC), the pulsed sieve tray extractor (PSE, d_h = 2 mm) and the pulsed extractor with structured packings (PESP, Montz-Pak B1-350) for toluene (d)/acetone/water (diagram A) and butyl acetate (d)/acetone/water (diagram B) for a phase ratio of v_d / v_c = 1.2

10 Summary

In recent years liquid/liquid-extraction has become a widely used separation technique in a variety of industrial applications. However, the choice of the optimal extractor and its dimensioning are still associated with uncertainties. Preliminary tests cannot be abandoned for a reliable dimensioning of an extraction column. To reduce the experimental effort, new methods have been introduced for dimensioning extraction columns only on the basis of experiments with single particles (single rigid spheres or drops). The results of the single particle investigations can be combined with drop population balance models (DPBMs), which represent efficient computer simulation programs for predicting the fluiddynamics and mass transfer rates of extractors.

The experiments with single rigid polypropylene spheres, single toluene drops and single butyl acetate drops show how characteristic velocities, drop breakage and mass transfer rates are influenced by the relevant parameters. The investigations in pulsed columns with different types of sieve trays and with structured packings as well as in agitated columns with rotating discs and Kühni blade agitators reveal that the characteristic velocity is mainly influenced by the particle size and the geometry of the column internals. Particularly in columns with Kühni blade agitators, the rotational speed also significantly affects the velocity of single particles. In addition to drop size and energy input, breakage and mass transfer rates of single drops are strongly influenced by the physical properties of the liquid/liquid-system.

Beside the experiments with single rigid spheres and drops, correlations were developed to predict the characteristic velocity of single particles as well as the breakage of single drops. Correlations for the characteristic velocities show a good agreement with own experimental data and with data from the literature. The derived correlations for predicting the breakage probability, the number of generated daughter drops and their drop size distribution agree very well with the experimental results. For pulsed columns with sieve trays and structured packings the derived correlations allow the breakage of single drops to be precisely described through a small number of experiments only. For agitated RDC- and Kühni-columns, these correlations also permit the single drop breakage to be accurately determined.

The experiments with swarms of rigid spheres and drops give information about the influence of hold-up on swarm velocities, i. e. about the swarm influence. Based on these investigations, a novel model for predicting the swarm influence was developed. With this model the swarm influence is determined from the characteristic velocities of single particles only. The validity of the new swarm model for drops in different extractors was verified through numerous experiments in a pilot plant extractor as well as by data from the literature. Thus, the swarm influence in extractors can be accurately predicted from single drop experiments only.

The investigation of the swarm influence in different pilot plant extractors was carried out under mass transfer conditions. The performance of the different extractors shows that a pulsed extractor with structured packings (Montz-Pak B1-350) combines very high mass transfer rates with very high throughputs. Very low mass transfer rates are obtained in an agitated RDC-column, which is due to the low energy input of the rotating discs and the low breakage rates.

With the help of DPBMs and the derived correlations in this work, the performance of an extractor can be predicted on the basis of a few single drop experiments. This results in a significant reduction of the effort and costs of the preliminary experiments necessary for dimensioning an extractor.

Further development of the introduced correlations by investigations with other liquid/liquid-systems and extensive investigations of coalescence behaviour and axial mixing are recommended. The prediction of coalescence rates in liquid/liquid-systems is still uncertain since small amounts of impurities and surfactants can cause a significant change of the coalescence behaviour. The investigation of axial mixing is difficult due to the large experimental effort required and the need for columns with large dimensions. However, further improvement in the prediction of fluiddynamics and mass transfer rates of industrial extractors can surely be achieved by a more accurate description of coalescence and axial mixing.

11 Nomenclature

Symbol	Description	Unit
a	amplitude of pulsation, volumetric mass transfer area	m, m^2/m^3
A	interfacial area	m^2
A_C	cross-sectional area of an extraction column	m^2
$a \cdot f$	pulsation intensity	m/s
a_P	volumetric surface area of a packing	m^2/m^3
A_P	cross-sectional area of a packing	m^2
B	total throughput, $B = v_c + v_d$	$m^3/(m^2 \cdot s)$
C	constant parameter	-
C_{IP}	interface instability parameter	-
$c_{d,o}$	drag coefficient of a single particle	-
$c_{d,o}(Re_o)$	drag coefficient of a single particle with Reynolds number Re_o	-
$c_{d,o}(Re_s)$	drag coefficient of a single particle within a particle swarm with Re_s	-
$c_{d,s}$	drag coefficient of a swarm of particles	-
d	drop diameter	m
$d_{1,2}$	sauter diameter, also referred to as $d_{3,2}$	m
d_{100}	characteristic drop diameter due to a breakage probability of 100 %	m
d_A	diameter of an agitator/stirrer	m
$D_{ax,c}$	axial back mixing coefficient of continuous phase	m^2/s
$D_{ax,d}$	axial back mixing coefficient of dispersed phase	m^2/s
D_c	diffusion coefficient in continuous phase	m^2/s
D_C	column diameter within the active part	m
d_{cap}	inner diameter of a glass capillary	m
d_{crit}	critical drop diameter	m
D_d	diffusion coefficient in dispersed phase	m^2/s
$D_{d,eff}$	effective diffusion coefficient in the dispersed phase	m^2/s
D_P	diameter of a packing	m
D_{st}	diameter of a sieve tray	m
d_{dd}	daughter drop diameter	m
d_{hP}	hole diameter of punched sheets of a packing	m

d_h	diameter of sieve tray holes	m
d_M	mother drop diameter	m
d_{max}	maximum diameter of a drop size distribution	m
d_p	particle diameter	m
d_{RP}	diameter of a random packing	m
d_s	inner diameter of a stator of an agitated compartment	m
d_{sh}	diameter of a rotating shaft	m
d_{stab}	stable drop diameter	m
f	continuous phase back mixing coefficient or frequency of pulsation	- , 1/s
g	dispersed phase back mixing coefficient	-
$g(t,z,d)$	breakage frequency for drops with diameter d at height z and time t	1/s
$h(d_1,d_2)$	collision frequency of drops with a diameter of d_1 and d_2	m^3/s
h_A	height of an agitator	m
H_{ac}	active height of an extraction column	m
h_c	volume fraction of continuous phase or compartment height	m^3/m^3, m
H_{coal}	height of volume of coalesced dispersed phase	m
h_d	hold-up (volume fraction of dispersed phase)	m^3/m^3
$h_{d,f}$	hold-up at the flooding point	m^3/m^3
h_P	height of a packing	m
h_{pb}	volume fraction of particles in a densely packed bed	m^3/m^3
H_{pb}	height of a packed bed of particles	m
h_s	height of a stage, see *chapter 2.1*	m
h_{st}	height of a sieve tray compartment	m
K'_{HR}	modified Hadamard-Rybczynski factor, see *chapter 2.2*	-
L	length of a measuring section	m
l_d	length of a cylindrical deformed drop	m
m	distribution coefficient: $m = y^*/x$	kg/kg
$\dot{M}_c$	mass flow rate of continuous phase	kg/s
$\dot{M}_d$	mass flow rate of dispersed phase	kg/s
m_s	overall mass transport of an entire drop spectrum	1/s
n	swarm exponent	-
$N(t,z,d)$	number of drops per column unit volume	$1/m^3$
n_{coal}	number of coalescence events	-

n_D	refractive index	-
n_{dd}	averaged number of daughter drops per breakage	-
N_P	dimensionless energy input, see *Kumar and Hartland 1996*	-
n_R	rotational speed	1/s
$n_{R,\,crit}$	critical rotational speed	1/s
n_{th}	number of equilibrium stages	-
P	energy input per compartment	W
$P(t,z,d)$	volumetric drop size density distribution for drops	
	with a diameter of d at height z and time t	1/m
p_B	breakage probability of single drops	-
p_c	coalescence probability	-
q_3	volumetric density distribution	1/m
R	dimensionless enhancement factor for mass transfer	-
s	thickness of a sieve tray	m
S_B	source term characterising the breakage of drops	1/(m · s)
S_C	source term characterising the coalescence of drops	1/(m · s)
$S_{F,d}$	source term characterising the feed and drop size distribution	
	at the inlet of the dispersed phase	1/(m · s)
$S_{F,c}$	source term characterising the feed inlet of the continuous phase	1/(m · s)
t	time	s
T	temperature	°C
t_{res}	residence time	s
T_y	mixing term due to breakage and coalescence during mass transfer	1/(m · s)
$\dot{V}$	volumetric flow rate	m^3/s
$V(d)$	volume of a drop with diameter d	m^3
v_c	superficial velocity of the continuous phase	m/s
$v_{c,e}$	effective velocity of the continuous phase in the column	m/s
$v_{c,f}$	superficial velocity of the continuous phase at flooding	m/s
$v_{char,o}$	characteristic velocity of single particles in columns with internals	m/s
V_{Comp}	volume of a compartment	m^3
v_d	superficial velocity of the dispersed phase	m/s
$v_{d,e}$	effective drop velocity in the column	m/s
$v_{d,f}$	superficial velocity of the dispersed phase at flooding	m/s

$V_{i,coal}$	volume of a drop with diameter d produced by coalescence	m^3
v_o	terminal velocity of single particles (in columns without internals)	m/s
v_{rs}	relative swarm velocity	m/s
v_s	superficial swarm velocity	m/s
V_{total}	volume of all swarm drops in a volume V_{Comp}	m^3
$w(d_1,d_2)$	coalescence rate for drops with a diameter of d_1 and d_2	m^3/s
x	solute concentration of the continuous phase	kg/kg
X	solute fraction in the continuous phase (solute free bases)	kg/kg
x_{if}	solute concentration of the continuous phase at the interface	kg/kg
x_{in}	solute concentration of the continuous phase at the entry	kg/kg
X_{in}	solute fraction in the continuous phase (solute free bases) at the entry	kg/kg
x_o	initial solute concentration of the continuous phase	kg/kg
X_{out}	solute fraction in the continuous phase (solute free bases) at the exit	kg/kg
$x_o - y_o$	initial solute concentration difference	kg/kg
y	solute concentration of the dispersed phase	kg/kg
Y	solute fraction in the dispersed phase (solute free bases)	kg/kg
y^*	solute concentration of the dispersed phase at equilibrium	kg/kg
y_{if}	solute concentration of the dispersed phase at the interface	kg/kg
y_{in}	solute concentration of the dispersed phase at the entry	kg/kg
Y_{in}	solute fraction in the dispersed phase (solute free bases) at the entry	kg/kg
y_o	initial solute concentration of the dispersed phase	kg/kg
Y_{out}	solute fraction in the dispersed phase (solute free bases) at the exit	kg/kg
z	height coordinate	m

Greek symbols

β_c	individual mass transfer coefficient in the continuous phase	m/s
β_d	individual mass transfer coefficient in the dispersed phase	m/s
β_{oc}	overall continuous phase mass transfer coefficient	m/s

β_{od}	overall dispersed phase mass transfer coefficient	m/s
$\beta_{od,s}$	overall dispersed phase mass transfer coefficient of a drop swarm	m/s
η_c	dynamic viscosity of the continuous phase	Pa · s
η_d	dynamic viscosity of the dispersed phase	Pa · s
κ	conductivity of water	S/m
λ	extraction factor: $\lambda = m/(\dot{M}_c/\dot{M}_d)$	-
$\lambda(d_1,d_2)$	coalescence efficiency of two collided drops	-
λ_i	eigen values	-
λ_{ls}	wave length of a light source	m
ρ_c	density of the continuous phase	kg/m^3
ρ_d	density of the dispersed phase	kg/m^3
σ	interfacial tension of a liquid/liquid-system	N/m
ϕ	energy dissipation	m^2/s^3
φ_P	voidage fraction of a packing	m^3/m^3
φ_s	relative free cross-sectional area of a stator	m^2/m^2
φ_{st}	relative free cross-sectional area of a sieve tray plate	m^2/m^2
Ψ_m	drag coefficient of a packing, see *Mackowiak 1993*	-

Dimensionless numbers

$Ar = \rho_c \cdot \lvert\rho_c - \rho_d\rvert \cdot g \cdot d^3/\eta_c^2$	Archimedes number
$Br = m \cdot \sqrt{D_d/D_c}$	Brauer number
$Eö = g \cdot d^2 \cdot \lvert\rho_c - \rho_d\rvert/\sigma$	Eötvos number
$Fo_c = 4 \cdot D_c \cdot t/d^2$	continuous phase Fourier number
$Fo_d = 4 \cdot D_d \cdot t/d^2$	dispersed phase Fourier number
$K_l = \sigma^3 \cdot \rho_c^2/(g \cdot \eta_c^4 \cdot \Delta\rho)$	number characterising the liquid/liquid-system
$Pe_c = v_{c,e} \cdot L/D_{ax,c}$	Peclet number of the continuous phase
$Pe_d = v_{d,e} \cdot L/D_{ax,d}$	Peclet number of the dispersed phase
$Q = (y_2 - y_1)/(y^* - y_1)$	extraction efficiency
$Re_o = v_o \cdot d \cdot \rho_c/\eta_c$	Reynolds number of a single particle
$Re_R = n_R \cdot d_A^2 \cdot \rho_c/\eta_c$	Reynolds number of an agitator
$Re_s = v_s \cdot d \cdot \rho_c/\eta_c$	Reynolds number of a swarm of particles

$Sc_c = \eta_c/(\rho_c \cdot D_c)$	Schmidt number of the continuous phase
$Sc_d = \eta_d/(\rho_d \cdot D_d)$	Schmidt number of the dispersed phase
$Sh_c = \beta_c \cdot d/D_c$	Sherwood number of the continuous phase
$Sh_d = \beta_d \cdot d/D_d$	Sherwood number of the dispersed phase
$\pi_{af} = a \cdot f \cdot (\rho_c^2/(\eta_c \cdot \Delta\rho \cdot g))^{1/3}$	pulsation intensity
$\pi_{a_P} = a_P \cdot (\eta_c^2/(\rho_c \cdot \Delta\rho \cdot g))^{1/3}$	volumetric surface area of a packing
$\pi_d = d \cdot (\rho_c \cdot \Delta\rho \cdot g/\eta_c^2)^{1/3}$	drop diameter
$\pi_{h_P} = h_P \cdot (\rho_c \cdot \Delta\rho \cdot g/\eta_c^2)^{1/3}$	height of a packing
$\pi_\sigma = \sigma \cdot (\rho_c^2/(\eta_c^4 \cdot \Delta\rho \cdot g))^{1/3}$	interfacial tension
$\pi_v = v \cdot (\rho_c^2/(\eta_c \cdot \Delta\rho \cdot g))^{1/3}$	drop velocity

Abbreviations

DPBMs	drop population balance models
PSE	pulsed sieve tray extractor
PESP	pulsed extractor with structured packings
PERP	pulsed extractor with random packings
RDC	rotating disc contactor
Kühni	extractor with Kühni blade agitators
c to d	denotes the mass transfer direction: from continuous to dispersed phase
d to c	denotes the mass transfer direction: from dispersed to continuous phase
pp	polypropylene: was used as material for the rigid spheres
p. a.	pro analysis: denotes the purity of a substance
equil.	equilibrium
t	toluene
bu-ac	butyl acetate
a	acetone
w	water

12 References

Al Aswad et al. 1985 — Al Aswad, K. K.; Mumford, C. J.; Jeffreys, G. V.: The Application of Drop Size Distribution and Discrete Drop Mass Transfer Models to Assess the Performance of a Rotating Disc Contactor, AIChE Journal 31, 9, p. 1488-1497

Al Khani et al. 1989 — Al Khani, D. S.; Gourdon, C.; Casamatta, G.: Dynamic and Steady-State Simulation of Hydrodynamics and Mass Transfer In Liquid-Liquid Extraction Column, Chem. Eng. Sci 44, 6, p. 1295-1305

Anderson 1961 — Anderson, K. E. B.: Pressure Drop in Ideal Fluidisation, Chem. Eng. Sci. 15, p. 276-283

Attarakih 2004 — Attarakih, M.: Solution Methodologies for the Population Balance Equations Describing the Hydrodynamics of Liquid-Liquid Extraction Contactors, Dissertation, Technical University of Kaiserslautern, Germany

Attarakih et al. 2005 — Attarakih, M.; Bart, H.-J.; Faqir, N. M.: Numerical Solution of Bivariate Population Balance Equation for the Interacting of Hydrodynamics and Mass Transfer in Liquid-Liquid Extraction Columns, Chem. Eng. Sci.

Aufderheide 1985 — Aufderheide, E.: Hydrodynamische Untersuchungen an Pulsierten Siebbodenextraktionskolonnen, Dissertation, Technical University of Clausthal, Germany

Bäcker et al. 1991 — Bäcker, W.; Schäfer, J.-P.; Schröter, J. (1991): Einsatz von geordneten Packungen in der Flüssig/flüssig-Extraktion, Chem. Ing. Tech. 63 (10), p. 1008-1011

Bahmanyar and Slater 1991 — Bahmanyar, H.; Slater, M. J.: Studies of Breakage in Liquid-Liquid Systems in a Rotating Disc Contactor, Part I: Conditions of no mass transfer, Chem. Eng. Technol. 14, p. 79-89

Bailes et al. 1986	Bailes, P. J.; Gledhill, J.; Godfrey, J. C.; Slater, M. J.: Hydrodynamic Behaviour of Packed, Rotating Disc and Kühni Liquid/Liquid Extraction Columns, Chem. Eng. Res. Des. 14, p. 43-55
Barnea and Mizrahi 1975	Barnea, E.; Mizrahi, J.: A Generalized Approach to the Fluid Dynamics of Particulate Systems, Can. J. Chem. Eng. 53, p. 461-468
Bauer 1976	Bauer, R.: Die Längsvermischung beider Phasen in einer gerührten Fest-Flüssig-Extraktionskolonne, Dissertation, ETH Zurich, Switzerland
Bell and Babb 1969	Bell, R. L.; Babb, A. L.: Holdup and Axial Distribution of Holdup in a Pulsed Sieve-Plate Solvent Extraction Column, Ind. Eng. Chem., Process Des. Dev. 8, p. 392-400
Blaß 1990	Blaß, E.: Formation and Coalescence of Bubbles and Droplets, Int. Chem. Eng. 30, p. 206-221
Blaß 1997	Blaß, E.: Entwicklung verfahrenstechnischer Prozesse, second edition, Springer-Verlag, Berlin
Blaß et al. 2000	Blaß, E. et al.: Transportmechanisms across Fluid Interfaces, Dechema Monograph, Wiley-VCH Verlag GmbH, Weinheim
Böcker 1997	Böcker, J.: Chromatographie, Würzburg, Germany, Vogel-Verlag
Boyadzhiev et al. 1969	Boyadzhiev, L.; Elenkov, D.; Kyuchukov, G. (1969): On Liquid-Liquid Mass Transfer inside Drops in a Turbulent Flow Field, Can. J. Chem. Eng. 47, p. 42-44
Brandner and Brauer 1993	Brandner, B.; Brauer, H.: Impuls- und Stofftransport durch die Phasen-grenzfläche von kugelförmigen fluiden Partikeln, Fortschrittsberichte VDI 3/326 (Reihe/Nr.), Germany
Brauer 1971	Brauer, H.: Grundlagen der Einphasen- und Mehrphasenströmungen, Verlag Sauerländer, Frankfurt am Main, Germany
Brauer 1971	Brauer, H.: Stoffaustausch einschließlich chemischer Reaktionen, Verlag Sauerländer, Aarau, Switzerland

Casamatta and Vogelpohl 1985	Casamatta, G.; Vogelpohl, A.: Modelling of Fluiddynamics and Mass Transfer in Extraction Columns, Ger. Chem. Eng. 8, p. 96-103
Cauwenberg 1995	Cauwenberg, V.: Hydrodynamics and Physico-Chemical Aspects of Liquid-Liquid Extraction, Dissertation, Catholic University Leuven, Germany
Chen and Lee 2000	Chen, L.-H.; Lee, Y.-L.: Adsorption Behavior of Surfactants and Mass Transfer in Single-Drop Extraction, AIChE 46, 1, p. 160-168
Clift et al. 1978	Clift, R.; Grace, J. R.; Weber, M. E.: Bubbles, Drops and Particles, Academic Press, London
Coulaloglou and Tavlarides 1976	Coulaloglou, C. A.; Tavlarides, L. L.: Drop Size Distribution and Coalescence Frequencies of Liquid/Liquid Dispersions in Flow Vessels, AIChE J. 22, 2
Coulaloglou and Tavlarides 1977	Coulaloglou, C. A.; Tavlarides, L. L.: Description of Interaction Processes in Agitated Liquid/Liquid Dispersions, Chem. Eng. Sci. 32, p. 1289-1297
Cruz-Pinto 1979	Cruz-Pinto, J. J. C.: Experimental and Theoretical Modelling Studies of the Hydrodynamic and Mass Transfer Processes in Countercurrent Flow Liquid-Liquid Extraction Columns, Dissertation, University of Manchester, England
Cruz-Pinto and Korchinsky 1980	Cruz-Pinto, J. J. C.; Korchinsky, W. J.: Experimental Confirmation of the Influence of Drop Size Distribution on Liquid-Liquid Extraction Column Performance, Chem. Eng. Sci. 35, p. 2213-2219
Cruz-Pinto and Korchinsky 1981	Cruz-Pinto, J. J. C.; Korchinsky, W. J.: Drop Breakage in Counter Current Flow Liquid-Liquid Extraction Columns, Chem. Eng. Sci. 36, p. 687-694

Delplancq and Delvosalle 1996	Delplancq, E.; Delvosalle, C.: Hold-up and Flooding in Stagewise Multi-Agitated Liquid Extractors: Pilot-Plant Experimentation and Scale-up Procedure, 12th International Congress of Chemical and Process Engineering, Chisa, Praha, Czech Republic
EFCE 1984	Misek, T.; Berger, R. Schröter, J.: Standard Test Systems for Liquid Extraction, Inst. Chem. Eng., 2th edition, Warwickshire
Elzina and Banchero 1959	Elzina, E. R.; Banchero, J. T.: Film Coefficients for Heat Transfer to Liquid Drops, Chem. Eng. Prog. Symp. Ser.-No. 29, 55, p. 149 et seqq.
Fan et al. 1987	Fan, Z.; Oloidi, J. O.; Slater, M. J.: Liquid-Liquid Extraction Column Design Data Acquisition from Short Columns, Chem. Eng. Res. Des. 65, p. 243-250
Fang et al. 1995	Fang, J.; Godfrey, J. C.; Mao, Z.-Q.; Slater, M. J.; Gourdon, C.: Single Liquid Drop Breakage Probabilities and Characteristic Velocities in Kühni Columns, Chem. Eng. Technol. 18, p. 41-48
Final Report AiF 40 ZN 2004	Final Report AiF 40 ZN: Vom Einzeltropfenexperiment zur Extraktionskolonne, 01.01.2001-31.10.2004, Forschungs-Gesellschaft Verfahrens-Technik e. V., Frankfurt am Main, Germany (a link to the final report can be found in the internet: www.tvt.rwth-aachen.de)
Fischer 1973	Fischer, E. A.: Hydrodynamik und Stoffaustausch in einer Flüssig-Flüssig-Rührextraktionskolonne, Dissertation, Technical University of Zurich, Switzerland
Gayler et al. 1953	Gayler, R.; Roberts, N. W.; Pratt, H. R. C.: Liquid-Liquid Extraction: Part IV: A Further Study of Holdup in Packed Columns, Trans. Inst. Chem. Eng. 31, p. 69-82
Godfrey and Slater 1991	Godfrey, J. C.; Slater, M. J.: Slip Velocity Relationships for Liquid-Liquid Extraction Columns, Trans. IChemE. 69 (3) Part A, p. 130-141
Godfrey and Slater 1994	Godfrey, J. C.; Slater, M. J.: Liquid-Liquid Extraction Equipment, John Wiley & Sons, New York

Goldmann 1986	Goldmann, G.: Ermittlung und Interpretation von Kennlinienfelder einer gerührten Extraktionskolonne, Dissertation, Technical University of Munich, Germany
Goldmann and Blaß 1986	Goldmann, G.; Blaß, E.: Mass Transfer Characteristics of an Agitated Extraction Column Depending on Material Properties, Proceedings ISEC, p. 1-9
Golovin 1992	Golovin, A. A.: Mass Transfer under Interfacial Turbulence: Kinetic Regularities, Chem. Eng. Sci. 47, 8, p. 2069-2080
Grace et al. 1976	Grace, W.; Wairegi, J.; Nguyen, N.: Shapes and Velocities of Single Drops and Bubbles Moving Freely through Immiscible Liquids, Trans. Inst. Chem. Eng. 54, p. 167-173
Grömping 2004	Grömping, T.: in: Final Report AiF 40 ZN: Vom Einzeltropfenexperiment zur Extraktionskolonne, 01.01.2001-31.10.2004, Forschungs-Gesellschaft Verfahrens-Technik e. V., Frankfurt am Main, Germany
Hafez et al. 1974	Hafez, M. M.; Nemecek, N.; Prochazka, J.: Holdup and Flooding in a Reciprocating-Plate Extractor, Proc. Int. Solvent Extraction Conf. 2, Soc. Chem. Ind. , p. 1671-1688
Hancil and Rod 1988	Hancil, V.; Rod, V.: Break-up of a Drop in a Stirred Tank, Chem. Eng. Process 23, p. 189-193
Handlos and Baron 1957	Handlos, A. E.; Baron, T.: Mass and Heat Transfer from Drops in Liquid-Liquid Extraction, AIChE 3, p. 127-136
Hähnsen 1989	Hähnsen, A.: Inbetriebnahme von zwei pulsierten Packungsextraktoren, sowie vergleichende Untersuchungen der Fluiddynamik und des Stoffaustausches zur Optimierung der Packungsabmessungen und der Packungsoberflächen, Diploma Thesis, Technical University of Clausthal, Germany
Häntsch and Weiss 1976	Häntsch, W.; Weiss, S.: Zur axialen Durchmischung der dispersen Phase in Drehscheibenextraktoren, Chem. Tech. 28. p. 334 et seqq.

Haverland 1988	Haverland, H.: Untersuchungen zur Tropfendispergierung in flüssigkeitspulsierten Siebboden-Extraktionskolonnen, Dissertation, Technical University of Clausthal, Germany
Heertjes et al. 1954	Heertjes, P. M.; Holve, W. A.; Talsma, H.: Mass Transfer between Isobutanol and Water in a Spray Column, Chem. Eng. Sci. 3, p. 122 et seqq.
Henschke 2003	Henschke, M.: Auslegung pulsierter Siebboden-Extraktionskolonnen, Professorial Dissertation, RWTH Aachen, Germany
Hoting 1996	Hoting, B.: Untersuchungen zur Fluiddynamik und Stoffübertragung in Extraktionskolonnen mit strukturierten Packungen, Dissertation, Technical University of Clausthal, Germany
Hu and Kintner 1955	Hu, S.; Kintner, R. S.: The Fall of Single Liquid Drops Through Water, AIChE 1 (1), p. 42-48
Ihme et al. 1972	Ihme, F; Schmidt-Traub, H.; Brauer, H.: Theoretische Untersuchung über die Umströmung und den Stoffübergang an Kugeln, Chem. Ing. Tech. 44, 5, p. 306-313
Ingham et al. 1974	Ingham, J.; Bourne, J. R.; Mogli, A.: Backmixing in a Kühni Liquid-Liquid Extraction Column, Proc. ISEC 2, p. 1299 et seqq.
Ishii and Zuber 1979	Ishii, M.; Zuber, N.: Drag Coefficient and Relative Velocity in Bubble, Droplet or Particulate Flows, AIChE 25 (5), p. 843-855
Ismail et al. 1988	Ismail, A. M.; Korchinsky, W. J.: Mass-Transfer Parameters in Rotating Disc Contactors: Influence of Column Diameter, J. Chem. Tech. Biotechnol. 43. p. 147-158
Kaskas 1971	Kaskas, I. in: Brauer, H.: Grundlagen der Einphasen- und Mehrphasenströmungen, Verlag Sauerländer, Frankfurt am Main, Germany

Kirou et al. 1988	Kirou, V. I.; Tavlarides, L. L.; Bonnet, J. C.: Flooding, Holdup, and Drop Size Measurements in a Multistage Column Extractor, AIChE 34 (2), p. 283-292
Klee and Treybal 1956	Klee, A. J.; Treybal, R. E.: Rate of Rise or Fall of Liquid Drops, AIChE 2 (4), p. 444-447
Kolb 2003	Kolb, B.: Gaschromatographie in Bildern, Weinheim, Wiley-VCH Verlag
Kolmogorov 1958	Kolmogorov, A. N.: Sammelband zur Theorie der statistischen Turbulenz, Akademie-Verlag, Berlin, Germany
Korchinsky et al. 1986	Korchinsky, W. J.; Al-Husseini, R.: Liquid-Liquid Extraction Column (Rotating Disc Contactor) - Model Parameters from Drop Size Distribution and Solute Concentration Measurements, J. Chem. Tech. Biotechnol. 36, p. 295-409
Korchinsky and Ismail 1988	Korchinsky, W. J.; Ismail, A. M.: Mass-Transfer Parameters in Rotating Disc Contactors: Influence of Column Diameter, J. Chem. Tech. Biotechnol. 43. p. 147-158
Korchinsky and Sheikh 1992	Korchinsky, W. J.; Sheikh, Q. M.: “Forward Mixing“ Model: Application to Pulsed Plate Extraction Column Operation in the Emulsion Region, Chem. Eng. Comm. 115, p. 95-115
Korchinsky und Young 1986	Korchinsky, W. J.; Young, C. H.: High Flux Mass Transfer: Comparison of Liquid-Liquid Extraction Column and Drop (Handlos-Baron) Model Predictions with Rotating Disc Contactor Performance, Chem. Eng. Sci. 41, 12, p. 3053-3061
Kronberger et al. 1995	Kronberger, T.; Ortner, A.; Zulehner, W.; Bart, H.-J.: Numerical Simulation of Extraction Columns Using a Drop Population Model, Computers Chemical Engineering 19, p. 639-644
Kronik and Brink 1950	Kronik, R.; Brink, J. C.: On the Theory of Extraction from Falling Droplets, Appl. Sci. Res. A2, p. 142-154

Kumar 1985 — Kumar, A.: Hydrodynamics and Mass Transfer in Kühni Extractor, Dissertation, Swiss Federal Institute of Technology, Zurich

Kumar and Hartland 1989 — Kumar, A.; Hartland, S.: Independent Prediction of Slip Velocity and Dispersed Phase Hold-up in Liquid/Liquid Extraction Columns, Can. J. Chem. Eng. 67 (2), p. 17-25

Kumar and Hartland 1994 — Kumar, A.; Hartland, S.: Empirical Prediction of operating variables, in: Liquid-Liquid Extraction Equipment, John Wiley & Sons, New York, p. 625-735

Kumar and Hartland 1995 — Kumar, A.; Hartland, S.: A Unified Correlation for the Prediction of Dispersed-Phase Hold-up in Liquid-Liquid Extraction Columns, Ind. Eng. Chem. Res. 34, p. 3925-3940

Kumar and Hartland 1996 — Kumar, A.; Hartland, S.: Unified Correlation for the Prediction of Drop Size in Liquid-Liquid Extraction Columns, Ind. Eng. Chem. Res. 35, p. 2682-2695

Kumar and Hartland 1999 — Kumar , A.; Hartland, S.: Correlations for Prediction of Mass Transfer Coefficients in Single Drop Systems and Liquid-Liquid Extraction Columns, Trans IChemE 77, p. 372-384

Kumar et al. 1986 — Kumar, A.; Steiner, L.; Hartland, S.: Capacity and Hydrodynamics of an Agitated Extraction Column, Ind. Eng. Chem. Process Des. Dev. 25, p. 728-733

Laddha et al. 1978 — Laddha, G. S.; Degaleesan, T. E.; Kannappan, R.: Hydrodynamics and Mass Transport in Rotary Disc Contactors, Can. J. Chem. Eng. 56, p. 137-150

Leu 1995 — Leu, J. T.: Beitrag zur Fluiddynamik von Extraktionskolonnen mit geordneten Packungen, Dissertation, Technical University of Clausthal, Germany

Liang and Slater 1990	Liang, T.-B; Slater, M. J.: Liquid-Liquid Extraction Drop Formation: Mass Transfer and the Influence of Surfactants, Chem. Eng. Sci. 45, 1, p. 97-105
Logsdail et al. 1957	Logsdail, D. H.; Thornton J. D.; Pratt, H. R. C.: Liquid-Liquid Extraction Part XII: Flooding Rates and Performance Data for a Rotary Disc Contactor, Trans. Instn. Chem. Engrs. 35, p. 301-315
Lorenz 1990	Lorenz, M.: Untersuchungen zum fluiddynamischen Verhalten von pulsierten Siebboden-Extraktionskolonnen, Dissertation, Technical University of Clausthal, Germany
Mackowiak 1993	Mackowiak, J: Grenzbelastungen von unpulsierten Füllkörperkolonnen bei der Flüssig/Flüssig-Extraktion, Chem.-Ing.-Tech. 65 (4), p. 423-429
Mao et al. 1995	Mao, Z.-Q.; Godfrey, J. C.; Slater, M. J.: Single Liquid Drop Velocities and Breakage Mechanism in Sections of Structured Packings, Chem. Eng. Technol. 18, p. 33-40
Marr et al. 1975	Marr, R.; Moser, F.; Husung, G.: Hydrodynamische Auslegung von Drehscheiben-Extraktoren (RDC), Chem. Ing. Tech. 47 (5), p. 1-16
McAllister et al. 1967	McAllister, R. A.; Groenier, W. S.; Ryon, A. D.: Correlation of Flooding in Pulsed Perforated-Plate Extraction Columns, Chem. Eng. Sci. 22, p. 931-944
Mecklenburg and Hartland 1966	Mecklenburg, J. C.; Hartland, S.: A Comparison of Differential and Stagewise Counter Current Extraction with Backmixing, Chem. Eng. Sci. 21, p. 1209 et seqq.
Mersmann 1980	Mersmann, A.: Zum Flutpunkt in Flüssig/Flüssig-Gegenstromkolonnen, Chem. Ing. Tech. 52, p. 933-942
Mersmann 1986	Mersmann, A.: Stoffübertragung, Springer-Verlag, Berlin, Heidelberg, New York, Tokyo, p. 82 et seqq.

Mersmann et al. 2005 — Mermann, A.; Kind, M.; Stichlmair, J.: Thermische Verfahrenstechnik - Grundlagen und Methoden, 2. wesentlich erweiterte und aktualisierte Auflage, Springer-Verlag, Berlin Heidelberg, Germany

Misek 1963 — Misek, T.: Hydrodynamic Behaviour of Agitated Liquid Extractors, Czech. Chem. Commun. 28, p. 1631 et seqq.

Miyauchi and Oya 1965 — Miyauchi, T.; Qya, H.: Longitudinal Dispersion in Pulsed Perforated Plate Columns, AIChE 11, p. 395-402

Modes 1999 — Modes, G.: Grundsätzliche Studie zur Populationsdynamik einer Extraktionskolonne auf Basis von Einzeltropfenuntersuchungen, Dissertation, Technische Universität Kaiserslautern, Germany

Molinier 1976 — Molinier, J.: Fonctionnement des Colonnes Pulsèes en Extraction Liquide/ Liquide: Transfert de Matière Entre une Goutte et un Liquide, Dissertation, Institut National Polytechnique, Toulouse, France

Narsimhan 1979 — Narsimhan, G.; Gupta, J. P.; Ramkrishna, D.: A Model for Transitional Breakage Probability of Droplets in Agitated Liquid-Liquid Dispersions, Chem. Eng. Sci. 34, p. 257-265

Nedungadi 1991 — Nedungadi, K.: On the Performance of a Liquid-Liquid Extraction Column packed with Sulzer SMV Static Mixers, Dissertation, Swiss Federal Institute of Technology Zurich

Newman 1931 — Newman, A. B.: The Drying of Porous Solids: Diffusion and Surface Emission Equations, Trans. AIChE 27, p. 203-220

Niebuhr 1982 — Niebuhr, D.: Untersuchungen zur Fluiddynamik in Pulsierten Siebbodenextraktionskolonnen, Dissertation, Technical University of Clausthal, Germany

Nishimura and Ishii 1980 — Nishimura, Y.; Ishii, T.: An Analysis of Transport Phenomena of Multisolid Particle Systems at Higher Reynolds Numbers by a Standard Karman-Pohlhausen Method. II. Mass Transfer, Chem. Eng. Sci. 35, 5, p. 1205-1209

Olney 1964 — Olney, R. B.: Droplet Characterisation in a Countercurrent Contactor, AIChE Journal 10, p. 827-835

Ortner et al. 1995 — Ortner, A.; Kronberger, T.; Zulehner, W.; Bart, H.-J.: Tropfenbilanzmodell am Beispiel einer gerührten Extraktionskolonne, Chem. Ing. Tech. 67, 8, p. 984-988

Petersen 1994 — Petersen, M.: Einfluß des Stoffübergangs auf die Fluiddynamik und die Trennleistung einer pulsierten Extraktionskolonne mit geordneten Packungen, Diploma Thesis, Technical University of Clausthal, Germany

Pfennig et al. 2005 — Pfennig, A.; Bart, H.-J.; Garthe, D.; Grömping, T.; Schmidt, S.; Stichlmair, J.: Vom Einzeltropfen zur Extraktionskolonne, Chem. Ing. Tech., will soon be published

Pietzsch 1984 — Pietzsch, W.: Beitrag zur Auslegung pulsierter Siebbodenextraktoren, Dissertation, Technical University of Munich, Germany

Pietzsch and Blaß 1987 — Pietzsch, W.; Blaß, E.: A new Method for the Prediction of Liquid Pulsed Sieve-Tray Extractors, Chem. Eng. Technol. 10 (73), p. 73-86

Pilhofer 1974 — Pilhofer, T.: Hydrodynamik von Tropfenschwärmen in Flüssig-Flüssig Sprühkolonnen, Chem. Ing. Tech. 46, p. 783 et seqq.

Pilhofer 1977 — Pilhofer, T.: Partikelmeßtechnik für Blasen und Tropfen in Flüssigkeiten, Fortschritte der Verfahrenstechnik 15, p. 92 et seqq.

Pilhofer 1978 — Pilhofer, T.: Verfahrenstechnische Auslegung von Flüssig-Flüssig Gegenstromkolonnen, Professorial Dissertation, Technical University of Munich, Germany

Pilhofer 1989 — Pilhofer, T.: Industrielle Anwendungen von Flüssig-flüssig Extraktionsprozessen, Dechema-Monographie, 114, S. 303-313

Qi 1992 — Qi, M.: Untersuchungen zum Stoffaustausch am Einzeltropfen in flüssigkeitspulsierten Siebboden-Extraktionskolonnen, Dissertation, Technical University of Clausthal, Germany

Rauber and Steiner 1997 — Rauber, J.; Steiner, R.: Untersuchungen zum Trennverhalten von strukturierten Packungen bei der Flüssig/Flüssig-Extraktion mit hohem Phasenverhältnis, Chem. Ing. Tech. 69, p. 320-323

Rauscher 1992 — Rauscher, H.: Untersuchung einer pulsierten Siebboden-Extraktionskolonne bei extremen Phasenverhältnissen, Dissertation, Technical University of Munich, Germany

Reissinger 1985 — Reissinger K.-H.: Auslegung pulsierter Siebboden-Extraktoren (PSE) unter Berücksichtigung von Tropfengrößen- und Verweilzeitverteilungen, Dissertation, Technical University of Graz, Austria

Richardson and Zaki 1954 — Richardson, J. F.; Zaki, W.: Sedimentation and Fluidisation: Part I, Trans. Institution of chemical Engineers 32, p. 35-53

Rod 1968 — Rod, V.: Longitudinal Mixing in the Dispersed Phase in Rotating Disc Extractors, Coll. Czech. Chem. Com. 33, p. 2855 et seqq.

Rohlfing 1991 — Rohlfing, E.: Untersuchungen zum fluiddynamischen Verhalten einer pulsierten Füllkörperextraktionskolonne, Dissertation, RWTH Aachen, Germany

Roock 1985 — Roock, D.: Vergleichende Messungen in einer Füllkörperkolonne mit geordneten Einbauten, Diploma Thesis, University of applied sciences (FH) of Cologne, Germany

Rozen et al. 1970 — Rozen, A. M.; Rubezhnyv, Y. G.; Martynov, B. V.: Longitudinal Mixing in Pulsating Extraction Column, Sov. Chem. Ind. 2, p. 66-73

Rydberg et al. 1992 — Rydberg, J.; Musikas, C.; Choppin, G. R.: Principles and Practices of Solvent Extraction, Marcel Dekker Inc., New York

Schmidt 1994 — Schmidt, R.: ACHEMA Berichte: Anlagen und Apparate für Destillation, Rektifikation, Sorption, Permeation, Extraktion, Chem.-Ing.-Tech. 66, 11, p. 1448-1462

Schmidt 2004 — Schmidt, S.: in: Final Report AiF 40 ZN: Vom Einzeltropfenexperiment zur Extraktionskolonne, 01.01.2001-31.10.2004, Forschungs-Gesellschaft Verfahrens-Technik e. V., Frankfurt am Main, Germany

Schweitzer et al. 1996 — Schweitzer et al.: Handbook of Separation Techniques for Chemical Engineers, third edition, McGraw-Hill, New York

Seibert 1986 — Seibert, A. F.: Hydrodynamics and Mass Transfer in Spray and Packed Liquid-Liquid Extraction Columns, Dissertation, University of Texas at Austin, America

Simon et al. 2003 — Simon, M.; Schmidt, S.; Bart, H.-J.: The Droplet Population Balance Model - Estimation of Breakage and Coalescence, Chem. Eng. Technol. 26, p. 745-750

Skelland and Wellek 1964 — Skelland, A. H.; Wellek, R. M.: Resistance to Mass Transfer inside Droplets, AIChE 10, p. 491 et seqq

Slater 1994 — Slater, M. J.: Rate Coefficients in Liquid-Liquid Extraction Systems, in: Liquid-Liquid Extraction Equipment, Godfrey, J. C.; Slater, M. J. (1994), John Wiley & Sons, New York, p. 45-94

Slater 1995 — Slater, M. J.: A combined Model of Mass Transfer Coefficients for Contaminated Drop Liquid/Liquid-Systems. Can. J. Chem. Eng. 73, p. 462-469

Sovova 1981 — Sovova, H.: Breakage and Coalescence of Drops in a batch stirred Vessel-II. Comparison of Model and Experiments, Chem. Eng. Sci. 36, p. 1567-1573

Sovova 1990 — Sovova, H.: Countercurrent Pulsed and Reciprocating Plate Extractors. Prediction of Sauter Mean Drop Diameter, Collect. Czech. Chem. Commun. 55, p. 409-425

Sovova and Prochazka 1981 — Sovova, H.; Prochazka, J.: Breakage and Coalescence of Drops in a Batch Stirred Vessel-I. Comparison of Continuous and Discrete Models, Chem. Eng. Sci. 36, p. 163-171

Spaay et al. 1971 — Spaay, N. M.; Simons, A. J. F.; Brink, G. P.: Design and Operation of a Pulsed Packed Column for Liquid-Liquid Extraction, Proc. ISEC 1, p. 281-298

Steiner 1986 — Steiner, L.: Mass-transfer Rates from Single Drops and Drop Swarms, Chem. Eng. Sci. 41, p. 1979-1986

Steiner 1988 — Steiner, L.: Rechnerische Erfassung der Arbeitsweise von Flüssig-Flüssig Extraktionskolonnen, VDI-Reihe 3, 154, Düsseldorf, Germany

Steiner et al. 1998 — Steiner, L.; Balmelli, M.; Hartland, S.: Simulation of Hydrodynamic Performance of a Stirred Extraction Column, 13th International Congress of Chemical and Process Engineering, Chisa, Praha, Czech Republic

Stichlmair 1980 — Stichlmair, J.: Leistungs- und Kostenvergleich verschiedener Apparatebauarten für die Flüssig/flüssig-Extraktion, Chem. Ing. Tech. 3, p. 253-255

Stichlmair 2001 — Stichlmair, J.: Scale-up Engineering, Begell House Verlag, New York

Stichlmair 2005 — Stichlmair, J.: Extraktion, in: Thermische Verfahrenstechnik - Grundlagen und Methoden, 2. wesentlich erweiterte und aktualisierte Auflage, Springer-Verlag, Berlin Heidelberg, Germany

Stichlmair et al. 1989 — Stichlmair, J.; Bravo, J. L., Fair, J. R.: General Model for Prediction of Pressure Drop and Capacity of Countercurrent Gas/Liquid Packed Columns, Gas Separation & Purification 3, p. 19-26

Stichlmair and Steude 1990 — Stichlmair, J.; Steude, H. E.: Abtrennen und Rückgewinnung von Stofffen aus Abwasser und Abfallflüssigkeiten - Stofftrenntechnik in der Umwelttechnik, Diskussionstagung 4./5.12.1990, VDI-GVC, Düsseldorf, Germany

Strand et al. 1962 — Strand, C. P.; Olney, R. B.; Ackermann, G. H.: Fundamental Aspects of Rotating Disc Contactor Performance, AIChE 8, p. 252-261

Thornton 1957 — Thornton, J. D.: Liquid-Liquid Extraction Part XIII: The Effect of Pulse Wave-Form and Plate Geometry on the Performance and Throughput of a pulsed column, Trans. Instn. Chem. Engrs. 35, p. 317-330

Thorsen et al. 1968 — Thorsen, G.; Stordalen, R. M.; Terjesen, S. G.: On the Terminal Velocity of Circulating and Oscillating Liquid Drops, Chem. Eng. Sci. 23, p. 413-426

Tobin and Ramkrishna 1999 — Tobin, T.; Ramkrishna, D.: Modelling the Effect of Drop Charge on Coalescence in Turbulent Liquid-Liquid Dispersions, Can. J. Chem. Eng. 77, p. 1090-1104

Tourneau 2004 — Tourneau, M.: Stoffübergang im Tropfenschwarm unter dem Einfluss von Marangonikonvektionen, Dissertation, Technical University of Munich, Germany

Toutain et al. 1998 — Toutain, J.; Le Lann, J. M.; Gourdon, C.; Joulia, X.: Maxwell-Stefan Approach Coupled Drop Population Model for the Dynamic Simulation of Liquid/liquid Extraction Pulsed Column, Computers Chem. Eng. 22, p. 379-386

Tsouris and Tavlarides 1994 — Tsouris, C.; Tavlarides, L. L.: Breakage and Coalescence Models for Drops in Turbulent Dispersions, AIChE J. 40, 3, p. 395-406

Wagner 1994 — Wagner, G.: Der Einfluß der Viskosität auf die Strömung in Apparaten für die Flüssig-flüssig-Extraktion, Dissertation, Technical University of Munich, Germany

Wagner 1999 — Wagner, I.: Der Einfluß der Viskosität auf den Stoffübergang in Flüssig-flüssig-Extraktionskolonnen, Dissertation, Technical University of Munich, Germany

Wagner and Blaß 1999 — Wagner, G.; Blaß, E.: Modeling of Drop Disintegration in Liquid Pulsed Sieve-Tray Extractors with Regard to Viscosity, Chem. Eng. Technol. 21 (6), p. 475-479

Wagner 2003 — Wagner, R.: Nichts als Wasser - Reinstwassersysteme für Analytik und Life Science, LABO 2003, p. 6-7, Germany

Wasowski and Blaß 1987	Wasowski, T.; Blaß, E.: Wake-Phänomene hinter festen und fluiden Partikeln, Chem. Ing. Tech. 59, p. 544-555
Weiss et. al 1995	Weiss, J.; Steiner, L.; Hartland, S.: Determination of Actual Drop Velocities in Agitated Extraction Columns, Chem. Eng. Sci. 50 (2), p. 255-261
Wesselingh and Bollen 1999	Wesselingh, J. A.; Bollen, A. M.: Single Particles, Bubbles and Drops: Their Velocities and Mass Transfer Coefficients, Trans IChemE. 77 (Part A), p. 89-96
Widmer 1973	Widmer, F.: Tropfengröße, Tropfenverhalten und Stoffaustausch in pulsierten Füllkörper-Extraktionskolonnen, Chem. Ing. Tech. 45 (2), p. 67-74
Wolf 1999	Wolf, S.: Phasengrenzkonvektionen beim Stoffübergang in Flüssig-Flüssig-Systemen, Dissertation, Technical University of Munich, Germany
Wolschner 1980	Wolschner, B.: Konzentrationsprofile in Drehscheibenextraktoren, Dissertation, Technical University of Graz, Austria
Yaron and Gal-Or 1971	Yaron, I.; Gal-Or, B.: Relative Velocity and Pressure Drops in clouds of drops, bubbles or solid particles, AIChE 17, p. 1064-1067
Young et al. 1986	Young, C. H.; Korchinsky, W. J.: High Flux Mass Transfer: Comparison of Liquid-Liquid Extraction Column and Drop (Handlos-Baron) Model Predictions with Rotating Disc Contactor Performance, Chem. Eng. Sci. 41, 12, p. 3053-3061
Zamponi 1996	Zamponi, G.: Das dynamische Verhalten einer gerührten Solventextraktionskolonne, Dissertation, Technical University of Munich, Germany
Zhang et al. 1985	Zhang, S. H.; Yu, S. C.; Zhou, Y. C.; Su, Y. F.: A Model for Liquid-Liquid Extraction Column Performance - The Influence of Drop Size Distribution on Extraction Efficiency, Can. J. of Chem. Eng. 63, p. 212-226

A Appendix

Experiments with single particles and swarms of particles were performed with rigid polypropylene spheres and two different liquid/liquid-systems. Two standard systems recommended by the European Federation of Chemical Engineering, see *EFCE 1984*, were used as the liquid/liquid-systems: toluene/acetone/water and butyl acetate/acetone/water. The physical properties of both liquid/liquid-systems can be found in *chapter 3.2*. The thermodynamic phase equilibria of both test systems will be discussed in the following section.

A.1 Phase Equilibria: Toluene/Acetone/Water and Butyl Acetate/Acetone/Water

The phase equilibria for toluene/acetone/water and butyl acetate/acetone/water are shown in *figure (A.1)* and *figure (A.2)*. The diagrams show the miscibility gap calculated from correlations presented in *EFCE 1984* and show experimental results of own phase equilibrium studies.

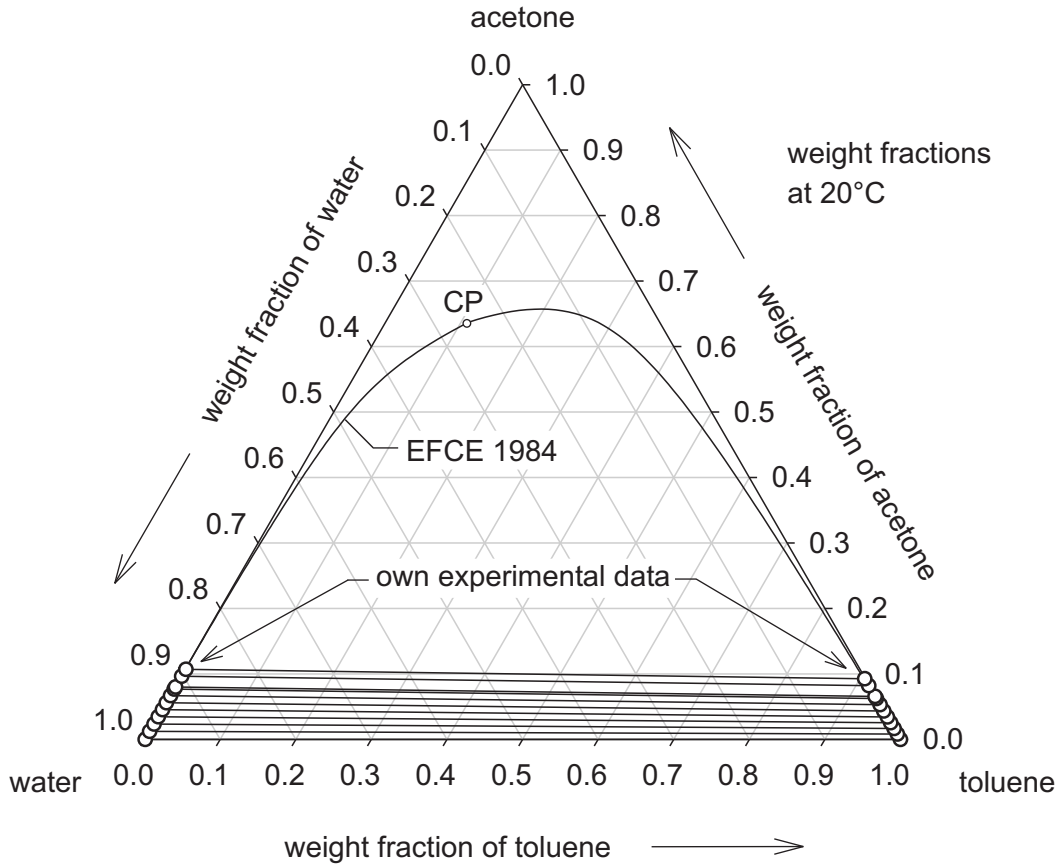

Figure A.1: Phase equilibrium and miscibility gap of toluene/acetone/water; comparison of experimental data with the correlation for the prediction of the thermodynamic phase equilibrium presented in EFCE 1984

Both liquid/liquid-systems show a wide miscibility gap in a wide range of acetone concentrations. For toluene/acetone/water almost no miscibility of the two phases is observed for acetone concentrations up to 10 wt.-%. In contrast, butyl acetate/acetone/water shows a low miscibility, particularly in the butyl acetate phase in the same acetone concentration range.

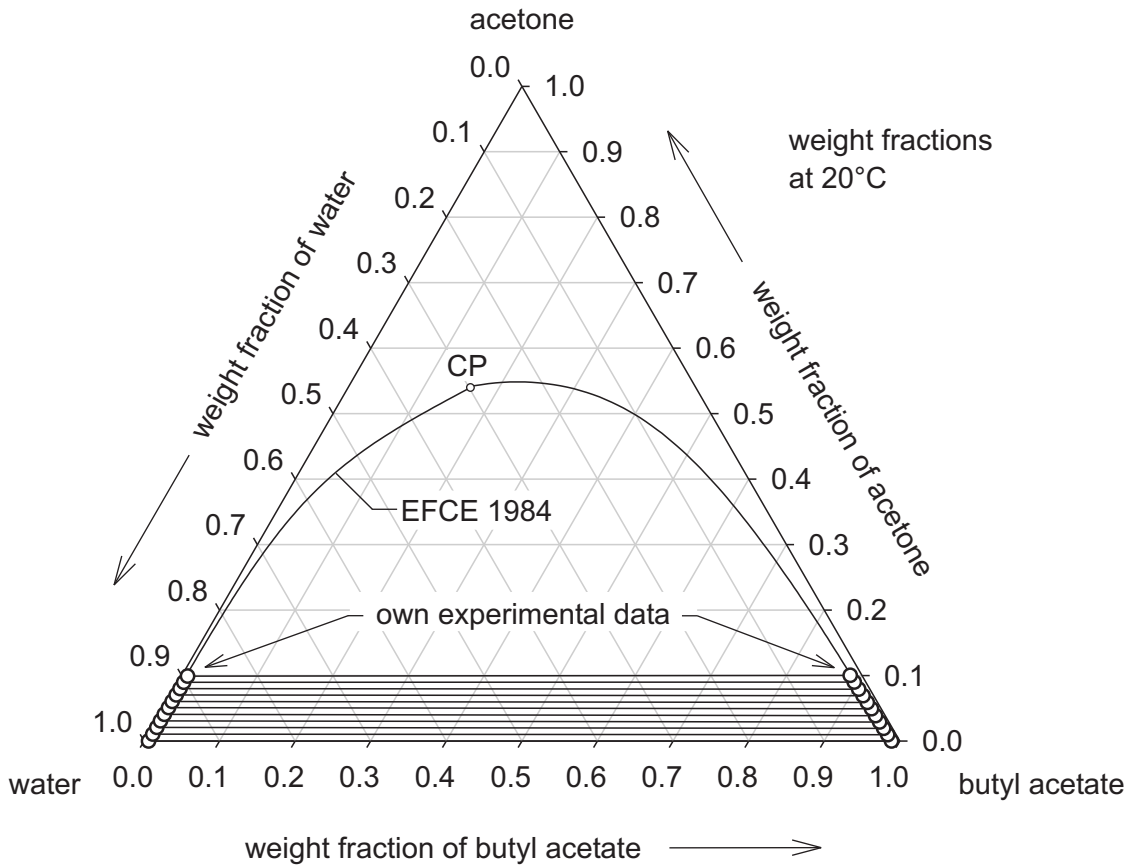

Figure A.2: Phase equilibrium and miscibility gap of butyl acetate/acetone/water; comparison of experimental data with the correlation for the phase equilibrium presented in EFCE 1984

A.2 Extraction Plant, Sliding Valves and Column Internals

A schematic of the entire extraction plant, used for the investigations of drop swarms, including the distillation column for the reprocessing treatment of the solvent, is seen in *figure (A.3)*. Structured packings were used as internals in the distillation column. The diameter of the distillation column was 150 mm and the total height was approximately 7 m. The dimensions of the extraction column are given in *chapter 4.4*.

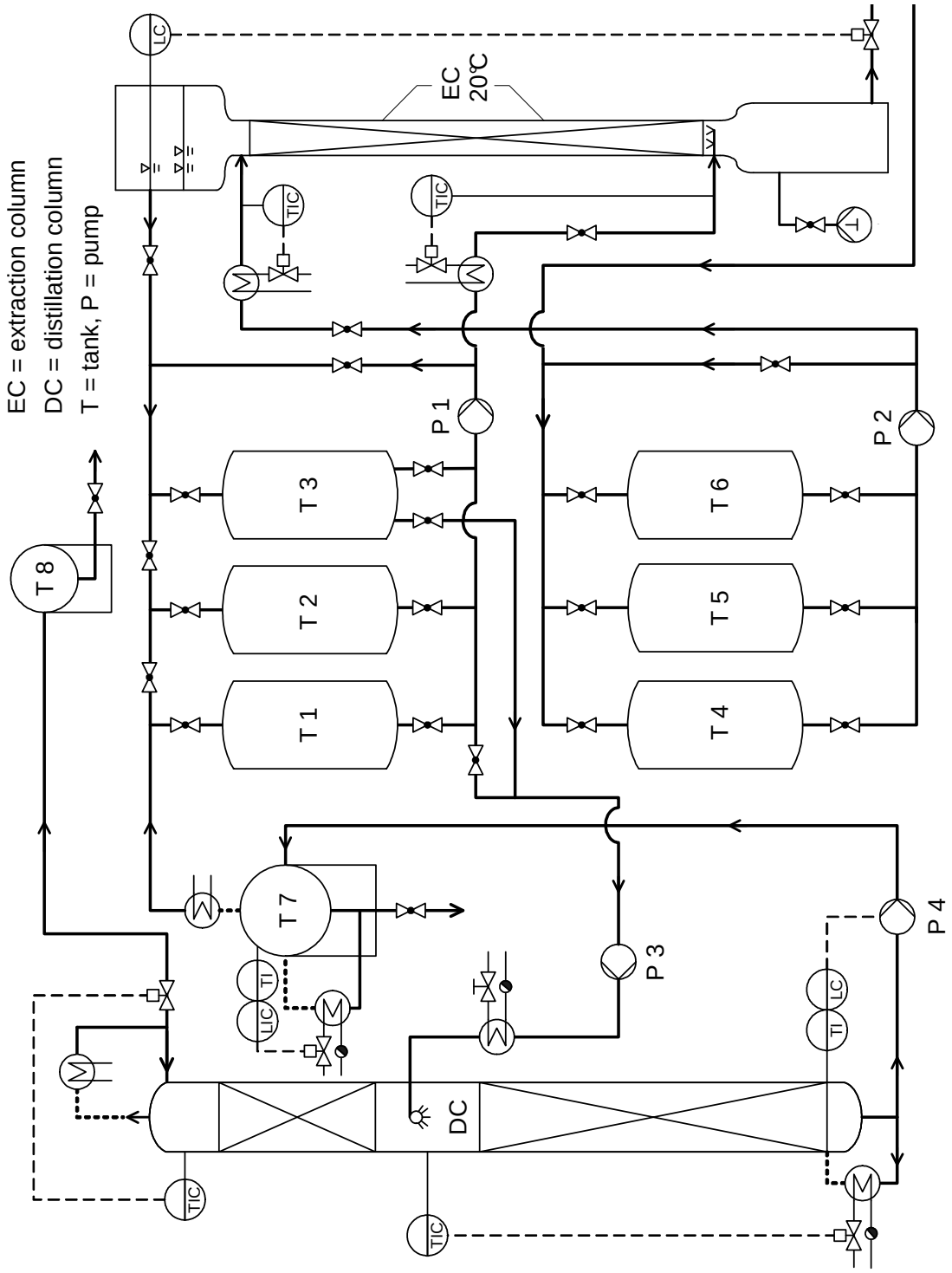

Figure A.3: Schematic of the entire extraction plant including the extraction column "EC" and the distillation column "DC"

During the experiments in the drop swarm extractor and the rigid sphere swarm extractor, the hold-up was determined with slide valves, see *chapter 4*. After the entire cross-section of the columns was closed for the dispersed phases with the help of different closing plates within the slide valves, the hold-up was determined by measuring the height of the rigid particle bed or the height of coalescence beneath the closing plates. In *figure (A.4)* photos of the closing plates for both the rigid sphere swarm extractor (top row) and the drop swarm extractor (second row) are shown. Aluminium, poly-vinyl chloride (PVC), silicone and stainless steel were used as construction materials for the slide valves and closing plates of the rigid sphere swarm extractor. The slide valves of the drop swarm extractor were made of stainless steel and the closing plates consisted of teflon.

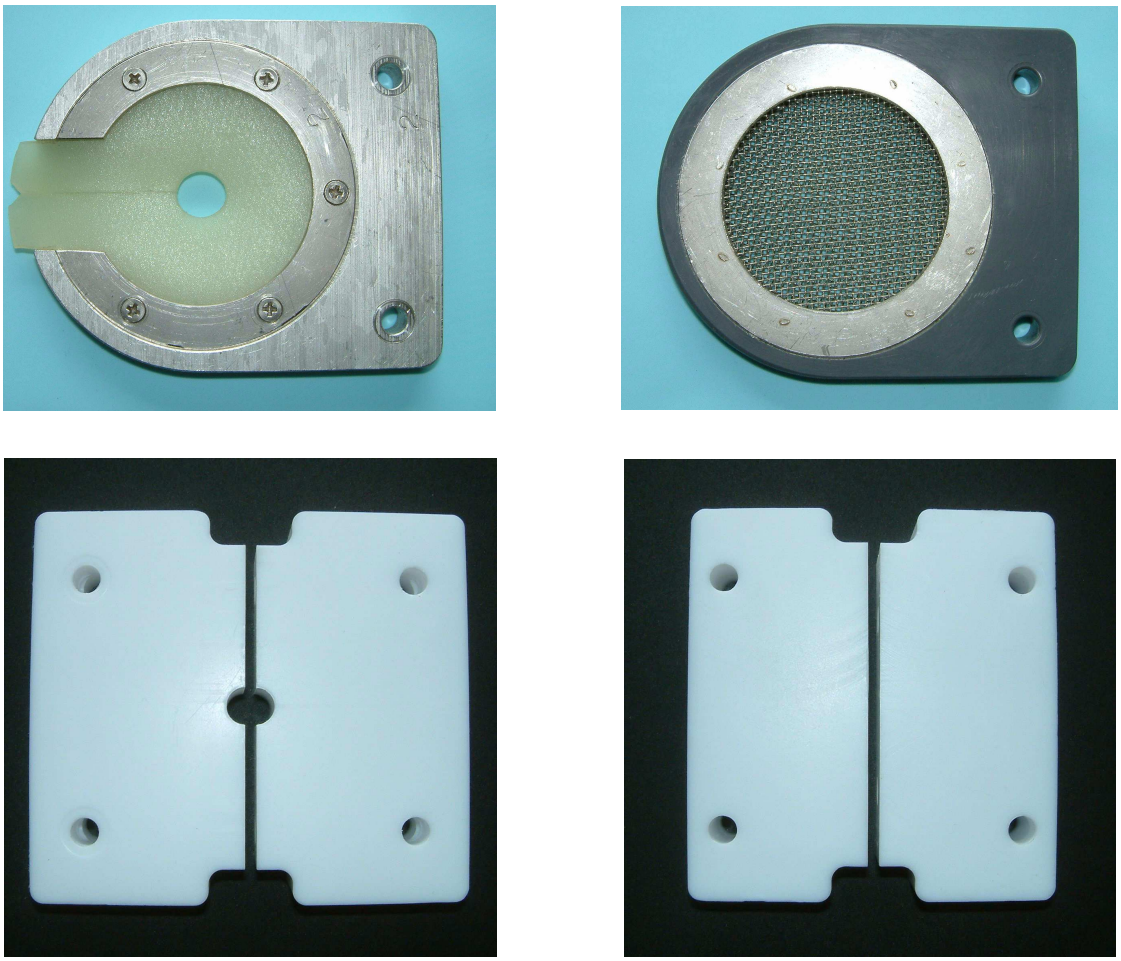

Figure A.4: Photos of closing plates: top row = closing plates for the agitated (left) and pulsed (right) rigid sphere swarm extractor, second row = teflon closing plates for the agitated (left) and pulsed (right) drop swarm extractor

Two different types of sieve trays, structured packings (Montz-Pak B1-350), rotating discs and Kühni blade agitators were used as internals in the pulsed and agitated columns. Sketches of the installed compartments are given in *chapter 4.5*. The dimensions of the internals are listed in the following table.

Table A.1: Geometrical data of used internals: Two different types of sieve trays, structured packings (Montz-Pak B1-350) and two different agitator types (rotating disc and Kühni blade agitator) were installed inside the active part of the columns.

Sieve tray - d_h = 2 mm	Sieve tray - d_h = 4 mm	Montz-Pak B1-350
diameter of sieve tray D_{st} = 79 mm	diameter of sieve tray D_{st} = 79 mm	diameter of a packing D_P = 79 mm
diameter of holes d_h = 2 mm	diameter of holes d_h = 4 mm	volumetric surface area a_P = 350 m^2/m^3
rel. free cross-sectional area φ_{st} = 0.20 m^2/m^2	rel. free cross-sectional area φ_{st} = 0.40 m^2/m^2	void fraction φ_P = 0.97 m^3/m^3
height of compartment h_{st} = 100 mm	height of compartment h_{st} = 100 mm	height of a packing h_P = 100 mm
thickness of sieve tray s = 1.0 mm	thickness of sieve tray s = 2.0 mm	hole diameter of punched sheets d_{hP} = 4 mm

Rotating disc	Kühni - 6 blade agitator
diameter of agitator d_A = 45 mm	diameter of agitator d_A = 45 mm
height of agitator h_A = 1.5 mm	height of agitator h_A = 7 mm
rel. free cross-sectional stator area φ_s = 0.40 m^2/m^2	rel. free cross-sectional stator area φ_s = 0.40 m^2/m^2
height of compartment h_c = 50 mm	height of compartment h_c = 50 mm
diameter of rotating shaft d_{sh} = 10 mm	diameter of rotating shaft d_{sh} = 10 mm

A.3 Survey of Experimental Data

The following sections show the results of the experiments with single particles and swarms of particles which include the single particle velocities in extraction columns with and without internals.

A.3.1 Velocities of Single Drops

Experiments with single rigid spheres and liquid drops were carried out to study the effect of surface mobility and form oscillations on the terminal velocity of single drops. The terminal velocity of single rigid pp-spheres, toluene drops and butyl acetate drops in an extraction column without internals, where no mass transfer was present, are listed in *table (A.2)*.

Table A.2: Terminal velocity v_o of single particles in an extraction column without internals (where no mass transfer was present); binary test systems: rigid pp-spheres/water, toluene (d)/water and butyl acetate (d)/water;

single rigid spheres - single liquid drops	particle/drop-diameter d_p /d [mm]	terminal velocity v_o [cm/s]
pp-spheres	1.9	4.6
pp-spheres	2.0	5.4
pp-spheres	2.5	7.2
pp-spheres	3.0	8.6
pp-spheres	3.4	9.8
pp-spheres	4.0	10.2
toluene drops, charge A	1.5	5.0
toluene drops, charge A	2.0	6.4
toluene drops, charge A	2.5	8.2
toluene drops, charge A	3.0	9.1
toluene drops, charge A	3.5	10.3
toluene drops, charge A	4.0	11.7
toluene drops, charge A	5.0	12.7
toluene drops, charge A	6.0	13.7
toluene drops, charge B	1.5	4.6
toluene drops, charge B	2.0	6.8
toluene drops, charge B	2.5	9.0
toluene drops, charge B	3.0	9.8

Table A.2: Terminal velocity v_o of single particles in an extraction column without internals (where no mass transfer was present); binary test systems: rigid pp-spheres/water, toluene (d)/water and butyl acetate (d)/water; (continued)

single rigid spheres - single liquid drops	particle/drop-diameter d_p /d [mm]	terminal velocity v_o [cm/s]
toluene drops, charge B	3.5	11.7
toluene drops, charge B	4.0	12.6
toluene drops, charge B	4.5	13.0
toluene drops, charge B	5.0	13.9
toluene drops, charge B	5.5	14.2
toluene drops, charge B	5.8	14.3
toluene drops, charge B	6.0	14.7
toluene drops, charge B	6.3	14.6
toluene drops, charge B	6.5	14.7
toluene drops, charge B	7.0	14.0
toluene drops, charge B	7.5	13.8
toluene drops, charge B	8.0	13.6
butyl acetate drops	1.5	4.5
butyl acetate drops	2.0	7.3
butyl acetate drops	2.5	10.1
butyl acetate drops	3.0	12.0
butyl acetate drops	3.5	12.3
butyl acetate drops	3.8	12.2
butyl acetate drops	4.0	12.1
butyl acetate drops	4.3	12.1
butyl acetate drops	4.5	11.7
butyl acetate drops	4.8	11.3
butyl acetate drops	5.0	11.0
butyl acetate drops	5.5	10.7
butyl acetate drops	6.0	10.2

The investigation of the characteristic velocity of single particles in columns with different internals were mainly conducted to determine the influence of particle size, physical properties of the test systems and energy input on the flow of single particles. The characteristic velocities of single rigid pp-spheres, toluene drops and butyl acetate drops in pulsed and agitated compartments are listed in *table (A.3)* and in *table (A.3)*. The characteristic velocities presented in these tables were determined in the mini plants in absence of mass transfer.

Table A.3: Characteristic velocity $v_{char,o}$ of single particles in pulsed compartments with different internals (where no mass transfer was present); binary test systems: rigid pp-spheres/water, toluene (d)/water, butyl acetate (d)/water;

compartment type	single rigid spheres - single liquid drops	d_p or d [mm]	a · f [cm/s]	$v_{char,o}$ [cm/s]
sieve-tray d_h = 4 mm	pp-spheres	1.9	1.0	4.0
sieve-tray d_h = 4 mm	pp-spheres	2.0	1.0	4.6
sieve-tray d_h = 4 mm	pp-spheres	2.5	1.0	5.1
sieve-tray d_h = 4 mm	pp-spheres	3.0	1.0	6.4
sieve-tray d_h = 4 mm	pp-spheres	3.4	1.0	6.1
sieve-tray d_h = 4 mm	pp-spheres	1.9	1.5	4.3
sieve-tray d_h = 4 mm	pp-spheres	2.0	1.5	5.0
sieve-tray d_h = 4 mm	pp-spheres	2.5	1.5	5.4
sieve-tray d_h = 4 mm	pp-spheres	3.0	1.5	6.5
sieve-tray d_h = 4 mm	pp-spheres	3.4	1.5	7.1
sieve-tray d_h = 4 mm	pp-spheres	1.9	2.0	4.2
sieve-tray d_h = 4 mm	pp-spheres	2.0	2.0	4.8
sieve-tray d_h = 4 mm	pp-spheres	2.5	2.0	5.6
sieve-tray d_h = 4 mm	pp-spheres	3.0	2.0	6.5
sieve-tray d_h = 4 mm	pp-spheres	3.4	2.0	6.6
sieve-tray d_h = 4 mm	toluene drops, charge A	1.5	0.0	4.4
sieve-tray d_h = 4 mm	toluene drops, charge A	2.0	0.0	5.3
sieve-tray d_h = 4 mm	toluene drops, charge A	2.5	0.0	6.3
sieve-tray d_h = 4 mm	toluene drops, charge A	3.0	0.0	7.1
sieve-tray d_h = 4 mm	toluene drops, charge A	3.5	0.0	7.4
sieve-tray d_h = 4 mm	toluene drops, charge A	4.0	0.0	7.8
sieve-tray d_h = 4 mm	toluene drops, charge A	1.5	0.5	4.2
sieve-tray d_h = 4 mm	toluene drops, charge A	2.0	0.5	5.4
sieve-tray d_h = 4 mm	toluene drops, charge A	2.5	0.5	6.3
sieve-tray d_h = 4 mm	toluene drops, charge A	3.0	0.5	6.7

Table A.3: Characteristic velocity $v_{char,o}$ of single particles in pulsed compartments with different internals (where no mass transfer was present); binary test systems: rigid pp-spheres/water, toluene (d)/water, butyl acetate (d)/water; (continued)

compartment type	single rigid spheres - single liquid drops	d_p or d [mm]	a · f [cm/s]	$v_{char,o}$ [cm/s]
sieve-tray d_h = 4 mm	toluene drops, charge A	3.5	0.5	7.2
sieve-tray d_h = 4 mm	toluene drops, charge A	4.0	0.5	7.5
sieve-tray d_h = 4 mm	toluene drops, charge A	1.5	1.0	4.2
sieve-tray d_h = 4 mm	toluene drops, charge A	2.0	1.0	5.5
sieve-tray d_h = 4 mm	toluene drops, charge A	2.5	1.0	5.7
sieve-tray d_h = 4 mm	toluene drops, charge A	3.0	1.0	6.4
sieve-tray d_h = 4 mm	toluene drops, charge A	3.5	1.0	6.9
sieve-tray d_h = 4 mm	toluene drops, charge A	4.0	1.0	7.2
sieve-tray d_h = 4 mm	toluene drops, charge A	1.5	1.5	4.4
sieve-tray d_h = 4 mm	toluene drops, charge A	2.0	1.5	5.4
sieve-tray d_h = 4 mm	toluene drops, charge A	2.5	1.5	6.0
sieve-tray d_h = 4 mm	toluene drops, charge A	3.0	1.5	6.7
sieve-tray d_h = 4 mm	toluene drops, charge A	3.5	1.5	7.1
sieve-tray d_h = 4 mm	toluene drops, charge A	4.0	1.5	7.7
sieve-tray d_h = 4 mm	toluene drops, charge A	1.5	2.0	4.2
sieve-tray d_h = 4 mm	toluene drops, charge A	2.0	2.0	5.3
sieve-tray d_h = 4 mm	toluene drops, charge A	2.5	2.0	6.2
sieve-tray d_h = 4 mm	toluene drops, charge A	3.0	2.0	7.1
sieve-tray d_h = 4 mm	toluene drops, charge A	3.5	2.0	7.4
sieve-tray d_h = 4 mm	toluene drops, charge A	4.0	2.0	7.6
sieve-tray d_h = 4 mm	butyl acetate drops	1.5	0.0	4.4
sieve-tray d_h = 4 mm	butyl acetate drops	2.0	0.0	5.4
sieve-tray d_h = 4 mm	butyl acetate drops	2.5	0.0	6.8
sieve-tray d_h = 4 mm	butyl acetate drops	3.0	0.0	8.1
sieve-tray d_h = 4 mm	butyl acetate drops	3.5	0.0	8.0
sieve-tray d_h = 4 mm	butyl acetate drops	4.0	0.0	8.4
sieve-tray d_h = 4 mm	butyl acetate drops	1.5	0.5	4.2
sieve-tray d_h = 4 mm	butyl acetate drops	2.0	0.5	5.7
sieve-tray d_h = 4 mm	butyl acetate drops	2.5	0.5	7.0
sieve-tray d_h = 4 mm	butyl acetate drops	3.0	0.5	8.0
sieve-tray d_h = 4 mm	butyl acetate drops	3.5	0.5	8.0
sieve-tray d_h = 4 mm	butyl acetate drops	4.0	0.5	8.5
sieve-tray d_h = 4 mm	butyl acetate drops	1.5	1.0	4.0
sieve-tray d_h = 4 mm	butyl acetate drops	2.0	1.0	5.5

Table A.3: Characteristic velocity $v_{char,o}$ of single particles in pulsed compartments with different internals (where no mass transfer was present); binary test systems: rigid pp-spheres/water, toluene (d)/water, butyl acetate (d)/water; (continued)

compartment type	single rigid spheres - single liquid drops	d_p or d [mm]	a · f [cm/s]	$v_{char,o}$ [cm/s]
sieve-tray d_h = 4 mm	butyl acetate drops	2.5	1.0	7.2
sieve-tray d_h = 4 mm	butyl acetate drops	3.0	1.0	8.0
sieve-tray d_h = 4 mm	butyl acetate drops	3.5	1.0	8.2
sieve-tray d_h = 4 mm	butyl acetate drops	4.0	1.0	8.8
sieve-tray d_h = 4 mm	butyl acetate drops	1.5	1.5	4.5
sieve-tray d_h = 4 mm	butyl acetate drops	2.0	1.5	5.7
sieve-tray d_h = 4 mm	butyl acetate drops	2.5	1.5	7.0
sieve-tray d_h = 4 mm	butyl acetate drops	3.0	1.5	8.0
sieve-tray d_h = 4 mm	butyl acetate drops	3.5	1.5	8.3
sieve-tray d_h = 4 mm	butyl acetate drops	4.0	1.5	8.3
sieve-tray d_h = 4 mm	butyl acetate drops	1.5	2.0	4.3
sieve-tray d_h = 4 mm	butyl acetate drops	2.0	2.0	5.5
sieve-tray d_h = 4 mm	butyl acetate drops	2.5	2.0	7.0
sieve-tray d_h = 4 mm	butyl acetate drops	3.0	2.0	7.4
Montz-Pak B1-350	pp-spheres	1.9	0.0	3.4
Montz-Pak B1-350	pp-spheres	2.0	0.0	3.3
Montz-Pak B1-350	pp-spheres	2.5	0.0	3.4
Montz-Pak B1-350	pp-spheres	3.0	0.0	3.7
Montz-Pak B1-350	pp-spheres	3.4	0.0	3.9
Montz-Pak B1-350	pp-spheres	1.9	0.5	2.9
Montz-Pak B1-350	pp-spheres	2.0	0.5	3.3
Montz-Pak B1-350	pp-spheres	2.5	0.5	3.4
Montz-Pak B1-350	pp-spheres	3.0	0.5	3.2
Montz-Pak B1-350	pp-spheres	3.4	0.5	3.5
Montz-Pak B1-350	pp-spheres	1.9	1.0	2.9
Montz-Pak B1-350	pp-spheres	2.0	1.0	2.7
Montz-Pak B1-350	pp-spheres	2.5	1.0	3.5
Montz-Pak B1-350	pp-spheres	3.0	1.0	3.2
Montz-Pak B1-350	pp-spheres	3.4	1.0	3.5
Montz-Pak B1-350	pp-spheres	1.9	1.5	3.1
Montz-Pak B1-350	pp-spheres	2.0	1.5	3.4
Montz-Pak B1-350	pp-spheres	2.5	1.5	3.5
Montz-Pak B1-350	pp-spheres	3.0	1.5	3.3
Montz-Pak B1-350	pp-spheres	3.4	1.5	3.7

Table A.3: Characteristic velocity $v_{char,o}$ of single particles in pulsed compartments with different internals (where no mass transfer was present); binary test systems: rigid pp-spheres/water, toluene (d)/water, butyl acetate (d)/water; (continued)

compartment type	single rigid spheres - single liquid drops	d_p or d [mm]	a · f [cm/s]	$v_{char,o}$ [cm/s]
Montz-Pak B1-350	pp-spheres	1.9	2.0	2.5
Montz-Pak B1-350	pp-spheres	2.0	2.0	3.0
Montz-Pak B1-350	pp-spheres	2.5	2.0	3.2
Montz-Pak B1-350	pp-spheres	3.0	2.0	3.2
Montz-Pak B1-350	pp-spheres	3.4	2.0	3.8
Montz-Pak B1-350	toluene drops, charge A	2.0	0.0	3.1
Montz-Pak B1-350	toluene drops, charge A	2.5	0.0	4.0
Montz-Pak B1-350	toluene drops, charge A	3.0	0.0	3.5
Montz-Pak B1-350	toluene drops, charge A	3.5	0.0	3.3
Montz-Pak B1-350	toluene drops, charge A	4.0	0.0	3.2
Montz-Pak B1-350	toluene drops, charge A	1.5	0.5	2.9
Montz-Pak B1-350	toluene drops, charge A	2.0	0.5	2.8
Montz-Pak B1-350	toluene drops, charge A	2.5	0.5	3.8
Montz-Pak B1-350	toluene drops, charge A	3.0	0.5	3.4
Montz-Pak B1-350	toluene drops, charge A	3.5	0.5	3.3
Montz-Pak B1-350	toluene drops, charge A	4.0	0.5	3.1
Montz-Pak B1-350	toluene drops, charge A	1.5	1.0	3.0
Montz-Pak B1-350	toluene drops, charge A	2.0	1.0	3.2
Montz-Pak B1-350	toluene drops, charge A	2.5	1.0	3.8
Montz-Pak B1-350	toluene drops, charge A	3.0	1.0	3.6
Montz-Pak B1-350	toluene drops, charge A	3.5	1.0	3.5
Montz-Pak B1-350	toluene drops, charge A	4.0	1.0	3.5
Montz-Pak B1-350	toluene drops, charge A	1.5	1.5	2.8
Montz-Pak B1-350	toluene drops, charge A	2.0	1.5	3.3
Montz-Pak B1-350	toluene drops, charge A	2.5	1.5	3.7
Montz-Pak B1-350	toluene drops, charge A	3.0	1.5	3.7
Montz-Pak B1-350	toluene drops, charge A	3.5	1.5	3.9
Montz-Pak B1-350	toluene drops, charge A	4.0	1.5	4.0
Montz-Pak B1-350	butyl acetate drops	1.5	0.0	2.7
Montz-Pak B1-350	butyl acetate drops	2.0	0.0	3.5
Montz-Pak B1-350	butyl acetate drops	2.5	0.0	3.7
Montz-Pak B1-350	butyl acetate drops	3.0	0.0	3.7
Montz-Pak B1-350	butyl acetate drops	3.5	0.0	3.4

Table A.3: Characteristic velocity $v_{char,o}$ of single particles in pulsed compartments with different internals (where no mass transfer was present); binary test systems: rigid pp-spheres/water, toluene (d)/water, butyl acetate (d)/water; (continued)

compartment type	single rigid spheres - single liquid drops	d_p or d [mm]	a · f [cm/s]	$v_{char,o}$ [cm/s]
Montz-Pak B1-350	butyl acetate drops	4.0	0.0	3.6
Montz-Pak B1-350	butyl acetate drops	1.5	0.5	3.1
Montz-Pak B1-350	butyl acetate drops	2.0	0.5	3.6
Montz-Pak B1-350	butyl acetate drops	2.5	0.5	3.8
Montz-Pak B1-350	butyl acetate drops	3.0	0.5	3.7
Montz-Pak B1-350	butyl acetate drops	3.5	0.5	3.3
Montz-Pak B1-350	butyl acetate drops	4.0	0.5	3.2
Montz-Pak B1-350	butyl acetate drops	1.5	1.0	3.2
Montz-Pak B1-350	butyl acetate drops	2.0	1.0	3.5
Montz-Pak B1-350	butyl acetate drops	2.5	1.0	3.7
Montz-Pak B1-350	butyl acetate drops	3.0	1.0	3.7
Montz-Pak B1-350	butyl acetate drops	3.5	1.0	3.5
Montz-Pak B1-350	butyl acetate drops	4.0	1.0	3.5
Montz-Pak B1-350	butyl acetate drops	1.5	1.5	3.6
Montz-Pak B1-350	butyl acetate drops	2.0	1.5	4.0
Montz-Pak B1-350	butyl acetate drops	2.5	1.5	3.9
Montz-Pak B1-350	butyl acetate drops	3.0	1.5	3.9
Montz-Pak B1-350	butyl acetate drops	3.5	1.5	4.0
Montz-Pak B1-350	butyl acetate drops	4.0	1.5	3.6
Montz-Pak B1-350	butyl acetate drops	1.5	2.0	3.5
Montz-Pak B1-350	butyl acetate drops	2.0	2.0	3.8
Montz-Pak B1-350	butyl acetate drops	2.5	2.0	4.2
Montz-Pak B1-350	butyl acetate drops	3.0	2.0	4.2
Montz-Pak B1-350	butyl acetate drops	3.5	2.0	4.0

Table A.4: Characteristic velocity $v_{char,o}$ of single particles in agitated compartments with different agitators (where no mass transfer was present); binary test systems: rigid pp-spheres/water, toluene (d)/water, butyl acetate (d)/water;

compartment type	single rigid spheres - single liquid drops	d_p or d [mm]	a · f [cm/s]	$v_{char,o}$ [cm/s]
RDC-compartment	pp-spheres	1.9	100	2.8
RDC-compartment	pp-spheres	2.0	100	3.3
RDC-compartment	pp-spheres	2.5	100	3.4
RDC-compartment	pp-spheres	3.0	100	3.5
RDC-compartment	pp-spheres	3.4	100	3.7
RDC-compartment	pp-spheres	4.0	100	3.4
RDC-compartment	pp-spheres	1.9	200	3.2
RDC-compartment	pp-spheres	2.0	200	3.6
RDC-compartment	pp-spheres	2.5	200	3.7
RDC-compartment	pp-spheres	3.0	200	3.9
RDC-compartment	pp-spheres	3.4	200	4.3
RDC-compartment	pp-spheres	4.0	200	3.4
RDC-compartment	pp-spheres	1.9	300	2.9
RDC-compartment	pp-spheres	2.0	300	3.8
RDC-compartment	pp-spheres	2.5	300	3.8
RDC-compartment	pp-spheres	3.0	300	3.8
RDC-compartment	pp-spheres	3.4	300	4.1
RDC-compartment	pp-spheres	4.0	300	3.9
RDC-compartment	pp-spheres	1.9	400	3.3
RDC-compartment	pp-spheres	2.0	400	4.0
RDC-compartment	pp-spheres	2.5	400	3.6
RDC-compartment	pp-spheres	3.0	400	3.9
RDC-compartment	pp-spheres	3.4	400	4.5
RDC-compartment	pp-spheres	4.0	400	4.6
RDC-compartment	toluene drops, charge A	1.5	100	3.6
RDC-compartment	toluene drops, charge A	2.0	100	3.6
RDC-compartment	toluene drops, charge A	2.5	100	4.9
RDC-compartment	toluene drops, charge A	3.0	100	5.1
RDC-compartment	toluene drops, charge A	3.5	100	5.1
RDC-compartment	toluene drops, charge A	4.0	100	5.3
RDC-compartment	toluene drops, charge A	1.5	200	3.3
RDC-compartment	toluene drops, charge A	2.0	200	4.2
RDC-compartment	toluene drops, charge A	2.5	200	4.6
RDC-compartment	toluene drops, charge A	3.0	200	5.0

Table A.4: Characteristic velocity $v_{char,o}$ of single particles in agitated compartments with different agitators (where no mass transfer was present); binary test systems: rigid pp-spheres/water, toluene (d)/water, butyl acetate (d)/water; (continued)

compartment type	single rigid spheres - single liquid drops	d_p or d [mm]	a · f [cm/s]	$v_{char,o}$ [cm/s]
RDC-compartment	toluene drops, charge A	3.5	200	4.8
RDC-compartment	toluene drops, charge A	4.0	200	4.8
RDC-compartment	toluene drops, charge A	1.5	300	3.1
RDC-compartment	toluene drops, charge A	2.0	300	3.8
RDC-compartment	toluene drops, charge A	2.5	300	4.5
RDC-compartment	toluene drops, charge A	3.0	300	4.8
RDC-compartment	toluene drops, charge A	3.5	300	4.9
RDC-compartment	toluene drops, charge A	4.0	300	4.8
RDC-compartment	toluene drops, charge A	1.5	400	3.4
RDC-compartment	toluene drops, charge A	2.0	400	3.6
RDC-compartment	toluene drops, charge A	2.5	400	4.0
RDC-compartment	toluene drops, charge A	3.0	400	4.3
RDC-compartment	toluene drops, charge A	3.5	400	4.3
RDC-compartment	toluene drops, charge A	4.0	400	4.6
RDC-compartment	butyl acetate drops	1.5	100	3.6
RDC-compartment	butyl acetate drops	2.0	100	4.7
RDC-compartment	butyl acetate drops	2.5	100	5.0
RDC-compartment	butyl acetate drops	3.0	100	5.1
RDC-compartment	butyl acetate drops	3.5	100	5.0
RDC-compartment	butyl acetate drops	4.0	100	5.3
RDC-compartment	butyl acetate drops	1.5	200	3.5
RDC-compartment	butyl acetate drops	2.0	200	4.1
RDC-compartment	butyl acetate drops	2.5	200	5.3
RDC-compartment	butyl acetate drops	3.0	200	5.7
RDC-compartment	butyl acetate drops	3.5	200	6.4
RDC-compartment	butyl acetate drops	4.0	200	6.1
RDC-compartment	butyl acetate drops	1.5	300	3.6
RDC-compartment	butyl acetate drops	2.0	300	4.4
RDC-compartment	butyl acetate drops	2.5	300	5.2
RDC-compartment	butyl acetate drops	3.0	300	5.9
RDC-compartment	butyl acetate drops	3.5	300	6.5
RDC-compartment	butyl acetate drops	4.0	300	5.9
RDC-compartment	butyl acetate drops	1.5	400	3.6
RDC-compartment	butyl acetate drops	2.0	400	4.3

Table A.4: Characteristic velocity $v_{char,o}$ of single particles in agitated compartments with different agitators (where no mass transfer was present); binary test systems: rigid pp-spheres/water, toluene (d)/water, butyl acetate (d)/water; (continued)

compartment type	single rigid spheres - single liquid drops	d_p or d [mm]	a · f [cm/s]	$v_{char,o}$ [cm/s]
RDC-compartment	butyl acetate drops	2.5	400	5.3
RDC-compartment	butyl acetate drops	3.0	400	6.0
RDC-compartment	butyl acetate drops	3.5	400	6.0
RDC-compartment	butyl acetate drops	4.0	400	5.8
Kühni-compartment	pp-spheres	1.9	100	3.9
Kühni-compartment	pp-spheres	2.0	100	4.5
Kühni-compartment	pp-spheres	2.5	100	6.1
Kühni-compartment	pp-spheres	3.0	100	6.7
Kühni-compartment	pp-spheres	3.4	100	7.1
Kühni-compartment	pp-spheres	4.0	100	6.7
Kühni-compartment	pp-spheres	1.9	200	3.4
Kühni-compartment	pp-spheres	2.0	200	3.8
Kühni-compartment	pp-spheres	2.5	200	5.4
Kühni-compartment	pp-spheres	3.0	200	6.4
Kühni-compartment	pp-spheres	3.4	200	6.6
Kühni-compartment	pp-spheres	4.0	200	6.1
Kühni-compartment	pp-spheres	1.9	300	2.3
Kühni-compartment	pp-spheres	2.0	300	2.9
Kühni-compartment	pp-spheres	2.5	300	4.6
Kühni-compartment	pp-spheres	3.0	300	4.3
Kühni-compartment	pp-spheres	3.4	300	5.7
Kühni-compartment	pp-spheres	4.0	300	4.8
Kühni-compartment	pp-spheres	1.9	400	2.9
Kühni-compartment	pp-spheres	2.0	400	2.4
Kühni-compartment	pp-spheres	2.5	400	4.2
Kühni-compartment	pp-spheres	3.0	400	4.0
Kühni-compartment	pp-spheres	3.4	400	4.0
Kühni-compartment	pp-spheres	4.0	400	3.1
Kühni-compartment	toluene drops, charge A	1.5	50	4.1
Kühni-compartment	toluene drops, charge A	2.0	50	4.9
Kühni-compartment	toluene drops, charge A	2.5	50	5.8
Kühni-compartment	toluene drops, charge A	3.0	50	6.8
Kühni-compartment	toluene drops, charge A	3.5	50	7.8

Table A.4: Characteristic velocity $v_{char,o}$ of single particles in agitated compartments with different agitators (where no mass transfer was present); binary test systems: rigid pp-spheres/water, toluene (d)/water, butyl acetate (d)/water; (continued)

compartment type	single rigid spheres - single liquid drops	d_p or d [mm]	a · f [cm/s]	$v_{char,o}$ [cm/s]
Kühni-compartment	toluene drops, charge A	4.0	50	7.9
Kühni-compartment	toluene drops, charge A	1.5	100	3.3
Kühni-compartment	toluene drops, charge A	2.0	100	4.0
Kühni-compartment	toluene drops, charge A	2.5	100	4.9
Kühni-compartment	toluene drops, charge A	3.0	100	5.7
Kühni-compartment	toluene drops, charge A	3.5	100	6.0
Kühni-compartment	toluene drops, charge A	4.0	100	6.5
Kühni-compartment	toluene drops, charge A	1.5	150	2.9
Kühni-compartment	toluene drops, charge A	2.0	150	3.4
Kühni-compartment	toluene drops, charge A	2.5	150	3.8
Kühni-compartment	toluene drops, charge A	3.0	150	4.9
Kühni-compartment	toluene drops, charge A	3.5	150	5.0
Kühni-compartment	toluene drops, charge A	4.0	150	5.3
Kühni-compartment	toluene drops, charge A	1.5	200	3.0
Kühni-compartment	toluene drops, charge A	2.0	200	3.0
Kühni-compartment	toluene drops, charge A	2.5	200	4.1
Kühni-compartment	toluene drops, charge A	3.0	200	3.9
Kühni-compartment	toluene drops, charge A	3.5	200	4.7
Kühni-compartment	toluene drops, charge A	4.0	200	5.0
Kühni-compartment	toluene drops, charge A	1.5	250	2.6
Kühni-compartment	toluene drops, charge A	2.0	250	3.2
Kühni-compartment	butyl acetate drops	1.5	50	3.9
Kühni-compartment	butyl acetate drops	2.0	50	5.1
Kühni-compartment	butyl acetate drops	2.5	50	6.9
Kühni-compartment	butyl acetate drops	3.0	50	7.2
Kühni-compartment	butyl acetate drops	3.5	50	8.5
Kühni-compartment	butyl acetate drops	4.0	50	8.5
Kühni-compartment	butyl acetate drops	1.5	100	4.2
Kühni-compartment	butyl acetate drops	2.0	100	4.3
Kühni-compartment	butyl acetate drops	2.5	100	5.4
Kühni-compartment	butyl acetate drops	3.0	100	6.4
Kühni-compartment	butyl acetate drops	3.5	100	6.8
Kühni-compartment	butyl acetate drops	4.0	100	7.1
Kühni-compartment	butyl acetate drops	1.5	150	3.5

Table A.4: Characteristic velocity $v_{char,o}$ of single particles in agitated compartments with different agitators (where no mass transfer was present); binary test systems: rigid pp-spheres/water, toluene (d)/water, butyl acetate (d)/water; (continued)

compartment type	single rigid spheres - single liquid drops	d_p or d [mm]	a · f [cm/s]	$v_{char,o}$ [cm/s]
Kühni-compartment	butyl acetate drops	2.0	150	3.6
Kühni-compartment	butyl acetate drops	2.5	150	4.9
Kühni-compartment	butyl acetate drops	3.0	150	5.0
Kühni-compartment	butyl acetate drops	3.5	150	6.2
Kühni-compartment	butyl acetate drops	4.0	150	6.3
Kühni-compartment	butyl acetate drops	1.5	200	3.4
Kühni-compartment	butyl acetate drops	2.0	200	4.2

A.3.2 Mass Transfer Data of Single Drops

Mass transfer of single drops was investigated in the single drop mini plant with and without internals. During the mass transfer experiments, the change of the single drop concentration in a stationary continuous liquid with an acetone mass fraction of x_o was determined over a measuring distance *L*. Organic phase with an initial concentration y_o was dispersed in single drops with a definite drop diameter. The concentration of the drops was determined at a measuring position 1, which was 100 mm above the inlet of the dispersed phase, and a measuring position 2, which was a distance *L* above position 1, see also *chapter 4.2*. From the determined drop concentrations, continuous phase concentration and the drop velocity within the measuring section *L*, the overall mass transfer coefficients β_{od} were calculated by

$$\beta_{od} = \frac{d}{6 \cdot \Delta t} \cdot \ln\left(\frac{y^* - y_1}{y^* - y_2}\right) \tag{A.1}$$

where y^* is the equilibrium acetone concentration given by $y^* = m \cdot x_o$ and Δt is the time that a drop needs to pass the measuring distance *L*, see *figure (A.5)*.

Table (A.5), *table (A.6)* and *table (A.7)* show the velocities of single drops and the corresponding drop and water phase concentrations for the mass transfer investigations in columns with and without internals.

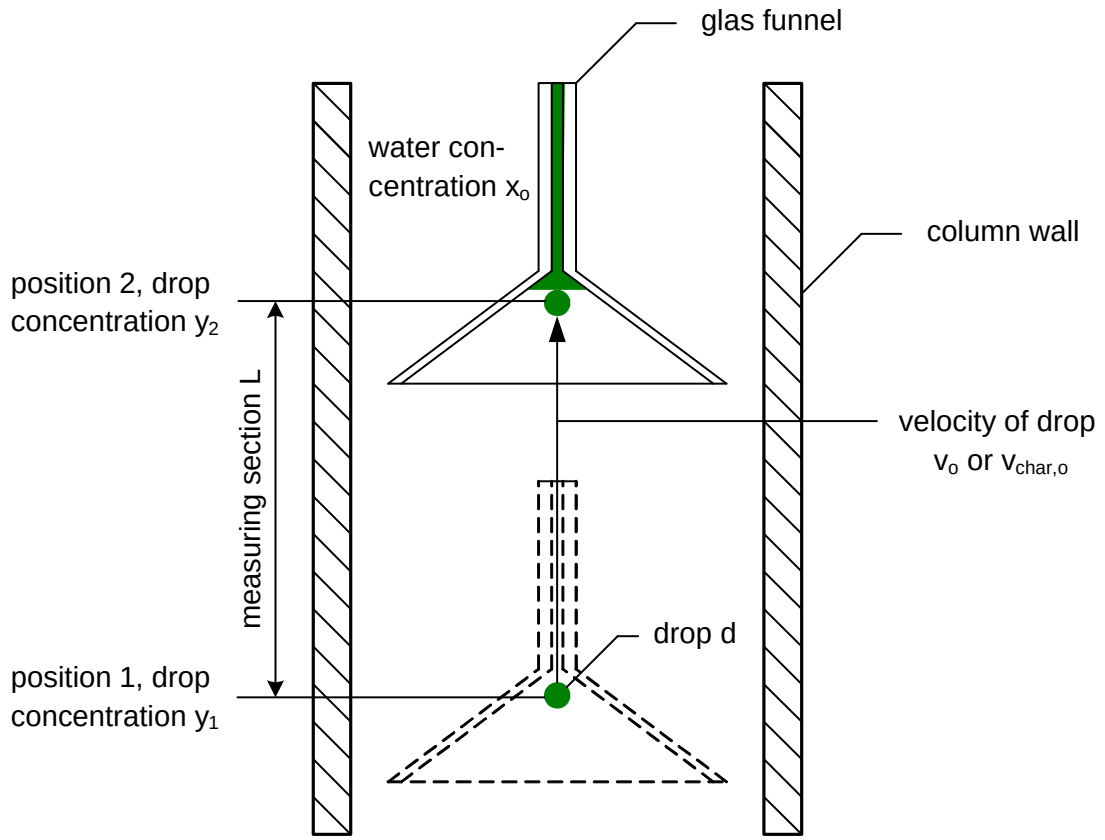

Figure A.5: Illustration of the determination of the overall mass transfer coefficients β_{od} of single drops by the measurement of the drop concentration change within a measuring distance L

Table A.5: Terminal velocity v_o and mass transfer data of single drops in extraction columns without internals within a measuring section L for different directions of mass transfer; ternary test systems: toluene (d)/acetone/water and butyl acetate (d)/ acetone/water;

liquid/liquid-system direction of mass transfer	d [mm]	v_o [cm/s]	L [cm]	y_o [%]	y_1 [%]	y_2 [%]	x_o [%]
t (d)/a/w, c to d	2.0	5.5	20	0.00	1.17	1.61	3.02
t (d)/a/w, c to d	2.5	6.8	20	0.00	1.05	1.57	3.29
t (d)/a/w, c to d	3.0	8.3	20	0.00	0.86	1.39	3.35
t (d)/a/w, c to d	3.5	8.8	20	0.00	0.95	1.31	2.74
t (d)/a/w, c to d	4.0	9.4	20	0.00	0.75	1.19	2.77
t (d)/a/w, d to c	2.0	5.5	23	3.00	1.08	0.43	0.00
t (d)/a/w, d to c	2.5	7.0	23	3.00	1.41	0.64	0.00
t (d)/a/w, d to c	3.0	8.0	23	3.00	1.69	0.88	0.00

Table A.5: Terminal velocity v_o and mass transfer data of single drops in extraction columns without internals within a measuring section L for different directions of mass transfer; ternary test systems: toluene (d)/acetone/water and butyl acetate (d)/ acetone/water; (continued)

liquid/liquid-system direction of mass transfer	d [mm]	v_o [cm/s]	L [cm]	y_o [%]	y_1 [%]	y_2 [%]	x_o [%]
t (d)/a/w, d to c	3.5	9.1	23	3.00	1.83	1.10	0.00
t (d)/a/w, d to c	4.0	10.1	23	3.00	1.89	1.19	0.00
bu-ac (d)/a/w, c to d	2.0	6.0	23	0.00	1.79	2.37	3.11
bu-ac (d)/a/w, c to d	2.5	7.9	23	0.00	1.54	2.14	3.10
bu-ac (d)/a/w, c to d	3.0	10.1	23	0.00	1.33	1.95	3.10
bu-ac (d)/a/w, c to d	3.5	10.8	23	0.00	1.17	1.84	3.14
bu-ac (d)/a/w, c to d	4.0	10.6	23	0.00	0.98	1.71	3.13
bu-ac (d)/a/w, d to c	2.0	5.3	23	3.00	1.76	0.65	0.00
bu-ac (d)/a/w, d to c	2.5	7.3	23	3.00	1.85	0.85	0.00
bu-ac (d)/a/w, d to c	3.0	8.3	23	3.00	2.01	1.01	0.00
bu-ac (d)/a/w, d to c	3.5	9.5	23	3.00	2.16	1.21	0.00
bu-ac (d)/a/w, d to c	4.0	11.0	23	3.00	2.29	1.43	0.00
bu-ac (d)/a/w, c to d	2.0	5.4	23	0.00	3.51	4.99	6.23
bu-ac (d)/a/w, c to d	2.5	7.2	23	0.00	3.05	4.65	6.23
bu-ac (d)/a/w, c to d	3.0	9.0	23	0.00	2.45	4.18	6.23
bu-ac (d)/a/w, c to d	3.5	10.1	23	0.00	2.21	3.83	6.23
bu-ac (d)/a/w, c to d	4.0	10.1	23	0.00	2.06	3.65	6.23

Table A.6: Characteristic velocity $v_{char,o}$ and mass transfer of single liquid drops in pulsed compartments with different internals for a mass transfer direction from the continuous to the dispersed phase (y_o = 0.0 %) within a measuring distance L (L = 20 cm); ternary test systems: toluene (d)/acetone/water and butyl acetate (d)/ acetone/water;

compartment type	liquid/liquid-system direction of mass transfer	d [mm]	a · f [cm/s]	$v_{char,o}$ [cm/s]	y_1 [%]	y_2 [%]	x_o [%]
sieve-tray d_h = 4 mm	t (d)/a/w, c to d	2.0	0.0	4.8	1.17	1.65	2.84
sieve-tray d_h = 4 mm	t (d)/a/w, c to d	2.5	0.0	6.3	1.05	1.56	2.75
sieve-tray d_h = 4 mm	t (d)/a/w, c to d	3.0	0.0	6.8	0.86	1.47	3.01
sieve-tray d_h = 4 mm	t (d)/a/w, c to d	3.5	0.0	7.3	0.95	1.41	2.74
sieve-tray d_h = 4 mm	t (d)/a/w, c to d	4.0	0.0	7.5	0.75	1.30	2.74
sieve-tray d_h = 4 mm	t (d)/a/w, c to d	2.0	0.5	4.9	1.17	1.68	2.84
sieve-tray d_h = 4 mm	t (d)/a/w, c to d	2.5	0.5	6.0	1.05	1.58	2.75
sieve-tray d_h = 4 mm	t (d)/a/w, c to d	3.0	0.5	6.6	0.86	1.49	3.01
sieve-tray d_h = 4 mm	t (d)/a/w, c to d	3.5	0.5	7.3	0.95	1.41	2.74
sieve-tray d_h = 4 mm	t (d)/a/w, c to d	4.0	0.5	7.4	0.75	1.34	2.74
sieve-tray d_h = 4 mm	t (d)/a/w, c to d	2.0	1.0	5.0	1.17	1.71	2.84
sieve-tray d_h = 4 mm	t (d)/a/w, c to d	2.5	1.0	6.0	1.05	1.58	2.75
sieve-tray d_h = 4 mm	t (d)/a/w, c to d	3.0	1.0	6.4	0.86	1.52	3.01
sieve-tray d_h = 4 mm	t (d)/a/w, c to d	3.5	1.0	7.1	0.95	1.43	2.74
sieve-tray d_h = 4 mm	t (d)/a/w, c to d	4.0	1.0	7.3	0.75	1.33	2.74
sieve-tray d_h = 4 mm	t (d)/a/w, c to d	2.0	1.5	5.1	1.17	1.79	2.84
sieve-tray d_h = 4 mm	t (d)/a/w, c to d	2.5	1.5	6.1	1.05	1.66	2.75
sieve-tray d_h = 4 mm	t (d)/a/w, c to d	3.0	1.5	6.6	0.86	1.55	3.01
sieve-tray d_h = 4 mm	t (d)/a/w, c to d	3.5	1.5	7.3	0.95	1.50	2.74
sieve-tray d_h = 4 mm	t (d)/a/w, c to d	4.0	1.5	8.0	0.75	1.36	2.74
sieve-tray d_h = 4 mm	t (d)/a/w, c to d	2.0	2.0	5.2	1.17	1.81	2.84
sieve-tray d_h = 4 mm	t (d)/a/w, c to d	2.5	2.0	6.6	1.05	1.68	2.75
sieve-tray d_h = 4 mm	t (d)/a/w, c to d	3.0	2.0	7.2	0.86	1.62	3.01
sieve-tray d_h = 2 mm	t (d)/a/w, c to d	2.0	0.0	4.3	1.17	1.80	3.04
sieve-tray d_h = 2 mm	t (d)/a/w, c to d	2.0	0.5	4.0	1.17	1.83	3.04
sieve-tray d_h = 2 mm	t (d)/a/w, c to d	2.0	1.0	4.2	1.17	1.86	3.04
sieve-tray d_h = 2 mm	t (d)/a/w, c to d	2.5	1.0	4.5	1.05	1.78	3.19
sieve-tray d_h = 2 mm	t (d)/a/w, c to d	3.0	1.0	4.6	0.86	1.80	3.01
sieve-tray d_h = 2 mm	t (d)/a/w, c to d	2.0	1.5	4.4	1.17	1.85	3.04
sieve-tray d_h = 2 mm	t (d)/a/w, c to d	2.5	1.5	5.5	1.05	1.84	3.19
sieve-tray d_h = 2 mm	t (d)/a/w, c to d	2.0	2.0	4.5	1.17	1.87	3.04
sieve-tray d_h = 2 mm	t (d)/a/w, c to d	2.5	2.0	4.8	1.05	1.94	3.19

Table A.6: Characteristic velocity $v_{char,o}$ and mass transfer of single liquid drops in pulsed compartments with different internals for a mass transfer direction from the continuous to the dispersed phase (y_o = 0.0 %) within a measuring distance L (L = 20 cm); ternary test systems: toluene (d)/acetone/water and butyl acetate (d)/ acetone/water; (continued)

compartment type	liquid/liquid-system direction of mass transfer	d [mm]	a · f [cm/s]	$v_{char,o}$ [cm/s]	y_1 [%]	y_2 [%]	x_o [%]
sieve-tray d_h = 4 mm	bu-ac (d)/a/w, c to d	2.0	0.0	5.5	1.79	2.55	3.05
sieve-tray d_h = 4 mm	bu-ac (d)/a/w, c to d	2.5	0.0	6.5	1.54	2.36	3.05
sieve-tray d_h = 4 mm	bu-ac (d)/a/w, c to d	3.0	0.0	7.7	1.33	2.15	3.01
sieve-tray d_h = 4 mm	bu-ac (d)/a/w, c to d	3.5	0.0	8.0	1.17	1.95	3.02
sieve-tray d_h = 4 mm	bu-ac (d)/a/w, c to d	4.0	0.0	7.8	0.98	1.86	3.03
sieve-tray d_h = 4 mm	bu-ac (d)/a/w, c to d	2.0	0.5	5.4	1.79	2.54	3.05
sieve-tray d_h = 4 mm	bu-ac (d)/a/w, c to d	2.5	0.5	6.4	1.54	2.38	3.05
sieve-tray d_h = 4 mm	bu-ac (d)/a/w, c to d	3.0	0.5	7.8	1.33	2.20	3.01
sieve-tray d_h = 4 mm	bu-ac (d)/a/w, c to d	3.5	0.5	8.0	1.17	1.99	3.02
sieve-tray d_h = 4 mm	bu-ac (d)/a/w, c to d	4.0	0.5	7.7	0.98	1.93	3.03
sieve-tray d_h = 4 mm	bu-ac (d)/a/w, c to d	2.0	1.0	5.7	1.79	2.54	3.05
sieve-tray d_h = 4 mm	bu-ac (d)/a/w, c to d	2.5	1.0	6.7	1.54	2.35	3.05
sieve-tray d_h = 4 mm	bu-ac (d)/a/w, c to d	3.0	1.0	7.8	1.33	2.21	3.01
sieve-tray d_h = 4 mm	bu-ac (d)/a/w, c to d	2.0	1.5	5.7	1.79	2.63	3.05
sieve-tray d_h = 4 mm	bu-ac (d)/a/w, c to d	2.5	1.5	7.1	1.54	2.39	3.05
sieve-tray d_h = 4 mm	bu-ac (d)/a/w, c to d	3.0	1.5	7.6	1.33	2.23	3.01
sieve-tray d_h = 4 mm	bu-ac (d)/a/w, c to d	2.0	2.0	5.5	1.79	2.63	3.05
sieve-tray d_h = 4 mm	bu-ac (d)/a/w, c to d	2.5	2.0	7.3	1.54	2.40	3.05
sieve-tray d_h = 2 mm	bu-ac (d)/a/w, c to d	2.0	0.5	4.6	1.79	2.56	2.93
sieve-tray d_h = 2 mm	bu-ac (d)/a/w, c to d	2.5	0.5	4.6	1.54	2.45	2.93
sieve-tray d_h = 2 mm	bu-ac (d)/a/w, c to d	2.0	1.0	4.3	1.79	2.60	2.93
sieve-tray d_h = 2 mm	bu-ac (d)/a/w, c to d	2.5	1.0	5.1	1.54	2.46	2.93
sieve-tray d_h = 2 mm	bu-ac (d)/a/w, c to d	2.0	1.5	4.8	1.79	2.57	2.93
Montz-Pak B1-350	t (d)/a/w, c to d	2.0	0.0	3.7	1.17	2.01	3.03
Montz-Pak B1-350	t (d)/a/w, c to d	2.5	0.0	4.0	1.05	2.03	3.03
Montz-Pak B1-350	t (d)/a/w, c to d	3.0	0.0	3.9	0.86	1.94	3.03
Montz-Pak B1-350	t (d)/a/w, c to d	3.5	0.0	3.7	0.95	1.86	2.93
Montz-Pak B1-350	t (d)/a/w, c to d	4.0	0.0	3.4	0.75	1.83	2.93
Montz-Pak B1-350	t (d)/a/w, c to d	2.0	0.5	3.7	1.17	2.12	3.03
Montz-Pak B1-350	t (d)/a/w, c to d	2.5	0.5	4.0	1.05	2.00	3.03

Table A.6: Characteristic velocity $v_{char,o}$ and mass transfer of single liquid drops in pulsed compartments with different internals for a mass transfer direction from the continuous to the dispersed phase (y_o = 0.0 %) within a measuring distance L (L = 20 cm); ternary test systems: toluene (d)/acetone/water and butyl acetate (d)/ acetone/water; (continued)

compartment type	liquid/liquid-system direction of mass transfer	d [mm]	a · f [cm/s]	$v_{char,o}$ [cm/s]	y_1 [%]	y_2 [%]	x_o [%]
Montz-Pak B1-350	t (d)/a/w, c to d	3.0	0.5	4.0	0.86	1.91	3.03
Montz-Pak B1-350	t (d)/a/w, c to d	3.5	0.5	3.7	0.95	1.88	2.93
Montz-Pak B1-350	t (d)/a/w, c to d	4.0	0.5	3.4	0.75	1.82	2.93
Montz-Pak B1-350	t (d)/a/w, c to d	2.0	1.0	3.7	1.17	2.13	3.03
Montz-Pak B1-350	t (d)/a/w, c to d	2.5	1.0	4.1	1.05	2.06	3.03
Montz-Pak B1-350	t (d)/a/w, c to d	3.0	1.0	3.9	0.86	1.94	3.03
Montz-Pak B1-350	t (d)/a/w, c to d	3.5	1.0	3.8	0.95	1.87	2.93
Montz-Pak B1-350	t (d)/a/w, c to d	4.0	1.0	3.5	0.75	1.85	2.93
Montz-Pak B1-350	t (d)/a/w, c to d	2.0	1.5	3.9	1.17	2.15	3.03
Montz-Pak B1-350	t (d)/a/w, c to d	2.5	1.5	4.1	1.05	2.04	3.03
Montz-Pak B1-350	t (d)/a/w, c to d	3.0	1.5	4.0	0.86	1.95	3.03
Montz-Pak B1-350	t (d)/a/w, c to d	3.5	1.5	3.9	0.95	1.89	2.93
Montz-Pak B1-350	t (d)/a/w, c to d	2.0	2.0	4.0	1.17	2.18	3.03
Montz-Pak B1-350	t (d)/a/w, c to d	2.5	2.0	4.3	1.05	2.06	3.03
Montz-Pak B1-350	t (d)/a/w, c to d	3.0	2.0	4.0	0.86	1.99	3.03
Montz-Pak B1-350	bu-ac (d)/a/w, c to d	2.0	0.0	3.4	1.79	2.55	2.96
Montz-Pak B1-350	bu-ac (d)/a/w, c to d	2.5	0.0	3.7	1.54	2.39	2.93
Montz-Pak B1-350	bu-ac (d)/a/w, c to d	3.0	0.0	3.7	1.33	2.43	3.03
Montz-Pak B1-350	bu-ac (d)/a/w, c to d	3.5	0.0	3.4	1.17	2.46	3.03
Montz-Pak B1-350	bu-ac (d)/a/w, c to d	4.0	0.0	3.4	0.98	2.41	3.03
Montz-Pak B1-350	bu-ac (d)/a/w, c to d	2.0	0.5	3.4	1.79	2.58	2.96
Montz-Pak B1-350	bu-ac (d)/a/w, c to d	2.5	0.5	3.7	1.54	2.47	2.93
Montz-Pak B1-350	bu-ac (d)/a/w, c to d	3.0	0.5	3.7	1.33	2.50	3.03
Montz-Pak B1-350	bu-ac (d)/a/w, c to d	3.5	0.5	3.5	1.17	2.47	3.03
Montz-Pak B1-350	bu-ac (d)/a/w, c to d	2.0	1.0	3.3	1.79	2.63	2.96
Montz-Pak B1-350	bu-ac (d)/a/w, c to d	2.5	1.0	3.6	1.54	2.49	2.93
Montz-Pak B1-350	bu-ac (d)/a/w, c to d	3.0	1.0	3.7	1.33	2.56	3.03
Montz-Pak B1-350	bu-ac (d)/a/w, c to d	2.0	1.5	3.7	1.79	2.62	2.96
Montz-Pak B1-350	bu-ac (d)/a/w, c to d	2.5	1.5	3.8	1.54	2.53	2.93
Montz-Pak B1-350	bu-ac (d)/a/w, c to d	2.0	2.0	3.7	1.79	2.65	2.96

Table A.7: Characteristic velocity $v_{char,o}$ and mass transfer of single liquid drops in agitated compartments with different internals for a mass transfer direction from the continuous to the dispersed phase (y_o = 0.0 %) within a measuring distance L (L = 20 cm); ternary test systems: toluene (d)/acetone/water and butyl acetate (d)/ acetone/water;

compartment type	liquid/liquid-system direction of mass transfer	d [mm]	n_R [1/min]	$v_{char,o}$ [cm/s]	y_1 [%]	y_2 [%]	x_o [%]
RDC-compartment	t (d)/a/w, c to d	2.0	100	3.9	1.17	1.97	3.11
RDC-compartment	t (d)/a/w, c to d	2.5	100	4.8	1.05	1.81	3.11
RDC-compartment	t (d)/a/w, c to d	3.0	100	4.7	0.86	1.71	3.08
RDC-compartment	t (d)/a/w, c to d	3.5	100	5.1	0.95	1.69	3.08
RDC-compartment	t (d)/a/w, c to d	4.0	100	5.3	0.75	1.59	3.04
RDC-compartment	t (d)/a/w, c to d	2.0	200	3.4	1.17	2.08	3.11
RDC-compartment	t (d)/a/w, c to d	2.5	200	3.9	1.05	1.84	3.11
RDC-compartment	t (d)/a/w, c to d	3.0	200	4.4	0.86	1.79	3.08
RDC-compartment	t (d)/a/w, c to d	3.5	200	4.5	0.95	1.70	3.08
RDC-compartment	t (d)/a/w, c to d	4.0	200	4.9	0.75	1.80	3.04
RDC-compartment	t (d)/a/w, c to d	2.0	300	3.3	1.17	2.15	3.11
RDC-compartment	t (d)/a/w, c to d	2.5	300	4.0	1.05	1.97	3.11
RDC-compartment	t (d)/a/w, c to d	3.0	300	4.2	0.86	1.93	3.08
RDC-compartment	t (d)/a/w, c to d	3.5	300	4.6	0.95	1.78	3.08
RDC-compartment	t (d)/a/w, c to d	4.0	300	4.9	0.75	1.84	3.04
RDC-compartment	t (d)/a/w, c to d	2.0	400	3.7	1.17	2.18	3.11
RDC-compartment	t (d)/a/w, c to d	2.5	400	4.3	1.05	2.00	3.11
RDC-compartment	t (d)/a/w, c to d	3.0	400	4.4	0.86	1.96	3.08
RDC-compartment	t (d)/a/w, c to d	3.5	400	4.7	0.95	1.85	3.08
RDC-compartment	t (d)/a/w, c to d	4.0	400	4.9	0.75	1.94	3.04
RDC-compartment	bu-ac (d)/a/w, c to d	2.0	100	3.7	1.79	2.50	2.99
RDC-compartment	bu-ac (d)/a/w, c to d	2.5	100	4.4	1.54	2.47	2.99
RDC-compartment	bu-ac (d)/a/w, c to d	3.0	100	5.4	1.33	2.31	2.99
RDC-compartment	bu-ac (d)/a/w, c to d	3.5	100	5.5	1.17	2.24	2.99
RDC-compartment	bu-ac (d)/a/w, c to d	4.0	100	5.7	0.98	2.05	2.99
RDC-compartment	bu-ac (d)/a/w, c to d	2.0	200	3.8	1.79	2.55	2.99
RDC-compartment	bu-ac (d)/a/w, c to d	2.5	200	4.0	1.54	2.55	2.99
RDC-compartment	bu-ac (d)/a/w, c to d	3.0	200	4.3	1.33	2.42	2.99
RDC-compartment	bu-ac (d)/a/w, c to d	3.5	200	4.4	1.17	2.34	2.99
RDC-compartment	bu-ac (d)/a/w, c to d	4.0	200	4.5	0.98	2.25	2.99
RDC-compartment	bu-ac (d)/a/w, c to d	2.0	300	3.5	1.79	2.62	2.99
RDC-compartment	bu-ac (d)/a/w, c to d	2.5	300	4.1	1.54	2.61	2.99

Table A.7: Characteristic velocity $v_{char,o}$ and mass transfer of single liquid drops in agitated compartments with different internals for a mass transfer direction from the continuous to the dispersed phase (y_o = 0.0 %) within a measuring distance L (L = 20 cm); ternary test systems: toluene (d)/acetone/water and butyl acetate (d)/ acetone/water; (continued)

compartment type	liquid/liquid-system direction of mass transfer	d [mm]	n_R [1/min]	$v_{char,o}$ [cm/s]	y_1 [%]	y_2 [%]	x_o [%]
RDC-compartment	bu-ac (d)/a/w, c to d	3.0	300	4.7	1.33	2.46	2.99
RDC-compartment	bu-ac (d)/a/w, c to d	3.5	300	4.5	1.17	2.42	2.99
RDC-compartment	bu-ac (d)/a/w, c to d	4.0	300	4.6	0.98	2.30	2.99
RDC-compartment	bu-ac (d)/a/w, c to d	2.0	400	3.4	1.79	2.62	2.99
RDC-compartment	bu-ac (d)/a/w, c to d	2.5	400	4.1	1.54	2.62	2.99
RDC-compartment	bu-ac (d)/a/w, c to d	3.0	400	4.5	1.33	2.52	2.99
Kühni-compartment	t (d)/a/w, c to d	2.0	50	4.7	1.17	1.75	3.08
Kühni-compartment	t (d)/a/w, c to d	2.5	50	6.1	1.05	1.63	3.08
Kühni-compartment	t (d)/a/w, c to d	3.0	50	7.0	0.86	1.59	3.12
Kühni-compartment	t (d)/a/w, c to d	3.5	50	7.2	0.95	1.50	3.08
Kühni-compartment	t (d)/a/w, c to d	4.0	50	7.7	0.75	1.50	3.12
Kühni-compartment	t (d)/a/w, c to d	2.0	100	3.9	1.17	1.88	3.08
Kühni-compartment	t (d)/a/w, c to d	2.5	100	4.8	1.05	1.87	3.08
Kühni-compartment	t (d)/a/w, c to d	3.0	100	5.3	0.86	1.77	3.12
Kühni-compartment	t (d)/a/w, c to d	3.5	100	6.0	0.95	1.71	3.12
Kühni-compartment	t (d)/a/w, c to d	4.0	100	6.2	0.75	1.73	3.12
Kühni-compartment	t (d)/a/w, c to d	2.0	150	2.9	1.17	2.05	3.08
Kühni-compartment	t (d)/a/w, c to d	2.5	150	3.7	1.05	2.09	3.08
Kühni-compartment	bu-ac (d)/a/w, c to d	2.0	50	5.1	1.79	2.64	3.01
Kühni-compartment	bu-ac (d)/a/w, c to d	2.5	50	6.2	1.54	2.55	3.01
Kühni-compartment	bu-ac (d)/a/w, c to d	3.0	50	7.1	1.33	2.38	3.01
Kühni-compartment	bu-ac (d)/a/w, c to d	3.5	50	7.4	1.17	2.36	3.01
Kühni-compartment	bu-ac (d)/a/w, c to d	4.0	50	7.4	0.98	2.19	3.01
Kühni-compartment	bu-ac (d)/a/w, c to d	2.0	100	3.9	1.79	2.71	3.01
Kühni-compartment	bu-ac (d)/a/w, c to d	2.5	100	4.9	1.54	2.66	3.01
Kühni-compartment	bu-ac (d)/a/w, c to d	3.0	100	5.6	1.33	2.52	3.01

A.3.3 Single Drop Breakage

The breakage behaviour of single mother drops was determined using two mutually saturated binary systems (toluene (d)/water and butyl acetate (d)/water) and two ternary systems (toluene (d)/acetone/water and butyl acetate (d)/acetone/water). For the investigation of the ternary test systems acetone was added to the water phase until an acetone weight concentration of 5 % was obtained. The aqueous phase was subsequently mixed with toluene or butyl acetate to mutually saturate both phases. Afterwards the aqueous phase was fed to the single drop mini plant and the organic phases were used to generate single mother drops with a known diameter d_M. The investigation of the drop breakage was always carried out in absence of mass transfer.

The results of the single drop breakage experiments are listed in the following tables. The characteristic drop diameters d_{stab} and d_{100}, which are important for the prediction of the breakage probability p_B in pulsed compartments by the correlations presented in *chapter 6.1*, are listed in *table (A.8). Table (A.9)* and *table (A.10)* show the breakage probability of mother drops with a diameter d_M and the average number of daughter drops n_{dd} produced by the breakage of a mother drop in single pulsed and agitated compartments.

*Table A.8: Characteristic drop diameter d_{stab} and d_{100} for the determination of the breakage probability in pulsed compartments with different internals; * = extrapolated values*

compartment type	liquid/liquid-system (mutually saturated)	a · f [cm/s]	d_{stab} [mm]	d_{100} [mm]
sieve-tray - d_h = 2 mm	toluene (d)/water	1.5	2.0	4.3
sieve-tray - d_h = 2 mm	toluene (d)/water	2.0	1.7	3.8
sieve-tray - d_h = 2 mm	toluene (d)/water	2.5	0.8*	3.6
sieve-tray - d_h = 2 mm	toluene (d)/acetone/water	1.5	1.7	4.1
sieve-tray - d_h = 2 mm	toluene (d)/acetone/water	2.0	0.5*	3.7
sieve-tray - d_h = 2 mm	toluene (d)/acetone/water	2.5	0.3*	3.3
sieve-tray - d_h = 2 mm	butyl acetate (d)/water	1.0	1.5	4.0
sieve-tray - d_h = 2 mm	butyl acetate (d)/water	1.5	1.0	3.5
sieve-tray - d_h = 2 mm	butyl acetate (d)/water	2.0	0.5*	2.8
sieve-tray - d_h = 2 mm	butyl acetate (d)/acetone/water	1.0	2.0	3.8
sieve-tray - d_h = 2 mm	butyl acetate (d)/acetone/water	1.5	0.8*	3.4
sieve-tray - d_h = 2 mm	butyl acetate (d)/acetone/water	2.0	0.3*	3.0

*Table A.8: Characteristic drop diameter d_{stab} and d_{100} for the determination of the breakage probability in pulsed compartments with different internals; * = extrapolated values (continued)*

compartment type	liquid/liquid-system (mutually saturated)	a · f [cm/s]	d_{stab} [mm]	d_{100} [mm]
sieve-tray - d_h = 4 mm	toluene (d)/water	1.5	2.7	6.7
sieve-tray - d_h = 4 mm	toluene (d)/water	2.0	2.0	6.2
sieve-tray - d_h = 4 mm	toluene (d)/water	2.5	1.3	6.0
sieve-tray - d_h = 4 mm	toluene (d)/acetone/water	1.5	2.3	6.3
sieve-tray - d_h = 4 mm	toluene (d)/acetone/water	2.0	1.7	5.5
sieve-tray - d_h = 4 mm	toluene (d)/acetone/water	2.5	1.0	5.2
sieve-tray - d_h = 4 mm	butyl acetate (d)/water	1.0	2.3	5.8
sieve-tray - d_h = 4 mm	butyl acetate (d)/water	1.5	1.8	5.1
sieve-tray - d_h = 4 mm	butyl acetate (d)/water	2.0	1.3	4.6
sieve-tray - d_h = 4 mm	butyl acetate (d)/acetone/water	1.0	2.5	5.3
sieve-tray - d_h = 4 mm	butyl acetate (d)/acetone/water	1.5	1.3	4.5
sieve-tray - d_h = 4 mm	butyl acetate (d)/acetone/water	2.0	0.9*	4.4
Montz-Pak B1-350	toluene (d)/water	1.0	3.4	8.5
Montz-Pak B1-350	toluene (d)/water	1.5	2.3	7.0
Montz-Pak B1-350	toluene (d)/water	2.0	1.7	5.5
Montz-Pak B1-350	toluene (d)/water	2.5	1.5	4.7
Montz-Pak B1-350	toluene (d)/acetone/water	1.0	3.3	7.5
Montz-Pak B1-350	toluene (d)/acetone/water	1.5	3.0	6.5
Montz-Pak B1-350	toluene (d)/acetone/water	2.0	1.5	4.5
Montz-Pak B1-350	toluene (d)/acetone/water	2.5	1.2	4.0
Montz-Pak B1-350	butyl acetate (d)/water	0.5	2.5	4.6
Montz-Pak B1-350	butyl acetate (d)/water	1.0	2.3	4.2
Montz-Pak B1-350	butyl acetate (d)/water	1.5	1.5	3.8
Montz-Pak B1-350	butyl acetate (d)/water	2.0	1.0	3.4
Montz-Pak B1-350	butyl acetate (d)/acetone/water	1.0	2.2	4.0
Montz-Pak B1-350	butyl acetate (d)/acetone/water	1.5	1.3	3.5
Montz-Pak B1-350	butyl acetate (d)/acetone/water	2.0	0.8*	3.1

Table A.9: Breakage probability p_B of single mother drops and average number of daughter drops n_{dd} produced from breakage of mother drops in a single pulsed compartment with different internals (where no mass transfer was present);

compartment type	liquid/liquid-system (mutually saturated)	a · f [cm/s]	d_M [mm]	p_B [-]	n_{dd} [-]
sieve-tray d_h = 4 mm	t (d)/w	1.5	3.0	0.04	2.0
sieve-tray d_h = 4 mm	t (d)/w	1.5	3.5	0.08	2.5
sieve-tray d_h = 4 mm	t (d)/w	1.5	4.0	0.21	2.3
sieve-tray d_h = 4 mm	t (d)/w	1.5	4.6	0.44	2.3
sieve-tray d_h = 4 mm	t (d)/w	1.5	5.1	0.58	2.7
sieve-tray d_h = 4 mm	t (d)/w	1.5	5.6	0.69	2.6
sieve-tray d_h = 4 mm	t (d)/w	1.5	5.9	0.81	2.5
sieve-tray d_h = 4 mm	t (d)/w	1.5	6.4	0.94	3.5
sieve-tray d_h = 4 mm	t (d)/w	2.0	2.5	0.07	2.3
sieve-tray d_h = 4 mm	t (d)/w	2.0	3.0	0.19	2.7
sieve-tray d_h = 4 mm	t (d)/w	2.0	3.5	0.33	2.8
sieve-tray d_h = 4 mm	t (d)/w	2.0	4.0	0.45	2.6
sieve-tray d_h = 4 mm	t (d)/w	2.0	4.6	0.66	3.1
sieve-tray d_h = 4 mm	t (d)/w	2.0	5.1	0.76	3.5
sieve-tray d_h = 4 mm	t (d)/w	2.0	5.6	0.84	3.2
sieve-tray d_h = 4 mm	t (d)/w	2.0	5.9	0.95	4.5
sieve-tray d_h = 4 mm	t (d)/w	2.5	1.5	0.02	2.2
sieve-tray d_h = 4 mm	t (d)/w	2.5	2.0	0.07	2.7
sieve-tray d_h = 4 mm	t (d)/w	2.5	2.5	0.23	2.7
sieve-tray d_h = 4 mm	t (d)/w	2.5	3.0	0.36	3.3
sieve-tray d_h = 4 mm	t (d)/w	2.5	3.5	0.45	3.6
sieve-tray d_h = 4 mm	t (d)/w	2.5	4.0	0.57	4.0
sieve-tray d_h = 4 mm	t (d)/w	2.5	4.6	0.75	4.7
sieve-tray d_h = 4 mm	t (d)/w	2.5	5.1	0.86	5.5
sieve-tray d_h = 4 mm	t (d)/w	2.5	5.6	0.95	5.4
sieve-tray d_h = 4 mm	bu-ac (d)/w	1.0	2.5	0.03	2.0
sieve-tray d_h = 4 mm	bu-ac (d)/w	1.0	3.0	0.11	2.2
sieve-tray d_h = 4 mm	bu-ac (d)/w	1.0	3.5	0.36	2.3
sieve-tray d_h = 4 mm	bu-ac (d)/w	1.0	4.0	0.55	2.8
sieve-tray d_h = 4 mm	bu-ac (d)/w	1.0	4.6	0.72	3.3
sieve-tray d_h = 4 mm	bu-ac (d)/w	1.0	4.6	0.71	3.2
sieve-tray d_h = 4 mm	bu-ac (d)/w	1.0	5.1	0.88	3.9
sieve-tray d_h = 4 mm	bu-ac (d)/w	1.0	5.6	0.93	4.3
sieve-tray d_h = 4 mm	bu-ac (d)/w	1.0	5.6	0.96	4.7

Table A.9: Breakage probability p_B of single mother drops and average number of daughter drops n_{dd} produced from breakage of mother drops in a single pulsed compartment with different internals (where no mass transfer was present); (continued)

compartment type	liquid/liquid-system (mutually saturated)	a · f [cm/s]	d_M [mm]	p_B [-]	n_{dd} [-]
sieve-tray d_h = 4 mm	bu-ac (d)/w	1.5	2.0	0.03	2.0
sieve-tray d_h = 4 mm	bu-ac (d)/w	1.5	2.5	0.15	2.0
sieve-tray d_h = 4 mm	bu-ac (d)/w	1.5	2.5	0.13	2.2
sieve-tray d_h = 4 mm	bu-ac (d)/w	1.5	3.0	0.35	2.4
sieve-tray d_h = 4 mm	bu-ac (d)/w	1.5	3.0	0.29	2.2
sieve-tray d_h = 4 mm	bu-ac (d)/w	1.5	3.5	0.53	3.0
sieve-tray d_h = 4 mm	bu-ac (d)/w	1.5	3.5	0.58	3.3
sieve-tray d_h = 4 mm	bu-ac (d)/w	1.5	4.0	0.79	3.3
sieve-tray d_h = 4 mm	bu-ac (d)/w	1.5	4.0	0.77	3.6
sieve-tray d_h = 4 mm	bu-ac (d)/w	1.5	4.6	0.83	4.1
sieve-tray d_h = 4 mm	bu-ac (d)/w	1.5	4.6	0.90	4.0
sieve-tray d_h = 4 mm	bu-ac (d)/w	1.5	5.1	0.97	5.2
sieve-tray d_h = 4 mm	bu-ac (d)/w	1.5	5.1	0.95	5.7
sieve-tray d_h = 4 mm	bu-ac (d)/w	2.0	1.6	0.06	2.5
sieve-tray d_h = 4 mm	bu-ac (d)/w	2.0	1.6	0.07	2.4
sieve-tray d_h = 4 mm	bu-ac (d)/w	2.0	1.8	0.14	2.7
sieve-tray d_h = 4 mm	bu-ac (d)/w	2.0	1.8	0.14	2.9
sieve-tray d_h = 4 mm	bu-ac (d)/w	2.0	2.0	0.17	3.0
sieve-tray d_h = 4 mm	bu-ac (d)/w	2.0	2.0	0.12	2.5
sieve-tray d_h = 4 mm	bu-ac (d)/w	2.0	2.5	0.32	3.3
sieve-tray d_h = 4 mm	bu-ac (d)/w	2.0	2.5	0.28	3.6
sieve-tray d_h = 4 mm	bu-ac (d)/w	2.0	3.0	0.42	3.7
sieve-tray d_h = 4 mm	bu-ac (d)/w	2.0	3.5	0.67	4.2
sieve-tray d_h = 4 mm	bu-ac (d)/w	2.0	3.5	0.65	4.4
sieve-tray d_h = 4 mm	bu-ac (d)/w	2.0	4.0	0.88	4.6
sieve-tray d_h = 4 mm	bu-ac (d)/w	2.0	4.0	0.90	4.8
sieve-tray d_h = 4 mm	bu-ac (d)/w	2.0	4.6	0.98	5.8
sieve-tray d_h = 4 mm	bu-ac (d)/w	2.0	4.6	0.96	5.1
sieve-tray d_h = 4 mm	t (d)/a/w	1.5	2.3	0.01	2.0
sieve-tray d_h = 4 mm	t (d)/a/w	1.5	2.5	0.07	2.1
sieve-tray d_h = 4 mm	t (d)/a/w	1.5	3.0	0.19	2.3
sieve-tray d_h = 4 mm	t (d)/a/w	1.5	4.0	0.36	2.8
sieve-tray d_h = 4 mm	t (d)/a/w	1.5	4.5	0.65	2.5
sieve-tray d_h = 4 mm	t (d)/a/w	1.5	5.5	0.79	2.8

Table A.9: Breakage probability p_B of single mother drops and average number of daughter drops n_{dd} produced from breakage of mother drops in a single pulsed compartment with different internals (where no mass transfer was present); (continued)

compartment type	liquid/liquid-system (mutually saturated)	a · f [cm/s]	d_M [mm]	p_B [-]	n_{dd} [-]
sieve-tray d_h = 4 mm	t (d)/a/w	1.5	6.0	0.96	3.9
sieve-tray d_h = 4 mm	t (d)/a/w	2.0	2.0	0.07	2.4
sieve-tray d_h = 4 mm	t (d)/a/w	2.0	3.0	0.29	3.5
sieve-tray d_h = 4 mm	t (d)/a/w	2.0	4.0	0.54	4.5
sieve-tray d_h = 4 mm	t (d)/a/w	2.0	5.1	0.93	5.5
sieve-tray d_h = 4 mm	t (d)/a/w	2.5	1.5	0.05	2.6
sieve-tray d_h = 4 mm	t (d)/a/w	2.5	2.0	0.18	2.8
sieve-tray d_h = 4 mm	t (d)/a/w	2.5	3.0	0.42	5.4
sieve-tray d_h = 4 mm	t (d)/a/w	2.5	4.0	0.70	4.3
sieve-tray d_h = 4 mm	t (d)/a/w	2.5	5.1	0.99	6.7
sieve-tray d_h = 4 mm	bu-ac (d)/a/w	1.0	2.8	0.04	2.0
sieve-tray d_h = 4 mm	bu-ac (d)/a/w	1.0	3.0	0.22	2.2
sieve-tray d_h = 4 mm	bu-ac (d)/a/w	1.0	3.5	0.44	2.4
sieve-tray d_h = 4 mm	bu-ac (d)/a/w	1.0	4.0	0.55	3.5
sieve-tray d_h = 4 mm	bu-ac (d)/a/w	1.0	4.5	0.72	3.1
sieve-tray d_h = 4 mm	bu-ac (d)/a/w	1.0	5.0	0.97	4.6
sieve-tray d_h = 4 mm	bu-ac (d)/a/w	1.5	1.5	0.03	2.1
sieve-tray d_h = 4 mm	bu-ac (d)/a/w	1.5	2.0	0.13	3.2
sieve-tray d_h = 4 mm	bu-ac (d)/a/w	1.5	2.5	0.26	3.7
sieve-tray d_h = 4 mm	bu-ac (d)/a/w	1.5	3.0	0.49	3.8
sieve-tray d_h = 4 mm	bu-ac (d)/a/w	1.5	3.5	0.63	4.4
sieve-tray d_h = 4 mm	bu-ac (d)/a/w	1.5	4.0	0.86	5.6
sieve-tray d_h = 4 mm	bu-ac (d)/a/w	1.5	4.4	0.96	5.5
sieve-tray d_h = 4 mm	bu-ac (d)/a/w	2.0	1.5	0.13	3.5
sieve-tray d_h = 4 mm	bu-ac (d)/a/w	2.0	2.0	0.23	3.2
sieve-tray d_h = 4 mm	bu-ac (d)/a/w	2.0	2.5	0.39	4.2
sieve-tray d_h = 4 mm	bu-ac (d)/a/w	2.0	3.0	0.54	4.7
sieve-tray d_h = 4 mm	bu-ac (d)/a/w	2.0	3.5	0.86	5.7
sieve-tray d_h = 4 mm	bu-ac (d)/a/w	2.0	4.0	0.93	6.8
sieve-tray d_h = 2 mm	t (d)/w	1.5	2.3	0.04	2.0
sieve-tray d_h = 2 mm	t (d)/w	1.5	2.5	0.17	2.6
sieve-tray d_h = 2 mm	t (d)/w	1.5	2.8	0.32	3.0
sieve-tray d_h = 2 mm	t (d)/w	1.5	3.0	0.39	3.6

Table A.9: Breakage probability p_B of single mother drops and average number of daughter drops n_{dd} produced from breakage of mother drops in a single pulsed compartment with different internals (where no mass transfer was present); (continued)

compartment type	liquid/liquid-system (mutually saturated)	a · f [cm/s]	d_M [mm]	p_B [-]	n_{dd} [-]
sieve-tray d_h = 2 mm	t (d)/w	1.5	3.3	0.58	4.0
sieve-tray d_h = 2 mm	t (d)/w	1.5	3.8	0.80	4.4
sieve-tray d_h = 2 mm	t (d)/w	1.5	4.0	0.91	4.6
sieve-tray d_h = 2 mm	t (d)/w	1.5	4.3	0.97	4.9
sieve-tray d_h = 2 mm	t (d)/w	2.0	2.0	0.09	2.3
sieve-tray d_h = 2 mm	t (d)/w	2.0	2.5	0.33	3.5
sieve-tray d_h = 2 mm	t (d)/w	2.0	3.0	0.59	3.8
sieve-tray d_h = 2 mm	t (d)/w	2.0	3.3	0.77	4.1
sieve-tray d_h = 2 mm	t (d)/w	2.0	3.5	0.86	4.4
sieve-tray d_h = 2 mm	t (d)/w	2.0	3.8	0.97	4.9
sieve-tray d_h = 2 mm	t (d)/w	2.5	1.5	0.17	2.1
sieve-tray d_h = 2 mm	t (d)/w	2.5	1.8	0.32	2.6
sieve-tray d_h = 2 mm	t (d)/w	2.5	2.0	0.38	3.1
sieve-tray d_h = 2 mm	t (d)/w	2.5	2.5	0.63	3.9
sieve-tray d_h = 2 mm	t (d)/w	2.5	3.0	0.81	5.2
sieve-tray d_h = 2 mm	t (d)/w	2.5	3.3	0.86	5.2
sieve-tray d_h = 2 mm	t (d)/w	2.5	3.5	0.97	7.2
sieve-tray d_h = 2 mm	bu-ac (d)/w	1.0	1.8	0.03	2.0
sieve-tray d_h = 2 mm	bu-ac (d)/w	1.0	2.3	0.20	2.1
sieve-tray d_h = 2 mm	bu-ac (d)/w	1.0	2.5	0.35	2.2
sieve-tray d_h = 2 mm	bu-ac (d)/w	1.0	2.8	0.52	2.9
sieve-tray d_h = 2 mm	bu-ac (d)/w	1.0	2.8	0.49	3.1
sieve-tray d_h = 2 mm	bu-ac (d)/w	1.0	3.0	0.62	3.0
sieve-tray d_h = 2 mm	bu-ac (d)/w	1.0	3.3	0.77	3.1
sieve-tray d_h = 2 mm	bu-ac (d)/w	1.0	3.3	0.72	2.8
sieve-tray d_h = 2 mm	bu-ac (d)/w	1.0	3.5	0.81	3.0
sieve-tray d_h = 2 mm	bu-ac (d)/w	1.0	3.5	0.78	2.9
sieve-tray d_h = 2 mm	bu-ac (d)/w	1.0	3.8	0.92	2.4
sieve-tray d_h = 2 mm	bu-ac (d)/w	1.5	1.5	0.16	2.2
sieve-tray d_h = 2 mm	bu-ac (d)/w	1.5	1.5	0.15	2.5
sieve-tray d_h = 2 mm	bu-ac (d)/w	1.5	1.8	0.31	2.7
sieve-tray d_h = 2 mm	bu-ac (d)/w	1.5	1.8	0.34	2.4
sieve-tray d_h = 2 mm	bu-ac (d)/w	1.5	2.0	0.46	3.7
sieve-tray d_h = 2 mm	bu-ac (d)/w	1.5	2.0	0.47	3.2

Table A.9: Breakage probability p_B of single mother drops and average number of daughter drops n_{dd} produced from breakage of mother drops in a single pulsed compartment with different internals (where no mass transfer was present); (continued)

compartment type	liquid/liquid-system (mutually saturated)	a · f [cm/s]	d_M [mm]	p_B [-]	n_{dd} [-]
sieve-tray d_h = 2 mm	bu-ac (d)/w	1.5	2.3	0.59	4.0
sieve-tray d_h = 2 mm	bu-ac (d)/w	1.5	2.5	0.67	4.6
sieve-tray d_h = 2 mm	bu-ac (d)/w	1.5	2.8	0.74	4.7
sieve-tray d_h = 2 mm	bu-ac (d)/w	1.5	3.0	0.85	5.5
sieve-tray d_h = 2 mm	bu-ac (d)/w	1.5	3.3	0.93	4.8
sieve-tray d_h = 2 mm	bu-ac (d)/w	1.5	3.3	0.92	5.4
sieve-tray d_h = 2 mm	bu-ac (d)/w	1.5	3.5	0.97	5.0
sieve-tray d_h = 2 mm	bu-ac (d)/w	1.5	3.5	0.98	5.3
sieve-tray d_h = 2 mm	bu-ac (d)/w	2.0	1.5	0.50	3.9
sieve-tray d_h = 2 mm	bu-ac (d)/w	2.0	1.8	0.59	4.1
sieve-tray d_h = 2 mm	bu-ac (d)/w	2.0	2.0	0.64	5.0
sieve-tray d_h = 2 mm	bu-ac (d)/w	2.0	2.0	0.68	5.2
sieve-tray d_h = 2 mm	bu-ac (d)/w	2.0	2.3	0.80	6.0
sieve-tray d_h = 2 mm	bu-ac (d)/w	2.0	2.5	0.88	8.1
sieve-tray d_h = 2 mm	bu-ac (d)/w	2.0	2.8	0.97	9.3
sieve-tray d_h = 2 mm	t (d)/a/w	1.5	1.7	0.02	2.0
sieve-tray d_h = 2 mm	t (d)/a/w	1.5	2.0	0.13	3.0
sieve-tray d_h = 2 mm	t (d)/a/w	1.5	2.3	0.26	3.2
sieve-tray d_h = 2 mm	t (d)/a/w	1.5	3.0	0.60	3.5
sieve-tray d_h = 2 mm	t (d)/a/w	1.5	3.3	0.73	5.1
sieve-tray d_h = 2 mm	t (d)/a/w	1.5	4.0	0.95	5.3
sieve-tray d_h = 2 mm	t (d)/a/w	2.0	1.5	0.29	2.9
sieve-tray d_h = 2 mm	t (d)/a/w	2.0	1.8	0.53	4.2
sieve-tray d_h = 2 mm	t (d)/a/w	2.0	2.0	0.68	4.6
sieve-tray d_h = 2 mm	t (d)/a/w	2.0	3.0	0.85	6.5
sieve-tray d_h = 2 mm	t (d)/a/w	2.0	3.5	0.93	9.1
sieve-tray d_h = 2 mm	t (d)/a/w	2.5	1.5	0.57	5.4
sieve-tray d_h = 2 mm	t (d)/a/w	2.5	2.0	0.79	7.1
sieve-tray d_h = 2 mm	t (d)/a/w	2.5	3.0	0.95	9.3
sieve-tray d_h = 2 mm	bu-ac (d)/a/w	1.0	2.0	0.01	2.0
sieve-tray d_h = 2 mm	bu-ac (d)/a/w	1.0	2.5	0.30	2.6
sieve-tray d_h = 2 mm	bu-ac (d)/a/w	1.0	3.0	0.50	3.2
sieve-tray d_h = 2 mm	bu-ac (d)/a/w	1.0	3.5	0.79	4.5

Table A.9: Breakage probability p_B of single mother drops and average number of daughter drops n_{dd} produced from breakage of mother drops in a single pulsed compartment with different internals (where no mass transfer was present); (continued)

compartment type	liquid/liquid-system (mutually saturated)	a · f [cm/s]	d_M [mm]	p_B [-]	n_{dd} [-]
sieve-tray d_h = 2 mm	bu-ac (d)/a/w	1.0	3.8	0.98	5.0
sieve-tray d_h = 2 mm	bu-ac (d)/a/w	1.5	1.5	0.24	2.4
sieve-tray d_h = 2 mm	bu-ac (d)/a/w	1.5	2.0	0.66	3.3
sieve-tray d_h = 2 mm	bu-ac (d)/a/w	1.5	2.5	0.81	5.5
sieve-tray d_h = 2 mm	bu-ac (d)/a/w	1.5	3.0	0.90	5.9
sieve-tray d_h = 2 mm	bu-ac (d)/a/w	1.5	3.3	0.97	7.5
sieve-tray d_h = 2 mm	bu-ac (d)/a/w	2.0	1.5	0.61	4.5
sieve-tray d_h = 2 mm	bu-ac (d)/a/w	2.0	2.0	0.81	7.4
sieve-tray d_h = 2 mm	bu-ac (d)/a/w	2.0	2.5	0.96	11.3
Montz-Pak B1-350	t (d)/w	1.0	3.9	0.07	2.0
Montz-Pak B1-350	t (d)/w	1.0	4.6	0.13	2.0
Montz-Pak B1-350	t (d)/w	1.0	5.1	0.44	2.1
Montz-Pak B1-350	t (d)/w	1.0	5.6	0.55	2.1
Montz-Pak B1-350	t (d)/w	1.0	5.9	0.56	2.2
Montz-Pak B1-350	t (d)/w	1.0	6.4	0.75	2.3
Montz-Pak B1-350	t (d)/w	1.0	7.0	0.82	2.4
Montz-Pak B1-350	t (d)/w	1.0	7.5	0.87	2.6
Montz-Pak B1-350	t (d)/w	1.0	8.0	0.94	2.8
Montz-Pak B1-350	t (d)/w	1.5	2.5	0.03	2.0
Montz-Pak B1-350	t (d)/w	1.5	3.0	0.14	2.1
Montz-Pak B1-350	t (d)/w	1.5	3.9	0.37	2.2
Montz-Pak B1-350	t (d)/w	1.5	4.5	0.48	2.3
Montz-Pak B1-350	t (d)/w	1.5	5.1	0.60	2.2
Montz-Pak B1-350	t (d)/w	1.5	5.6	0.76	2.7
Montz-Pak B1-350	t (d)/w	1.5	5.9	0.89	3.4
Montz-Pak B1-350	t (d)/w	1.5	6.4	0.95	3.5
Montz-Pak B1-350	t (d)/w	2.0	2.0	0.04	2.0
Montz-Pak B1-350	t (d)/w	2.0	2.5	0.13	2.0
Montz-Pak B1-350	t (d)/w	2.0	3.0	0.37	2.1
Montz-Pak B1-350	t (d)/w	2.0	4.0	0.56	2.5
Montz-Pak B1-350	t (d)/w	2.0	4.2	0.74	2.5
Montz-Pak B1-350	t (d)/w	2.0	4.6	0.85	2.6
Montz-Pak B1-350	t (d)/w	2.0	5.1	0.95	3.6
Montz-Pak B1-350	t (d)/w	2.5	1.6	0.02	2.0

Table A.9: Breakage probability p_B of single mother drops and average number of daughter drops n_{dd} produced from breakage of mother drops in a single pulsed compartment with different internals (where no mass transfer was present); (continued)

compartment type	liquid/liquid-system (mutually saturated)	a · f [cm/s]	d_M [mm]	p_B [-]	n_{dd} [-]
Montz-Pak B1-350	t (d)/w	2.5	2.0	0.11	2.1
Montz-Pak B1-350	t (d)/w	2.5	2.5	0.25	2.3
Montz-Pak B1-350	t (d)/w	2.5	3.0	0.54	2.4
Montz-Pak B1-350	t (d)/w	2.5	3.5	0.69	2.8
Montz-Pak B1-350	t (d)/w	2.5	4.0	0.86	3.5
Montz-Pak B1-350	t (d)/w	2.5	4.6	0.97	4.6
Montz-Pak B1-350	bu-ac (d)/w	0.5	2.5	0.03	2.0
Montz-Pak B1-350	bu-ac (d)/w	0.5	2.8	0.09	2.0
Montz-Pak B1-350	bu-ac (d)/w	0.5	3.0	0.26	2.0
Montz-Pak B1-350	bu-ac (d)/w	0.5	3.3	0.46	2.2
Montz-Pak B1-350	bu-ac (d)/w	0.5	3.3	0.44	2.2
Montz-Pak B1-350	bu-ac (d)/w	0.5	3.5	0.61	2.3
Montz-Pak B1-350	bu-ac (d)/w	0.5	3.5	0.62	2.3
Montz-Pak B1-350	bu-ac (d)/w	0.5	3.8	0.70	2.4
Montz-Pak B1-350	bu-ac (d)/w	0.5	4.0	0.85	2.0
Montz-Pak B1-350	bu-ac (d)/w	0.5	4.4	0.96	2.1
Montz-Pak B1-350	bu-ac (d)/w	1.0	2.5	0.10	2.0
Montz-Pak B1-350	bu-ac (d)/w	1.0	2.8	0.19	2.0
Montz-Pak B1-350	bu-ac (d)/w	1.0	4.0	0.98	2.0
Montz-Pak B1-350	bu-ac (d)/w	1.0	3.0	0.35	2.0
Montz-Pak B1-350	bu-ac (d)/w	1.0	3.0	0.32	2.1
Montz-Pak B1-350	bu-ac (d)/w	1.0	3.3	0.55	2.1
Montz-Pak B1-350	bu-ac (d)/w	1.0	3.3	0.58	2.2
Montz-Pak B1-350	bu-ac (d)/w	1.0	3.5	0.78	2.3
Montz-Pak B1-350	bu-ac (d)/w	1.0	3.5	0.75	2.3
Montz-Pak B1-350	bu-ac (d)/w	1.0	3.8	0.93	2.5
Montz-Pak B1-350	bu-ac (d)/w	1.5	1.6	0.03	2.0
Montz-Pak B1-350	bu-ac (d)/w	1.5	1.8	0.15	2.0
Montz-Pak B1-350	bu-ac (d)/w	1.5	2.0	0.17	2.0
Montz-Pak B1-350	bu-ac (d)/w	1.5	2.3	0.21	2.1
Montz-Pak B1-350	bu-ac (d)/w	1.5	2.3	0.25	2.1
Montz-Pak B1-350	bu-ac (d)/w	1.5	2.5	0.39	2.2
Montz-Pak B1-350	bu-ac (d)/w	1.5	2.8	0.46	2.3
Montz-Pak B1-350	bu-ac (d)/w	1.5	3.0	0.61	2.6

Table A.9: Breakage probability p_B of single mother drops and average number of daughter drops n_{dd} produced from breakage of mother drops in a single pulsed compartment with different internals (where no mass transfer was present); (continued)

compartment type	liquid/liquid-system (mutually saturated)	a · f [cm/s]	d_M [mm]	p_B [-]	n_{dd} [-]
Montz-Pak B1-350	bu-ac (d)/w	1.5	3.0	0.54	2.4
Montz-Pak B1-350	bu-ac (d)/w	1.5	3.3	0.78	2.8
Montz-Pak B1-350	bu-ac (d)/w	1.5	3.5	0.91	3.2
Montz-Pak B1-350	bu-ac (d)/w	1.5	3.8	0.98	3.1
Montz-Pak B1-350	bu-ac (d)/w	2.0	1.6	0.20	2.0
Montz-Pak B1-350	bu-ac (d)/w	2.0	1.8	0.33	2.2
Montz-Pak B1-350	bu-ac (d)/w	2.0	2.0	0.44	2.3
Montz-Pak B1-350	bu-ac (d)/w	2.0	2.3	0.53	2.2
Montz-Pak B1-350	bu-ac (d)/w	2.0	2.5	0.63	2.6
Montz-Pak B1-350	bu-ac (d)/w	2.0	2.8	0.74	3.0
Montz-Pak B1-350	bu-ac (d)/w	2.0	3.0	0.82	3.0
Montz-Pak B1-350	bu-ac (d)/w	2.0	3.0	0.82	3.1
Montz-Pak B1-350	bu-ac (d)/w	2.0	3.3	0.94	3.3
Montz-Pak B1-350	bu-ac (d)/w	2.0	3.3	0.93	3.6
Montz-Pak B1-350	bu-ac (d)/w	2.0	3.4	0.98	3.9
Montz-Pak B1-350	t (d)/a/w	1.0	3.5	0.03	2.0
Montz-Pak B1-350	t (d)/a/w	1.0	4.0	0.16	2.0
Montz-Pak B1-350	t (d)/a/w	1.0	4.6	0.44	2.0
Montz-Pak B1-350	t (d)/a/w	1.0	5.1	0.52	2.1
Montz-Pak B1-350	t (d)/a/w	1.0	6.0	0.80	2.5
Montz-Pak B1-350	t (d)/a/w	1.0	7.0	0.94	3.1
Montz-Pak B1-350	t (d)/a/w	1.5	3.0	0.03	2.0
Montz-Pak B1-350	t (d)/a/w	1.5	4.0	0.34	2.1
Montz-Pak B1-350	t (d)/a/w	1.5	4.6	0.62	2.2
Montz-Pak B1-350	t (d)/a/w	1.5	5.1	0.79	2.5
Montz-Pak B1-350	t (d)/a/w	1.5	6.0	0.95	3.2
Montz-Pak B1-350	t (d)/a/w	2.0	1.8	0.05	2.0
Montz-Pak B1-350	t (d)/a/w	2.0	2.0	0.18	2.1
Montz-Pak B1-350	t (d)/a/w	2.0	2.5	0.42	2.2
Montz-Pak B1-350	t (d)/a/w	2.0	3.0	0.56	2.3
Montz-Pak B1-350	t (d)/a/w	2.0	3.5	0.78	2.9
Montz-Pak B1-350	t (d)/a/w	2.0	4.0	0.95	3.3
Montz-Pak B1-350	t (d)/a/w	2.5	1.5	0.10	2.2
Montz-Pak B1-350	t (d)/a/w	2.5	2.0	0.34	2.2

Table A.9: Breakage probability p_B of single mother drops and average number of daughter drops n_{dd} produced from breakage of mother drops in a single pulsed compartment with different internals (where no mass transfer was present); (continued)

compartment type	liquid/liquid-system (mutually saturated)	a · f [cm/s]	d_M [mm]	p_B [-]	n_{dd} [-]
Montz-Pak B1-350	t (d)/a/w	2.5	2.5	0.62	2.6
Montz-Pak B1-350	t (d)/a/w	2.5	3.0	0.84	3.4
Montz-Pak B1-350	t (d)/a/w	2.5	3.5	0.91	3.8
Montz-Pak B1-350	bu-ac (d)/a/w	1.0	2.3	0.02	2.0
Montz-Pak B1-350	bu-ac (d)/a/w	1.0	2.8	0.13	2.1
Montz-Pak B1-350	bu-ac (d)/a/w	1.0	3.0	0.36	2.2
Montz-Pak B1-350	bu-ac (d)/a/w	1.0	3.5	0.73	2.4
Montz-Pak B1-350	bu-ac (d)/a/w	1.0	4.0	0.98	2.6
Montz-Pak B1-350	bu-ac (d)/a/w	1.5	1.5	0.07	2.0
Montz-Pak B1-350	bu-ac (d)/a/w	1.5	2.0	0.21	2.1
Montz-Pak B1-350	bu-ac (d)/a/w	1.5	2.5	0.56	2.0
Montz-Pak B1-350	bu-ac (d)/a/w	1.5	3.0	0.78	2.4
Montz-Pak B1-350	bu-ac (d)/a/w	1.5	3.5	0.97	3.0
Montz-Pak B1-350	bu-ac (d)/a/w	2.0	1.5	0.33	2.1
Montz-Pak B1-350	bu-ac (d)/a/w	2.0	1.8	0.52	2.3
Montz-Pak B1-350	bu-ac (d)/a/w	2.0	2.3	0.74	2.9
Montz-Pak B1-350	bu-ac (d)/a/w	2.0	2.5	0.85	3.0
Montz-Pak B1-350	bu-ac (d)/a/w	2.0	2.8	0.93	3.4
Montz-Pak B1-350	bu-ac (d)/a/w	2.0	3.1	0.99	4.8

Table A.10: Breakage probability p_B of single mother drops and average number of daughter drops n_{dd} produced from breakage of mother drops in a single agitated compartment with different internals (where no mass transfer was present);

compartment type (one compartment)	liquid/liquid-system (mutually saturated)	n_R [1/min]	d_M [mm]	p_B [-]	n_{dd} [-]
RDC-compartment	t (d)/w	800	2.0	0.10	2.0
RDC-compartment	t (d)/w	900	2.0	0.28	2.4
RDC-compartment	t (d)/w	1000	2.0	0.41	2.6
RDC-compartment	t (d)/w	1100	2.0	0.53	3.1
RDC-compartment	t (d)/w	1200	2.0	0.67	4.2
RDC-compartment	t (d)/w	700	3.0	0.10	2.4
RDC-compartment	t (d)/w	800	3.0	0.31	2.8
RDC-compartment	t (d)/w	900	3.0	0.47	2.8
RDC-compartment	t (d)/w	1000	3.0	0.61	3.6
RDC-compartment	t (d)/w	1100	3.0	0.71	4.4
RDC-compartment	t (d)/w	1200	3.0	0.81	5.9
RDC-compartment	t (d)/w	600	4.0	0.18	2.4
RDC-compartment	t (d)/w	700	4.0	0.34	2.7
RDC-compartment	t (d)/w	800	4.0	0.54	3.6
RDC-compartment	t (d)/w	900	4.0	0.63	3.9
RDC-compartment	t (d)/w	1000	4.0	0.81	5.4
RDC-compartment	t (d)/w	1100	4.0	0.86	6.6
RDC-compartment	bu-ac (d)/w	500	2.0	0.12	2.0
RDC-compartment	bu-ac (d)/w	600	2.0	0.36	2.4
RDC-compartment	bu-ac (d)/w	700	2.0	0.58	2.8
RDC-compartment	bu-ac (d)/w	800	2.0	0.77	3.8
RDC-compartment	bu-ac (d)/w	900	2.0	0.87	5.1
RDC-compartment	bu-ac (d)/w	400	3.0	0.15	2.2
RDC-compartment	bu-ac (d)/w	500	3.0	0.35	2.5
RDC-compartment	bu-ac (d)/w	600	3.0	0.57	3.5
RDC-compartment	bu-ac (d)/w	700	3.0	0.79	5.1
RDC-compartment	bu-ac (d)/w	800	3.0	0.86	6.6
RDC-compartment	bu-ac (d)/w	350	4.0	0.14	2.4
RDC-compartment	bu-ac (d)/w	400	4.0	0.25	2.7
RDC-compartment	bu-ac (d)/w	450	4.0	0.43	2.5
RDC-compartment	bu-ac (d)/w	500	4.0	0.63	3.6
RDC-compartment	bu-ac (d)/w	550	4.0	0.79	4.1
RDC-compartment	bu-ac (d)/w	600	4.0	0.87	5.5
RDC-compartment	t (d)/a/w	600	2.0	0.02	2.0

Table A.10: Breakage probability p_B of single mother drops and average number of daughter drops n_{dd} produced from breakage of mother drops in a single agitated compartment with different internals (where no mass transfer was present);

compartment type (one compartment)	liquid/liquid-system (mutually saturated)	n_R [1/min]	d_M [mm]	p_B [-]	n_{dd} [-]
RDC-compartment	t (d)/a/w	700	2.0	0.15	3.0
RDC-compartment	t (d)/a/w	800	2.0	0.37	2.4
RDC-compartment	t (d)/a/w	900	2.0	0.58	2.8
RDC-compartment	t (d)/a/w	1000	2.0	0.77	3.3
RDC-compartment	t (d)/a/w	1100	2.0	0.85	4.4
RDC-compartment	t (d)/a/w	500	3.0	0.03	2.0
RDC-compartment	t (d)/a/w	600	3.0	0.12	2.1
RDC-compartment	t (d)/a/w	700	3.0	0.35	2.5
RDC-compartment	t (d)/a/w	800	3.0	0.51	3.4
RDC-compartment	t (d)/a/w	900	3.0	0.76	3.9
RDC-compartment	t (d)/a/w	1000	3.0	0.87	5.0
RDC-compartment	t (d)/a/w	400	4.0	0.02	2.0
RDC-compartment	t (d)/a/w	500	4.0	0.20	2.3
RDC-compartment	t (d)/a/w	600	4.0	0.38	2.6
RDC-compartment	t (d)/a/w	700	4.0	0.57	3.3
RDC-compartment	t (d)/a/w	800	4.0	0.78	4.4
RDC-compartment	t (d)/a/w	900	4.0	0.93	7.1
RDC-compartment	bu-ac (d)/a/w	400	2.0	0.05	2.2
RDC-compartment	bu-ac (d)/a/w	500	2.0	0.26	2.6
RDC-compartment	bu-ac (d)/a/w	600	2.0	0.55	3.0
RDC-compartment	bu-ac (d)/a/w	700	2.0	0.71	3.6
RDC-compartment	bu-ac (d)/a/w	800	2.0	0.87	4.7
RDC-compartment	bu-ac (d)/a/w	300	3.0	0.06	2.0
RDC-compartment	bu-ac (d)/a/w	400	3.0	0.32	2.7
RDC-compartment	bu-ac (d)/a/w	500	3.0	0.56	2.7
RDC-compartment	bu-ac (d)/a/w	600	3.0	0.70	5.3
RDC-compartment	bu-ac (d)/a/w	700	3.0	0.92	8.3
RDC-compartment	bu-ac (d)/a/w	300	4.0	0.13	2.3
RDC-compartment	bu-ac (d)/a/w	350	4.0	0.32	2.5
RDC-compartment	bu-ac (d)/a/w	400	4.0	0.66	3.3
RDC-compartment	bu-ac (d)/a/w	450	4.0	0.75	4.3
RDC-compartment	bu-ac (d)/a/w	500	4.0	0.86	4.9
Kühni-compartment	t (d)/w	175	2.0	0.08	2.3
Kühni-compartment	t (d)/w	200	2.0	0.28	2.5

Table A.10: Breakage probability p_B of single mother drops and average number of daughter drops n_{dd} produced from breakage of mother drops in a single agitated compartment with different internals (where no mass transfer was present);

compartment type (one compartment)	liquid/liquid-system (mutually saturated)	n_R [1/min]	d_M [mm]	p_B [-]	n_{dd} [-]
Kühni-compartment	t (d)/w	225	2.0	0.46	2.6
Kühni-compartment	t (d)/w	250	2.0	0.60	3.4
Kühni-compartment	t (d)/w	125	3.0	0.04	2.0
Kühni-compartment	t (d)/w	150	3.0	0.24	2.5
Kühni-compartment	t (d)/w	175	3.0	0.39	3.1
Kühni-compartment	t (d)/w	200	3.0	0.50	3.3
Kühni-compartment	t (d)/w	225	3.0	0.65	4.0
Kühni-compartment	t (d)/w	250	3.0	0.81	5.3
Kühni-compartment	t (d)/w	100	4.0	0.03	2.0
Kühni-compartment	t (d)/w	125	4.0	0.16	2.6
Kühni-compartment	t (d)/w	150	4.0	0.38	2.8
Kühni-compartment	t (d)/w	175	4.0	0.49	3.4
Kühni-compartment	t (d)/w	200	4.0	0.69	4.2
Kühni-compartment	t (d)/w	225	4.0	0.85	5.2
Kühni-compartment	bu-ac (d)/w	100	2.0	0.07	2.1
Kühni-compartment	bu-ac (d)/w	125	2.0	0.27	2.2
Kühni-compartment	bu-ac (d)/w	150	2.0	0.49	3.2
Kühni-compartment	bu-ac (d)/w	175	2.0	0.72	3.6
Kühni-compartment	bu-ac (d)/w	200	2.0	0.85	4.8
Kühni-compartment	bu-ac (d)/w	75	3.0	0.06	2.0
Kühni-compartment	bu-ac (d)/w	100	3.0	0.27	2.7
Kühni-compartment	bu-ac (d)/w	125	3.0	0.52	3.9
Kühni-compartment	bu-ac (d)/w	150	3.0	0.68	5.3
Kühni-compartment	bu-ac (d)/w	175	3.0	0.87	7.4
Kühni-compartment	bu-ac (d)/w	50	4.0	0.05	2.0
Kühni-compartment	bu-ac (d)/w	75	4.0	0.21	2.8
Kühni-compartment	bu-ac (d)/w	100	4.0	0.41	3.0
Kühni-compartment	bu-ac (d)/w	125	4.0	0.69	6.1
Kühni-compartment	bu-ac (d)/w	150	4.0	0.91	7.1
Kühni-compartment	t (d)/a/w	125	2.0	0.05	2.2
Kühni-compartment	t (d)/a/w	150	2.0	0.22	2.3
Kühni-compartment	t (d)/a/w	175	2.0	0.51	2.7

Table A.10: Breakage probability p_B of single mother drops and average number of daughter drops n_{dd} produced from breakage of mother drops in a single agitated compartment with different internals (where no mass transfer was present);

compartment type (one compartment)	liquid/liquid-system (mutually saturated)	n_R [1/min]	d_M [mm]	p_B [-]	n_{dd} [-]
Kühni-compartment	t (d)/a/w	200	2.0	0.69	4.0
Kühni-compartment	t (d)/a/w	225	2.0	0.87	4.7
Kühni-compartment	t (d)/a/w	100	3.0	0.10	2.4
Kühni-compartment	t (d)/a/w	125	3.0	0.36	3.1
Kühni-compartment	t (d)/a/w	150	3.0	0.61	4.6
Kühni-compartment	t (d)/a/w	175	3.0	0.73	5.5
Kühni-compartment	t (d)/a/w	200	3.0	0.85	7.5
Kühni-compartment	t (d)/a/w	75	4.0	0.02	2.0
Kühni-compartment	t (d)/a/w	100	4.0	0.30	2.9
Kühni-compartment	t (d)/a/w	125	4.0	0.54	4.6
Kühni-compartment	t (d)/a/w	150	4.0	0.74	6.2
Kühni-compartment	t (d)/a/w	175	4.0	0.84	5.9
Kühni-compartment	bu-ac (d)/a/w	75	2.0	0.02	2.0
Kühni-compartment	bu-ac (d)/a/w	100	2.0	0.20	2.9
Kühni-compartment	bu-ac (d)/a/w	125	2.0	0.37	2.9
Kühni-compartment	bu-ac (d)/a/w	150	2.0	0.61	4.6
Kühni-compartment	bu-ac (d)/a/w	175	2.0	0.87	5.6
Kühni-compartment	bu-ac (d)/a/w	50	3.0	0.04	2.0
Kühni-compartment	bu-ac (d)/a/w	75	3.0	0.19	2.2
Kühni-compartment	bu-ac (d)/a/w	100	3.0	0.41	3.9
Kühni-compartment	bu-ac (d)/a/w	125	3.0	0.56	5.6
Kühni-compartment	bu-ac (d)/a/w	150	3.0	0.82	7.2
Kühni-compartment	bu-ac (d)/a/w	175	3.0	0.90	8.8
Kühni-compartment	bu-ac (d)/a/w	25	4.0	0.06	2.0
Kühni-compartment	bu-ac (d)/a/w	50	4.0	0.17	2.1
Kühni-compartment	bu-ac (d)/a/w	75	4.0	0.40	3.0
Kühni-compartment	bu-ac (d)/a/w	100	4.0	0.58	6.6
Kühni-compartment	bu-ac (d)/a/w	125	4.0	0.87	8.4

A.3.4 Performance of Counter Current Extraction Columns

The swarm influence on the fluiddynamic behaviour and the mass transfer rates of drop swarms were determined in extraction columns with different internals. During an experiment, the acetone concentration of the aqueous and of the organic phase was determined at the inlet and at the outlet. In addition, concentration profiles of both phases, hold-up distribution along the column height and drop size distribution within the extraction column were recorded during each experiment at three column sections. The location of the measuring sections and the position of the individual measuring points are shown in *figure (A.6)*. The exact position of the single measuring points can be found in *chapter 4.4*.

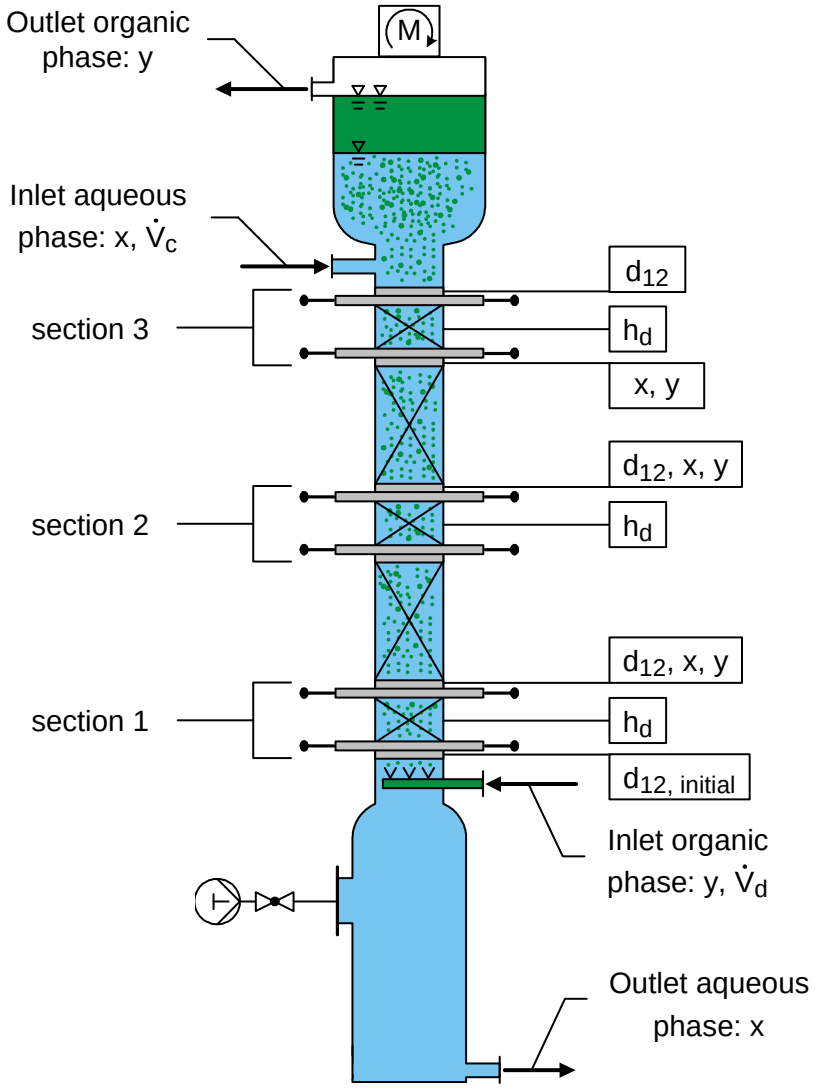

Figure A.6: Arrangement of the measuring sections and measuring points for the determination of the concentration profiles, hold-up profiles and drop size distributions along the column active height in the drop swarm extractor

Table (A.11) and *table (A.12)* show several examples of the initial drop size distribution of the toluene and butyl acetate phase determined immediately after the finger distributor, see *figure (A.6)*. No significant change of the initial drop size distribution was found during the experiments. Narrow drop size distributions were generated by the distributor with a sauter diameter $d_{12,initial}$ in the range from 2.0 to 2.4 mm.

*Table A.11: Examples for the initial drop size volume density distribution (Δd = 0.2 mm) of the dispersed **toluene phase** $q_3(d)_{initial}$*

example 1		example 2		example 3	
d [mm]	q_3(d) [1/mm]	d [mm]	q_3(d) [1/mm]	d [mm]	q_3(d) [1/mm]
0.1	0.000	0.1	0.000	0.1	0.000
0.3	0.000	0.3	0.000	0.3	0.000
0.5	0.000	0.5	0.000	0.5	0.000
0.7	0.000	0.7	0.000	0.7	0.000
0.9	0.000	0.9	0.000	0.9	0.000
1.1	0.066	1.1	0.080	1.1	0.056
1.3	0.113	1.3	0.097	1.3	0.111
1.5	0.213	1.5	0.138	1.5	0.214
1.7	0.226	1.7	0.210	1.7	0.289
1.9	0.340	1.9	0.274	1.9	0.340
2.1	0.527	2.1	0.485	2.1	0.598
2.3	0.632	2.3	0.541	2.3	0.752
2.5	0.758	2.5	0.630	2.5	0.894
2.7	0.540	2.7	0.730	2.7	0.526
2.9	0.622	2.9	0.554	2.9	0.410
3.1	0.424	3.1	0.359	3.1	0.182
3.3	0.159	3.3	0.350	3.3	0.137
3.5	0.105	3.5	0.219	3.5	0.033
3.7	0.149	3.7	0.117	3.7	0.039
3.9	0.058	3.9	0.083	3.9	0.045
4.1	0.068	4.1	0.096	4.1	0.053
4.3	0.000	4.3	0.037	4.3	0.182
4.5	0.000	4.5	0.000	4.5	0.139
4.7	0.000	4.7	0.000	4.7	0.000
4.9	0.000	4.9	0.000	4.9	0.000

*Table A.12: Examples for the initial drop size volume density distribution (Δd = 0.2 mm) of the dispersed **butyl acetate phase** $q_3(d)_{initial}$*

example 1		example 2		example 3	
d [mm]	q_3(d) [1/mm]	d [mm]	q_3(d) [1/mm]	d [mm]	q_3(d) [1/mm]
0.1	0.000	0.1	0.000	0.1	0.000
0.3	0.000	0.3	0.000	0.3	0.000
0.5	0.000	0.5	0.002	0.5	0.000
0.7	0.111	0.7	0.112	0.7	0.059
0.9	0.142	0.9	0.122	0.9	0.109
1.1	0.171	1.1	0.155	1.1	0.093
1.3	0.239	1.3	0.264	1.3	0.111
1.5	0.295	1.5	0.311	1.5	0.150
1.7	0.325	1.7	0.333	1.7	0.240
1.9	0.356	1.9	0.344	1.9	0.347
2.1	0.328	2.1	0.660	2.1	0.461
2.3	0.546	2.3	0.639	2.3	0.583
2.5	0.720	2.5	0.493	2.5	0.537
2.7	0.395	2.7	0.552	2.7	0.641
2.9	0.317	2.9	0.228	2.9	0.551
3.1	0.141	3.1	0.383	3.1	0.296
3.3	0.255	3.3	0.252	3.3	0.227
3.5	0.203	3.5	0.150	3.5	0.271
3.7	0.239	3.7	0.000	3.7	0.215
3.9	0.217	3.9	0.000	3.9	0.109
4.1	0.000	4.1	0.000	4.1	0.000
4.3	0.000	4.3	0.000	4.3	0.000
4.5	0.000	4.5	0.000	4.5	0.000
4.7	0.000	4.7	0.000	4.7	0.000
4.9	0.000	4.9	0.000	4.9	0.000

All experiments in the pilot plant extractor were carried out for a mass transfer direction from the continuous to the dispersed phase “c to d“. The following tables outline the results of a large number of experiments in the extractor. For each operating condition, the energy input ($a \cdot f$ or n_R), the volume flow of the continuous phase $\dot{V}_c$ and the dispersed phase $\dot{V}_d$ as well as the concentration profiles of both phases, the hold-up distribution along the column height and the sauter diameter profiles are shown.

*Table A.13: Drop swarm extractor: fluiddynamics and mass transfer of drop swarms in a pulsed sieve tray extractor **"PSE"** for different pulsation intensities; liquid/liquid-system: **toluene (d)/acetone/water***

column type:	concentration profile		hold-up profile	
PSE, sieve tray-d_h = 2 mm				
liquid/liquid-system:	aqueous phase	x [%]	measuring position	h_d [-]
t (d)/a/w	water inlet	5.44		
mass transfer direction:	section 3	4.51	section 3	0.077
c to d	section 2	3.86	section 2	0.092
pulsation intensity:	section 1	2.86	section 1	0.089
a · f = 1.0 cm/s	water outlet	2.37		
volume flow $\dot{V}_c$ [l/h]:			sauter diameter profile	
40.0	organic phase	y [%]		
volume flow $\dot{V}_d$ [l/h]:	organic phase outlet	3.57	measuring position	$d_{1,2}$ [mm]
48.0	section 3	3.20		
	section 2	2.67	section 3	1.9
	section 1	1.70	section 2	1.9
	organic phase inlet	0.76	section 1	2.3

column type:	concentration profile		hold-up profile	
PSE, sieve tray-d_h = 2 mm				
liquid/liquid-system:	aqueous phase	x [%]	measuring position	h_d [-]
t (d)/a/w	water inlet	5.44		
mass transfer direction:	section 3	4.19	section 3	0.095
c to d	section 2	3.49	section 2	0.092
pulsation intensity:	section 1	2.29	section 1	0.092
a · f = 1.0 cm/s	water outlet	2.09		
volume flow $\dot{V}_c$ [l/h]:			sauter diameter profile	
40.0	organic phase	y [%]		
volume flow $\dot{V}_d$ [l/h]:	organic phase outlet	3.50	measuring position	$d_{1,2}$ [mm]
48.0	section 3	3.10		
	section 2	2.45	section 3	2.0
	section 1	1.20	section 2	1.9
	organic phase inlet	0.36	section 1	2.4

column type:	concentration profile		hold-up profile	
PSE, sieve tray-d_h = 2 mm				
liquid/liquid-system:	aqueous phase	x [%]	measuring position	h_d [-]
t (d)/a/w	water inlet	5.52		
mass transfer direction:	section 3	4.55	section 3	0.129
c to d	section 2	3.75	section 2	0.129
pulsation intensity:	section 1	2.00	section 1	0.126
a · f = 1.0 cm/s	water outlet	1.60		
volume flow $\dot{V}_c$ [l/h]:			sauter diameter profile	
61.3	organic phase	y [%]		
volume flow $\dot{V}_d$ [l/h]:	organic phase outlet	3.82	measuring position	$d_{1,2}$ [mm]
74.1	section 3	3.33		
	section 2	2.56	section 3	2.1
	section 1	1.10	section 2	2.1
	organic phase inlet	0.15	section 1	2.3

*Table A.13: Drop swarm extractor: fluiddynamics and mass transfer of drop swarms in a pulsed sieve tray extractor **"PSE"** for different pulsation intensities; liquid/liquid-system: **toluene (d)/acetone/water** (continued)*

column type:	concentration profile		hold-up profile	
PSE, sieve tray-d_h = 2 mm				
liquid/liquid-system:	aqueous phase	x [%]	measuring position	h_d [-]
t (d)/a/w	water inlet	5.33		
mass transfer direction:	section 3	4.62	section 3	0.126
c to d	section 2	3.70	section 2	0.114
pulsation intensity:	section 1	2.05	section 1	0.117
a · f = 1.0 cm/s	water outlet	1.55		
volume flow $\dot{V}_c$ [l/h]:			sauter diameter profile	
61.3	organic phase	y [%]		
volume flow $\dot{V}_d$ [l/h]:	organic phase outlet	3.50	measuring position	$d_{1,2}$ [mm]
74.1	section 3	3.08		
	section 2	2.46	section 3	1.9
	section 1	1.13	section 2	2.2
	organic phase inlet	0.11	section 1	2.2

column type:	concentration profile		hold-up profile	
PSE, sieve tray-d_h = 2 mm				
liquid/liquid-system:	aqueous phase	x [%]	measuring position	h_d [-]
t (d)/a/w	water inlet	5.34		
mass transfer direction:	section 3	4.73	section 3	0.157
c to d	section 2	3.98	section 2	0.154
pulsation intensity:	section 1	2.46	section 1	0.135
a · f = 1.0 cm/s	water outlet	1.73		
volume flow $\dot{V}_c$ [l/h]:			sauter diameter profile	
71.9	organic phase	y [%]		
volume flow $\dot{V}_d$ [l/h]:	organic phase outlet	3.77	measuring position	$d_{1,2}$ [mm]
86.8	section 3	3.34		
	section 2	2.70	section 3	2.0
	section 1	1.42	section 2	2.2
	organic phase inlet	0.53	section 1	2.4

column type:	concentration profile		hold-up profile	
PSE, sieve tray-d_h = 2 mm				
liquid/liquid-system:	aqueous phase	x [%]	measuring position	h_d [-]
t (d)/a/w	water inlet	5.30		
mass transfer direction:	section 3	4.66	section 3	0.139
c to d	section 2	3.89	section 2	0.151
pulsation intensity:	section 1	2.14	section 1	0.135
a · f = 1.0 cm/s	water outlet	1.23		
volume flow $\dot{V}_c$ [l/h]:			sauter diameter profile	
71.9	organic phase	y [%]		
volume flow $\dot{V}_d$ [l/h]:	organic phase outlet	3.64	measuring position	$d_{1,2}$ [mm]
86.8	section 3	3.25		
	section 2	2.62	section 3	2.1
	section 1	1.25	section 2	2.1
	organic phase inlet	0.08	section 1	2.5

*Table A.13: Drop swarm extractor: fluiddynamics and mass transfer of drop swarms in a pulsed sieve tray extractor **"PSE"** for different pulsation intensities; liquid/liquid-system: **toluene (d)/acetone/water** (continued)*

column type:	concentration profile		hold-up profile	
PSE, sieve tray-d_h = 2 mm				
liquid/liquid-system:	aqueous phase	x [%]	measuring position	h_d [-]
t (d)/a/w	water inlet	5.92		
mass transfer direction:	section 3	4.98	section 3	0.326
c to d	section 2	4.42	section 2	0.345
pulsation intensity:	section 1	2.61	section 1	0.363
a · f = 1.0 cm/s	water outlet	1.36		
volume flow $\dot{V}_c$ [l/h]:			sauter diameter profile	
82.6	organic phase	y [%]		
volume flow $\dot{V}_d$ [l/h]:	organic phase outlet	4.19	measuring position	$d_{1,2}$ [mm]
99.6	section 3	3.81		
	section 2	2.93	section 3	2.2
	section 1	1.50	section 2	2.3
	organic phase inlet	0.13	section 1	2.3

column type:	concentration profile		hold-up profile	
PSE, sieve tray-d_h = 2 mm				
liquid/liquid-system:	aqueous phase	x [%]	measuring position	h_d [-]
t (d)/a/w	water inlet	5.49		
mass transfer direction:	section 3	4.96	section 3	0.259
c to d	section 2	4.31	section 2	0.308
pulsation intensity:	section 1	2.63	section 1	0.271
a · f = 1.0 cm/s	water outlet	1.62		
volume flow $\dot{V}_c$ [l/h]:			sauter diameter profile	
82.6	organic phase	y [%]		
volume flow $\dot{V}_d$ [l/h]:	organic phase outlet	3.87	measuring position	$d_{1,2}$ [mm]
99.6	section 3	3.53		
	section 2	2.92	section 3	2.3
	section 1	1.54	section 2	1.9
	organic phase inlet	0.54	section 1	2.5

column type:	concentration profile		hold-up profile	
PSE, sieve tray-d_h = 2 mm				
liquid/liquid-system:	aqueous phase	x [%]	measuring position	h_d [-]
t (d)/a/w	water inlet	5.35		
mass transfer direction:	section 3	4.86	section 3	0.277
c to d	section 2	4.24	section 2	0.255
pulsation intensity:	section 1	3.11	section 1	0.252
a · f = 1.0 cm/s	water outlet	1.83		
volume flow $\dot{V}_c$ [l/h]:			sauter diameter profile	
93.1	organic phase	y [%]		
volume flow $\dot{V}_d$ [l/h]:	organic phase outlet	4.02	measuring position	$d_{1,2}$ [mm]
111.8	section 3	3.73		
	section 2	3.24	section 3	2.6
	section 1	1.93	section 2	2.2
	organic phase inlet	0.73	section 1	2.6

*Table A.13: Drop swarm extractor: fluiddynamics and mass transfer of drop swarms in a pulsed sieve tray extractor **"PSE"** for different pulsation intensities; liquid/liquid-system: **toluene (d)/acetone/water** (continued)*

column type:	concentration profile		hold-up profile	
PSE, sieve tray-d_h = 2 mm				
liquid/liquid-system:	aqueous phase	x [%]	measuring position	h_d [-]
t (d)/a/w	water inlet	5.35		
mass transfer direction:	section 3	4.15	section 3	0.073
c to d	section 2	3.61	section 2	0.072
pulsation intensity:	section 1	2.69	section 1	0.072
a · f = 2.0 cm/s	water outlet	1.80		
volume flow $\dot{V}_c$ [l/h]:			sauter diameter profile	
40.0	organic phase	y [%]		
volume flow $\dot{V}_d$ [l/h]:	organic phase outlet	3.39	measuring position	$d_{1,2}$ [mm]
48.0	section 3	3.06		
	section 2	2.68	section 3	1.8
	section 1	1.58	section 2	1.9
	organic phase inlet	0.40	section 1	1.8

column type:	concentration profile		hold-up profile	
PSE, sieve tray-d_h = 2 mm				
liquid/liquid-system:	aqueous phase	x [%]	measuring position	h_d [-]
t (d)/a/w	water inlet	5.26		
mass transfer direction:	section 3	4.44	section 3	0.078
c to d	section 2	3.81	section 2	0.072
pulsation intensity:	section 1	2.41	section 1	0.077
a · f = 2.0 cm/s	water outlet	1.92		
volume flow $\dot{V}_c$ [l/h]:			sauter diameter profile	
40.0	organic phase	y [%]		
volume flow $\dot{V}_d$ [l/h]:	organic phase outlet	3.57	measuring position	$d_{1,2}$ [mm]
48.0	section 3	3.15		
	section 2	2.93	section 3	1.9
	section 1	1.61	section 2	1.8
	organic phase inlet	0.62	section 1	1.9

column type:	concentration profile		hold-up profile	
PSE, sieve tray-d_h = 2 mm				
liquid/liquid-system:	aqueous phase	x [%]	measuring position	h_d [-]
t (d)/a/w	water inlet	5.45		
mass transfer direction:	section 3	4.29	section 3	0.124
c to d	section 2	3.53	section 2	0.136
pulsation intensity:	section 1	2.33	section 1	0.121
a · f = 2.0 cm/s	water outlet	1.76		
volume flow $\dot{V}_c$ [l/h]:			sauter diameter profile	
61.3	organic phase	y [%]		
volume flow $\dot{V}_d$ [l/h]:	organic phase outlet	3.45	measuring position	$d_{1,2}$ [mm]
74.1	section 3	3.18		
	section 2	2.62	section 3	1.9
	section 1	1.32	section 2	2.0
	organic phase inlet	0.41	section 1	1.9

*Table A.13: Drop swarm extractor: fluiddynamics and mass transfer of drop swarms in a pulsed sieve tray extractor **"PSE"** for different pulsation intensities; liquid/liquid-system: **toluene (d)/acetone/water** (continued)*

column type:	concentration profile		hold-up profile	
PSE, sieve tray-d_h = 2 mm				
liquid/liquid-system:	aqueous phase	x [%]	measuring position	h_d [-]
t (d)/a/w	water inlet	5.31		
mass transfer direction:	section 3	4.57	section 3	0.145
c to d	section 2	3.90	section 2	0.125
pulsation intensity:	section 1	2.35	section 1	0.111
a · f = 2.0 cm/s	water outlet	1.81		
volume flow $\dot{V}_c$ [l/h]:			sauter diameter profile	
61.3	organic phase	y [%]		
volume flow $\dot{V}_d$ [l/h]:	organic phase outlet	3.96	measuring position	$d_{1,2}$ [mm]
74.1	section 3	3.61		
	section 2	2.94	section 3	1.8
	section 1	1.52	section 2	2.0
	organic phase inlet	0.62	section 1	2.0

column type:	concentration profile		hold-up profile	
PSE, sieve tray-d_h = 2 mm				
liquid/liquid-system:	aqueous phase	x [%]	measuring position	h_d [-]
t (d)/a/w	water inlet	5.22		
mass transfer direction:	section 3	4.63	section 3	0.167
c to d	section 2	3.98	section 2	0.165
pulsation intensity:	section 1	2.40	section 1	0.173
a · f = 2.0 cm/s	water outlet	1.64		
volume flow $\dot{V}_c$ [l/h]:			sauter diameter profile	
71.9	organic phase	y [%]		
volume flow $\dot{V}_d$ [l/h]:	organic phase outlet	4.06	measuring position	$d_{1,2}$ [mm]
86.8	section 3	3.77		
	section 2	3.08	section 3	2.1
	section 1	0.91	section 2	1.9
	organic phase inlet	0.62	section 1	2.2

column type:	concentration profile		hold-up profile	
PSE, sieve tray-d_h = 2 mm				
liquid/liquid-system:	aqueous phase	x [%]	measuring position	h_d [-]
t (d)/a/w	water inlet	5.36		
mass transfer direction:	section 3	4.76	section 3	0.215
c to d	section 2	3.86	section 2	0.209
pulsation intensity:	section 1	2.21	section 1	0.175
a · f = 2.0 cm/s	water outlet	1.46		
volume flow $\dot{V}_c$ [l/h]:			sauter diameter profile	
82.6	organic phase	y [%]		
volume flow $\dot{V}_d$ [l/h]:	organic phase outlet	4.28	measuring position	$d_{1,2}$ [mm]
99.6	section 3	3.86		
	section 2	3.04	section 3	1.9
	section 1	1.48	section 2	2.2
	organic phase inlet	0.53	section 1	2.0

*Table A.13: Drop swarm extractor: fluiddynamics and mass transfer of drop swarms in a pulsed sieve tray extractor **"PSE"** for different pulsation intensities; liquid/liquid-system: **toluene (d)/acetone/water** (continued)*

column type:	concentration profile		hold-up profile	
PSE, sieve tray-d_h = 2 mm				
liquid/liquid-system:	aqueous phase	x [%]	measuring position	h_d [-]
t (d)/a/w	water inlet	6.03		
mass transfer direction:	section 3	5.58	section 3	0.203
c to d	section 2	4.75	section 2	0.228
pulsation intensity:	section 1	3.12	section 1	0.200
$a \cdot f$ = 2.0 cm/s	water outlet	1.80		
volume flow $\dot{V}_c$ [l/h]:			sauter diameter profile	
82.6	organic phase	y [%]		
volume flow $\dot{V}_d$ [l/h]:	organic phase outlet	4.34	measuring position	$d_{1,2}$ [mm]
99.6	section 3	4.06		
	section 2	3.39	section 3	1.9
	section 1	1.89	section 2	1.8
	organic phase inlet	0.69	section 1	2.2

column type:	concentration profile		hold-up profile	
PSE, sieve tray-d_h = 2 mm				
liquid/liquid-system:	aqueous phase	x [%]	measuring position	h_d [-]
t (d)/a/w	water inlet	6.01		
mass transfer direction:	section 3	5.38	section 3	0.342
c to d	section 2	4.58	section 2	0.332
pulsation intensity:	section 1	2.93	section 1	0.300
$a \cdot f$ = 2.0 cm/s	water outlet	1.59		
volume flow $\dot{V}_c$ [l/h]:			sauter diameter profile	
93.2	organic phase	y [%]		
volume flow $\dot{V}_d$ [l/h]:	organic phase outlet	4.82	measuring position	$d_{1,2}$ [mm]
111.8	section 3	4.37		
	section 2	3.39	section 3	2.1
	section 1	2.05	section 2	2.0
	organic phase inlet	0.53	section 1	2.2

*Table A.14: Drop swarm extractor: fluiddynamics and mass transfer of drop swarms in a pulsed sieve tray extractor **"PSE"** for different pulsation intensities; liquid/liquid-system: **butyl acetate (d)/acetone/water***

column type:	concentration profile		hold-up profile	
PSE, sieve tray-d_h = 2 mm				
liquid/liquid-system:	aqueous phase	x [%]	measuring position	h_d [-]
bu-ac (d)/a/w	water inlet	5.17		
mass transfer direction:	section 3	3.33	section 3	0.062
c to d	section 2	2.36	section 2	0.074
pulsation intensity:	section 1	1.03	section 1	0.098
a · f = 1.0 cm/s	water outlet	0.59		
volume flow $\dot{V}_c$ [l/h]:			sauter diameter profile	
40.0	organic phase	y [%]		
volume flow $\dot{V}_d$ [l/h]:	organic phase outlet	4.37	measuring position	$d_{1,2}$ [mm]
48.0	section 3	2.92		
	section 2	2.01	section 3	1.8
	section 1	0.69	section 2	1.9
	organic phase inlet	0.16	section 1	2.0

column type:	concentration profile		hold-up profile	
PSE, sieve tray-d_h = 2 mm				
liquid/liquid-system:	aqueous phase	x [%]	measuring position	h_d [-]
bu-ac (d)/a/w	water inlet	5.26		
mass transfer direction:	section 3	3.41	section 3	0.062
c to d	section 2	2.59	section 2	0.074
pulsation intensity:	section 1	1.33	section 1	0.086
a · f = 1.0 cm/s	water outlet	0.90		
volume flow $\dot{V}_c$ [l/h]:			sauter diameter profile	
40.0	organic phase	y [%]		
volume flow $\dot{V}_d$ [l/h]:	organic phase outlet	4.52	measuring position	$d_{1,2}$ [mm]
48.0	section 3	3.05		
	section 2	2.27	section 3	1.8
	section 1	0.99	section 2	2.1
	organic phase inlet	0.45	section 1	1.9

column type:	concentration profile		hold-up profile	
PSE, sieve tray-d_h = 2 mm				
liquid/liquid-system:	aqueous phase	x [%]	measuring position	h_d [-]
bu-ac (d)/a/w	water inlet	5.25		
mass transfer direction:	section 3	3.36	section 3	0.108
c to d	section 2	2.43	section 2	0.095
pulsation intensity:	section 1	1.03	section 1	0.098
a · f = 1.0 cm/s	water outlet	0.53		
volume flow $\dot{V}_c$ [l/h]:			sauter diameter profile	
50.0	organic phase	y [%]		
volume flow $\dot{V}_d$ [l/h]:	organic phase outlet	4.60	measuring position	$d_{1,2}$ [mm]
60.0	section 3	3.13		
	section 2	2.11	section 3	1.9
	section 1	0.71	section 2	1.9
	organic phase inlet	0.09	section 1	2.0

*Table A.14: Drop swarm extractor: fluiddynamics and mass transfer of drop swarms in a pulsed sieve tray extractor **"PSE"** for different pulsation intensities; liquid/liquid-system: **butyl acetate (d)/acetone/water** (continued)*

column type:	concentration profile		hold-up profile	
PSE, sieve tray-d_h = 2 mm				
liquid/liquid-system:	aqueous phase	x [%]	measuring position	h_d [-]
bu-ac (d)/a/w	water inlet	5.27		
mass transfer direction:	section 3	3.60	section 3	0.097
c to d	section 2	2.45	section 2	0.098
pulsation intensity:	section 1	1.02	section 1	0.086
a · f = 1.0 cm/s	water outlet	0.49		
volume flow $\dot{V}_c$ [l/h]:			sauter diameter profile	
50.0	organic phase	y [%]		
volume flow $\dot{V}_d$ [l/h]:	organic phase outlet	4.69	measuring position	$d_{1,2}$ [mm]
60.0	section 3	3.09		
	section 2	2.07	section 3	2.0
	section 1	0.70	section 2	1.9
	organic phase inlet	0.00	section 1	1.8

column type:	concentration profile		hold-up profile	
PSE, sieve tray-d_h = 2 mm				
liquid/liquid-system:	aqueous phase	x [%]	measuring position	h_d [-]
bu-ac (d)/a/w	water inlet	5.23		
mass transfer direction:	section 3	3.59	section 3	0.117
c to d	section 2	2.33	section 2	0.092
pulsation intensity:	section 1	0.95	section 1	0.095
a · f = 1.0 cm/s	water outlet	0.48		
volume flow $\dot{V}_c$ [l/h]:			sauter diameter profile	
60.0	organic phase	y [%]		
volume flow $\dot{V}_d$ [l/h]:	organic phase outlet	4.58	measuring position	$d_{1,2}$ [mm]
72.0	section 3	3.25		
	section 2	1.98	section 3	1.8
	section 1	0.60	section 2	2.0
	organic phase inlet	0.00	section 1	2.1

column type:	concentration profile		hold-up profile	
PSE, sieve tray-d_h = 2 mm				
liquid/liquid-system:	aqueous phase	x [%]	measuring position	h_d [-]
bu-ac (d)/a/w	water inlet	5.46		
mass transfer direction:	section 3	3.54	section 3	0.154
c to d	section 2	2.28	section 2	0.154
pulsation intensity:	section 1	0.92	section 1	0.122
a · f = 1.0 cm/s	water outlet	0.46		
volume flow $\dot{V}_c$ [l/h]:			sauter diameter profile	
60.0	organic phase	y [%]		
volume flow $\dot{V}_d$ [l/h]:	organic phase outlet	4.60	measuring position	$d_{1,2}$ [mm]
72.0	section 3	3.20		
	section 2	1.90	section 3	1.7
	section 1	0.57	section 2	1.9
	organic phase inlet	0.00	section 1	2.1

*Table A.14: Drop swarm extractor: fluiddynamics and mass transfer of drop swarms in a pulsed sieve tray extractor **"PSE"** for different pulsation intensities; liquid/liquid-system: **butyl acetate (d)/acetone/water** (continued)*

column type:	concentration profile		hold-up profile	
PSE, sieve tray-d_h = 2 mm				
liquid/liquid-system:	aqueous phase	x [%]	measuring position	h_d [-]
bu-ac (d)/a/w	water inlet	5.40		
mass transfer direction:	section 3	3.55	section 3	0.332
c to d	section 2	2.33	section 2	0.363
pulsation intensity:	section 1	0.73	section 1	0.265
a · f = 1.0 cm/s	water outlet	0.44		
volume flow $\dot{V}_c$ [l/h]:			sauter diameter profile	
70.0	organic phase	y [%]		
volume flow $\dot{V}_d$ [l/h]:	organic phase outlet	4.52	measuring position	$d_{1,2}$ [mm]
84.0	section 3	3.12		
	section 2	2.02	section 3	2.0
	section 1	0.57	section 2	2.1
	organic phase inlet	0.00	section 1	2.2

column type:	concentration profile		hold-up profile	
PSE, sieve tray-d_h = 2 mm				
liquid/liquid-system:	aqueous phase	x [%]	measuring position	h_d [-]
bu-ac (d)/a/w	water inlet	5.36		
mass transfer direction:	section 3	3.64	section 3	0.283
c to d	section 2	2.21	section 2	0.246
pulsation intensity:	section 1	0.72	section 1	0.204
a · f = 1.0 cm/s	water outlet	0.42		
volume flow $\dot{V}_c$ [l/h]:			sauter diameter profile	
70.0	organic phase	y [%]		
volume flow $\dot{V}_d$ [l/h]:	organic phase outlet	4.53	measuring position	$d_{1,2}$ [mm]
84.0	section 3	3.03		
	section 2	1.94	section 3	2.1
	section 1	0.51	section 2	2.2
	organic phase inlet	0.00	section 1	2.1

column type:	concentration profile		hold-up profile	
PSE, sieve tray-d_h = 2 mm				
liquid/liquid-system:	aqueous phase	x [%]	measuring position	h_d [-]
bu-ac (d)/a/w	water inlet	5.35		
mass transfer direction:	section 3	3.60	section 3	0.205
c to d	section 2	2.16	section 2	0.179
pulsation intensity:	section 1	0.79	section 1	0.163
a · f = 2.0 cm/s	water outlet	0.41		
volume flow $\dot{V}_c$ [l/h]:			sauter diameter profile	
40.0	organic phase	y [%]		
volume flow $\dot{V}_d$ [l/h]:	organic phase outlet	4.59	measuring position	$d_{1,2}$ [mm]
48.0	section 3	3.13		
	section 2	1.88	section 3	1.3
	section 1	0.54	section 2	1.3
	organic phase inlet	0.00	section 1	1.4

*Table A.14: Drop swarm extractor: fluiddynamics and mass transfer of drop swarms in a pulsed sieve tray extractor **"PSE"** for different pulsation intensities; liquid/liquid-system: **butyl acetate (d)/acetone/water** (continued)*

column type:	concentration profile		hold-up profile	
PSE, sieve tray-d_h = 2 mm				
liquid/liquid-system:	aqueous phase	x [%]	measuring position	h_d [-]
bu-ac (d)/a/w	water inlet	5.45		
mass transfer direction:	section 3	4.08	section 3	0.165
c to d	section 2	2.45	section 2	0.179
pulsation intensity:	section 1	0.91	section 1	0.185
a · f = 2.0 cm/s	water outlet	0.42		
volume flow $\dot{V}_c$ [l/h]:			sauter diameter profile	
40.0	organic phase	y [%]		
volume flow $\dot{V}_d$ [l/h]:	organic phase outlet	4.54	measuring position	$d_{1,2}$ [mm]
48.0	section 3	3.44		
	section 2	2.15	section 3	1.4
	section 1	0.61	section 2	1.5
	organic phase inlet	0.00	section 1	1.4

column type:	concentration profile		hold-up profile	
PSE, sieve tray-d_h = 2 mm				
liquid/liquid-system:	aqueous phase	x [%]	measuring position	h_d [-]
bu-ac (d)/a/w	water inlet	5.02		
mass transfer direction:	section 3	3.51	section 3	0.249
c to d	section 2	2.65	section 2	0.263
pulsation intensity:	section 1	0.86	section 1	0.233
a · f = 2.0 cm/s	water outlet	0.35		
volume flow $\dot{V}_c$ [l/h]:			sauter diameter profile	
50.0	organic phase	y [%]		
volume flow $\dot{V}_d$ [l/h]:	organic phase outlet	4.51	measuring position	$d_{1,2}$ [mm]
60.0	section 3	3.10		
	section 2	2.11	section 3	1.6
	section 1	0.63	section 2	1.6
	organic phase inlet	0.00	section 1	1.7

column type:	concentration profile		hold-up profile	
PSE, sieve tray-d_h = 2 mm				
liquid/liquid-system:	aqueous phase	x [%]	measuring position	h_d [-]
bu-ac (d)/a/w	water inlet	5.15		
mass transfer direction:	section 3	3.85	section 3	0.298
c to d	section 2	2.67	section 2	0.382
pulsation intensity:	section 1	0.90	section 1	0.332
a · f = 2.0 cm/s	water outlet	0.33		
volume flow $\dot{V}_c$ [l/h]:			sauter diameter profile	
60.0	organic phase	y [%]		
volume flow $\dot{V}_d$ [l/h]:	organic phase outlet	4.57	measuring position	$d_{1,2}$ [mm]
72.0	section 3	3.11		
	section 2	2.04	section 3	1.9
	section 1	0.76	section 2	2.1
	organic phase inlet	0.00	section 1	2.0

*Table A.14: Drop swarm extractor: fluiddynamics and mass transfer of drop swarms in a pulsed sieve tray extractor **"PSE"** for different pulsation intensities; liquid/liquid-system: **butyl acetate (d)/acetone/water** (continued)*

column type:	concentration profile		hold-up profile	
PSE, sieve tray-d_h = 2 mm				
liquid/liquid-system:	aqueous phase	x [%]	measuring position	h_d [-]
bu-ac (d)/a/w	water inlet	5.41		
mass transfer direction:	section 3	3.68	section 3	0.283
c to d	section 2	2.45	section 2	0.329
pulsation intensity:	section 1	0.91	section 1	0.308
$a \cdot f$ = 2.0 cm/s	water outlet	0.34		
volume flow $\dot{V}_c$ [l/h]:			sauter diameter profile	
60.0	organic phase	y [%]		
volume flow $\dot{V}_d$ [l/h]:	organic phase outlet	4.54	measuring position	$d_{1,2}$ [mm]
72.0	section 3	3.09		
	section 2	2.15	section 3	1.9
	section 1	0.78	section 2	2.0
	organic phase inlet	0.00	section 1	1.9

*Table A.15: Drop swarm extractor: fluiddynamics and mass transfer of drop swarms in a pulsed extractor with structured packings **"PESP"** for different pulsation intensities; liquid/liquid-system: **toluene (d)/acetone/water***

column type:	concentration profile		hold-up profile	
PESP, Montz-Pak B1-350				
liquid/liquid-system:	aqueous phase	x [%]	measuring position	h_d [-]
t (d)/a/w	water inlet	5.73		
mass transfer direction:	section 3	4.32	section 3	0.067
c to d	section 2	3.46	section 2	0.071
pulsation intensity:	section 1	1.62	section 1	0.056
$a \cdot f$ = 1.0 cm/s	water outlet	1.25		
volume flow $\dot{V}_c$ [l/h]:			sauter diameter profile	
40.0	organic phase	y [%]		
volume flow $\dot{V}_d$ [l/h]:	organic phase outlet	3.81	measuring position	$d_{1,2}$ [mm]
48.0	section 3	3.22		
	section 2	2.41	section 3	2.9
	section 1	1.05	section 2	3.3
	organic phase inlet	0.00	section 1	2.4

column type:	concentration profile		hold-up profile	
PESP, Montz-Pak B1-350				
liquid/liquid-system:	aqueous phase	x [%]	measuring position	h_d [-]
t (d)/a/w	water inlet	5.71		
mass transfer direction:	section 3	4.64	section 3	0.072
c to d	section 2	3.64	section 2	0.078
pulsation intensity:	section 1	1.64	section 1	0.071
$a \cdot f$ = 1.0 cm/s	water outlet	1.31		
volume flow $\dot{V}_c$ [l/h]:			sauter diameter profile	
40.0	organic phase	y [%]		
volume flow $\dot{V}_d$ [l/h]:	organic phase outlet	4.15	measuring position	$d_{1,2}$ [mm]
48.0	section 3	3.46		
	section 2	2.62	section 3	2.9
	section 1	1.04	section 2	3.0
	organic phase inlet	0.00	section 1	2.8

column type:	concentration profile		hold-up profile	
PESP, Montz-Pak B1-350				
liquid/liquid-system:	aqueous phase	x [%]	measuring position	h_d [-]
t (d)/a/w	water inlet	5.69		
mass transfer direction:	section 3	4.89	section 3	0.149
c to d	section 2	4.04	section 2	0.152
pulsation intensity:	section 1	2.17	section 1	0.151
$a \cdot f$ = 1.0 cm/s	water outlet	1.15		
volume flow $\dot{V}_c$ [l/h]:			sauter diameter profile	
61.3	organic phase	y [%]		
volume flow $\dot{V}_d$ [l/h]:	organic phase outlet	4.02	measuring position	$d_{1,2}$ [mm]
74.5	section 3	3.50		
	section 2	2.84	section 3	2.8
	section 1	1.34	section 2	3.1
	organic phase inlet	0.00	section 1	2.9

*Table A.15: Drop swarm extractor: fluiddynamics and mass transfer of drop swarms in a pulsed extractor with structured packings **"PESP"** for different pulsation intensities; liquid/liquid-system: **toluene (d)/acetone/water** (continued)*

column type:	concentration profile		hold-up profile	
PESP, Montz-Pak B1-350				
liquid/liquid-system:	aqueous phase	x [%]	measuring position	h_d [-]
t (d)/a/w	water inlet	5.33		
mass transfer direction:	section 3	4.76	section 3	0.157
c to d	section 2	4.07	section 2	0.157
pulsation intensity:	section 1	1.58	section 1	0.154
a · f = 1.0 cm/s	water outlet	1.06		
volume flow $\dot{V}_c$ [l/h]:			sauter diameter profile	
61.3	organic phase	y [%]		
volume flow $\dot{V}_d$ [l/h]:	organic phase outlet	4.08	measuring position	$d_{1,2}$ [mm]
74.5	section 3	3.70		
	section 2	2.95	section 3	2.7
	section 1	1.35	section 2	2.8
	organic phase inlet	0.00	section 1	2.6

column type:	concentration profile		hold-up profile	
PESP, Montz-Pak B1-350				
liquid/liquid-system:	aqueous phase	x [%]	measuring position	h_d [-]
t (d)/a/w	water inlet	5.49		
mass transfer direction:	section 3	5.03	section 3	0.246
c to d	section 2	4.43	section 2	0.285
pulsation intensity:	section 1	2.58	section 1	0.263
a · f = 1.0 cm/s	water outlet	1.10		
volume flow $\dot{V}_c$ [l/h]:			sauter diameter profile	
82.56	organic phase	y [%]		
volume flow $\dot{V}_d$ [l/h]:	organic phase outlet	4.23	measuring position	$d_{1,2}$ [mm]
99.58	section 3	3.84		
	section 2	3.27	section 3	2.9
	section 1	1.72	section 2	3.3
	organic phase inlet	0.05	section 1	3.0

column type:	concentration profile		hold-up profile	
PESP, Montz-Pak B1-350				
liquid/liquid-system:	aqueous phase	x [%]	measuring position	h_d [-]
t (d)/a/w	water inlet	5.51		
mass transfer direction:	section 3	5.07	section 3	0.315
c to d	section 2	4.45	section 2	0.308
pulsation intensity:	section 1	2.64	section 1	0.289
a · f = 1.0 cm/s	water outlet	1.01		
volume flow $\dot{V}_c$ [l/h]:			sauter diameter profile	
82.6	organic phase	y [%]		
volume flow $\dot{V}_d$ [l/h]:	organic phase outlet	4.13	measuring position	$d_{1,2}$ [mm]
99.6	section 3	3.75		
	section 2	3.25	section 3	2.9
	section 1	1.67	section 2	3.3
	organic phase inlet	0.00	section 1	3.2

*Table A.15: Drop swarm extractor: fluiddynamics and mass transfer of drop swarms in a pulsed extractor with structured packings **"PESP"** for different pulsation intensities; liquid/liquid-system: **toluene (d)/acetone/water** (continued)*

column type:	concentration profile		hold-up profile	
PESP, Montz-Pak B1-350				
liquid/liquid-system:	aqueous phase	x [%]	measuring position	h_d [-]
t (d)/a/w	water inlet	5.48		
mass transfer direction:	section 3	5.12	section 3	0.345
c to d	section 2	4.74	section 2	0.361
pulsation intensity:	section 1	2.92	section 1	0.339
$a \cdot f$ = 1.0 cm/s	water outlet	1.01		
volume flow $\dot{V}_c$ [l/h]:			sauter diameter profile	
87.9	organic phase	y [%]		
volume flow $\dot{V}_d$ [l/h]:	organic phase outlet	4.14	measuring position	$d_{1,2}$ [mm]
106.0	section 3	3.83		
	section 2	3.38	section 3	3.2
	section 1	1.92	section 2	3.5
	organic phase inlet	0.00	section 1	3.6

column type:	concentration profile		hold-up profile	
PESP, Montz-Pak B1-350				
liquid/liquid-system:	aqueous phase	x [%]	measuring position	h_d [-]
t (d)/a/w	water inlet	5.84		
mass transfer direction:	section 3	4.87	section 3	0.078
c to d	section 2	4.04	section 2	0.081
pulsation intensity:	section 1	2.45	section 1	0.072
$a \cdot f$ = 2.0 cm/s	water outlet	1.76		
volume flow $\dot{V}_c$ [l/h]:			sauter diameter profile	
40.0	organic phase	y [%]		
volume flow $\dot{V}_d$ [l/h]:	organic phase outlet	4.09	measuring position	$d_{1,2}$ [mm]
48.0	section 3	3.59		
	section 2	2.88	section 3	1.9
	section 1	1.61	section 2	1.8
	organic phase inlet	0.61	section 1	2.1

column type:	concentration profile		hold-up profile	
PESP, Montz-Pak B1-350				
liquid/liquid-system:	aqueous phase	x [%]	measuring position	h_d [-]
t (d)/a/w	water inlet	5.79		
mass transfer direction:	section 3	4.80	section 3	0.074
c to d	section 2	3.99	section 2	0.062
pulsation intensity:	section 1	2.32	section 1	0.077
$a \cdot f$ = 2.0 cm/s	water outlet	1.56		
volume flow $\dot{V}_c$ [l/h]:			sauter diameter profile	
40.0	organic phase	y [%]		
volume flow $\dot{V}_d$ [l/h]:	organic phase outlet	4.06	measuring position	$d_{1,2}$ [mm]
48.0	section 3	3.37		
	section 2	2.73	section 3	1.8
	section 1	1.24	section 2	2.0
	organic phase inlet	0.34	section 1	2.6

*Table A.15: Drop swarm extractor: fluiddynamics and mass transfer of drop swarms in a pulsed extractor with structured packings **"PESP"** for different pulsation intensities; liquid/liquid-system: **toluene (d)/acetone/water** (continued)*

column type:	concentration profile		hold-up profile	
PESP, Montz-Pak B1-350				
liquid/liquid-system:	aqueous phase	x [%]	measuring position	h_d [-]
t (d)/a/w	water inlet	5.89		
mass transfer direction:	section 3	5.00	section 3	0.135
c to d	section 2	4.16	section 2	0.147
pulsation intensity:	section 1	2.39	section 1	0.132
$a \cdot f$ = 2.0 cm/s	water outlet	1.61		
volume flow $\dot{V}_c$ [l/h]:			sauter diameter profile	
61.3	organic phase	y [%]		
volume flow $\dot{V}_d$ [l/h]:	organic phase outlet	4.16	measuring position	$d_{1,2}$ [mm]
74.5	section 3	3.52		
	section 2	2.83	section 3	1.7
	section 1	1.52	section 2	1.8
	organic phase inlet	0.60	section 1	2.0

column type:	concentration profile		hold-up profile	
PESP, Montz-Pak B1-350				
liquid/liquid-system:	aqueous phase	x [%]	measuring position	h_d [-]
t (d)/a/w	water inlet	5.36		
mass transfer direction:	section 3	4.55	section 3	0.149
c to d	section 2	3.82	section 2	0.153
pulsation intensity:	section 1	2.13	section 1	0.140
$a \cdot f$ = 2.0 cm/s	water outlet	1.26		
volume flow $\dot{V}_c$ [l/h]:			sauter diameter profile	
61.3	organic phase	y [%]		
volume flow $\dot{V}_d$ [l/h]:	organic phase outlet	3.81	measuring position	$d_{1,2}$ [mm]
74.5	section 3	3.20		
	section 2	2.56	section 3	1.7
	section 1	1.34	section 2	1.8
	organic phase inlet	0.34	section 1	1.9

column type:	concentration profile		hold-up profile	
PESP, Montz-Pak B1-350				
liquid/liquid-system:	aqueous phase	x [%]	measuring position	h_d [-]
t (d)/a/w	water inlet	5.57		
mass transfer direction:	section 3	5.07	section 3	0.262
c to d	section 2	4.36	section 2	0.270
pulsation intensity:	section 1	2.62	section 1	0.262
$a \cdot f$ = 2.0 cm/s	water outlet	1.04		
volume flow $\dot{V}_c$ [l/h]:			sauter diameter profile	
82.6	organic phase	y [%]		
volume flow $\dot{V}_d$ [l/h]:	organic phase outlet	4.27	measuring position	$d_{1,2}$ [mm]
99.6	section 3	3.80		
	section 2	3.21	section 3	2.2
	section 1	1.37	section 2	2.6
	organic phase inlet	0.14	section 1	2.2

*Table A.15: Drop swarm extractor: fluiddynamics and mass transfer of drop swarms in a pulsed extractor with structured packings **"PESP"** for different pulsation intensities; liquid/liquid-system: **toluene (d)/acetone/water** (continued)*

column type:	concentration profile		hold-up profile	
PESP, Montz-Pak B1-350				
liquid/liquid-system:	aqueous phase	x [%]	measuring position	h_d [-]
t (d)/a/w	water inlet	5.65		
mass transfer direction:	section 3	5.00	section 3	0.326
c to d	section 2	4.27	section 2	0.275
pulsation intensity:	section 1	2.52	section 1	0.256
a · f = 2.0 cm/s	water outlet	1.10		
volume flow $\dot{V}_c$ [l/h]:			sauter diameter profile	
82.6	organic phase	y [%]		
volume flow $\dot{V}_d$ [l/h]:	organic phase outlet	4.15	measuring position	$d_{1,2}$ [mm]
99.6	section 3	3.77		
	section 2	3.19	section 3	2.1
	section 1	1.65	section 2	2.6
	organic phase inlet	0.15	section 1	2.3

column type:	concentration profile		hold-up profile	
PESP, Montz-Pak B1-350				
liquid/liquid-system:	aqueous phase	x [%]	measuring position	h_d [-]
t (d)/a/w	water inlet	5.59		
mass transfer direction:	section 3	4.88	section 3	0.324
c to d	section 2	4.20	section 2	0.296
pulsation intensity:	section 1	2.59	section 1	0.300
a · f = 2.0 cm/s	water outlet	1.29		
volume flow $\dot{V}_c$ [l/h]:			sauter diameter profile	
87.9	organic phase	y [%]		
volume flow $\dot{V}_d$ [l/h]:	organic phase outlet	3.99	measuring position	$d_{1,2}$ [mm]
106.0	section 3	3.44		
	section 2	2.09	section 3	2.0
	section 1	1.22	section 2	2.3
	organic phase inlet	0.34	section 1	2.9

column type:	concentration profile		hold-up profile	
PESP, Montz-Pak B1-350				
liquid/liquid-system:	aqueous phase	x [%]	measuring position	h_d [-]
t (d)/a/w	water inlet	5.59		
mass transfer direction:	section 3	5.05	section 3	0.262
c to d	section 2	4.33	section 2	0.289
pulsation intensity:	section 1	2.75	section 1	0.305
a · f = 2.0 cm/s	water outlet	1.27		
volume flow $\dot{V}_c$ [l/h]:			sauter diameter profile	
87.9	organic phase	y [%]		
volume flow $\dot{V}_d$ [l/h]:	organic phase outlet	4.11	measuring position	$d_{1,2}$ [mm]
106.0	section 3	3.53		
	section 2	2.93	section 3	2.1
	section 1	1.71	section 2	2.4
	organic phase inlet	0.33	section 1	2.9

*Table A.15: Drop swarm extractor: fluiddynamics and mass transfer of drop swarms in a pulsed extractor with structured packings **"PESP"** for different pulsation intensities; liquid/liquid-system: **toluene (d)/acetone/water** (continued)*

column type:	concentration profile		hold-up profile	
PESP, Montz-Pak B1-350				
liquid/liquid-system:	aqueous phase	x [%]	measuring position	h_d [-]
t (d)/a/w	water inlet	5.43		
mass transfer direction:	section 3	5.04	section 3	0.432
c to d	section 2	4.70	section 2	0.375
pulsation intensity:	section 1	3.30	section 1	0.391
a · f = 2.0 cm/s	water outlet	0.99		
volume flow $\dot{V}_c$ [l/h]:			sauter diameter profile	
93.2	organic phase	y [%]		
volume flow $\dot{V}_d$ [l/h]:	organic phase outlet	4.04	measuring position	$d_{1,2}$ [mm]
111.8	section 3	3.89		
	section 2	3.53	section 3	2.5
	section 1	2.18	section 2	3.7
	organic phase inlet	0.03	section 1	3.6

column type:	concentration profile		hold-up profile	
PESP, Montz-Pak B1-350				
liquid/liquid-system:	aqueous phase	x [%]	measuring position	h_d [-]
t (d)/a/w	water inlet	5.47		
mass transfer direction:	section 3	4.92	section 3	0.326
c to d	section 2	4.28	section 2	0.292
pulsation intensity:	section 1	2.96	section 1	0.323
a · f = 2.0 cm/s	water outlet	1.70		
volume flow $\dot{V}_c$ [l/h]:			sauter diameter profile	
93.2	organic phase	y [%]		
volume flow $\dot{V}_d$ [l/h]:	organic phase outlet	3.98	measuring position	$d_{1,2}$ [mm]
112.5	section 3	3.48		
	section 2	2.98	section 3	2.3
	section 1	1.90	section 2	2.5
	organic phase inlet	0.79	section 1	2.7

*Table A.16: Drop swarm extractor: fluiddynamics and mass transfer of drop swarms in a pulsed extractor with structured packings **"PESP"** for different pulsation intensities; liquid/liquid-system: **butyl acetate (d)/acetone/water***

column type:	concentration profile		hold-up profile	
PESP, Montz-Pak B1-350				
liquid/liquid-system:	aqueous phase	x [%]	measuring position	h_d [-]
bu-ac (d)/a/w	water inlet	5.22		
mass transfer direction:	section 3	3.51	section 3	0.074
c to d	section 2	2.68	section 2	0.068
pulsation intensity:	section 1	0.98	section 1	0.062
a · f = 1.0 cm/s	water outlet	0.54		
volume flow $\dot{V}_c$ [l/h]:			sauter diameter profile	
40.0	organic phase	y [%]		
volume flow $\dot{V}_d$ [l/h]:	organic phase outlet	4.48	measuring position	$d_{1,2}$ [mm]
48.0	section 3	2.83		
	section 2	1.93	section 3	2.0
	section 1	0.61	section 2	2.1
	organic phase inlet	0.00	section 1	2.3

column type:	concentration profile		hold-up profile	
PESP, Montz-Pak B1-350				
liquid/liquid-system:	aqueous phase	x [%]	measuring position	h_d [-]
bu-ac (d)/a/w	water inlet	5.27		
mass transfer direction:	section 3	3.37	section 3	0.068
c to d	section 2	2.30	section 2	0.062
pulsation intensity:	section 1	1.05	section 1	0.067
a · f = 1.0 cm/s	water outlet	0.56		
volume flow $\dot{V}_c$ [l/h]:			sauter diameter profile	
40.0	organic phase	y [%]		
volume flow $\dot{V}_d$ [l/h]:	organic phase outlet	4.52	measuring position	$d_{1,2}$ [mm]
48.0	section 3	2.90		
	section 2	1.93	section 3	2.1
	section 1	0.69	section 2	2.1
	organic phase inlet	0.00	section 1	2.2

column type:	concentration profile		hold-up profile	
PESP, Montz-Pak B1-350				
liquid/liquid-system:	aqueous phase	x [%]	measuring position	h_d [-]
bu-ac (d)/a/w	water inlet	5.35		
mass transfer direction:	section 3	3.82	section 3	0.100
c to d	section 2	2.99	section 2	0.112
pulsation intensity:	section 1	1.13	section 1	0.096
a · f = 1.0 cm/s	water outlet	0.55		
volume flow $\dot{V}_c$ [l/h]:			sauter diameter profile	
50.0	organic phase	y [%]		
volume flow $\dot{V}_d$ [l/h]:	organic phase outlet	4.37	measuring position	$d_{1,2}$ [mm]
60.0	section 3	2.93		
	section 2	2.00	section 3	1.8
	section 1	0.65	section 2	2.2
	organic phase inlet	0.00	section 1	2.1

*Table A.16: Drop swarm extractor: fluiddynamics and mass transfer of drop swarms in a pulsed extractor with structured packings **"PESP"** for different pulsation intensities; liquid/liquid-system: **butyl acetate (d)/acetone/water** (continued)*

column type:	concentration profile		hold-up profile	
PESP, Montz-Pak B1-350				
liquid/liquid-system:	aqueous phase	x [%]	measuring position	h_d [-]
bu-ac (d)/a/w	water inlet	5.52		
mass transfer direction:	section 3	3.81	section 3	0.105
c to d	section 2	2.72	section 2	0.092
pulsation intensity:	section 1	1.06	section 1	0.080
a · f = 1.0 cm/s	water outlet	0.56		
volume flow $\dot{V}_c$ [l/h]:			sauter diameter profile	
50.0	organic phase	y [%]		
volume flow $\dot{V}_d$ [l/h]:	organic phase outlet	4.51	measuring position	$d_{1,2}$ [mm]
60.0	section 3	2.95		
	section 2	2.05	section 3	2.1
	section 1	0.68	section 2	2.0
	organic phase inlet	0.00	section 1	2.3

column type:	concentration profile		hold-up profile	
PESP, Montz-Pak B1-350				
liquid/liquid-system:	aqueous phase	x [%]	measuring position	h_d [-]
bu-ac (d)/a/w	water inlet	5.10		
mass transfer direction:	section 3	3.62	section 3	0.125
c to d	section 2	2.73	section 2	0.128
pulsation intensity:	section 1	1.10	section 1	0.131
a · f = 1.0 cm/s	water outlet	0.52		
volume flow $\dot{V}_c$ [l/h]:			sauter diameter profile	
60.0	organic phase	y [%]		
volume flow $\dot{V}_d$ [l/h]:	organic phase outlet	4.07	measuring position	$d_{1,2}$ [mm]
72.0	section 3	2.71		
	section 2	1.88	section 3	2.2
	section 1	0.61	section 2	2.1
	organic phase inlet	0.00	section 1	2.2

column type:	concentration profile		hold-up profile	
PESP, Montz-Pak B1-350				
liquid/liquid-system:	aqueous phase	x [%]	measuring position	h_d [-]
bu-ac (d)/a/w	water inlet	5.40		
mass transfer direction:	section 3	3.86	section 3	0.138
c to d	section 2	2.98	section 2	0.126
pulsation intensity:	section 1	1.03	section 1	0.135
a · f = 1.0 cm/s	water outlet	0.50		
volume flow $\dot{V}_c$ [l/h]:			sauter diameter profile	
60.0	organic phase	y [%]		
volume flow $\dot{V}_d$ [l/h]:	organic phase outlet	4.54	measuring position	$d_{1,2}$ [mm]
72.0	section 3	2.96		
	section 2	2.03	section 3	2.1
	section 1	0.66	section 2	2.3
	organic phase inlet	0.00	section 1	2.3

*Table A.16: Drop swarm extractor: fluiddynamics and mass transfer of drop swarms in a pulsed extractor with structured packings **"PESP"** for different pulsation intensities; liquid/liquid-system: **butyl acetate (d)/acetone/water** (continued)*

column type:	concentration profile		hold-up profile	
PESP, Montz-Pak B1-350				
liquid/liquid-system:	aqueous phase	x [%]	measuring position	h_d [-]
bu-ac (d)/a/w	water inlet	5.31		
mass transfer direction:	section 3	3.32	section 3	0.157
c to d	section 2	2.28	section 2	0.148
pulsation intensity:	section 1	1.00	section 1	0.145
a · f = 1.0 cm/s	water outlet	0.49		
volume flow $\dot{V}_c$ [l/h]:			sauter diameter profile	
70.0	organic phase	y [%]		
volume flow $\dot{V}_d$ [l/h]:	organic phase outlet	4.57	measuring position	$d_{1,2}$ [mm]
84.0	section 3	2.91		
	section 2	1.98	section 3	2.4
	section 1	0.67	section 2	2.5
	organic phase inlet	0.00	section 1	2.2

column type:	concentration profile		hold-up profile	
PESP, Montz-Pak B1-350				
liquid/liquid-system:	aqueous phase	x [%]	measuring position	h_d [-]
bu-ac (d)/a/w	water inlet	5.23		
mass transfer direction:	section 3	3.77	section 3	0.192
c to d	section 2	2.63	section 2	0.206
pulsation intensity:	section 1	1.14	section 1	0.196
a · f = 1.0 cm/s	water outlet	0.58		
volume flow $\dot{V}_c$ [l/h]:			sauter diameter profile	
80.0	organic phase	y [%]		
volume flow $\dot{V}_d$ [l/h]:	organic phase outlet	4.23	measuring position	$d_{1,2}$ [mm]
96.0	section 3	2.95		
	section 2	1.99	section 3	2.2
	section 1	0.67	section 2	2.1
	organic phase inlet	0.09	section 1	2.2

column type:	concentration profile		hold-up profile	
PESP, Montz-Pak B1-350				
liquid/liquid-system:	aqueous phase	x [%]	measuring position	h_d [-]
bu-ac (d)/a/w	water inlet	5.36		
mass transfer direction:	section 3	3.74	section 3	0.201
c to d	section 2	2.79	section 2	0.193
pulsation intensity:	section 1	1.17	section 1	0.199
a · f = 1.0 cm/s	water outlet	0.61		
volume flow $\dot{V}_c$ [l/h]:			sauter diameter profile	
80.0	organic phase	y [%]		
volume flow $\dot{V}_d$ [l/h]:	organic phase outlet	4.22	measuring position	$d_{1,2}$ [mm]
96.0	section 3	2.88		
	section 2	1.97	section 3	2.1
	section 1	0.66	section 2	2.2
	organic phase inlet	0.10	section 1	2.2

*Table A.16: Drop swarm extractor: fluiddynamics and mass transfer of drop swarms in a pulsed extractor with structured packings **"PESP"** for different pulsation intensities; liquid/liquid-system: **butyl acetate (d)/acetone/water** (continued)*

column type:	concentration profile		hold-up profile	
PESP, Montz-Pak B1-350				
liquid/liquid-system:	aqueous phase	x [%]	measuring position	h_d [-]
bu-ac (d)/a/w	water inlet	5.20		
mass transfer direction:	section 3	3.97	section 3	0.219
c to d	section 2	2.87	section 2	0.235
pulsation intensity:	section 1	1.02	section 1	0.228
a · f = 1.0 cm/s	water outlet	0.52		
volume flow $\dot{V}_c$ [l/h]:			sauter diameter profile	
90.0	organic phase	y [%]		
volume flow $\dot{V}_d$ [l/h]:	organic phase outlet	4.30	measuring position	$d_{1,2}$ [mm]
108.0	section 3	3.09		
	section 2	1.82	section 3	2.3
	section 1	0.66	section 2	2.0
	organic phase inlet	0.08	section 1	2.3

column type:	concentration profile		hold-up profile	
PESP, Montz-Pak B1-350				
liquid/liquid-system:	aqueous phase	x [%]	measuring position	h_d [-]
bu-ac (d)/a/w	water inlet	5.60		
mass transfer direction:	section 3	4.13	section 3	0.257
c to d	section 2	3.19	section 2	0.265
pulsation intensity:	section 1	1.03	section 1	0.238
a · f = 1.0 cm/s	water outlet	0.53		
volume flow $\dot{V}_c$ [l/h]:			sauter diameter profile	
90.0	organic phase	y [%]		
volume flow $\dot{V}_d$ [l/h]:	organic phase outlet	4.53	measuring position	$d_{1,2}$ [mm]
108.0	section 3	3.23		
	section 2	2.33	section 3	2.3
	section 1	0.79	section 2	2.0
	organic phase inlet	0.00	section 1	2.3

column type:	concentration profile		hold-up profile	
PESP, Montz-Pak B1-350				
liquid/liquid-system:	aqueous phase	x [%]	measuring position	h_d [-]
bu-ac (d)/a/w	water inlet	5.61		
mass transfer direction:	section 3	3.66	section 3	0.090
c to d	section 2	2.33	section 2	0.102
pulsation intensity:	section 1	0.78	section 1	0.096
a · f = 2.0 cm/s	water outlet	0.38		
volume flow $\dot{V}_c$ [l/h]:			sauter diameter profile	
40.0	organic phase	y [%]		
volume flow $\dot{V}_d$ [l/h]:	organic phase outlet	4.64	measuring position	$d_{1,2}$ [mm]
48.0	section 3	3.03		
	section 2	1.89	section 3	1.7
	section 1	0.52	section 2	1.6
	organic phase inlet	0.00	section 1	1.7

*Table A.16: Drop swarm extractor: fluiddynamics and mass transfer of drop swarms in a pulsed extractor with structured packings **"PESP"** for different pulsation intensities; liquid/liquid-system: **butyl acetate (d)/acetone/water** (continued)*

column type:	concentration profile		hold-up profile	
PESP, Montz-Pak B1-350				
liquid/liquid-system:	aqueous phase	x [%]	measuring position	h_d [-]
bu-ac (d)/a/w	water inlet	5.37		
mass transfer direction:	section 3	3.46	section 3	0.108
c to d	section 2	2.15	section 2	0.116
pulsation intensity:	section 1	0.74	section 1	0.088
a · f = 2.0 cm/s	water outlet	0.34		
volume flow $\dot{V}_c$ [l/h]:			sauter diameter profile	
40.0	organic phase	y [%]		
volume flow $\dot{V}_d$ [l/h]:	organic phase outlet	4.49	measuring position	$d_{1,2}$ [mm]
48.0	section 3	2.88		
	section 2	1.75	section 3	1.6
	section 1	0.49	section 2	1.6
	organic phase inlet	0.00	section 1	1.8

column type:	concentration profile		hold-up profile	
PESP, Montz-Pak B1-350				
liquid/liquid-system:	aqueous phase	x [%]	measuring position	h_d [-]
bu-ac (d)/a/w	water inlet	5.46		
mass transfer direction:	section 3	3.41	section 3	0.154
c to d	section 2	2.09	section 2	0.139
pulsation intensity:	section 1	0.72	section 1	0.120
a · f = 2.0 cm/s	water outlet	0.36		
volume flow $\dot{V}_c$ [l/h]:			sauter diameter profile	
50.0	organic phase	y [%]		
volume flow $\dot{V}_d$ [l/h]:	organic phase outlet	4.56	measuring position	$d_{1,2}$ [mm]
60.0	section 3	2.84		
	section 2	1.71	section 3	1.6
	section 1	0.46	section 2	1.8
	organic phase inlet	0.00	section 1	1.8

column type:	concentration profile		hold-up profile	
PESP, Montz-Pak B1-350				
liquid/liquid-system:	aqueous phase	x [%]	measuring position	h_d [-]
bu-ac (d)/a/w	water inlet	5.35		
mass transfer direction:	section 3	3.45	section 3	0.154
c to d	section 2	2.11	section 2	0.133
pulsation intensity:	section 1	0.75	section 1	0.139
a · f = 2.0 cm/s	water outlet	0.36		
volume flow $\dot{V}_c$ [l/h]:			sauter diameter profile	
50.0	organic phase	y [%]		
volume flow $\dot{V}_d$ [l/h]:	organic phase outlet	4.45	measuring position	$d_{1,2}$ [mm]
60.0	section 3	2.87		
	section 2	1.70	section 3	1.8
	section 1	0.47	section 2	2.0
	organic phase inlet	0.00	section 1	1.9

*Table A.16: Drop swarm extractor: fluiddynamics and mass transfer of drop swarms in a pulsed extractor with structured packings **"PESP"** for different pulsation intensities; liquid/liquid-system: **butyl acetate (d)/acetone/water** (continued)*

column type:	concentration profile		hold-up profile	
PESP, Montz-Pak B1-350				
liquid/liquid-system:	aqueous phase	x [%]	measuring position	h_d [-]
bu-ac (d)/a/w	water inlet	5.21		
mass transfer direction:	section 3	3.50	section 3	0.197
c to d	section 2	2.24	section 2	0.203
pulsation intensity:	section 1	0.82	section 1	0.182
$a \cdot f$ = 2.0 cm/s	water outlet	0.31		
volume flow $\dot{V}_c$ [l/h]:			sauter diameter profile	
60.0	organic phase	y [%]		
volume flow $\dot{V}_d$ [l/h]:	organic phase outlet	4.38	measuring position	$d_{1,2}$ [mm]
72.0	section 3	2.81		
	section 2	1.78	section 3	1.7
	section 1	0.49	section 2	1.8
	organic phase inlet	0.00	section 1	2.0

column type:	concentration profile		hold-up profile	
PESP, Montz-Pak B1-350				
liquid/liquid-system:	aqueous phase	x [%]	measuring position	h_d [-]
bu-ac (d)/a/w	water inlet	5.20		
mass transfer direction:	section 3	3.54	section 3	0.228
c to d	section 2	2.19	section 2	0.217
pulsation intensity:	section 1	0.83	section 1	0.202
$a \cdot f$ = 2.0 cm/s	water outlet	0.34		
volume flow $\dot{V}_c$ [l/h]:			sauter diameter profile	
60.0	organic phase	y [%]		
volume flow $\dot{V}_d$ [l/h]:	organic phase outlet	4.31	measuring position	$d_{1,2}$ [mm]
72.0	section 3	2.81		
	section 2	1.76	section 3	1.6
	section 1	0.51	section 2	1.7
	organic phase inlet	0.00	section 1	1.9

column type:	concentration profile		hold-up profile	
PESP, Montz-Pak B1-350				
liquid/liquid-system:	aqueous phase	x [%]	measuring position	h_d [-]
bu-ac (d)/a/w	water inlet	5.77		
mass transfer direction:	section 3	3.81	section 3	0.314
c to d	section 2	2.87	section 2	0.340
pulsation intensity:	section 1	0.98	section 1	0.294
$a \cdot f$ = 2.0 cm/s	water outlet	0.34		
volume flow $\dot{V}_c$ [l/h]:			sauter diameter profile	
70.0	organic phase	y [%]		
volume flow $\dot{V}_d$ [l/h]:	organic phase outlet	4.77	measuring position	$d_{1,2}$ [mm]
84.0	section 3	3.12		
	section 2	2.30	section 3	1.9
	section 1	0.68	section 2	2.2
	organic phase inlet	0.00	section 1	1.9

*Table A.16: Drop swarm extractor: fluiddynamics and mass transfer of drop swarms in a pulsed extractor with structured packings **"PESP"** for different pulsation intensities; liquid/liquid-system: **butyl acetate (d)/acetone/water** (continued)*

column type:	concentration profile		hold-up profile	
PESP, Montz-Pak B1-350				
liquid/liquid-system:	aqueous phase	x [%]	measuring position	h_d [-]
bu-ac (d)/a/w	water inlet	5.71		
mass transfer direction:	section 3	3.84	section 3	0.312
c to d	section 2	2.62	section 2	0.355
pulsation intensity:	section 1	0.70	section 1	0.322
$a \cdot f$ = 2.0 cm/s	water outlet	0.33		
volume flow $\dot{V}_c$ [l/h]:			sauter diameter profile	
70.0	organic phase	y [%]		
volume flow $\dot{V}_d$ [l/h]:	organic phase outlet	4.75	measuring position	$d_{1,2}$ [mm]
84.0	section 3	3.17		
	section 2	2.15	section 3	1.9
	section 1	0.53	section 2	2.0
	organic phase inlet	0.00	section 1	1.8

*Table A.17: Drop swarm extractor: fluiddynamics and mass transfer of drop swarms in an agitated extractor with rotating discs **"RDC-extractor"**; liquid/liquid-system: **toluene (d)/acetone/water***

column type:	concentration profile		hold-up profile	
RDC-extractor				
liquid/liquid-system:	aqueous phase	x [%]	measuring position	h_d [-]
t (d)/a/w	water inlet	5.68		
mass transfer direction:	section 3	5.38	section 3	0.065
c to d	section 2	4.86	section 2	0.068
rotational speed:	section 1	2.99	section 1	0.080
n_R = 200 1/min	water outlet	1.92		
volume flow $\dot{V}_c$ [l/h]:			sauter diameter profile	
40.0	organic phase	y [%]		
volume flow $\dot{V}_d$ [l/h]:	organic phase outlet	3.95	measuring position	$d_{1,2}$ [mm]
48.0	section 3	3.62		
	section 2	3.06	section 3	2.6
	section 1	1.52	section 2	3.1
	organic phase inlet	0.10	section 1	3.0

column type:	concentration profile		hold-up profile	
RDC-extractor				
liquid/liquid-system:	aqueous phase	x [%]	measuring position	h_d [-]
t (d)/a/w	water inlet	5.77		
mass transfer direction:	section 3	5.29	section 3	0.068
c to d	section 2	4.52	section 2	0.074
rotational speed:	section 1	2.63	section 1	0.080
n_R = 200 1/min	water outlet	1.68		
volume flow $\dot{V}_c$ [l/h]:			sauter diameter profile	
40.0	organic phase	y [%]		
volume flow $\dot{V}_d$ [l/h]:	organic phase outlet	3.73	measuring position	$d_{1,2}$ [mm]
48.0	section 3	3.40		
	section 2	2.49	section 3	2.6
	section 1	1.35	section 2	3.1
	organic phase inlet	0.10	section 1	3.0

column type:	concentration profile		hold-up profile	
RDC-extractor				
liquid/liquid-system:	aqueous phase	x [%]	measuring position	h_d [-]
t (d)/a/w	water inlet	6.20		
mass transfer direction:	section 3	5.67	section 3	0.093
c to d	section 2	4.91	section 2	0.093
rotational speed:	section 1	2.92	section 1	0.123
n_R = 200 1/min	water outlet	1.71		
volume flow $\dot{V}_c$ [l/h]:			sauter diameter profile	
50.6	organic phase	y [%]		
volume flow $\dot{V}_d$ [l/h]:	organic phase outlet	4.07	measuring position	$d_{1,2}$ [mm]
61.3	section 3	3.71		
	section 2	3.08	section 3	2.6
	section 1	1.53	section 2	3.0
	organic phase inlet	0.02	section 1	2.9

*Table A.17: Drop swarm extractor: fluiddynamics and mass transfer of drop swarms in an agitated extractor with rotating discs **"RDC-extractor"**; liquid/liquid-system: **toluene (d)/acetone/water** (continued)*

column type:	concentration profile		hold-up profile	
RDC-extractor				
liquid/liquid-system:	aqueous phase	x [%]	measuring position	h_d [-]
t (d)/a/w	water inlet	6.18		
mass transfer direction:	section 3	5.75	section 3	0.100
c to d	section 2	5.01	section 2	0.109
rotational speed:	section 1	2.95	section 1	0.116
n_R = 200 1/min	water outlet	1.56		
volume flow $\dot{V}_c$ [l/h]:			sauter diameter profile	
50.6	organic phase	y [%]		
volume flow $\dot{V}_d$ [l/h]:	organic phase outlet	4.05	measuring position	$d_{1,2}$ [mm]
61.3	section 3	3.64		
	section 2	3.01	section 3	3.1
	section 1	1.44	section 2	2.9
	organic phase inlet	0.00	section 1	2.9

column type:	concentration profile		hold-up profile	
RDC-extractor				
liquid/liquid-system:	aqueous phase	x [%]	measuring position	h_d [-]
t (d)/a/w	water inlet	6.10		
mass transfer direction:	section 3	5.71	section 3	0.149
c to d	section 2	5.06	section 2	0.135
rotational speed:	section 1	3.41	section 1	0.159
n_R = 200 1/min	water outlet	1.49		
volume flow $\dot{V}_c$ [l/h]:			sauter diameter profile	
61.3	organic phase	y [%]		
volume flow $\dot{V}_d$ [l/h]:	organic phase outlet	4.16	measuring position	$d_{1,2}$ [mm]
74.0	section 3	3.74		
	section 2	3.26	section 3	2.8
	section 1	1.41	section 2	2.9
	organic phase inlet	0.09	section 1	2.7

column type:	concentration profile		hold-up profile	
RDC-extractor				
liquid/liquid-system:	aqueous phase	x [%]	measuring position	h_d [-]
t (d)/a/w	water inlet	6.35		
mass transfer direction:	section 3	6.00	section 3	0.138
c to d	section 2	5.32	section 2	0.123
rotational speed:	section 1	3.58	section 1	0.149
n_R = 200 1/min	water outlet	1.47		
volume flow $\dot{V}_c$ [l/h]:			sauter diameter profile	
61.3	organic phase	y [%]		
volume flow $\dot{V}_d$ [l/h]:	organic phase outlet	4.24	measuring position	$d_{1,2}$ [mm]
74.0	section 3	3.81		
	section 2	3.25	section 3	3.0
	section 1	1.87	section 2	3.1
	organic phase inlet	0.00	section 1	2.9

*Table A.17: Drop swarm extractor: fluiddynamics and mass transfer of drop swarms in an agitated extractor with rotating discs **"RDC-extractor"**; liquid/liquid-system: **toluene (d)/acetone/water** (continued)*

column type:	concentration profile		hold-up profile	
RDC-extractor				
liquid/liquid-system:	aqueous phase	x [%]	measuring position	h_d [-]
t (d)/a/w	water inlet	5.55		
mass transfer direction:	section 3	5.08	section 3	0.196
c to d	section 2	4.57	section 2	0.182
rotational speed:	section 1	3.20	section 1	0.204
n_R = 200 1/min	water outlet	1.33		
volume flow $\dot{V}_c$ [l/h]:			sauter diameter profile	
71.9	organic phase	y [%]		
volume flow $\dot{V}_d$ [l/h]:	organic phase outlet	3.72	measuring position	$d_{1,2}$ [mm]
86.8	section 3	3.28		
	section 2	2.80	section 3	3.0
	section 1	1.71	section 2	3.2
	organic phase inlet	0.00	section 1	3.0

column type:	concentration profile		hold-up profile	
RDC-extractor				
liquid/liquid-system:	aqueous phase	x [%]	measuring position	h_d [-]
t (d)/a/w	water inlet	5.68		
mass transfer direction:	section 3	5.17	section 3	0.183
c to d	section 2	4.55	section 2	0.180
rotational speed:	section 1	3.02	section 1	0.192
n_R = 200 1/min	water outlet	1.36		
volume flow $\dot{V}_c$ [l/h]:			sauter diameter profile	
71.9	organic phase	y [%]		
volume flow $\dot{V}_d$ [l/h]:	organic phase outlet	3.70	measuring position	$d_{1,2}$ [mm]
86.8	section 3	3.35		
	section 2	2.86	section 3	3.0
	section 1	1.71	section 2	3.1
	organic phase inlet	0.01	section 1	2.9

column type:	concentration profile		hold-up profile	
RDC-extractor				
liquid/liquid-system:	aqueous phase	x [%]	measuring position	h_d [-]
t (d)/a/w	water inlet	6.00		
mass transfer direction:	section 3	5.49	section 3	0.245
c to d	section 2	4.87	section 2	0.225
rotational speed:	section 1	3.46	section 1	0.231
n_R = 200 1/min	water outlet	1.65		
volume flow $\dot{V}_c$ [l/h]:			sauter diameter profile	
82.6	organic phase	y [%]		
volume flow $\dot{V}_d$ [l/h]:	organic phase outlet	4.03	measuring position	$d_{1,2}$ [mm]
99.6	section 3	3.62		
	section 2	3.01	section 3	3.1
	section 1	1.87	section 2	3.5
	organic phase inlet	0.16	section 1	3.1

*Table A.17: Drop swarm extractor: fluiddynamics and mass transfer of drop swarms in an agitated extractor with rotating discs **"RDC-extractor"**; liquid/liquid-system: **toluene (d)/acetone/water** (continued)*

column type:	concentration profile		hold-up profile	
RDC-extractor				
liquid/liquid-system:	aqueous phase	x [%]	measuring position	h_d [-]
t (d)/a/w	water inlet	5.66		
mass transfer direction:	section 3	4.89	section 3	0.068
c to d	section 2	4.13	section 2	0.074
rotational speed:	section 1	2.08	section 1	0.080
n_R = 400 1/min	water outlet	1.33		
volume flow $\dot{V}_c$ [l/h]:			sauter diameter profile	
40.0	organic phase	y [%]		
volume flow $\dot{V}_d$ [l/h]:	organic phase outlet	3.80	measuring position	$d_{1,2}$ [mm]
48.0	section 3	3.24		
	section 2	2.58	section 3	2.6
	section 1	1.20	section 2	2.5
	organic phase inlet	0.00	section 1	3.0

column type:	concentration profile		hold-up profile	
RDC-extractor				
liquid/liquid-system:	aqueous phase	x [%]	measuring position	h_d [-]
t (d)/a/w	water inlet	5.56		
mass transfer direction:	section 3	4.94	section 3	0.071
c to d	section 2	4.19	section 2	0.077
rotational speed:	section 1	2.44	section 1	0.089
n_R = 400 1/min	water outlet	1.38		
volume flow $\dot{V}_c$ [l/h]:			sauter diameter profile	
40.0	organic phase	y [%]		
volume flow $\dot{V}_d$ [l/h]:	organic phase outlet	3.65	measuring position	$d_{1,2}$ [mm]
48.0	section 3	3.25		
	section 2	2.64	section 3	2.7
	section 1	1.23	section 2	2.7
	organic phase inlet	0.00	section 1	3.0

column type:	concentration profile		hold-up profile	
RDC-extractor				
liquid/liquid-system:	aqueous phase	x [%]	measuring position	h_d [-]
t (d)/a/w	water inlet	5.74		
mass transfer direction:	section 3	5.26	section 3	0.157
c to d	section 2	4.64	section 2	0.157
rotational speed:	section 1	2.91	section 1	0.146
n_R = 400 1/min	water outlet	1.21		
volume flow $\dot{V}_c$ [l/h]:			sauter diameter profile	
61.3	organic phase	y [%]		
volume flow $\dot{V}_d$ [l/h]:	organic phase outlet	3.91	measuring position	$d_{1,2}$ [mm]
74.5	section 3	3.43		
	section 2	2.94	section 3	2.7
	section 1	1.57	section 2	2.6
	organic phase inlet	0.00	section 1	2.8

*Table A.17: Drop swarm extractor: fluiddynamics and mass transfer of drop swarms in an agitated extractor with rotating discs **"RDC-extractor"**; liquid/liquid-system: **toluene (d)/acetone/water** (continued)*

column type:	concentration profile		hold-up profile	
RDC-extractor				
liquid/liquid-system:	aqueous phase	x [%]	measuring position	h_d [-]
t (d)/a/w	water inlet	6.11		
mass transfer direction:	section 3	5.62	section 3	0.129
c to d	section 2	5.06	section 2	0.129
rotational speed:	section 1	3.28	section 1	0.157
n_R = 400 1/min	water outlet	1.27		
volume flow $\dot{V}_c$ [l/h]:			sauter diameter profile	
61.3	organic phase	y [%]		
volume flow $\dot{V}_d$ [l/h]:	organic phase outlet	4.16	measuring position	$d_{1,2}$ [mm]
74.5	section 3	3.55		
	section 2	3.09	section 3	2.8
	section 1	1.69	section 2	2.9
	organic phase inlet	0.00	section 1	2.6

column type:	concentration profile		hold-up profile	
RDC-extractor				
liquid/liquid-system:	aqueous phase	x [%]	measuring position	h_d [-]
t (d)/a/w	water inlet	6.00		
mass transfer direction:	section 3	5.62	section 3	0.182
c to d	section 2	4.91	section 2	0.172
rotational speed:	section 1	3.42	section 1	0.204
n_R = 400 1/min	water outlet	1.31		
volume flow $\dot{V}_c$ [l/h]:			sauter diameter profile	
71.9	organic phase	y [%]		
volume flow $\dot{V}_d$ [l/h]:	organic phase outlet	4.01	measuring position	$d_{1,2}$ [mm]
86.8	section 3	3.54		
	section 2	3.02	section 3	2.9
	section 1	1.84	section 2	2.9
	organic phase inlet	0.00	section 1	2.8

column type:	concentration profile		hold-up profile	
RDC-extractor				
liquid/liquid-system:	aqueous phase	x [%]	measuring position	h_d [-]
t (d)/a/w	water inlet	6.31		
mass transfer direction:	section 3	5.59	section 3	0.232
c to d	section 2	4.95	section 2	0.200
rotational speed:	section 1	3.47	section 1	0.216
n_R = 400 1/min	water outlet	1.32		
volume flow $\dot{V}_c$ [l/h]:			sauter diameter profile	
71.9	organic phase	y [%]		
volume flow $\dot{V}_d$ [l/h]:	organic phase outlet	4.35	measuring position	$d_{1,2}$ [mm]
86.8	section 3	3.65		
	section 2	3.08	section 3	2.7
	section 1	1.75	section 2	2.9
	organic phase inlet	0.00	section 1	2.8

*Table A.17: Drop swarm extractor: fluiddynamics and mass transfer of drop swarms in an agitated extractor with rotating discs **"RDC-extractor"**; liquid/liquid-system: **toluene (d)/acetone/water** (continued)*

column type:	concentration profile		hold-up profile	
RDC-extractor				
liquid/liquid-system:	aqueous phase	x [%]	measuring position	h_d [-]
t (d)/a/w	water inlet	5.85		
mass transfer direction:	section 3	5.47	section 3	0.092
c to d	section 2	4.77	section 2	0.095
rotational speed:	section 1	2.97	section 1	0.126
n_R = 400 1/min	water outlet	1.41		
volume flow $\dot{V}_c$ [l/h]:			sauter diameter profile	
50.6	organic phase	y [%]		
volume flow $\dot{V}_d$ [l/h]:	organic phase outlet	4.01	measuring position	$d_{1,2}$ [mm]
61.3	section 3	3.62		
	section 2	3.09	section 3	2.5
	section 1	1.58	section 2	2.7
	organic phase inlet	0.09	section 1	2.6

*Table A.18: Drop swarm extractor: fluiddynamics and mass transfer of drop swarms in an agitated extractor with rotating discs **"RDC-extractor"**; liquid/liquid-system: **butyl acetate (d)/acetone/water***

column type:	concentration profile		hold-up profile	
RDC-extractor				
liquid/liquid-system:	aqueous phase	x [%]	measuring position	h_d [-]
bu-ac (d)/a/w	water inlet	4.93		
mass transfer direction:	section 3	3.79	section 3	0.070
c to d	section 2	2.85	section 2	0.085
rotational speed:	section 1	1.59	section 1	0.082
n_R = 200 1/min	water outlet	0.98		
volume flow $\dot{V}_c$ [l/h]:			sauter diameter profile	
40.0	organic phase	y [%]		
volume flow $\dot{V}_d$ [l/h]:	organic phase outlet	3.60	measuring position	$d_{1,2}$ [mm]
48.0	section 3	2.64		
	section 2	2.08	section 3	2.2
	section 1	0.88	section 2	2.2
	organic phase inlet	0.13	section 1	2.3

column type:	concentration profile		hold-up profile	
RDC-extractor				
liquid/liquid-system:	aqueous phase	x [%]	measuring position	h_d [-]
bu-ac (d)/a/w	water inlet	4.87		
mass transfer direction:	section 3	3.81	section 3	0.080
c to d	section 2	2.91	section 2	0.079
rotational speed:	section 1	1.65	section 1	0.076
n_R = 200 1/min	water outlet	0.94		
volume flow $\dot{V}_c$ [l/h]:			sauter diameter profile	
40.0	organic phase	y [%]		
volume flow $\dot{V}_d$ [l/h]:	organic phase outlet	3.59	measuring position	$d_{1,2}$ [mm]
48.0	section 3	2.71		
	section 2	2.14	section 3	2.3
	section 1	0.92	section 2	2.2
	organic phase inlet	0.14	section 1	2.1

column type:	concentration profile		hold-up profile	
RDC-extractor				
liquid/liquid-system:	aqueous phase	x [%]	measuring position	h_d [-]
bu-ac (d)/a/w	water inlet	5.18		
mass transfer direction:	section 3	4.13	section 3	0.117
c to d	section 2	3.20	section 2	0.123
rotational speed:	section 1	1.87	section 1	0.123
n_R = 200 1/min	water outlet	0.85		
volume flow $\dot{V}_c$ [l/h]:			sauter diameter profile	
50.0	organic phase	y [%]		
volume flow $\dot{V}_d$ [l/h]:	organic phase outlet	3.86	measuring position	$d_{1,2}$ [mm]
60.0	section 3	3.06		
	section 2	2.31	section 3	2.0
	section 1	1.20	section 2	2.2
	organic phase inlet	0.00	section 1	2.1

*Table A.18: Drop swarm extractor: fluiddynamics and mass transfer of drop swarms in an agitated extractor with rotating discs **"RDC-extractor"**; liquid/liquid-system: **butyl acetate (d)/acetone/water** (continued)*

column type:	concentration profile		hold-up profile	
RDC-extractor				
liquid/liquid-system:	aqueous phase	x [%]	measuring position	h_d [-]
bu-ac (d)/a/w	water inlet	5.27		
mass transfer direction:	section 3	4.16	section 3	0.098
c to d	section 2	3.12	section 2	0.126
rotational speed:	section 1	1.93	section 1	0.129
n_R = 200 1/min	water outlet	0.88		
volume flow $\dot{V}_c$ [l/h]:			sauter diameter profile	
50.0	organic phase	y [%]		
volume flow $\dot{V}_d$ [l/h]:	organic phase outlet	3.90	measuring position	$d_{1,2}$ [mm]
60.0	section 3	3.09		
	section 2	2.34	section 3	1.7
	section 1	1.23	section 2	1.9
	organic phase inlet	0.00	section 1	2.1

column type:	concentration profile		hold-up profile	
RDC-extractor				
liquid/liquid-system:	aqueous phase	x [%]	measuring position	h_d [-]
bu-ac (d)/a/w	water inlet	4.78		
mass transfer direction:	section 3	3.88	section 3	0.156
c to d	section 2	3.12	section 2	0.159
rotational speed:	section 1	1.96	section 1	0.140
n_R = 200 1/min	water outlet	0.88		
volume flow $\dot{V}_c$ [l/h]:			sauter diameter profile	
60.0	organic phase	y [%]		
volume flow $\dot{V}_d$ [l/h]:	organic phase outlet	3.52	measuring position	$d_{1,2}$ [mm]
72.0	section 3	2.88		
	section 2	2.32	section 3	2.0
	section 1	1.27	section 2	2.2
	organic phase inlet	0.00	section 1	1.9

column type:	concentration profile		hold-up profile	
RDC-extractor				
liquid/liquid-system:	aqueous phase	x [%]	measuring position	h_d [-]
bu-ac (d)/a/w	water inlet	4.83		
mass transfer direction:	section 3	3.98	section 3	0.153
c to d	section 2	3.15	section 2	0.166
rotational speed:	section 1	2.07	section 1	0.140
n_R = 200 1/min	water outlet	0.92		
volume flow $\dot{V}_c$ [l/h]:			sauter diameter profile	
60.0	organic phase	y [%]		
volume flow $\dot{V}_d$ [l/h]:	organic phase outlet	3.47	measuring position	$d_{1,2}$ [mm]
72.0	section 3	2.84		
	section 2	2.01	section 3	1.9
	section 1	1.29	section 2	2.0
	organic phase inlet	0.00	section 1	2.2

*Table A.18: Drop swarm extractor: fluiddynamics and mass transfer of drop swarms in an agitated extractor with rotating discs **"RDC-extractor"**; liquid/liquid-system: **butyl acetate (d)/acetone/water** (continued)*

column type:	concentration profile		hold-up profile	
RDC-extractor				
liquid/liquid-system:	aqueous phase	x [%]	measuring position	h_d [-]
bu-ac (d)/a/w	water inlet	5.18		
mass transfer direction:	section 3	4.15	section 3	0.225
c to d	section 2	3.25	section 2	0.212
rotational speed:	section 1	2.17	section 1	0.266
n_R = 200 1/min	water outlet	0.91		
volume flow $\dot{V}_c$ [l/h]:			sauter diameter profile	
80.0	organic phase	y [%]		
volume flow $\dot{V}_d$ [l/h]:	organic phase outlet	3.78	measuring position	$d_{1,2}$ [mm]
96.0	section 3	3.00		
	section 2	2.29	section 3	1.9
	section 1	1.40	section 2	2.3
	organic phase inlet	0.05	section 1	2.0

column type:	concentration profile		hold-up profile	
RDC-extractor				
liquid/liquid-system:	aqueous phase	x [%]	measuring position	h_d [-]
bu-ac (d)/a/w	water inlet	5.76		
mass transfer direction:	section 3	4.26	section 3	0.105
c to d	section 2	3.01	section 2	0.098
rotational speed:	section 1	1.24	section 1	0.089
n_R = 400 1/min	water outlet	1.08		
volume flow $\dot{V}_c$ [l/h]:			sauter diameter profile	
40.0	organic phase	y [%]		
volume flow $\dot{V}_d$ [l/h]:	organic phase outlet	4.49	measuring position	$d_{1,2}$ [mm]
48.0	section 3	3.15		
	section 2	2.14	section 3	1.9
	section 1	1.01	section 2	1.9
	organic phase inlet	0.40	section 1	2.0

column type:	concentration profile		hold-up profile	
RDC-extractor				
liquid/liquid-system:	aqueous phase	x [%]	measuring position	h_d [-]
bu-ac (d)/a/w	water inlet	5.77		
mass transfer direction:	section 3	4.36	section 3	0.102
c to d	section 2	3.23	section 2	0.102
rotational speed:	section 1	1.73	section 1	0.098
n_R = 400 1/min	water outlet	1.12		
volume flow $\dot{V}_c$ [l/h]:			sauter diameter profile	
40.0	organic phase	y [%]		
volume flow $\dot{V}_d$ [l/h]:	organic phase outlet	4.43	measuring position	$d_{1,2}$ [mm]
48.0	section 3	3.28		
	section 2	2.40	section 3	1.9
	section 1	1.05	section 2	2.0
	organic phase inlet	0.37	section 1	2.0

*Table A.18: Drop swarm extractor: fluiddynamics and mass transfer of drop swarms in an agitated extractor with rotating discs **"RDC-extractor"**; liquid/liquid-system: **butyl acetate (d)/acetone/water** (continued)*

column type:	concentration profile		hold-up profile	
RDC-extractor				
liquid/liquid-system:	aqueous phase	x [%]	measuring position	h_d [-]
bu-ac (d)/a/w	water inlet	4.96		
mass transfer direction:	section 3	3.71	section 3	0.138
c to d	section 2	2.76	section 2	0.135
rotational speed:	section 1	1.44	section 1	0.153
n_R = 400 1/min	water outlet	0.64		
volume flow $\dot{V}_c$ [l/h]:			sauter diameter profile	
50.0	organic phase	y [%]		
volume flow $\dot{V}_d$ [l/h]:	organic phase outlet	3.89	measuring position	$d_{1,2}$ [mm]
60.0	section 3	2.94		
	section 2	1.96	section 3	1.8
	section 1	0.86	section 2	1.9
	organic phase inlet	0.05	section 1	1.9

column type:	concentration profile		hold-up profile	
RDC-extractor				
liquid/liquid-system:	aqueous phase	x [%]	measuring position	h_d [-]
bu-ac (d)/a/w	water inlet	5.03		
mass transfer direction:	section 3	3.81	section 3	0.132
c to d	section 2	2.76	section 2	0.135
rotational speed:	section 1	1.46	section 1	0.154
n_R = 400 1/min	water outlet	0.63		
volume flow $\dot{V}_c$ [l/h]:			sauter diameter profile	
50.0	organic phase	y [%]		
volume flow $\dot{V}_d$ [l/h]:	organic phase outlet	3.98	measuring position	$d_{1,2}$ [mm]
60.0	section 3	2.88		
	section 2	2.07	section 3	2.0
	section 1	0.88	section 2	2.1
	organic phase inlet	0.06	section 1	1.8

column type:	concentration profile		hold-up profile	
RDC-extractor				
liquid/liquid-system:	aqueous phase	x [%]	measuring position	h_d [-]
bu-ac (d)/a/w	water inlet	5.73		
mass transfer direction:	section 3	4.55	section 3	0.169
c to d	section 2	3.46	section 2	0.182
rotational speed:	section 1	2.30	section 1	0.203
n_R = 400 1/min	water outlet	1.07		
volume flow $\dot{V}_c$ [l/h]:			sauter diameter profile	
60.0	organic phase	y [%]		
volume flow $\dot{V}_d$ [l/h]:	organic phase outlet	4.48	measuring position	$d_{1,2}$ [mm]
72.0	section 3	3.43		
	section 2	2.61	section 3	2.0
	section 1	1.40	section 2	1.9
	organic phase inlet	0.41	section 1	1.9

*Table A.18: Drop swarm extractor: fluiddynamics and mass transfer of drop swarms in an agitated extractor with rotating discs **"RDC-extractor"**; liquid/liquid-system: **butyl acetate (d)/acetone/water** (continued)*

column type:	concentration profile		hold-up profile	
RDC-extractor				
liquid/liquid-system:	aqueous phase	x [%]	measuring position	h_d [-]
bu-ac (d)/a/w	water inlet	5.70		
mass transfer direction:	section 3	4.39	section 3	0.161
c to d	section 2	3.26	section 2	0.185
rotational speed:	section 1	1.96	section 1	0.175
n_R = 400 1/min	water outlet	0.89		
volume flow $\dot{V}_c$ [l/h]:			sauter diameter profile	
60.0	organic phase	y [%]		
volume flow $\dot{V}_d$ [l/h]:	organic phase outlet	4.34	measuring position	$d_{1,2}$ [mm]
72.0	section 3	3.35		
	section 2	2.50	section 3	2.0
	section 1	1.26	section 2	1.9
	organic phase inlet	0.18	section 1	2.0

column type:	concentration profile		hold-up profile	
RDC-extractor				
liquid/liquid-system:	aqueous phase	x [%]	measuring position	h_d [-]
bu-ac (d)/a/w	water inlet	5.65		
mass transfer direction:	section 3	4.42	section 3	0.202
c to d	section 2	3.34	section 2	0.229
rotational speed:	section 1	2.07	section 1	0.238
n_R = 400 1/min	water outlet	0.90		
volume flow $\dot{V}_c$ [l/h]:			sauter diameter profile	
70.0	organic phase	y [%]		
volume flow $\dot{V}_d$ [l/h]:	organic phase outlet	4.39	measuring position	$d_{1,2}$ [mm]
84.0	section 3	3.38		
	section 2	2.46	section 3	2.0
	section 1	1.30	section 2	1.9
	organic phase inlet	0.16	section 1	2.0

column type:	concentration profile		hold-up profile	
RDC-extractor				
liquid/liquid-system:	aqueous phase	x [%]	measuring position	h_d [-]
bu-ac (d)/a/w	water inlet	5.74		
mass transfer direction:	section 3	4.52	section 3	0.228
c to d	section 2	3.48	section 2	0.218
rotational speed:	section 1	2.14	section 1	0.254
n_R = 400 1/min	water outlet	0.92		
volume flow $\dot{V}_c$ [l/h]:			sauter diameter profile	
70.0	organic phase	y [%]		
volume flow $\dot{V}_d$ [l/h]:	organic phase outlet	4.33	measuring position	$d_{1,2}$ [mm]
84.0	section 3	3.40		
	section 2	2.54	section 3	1.7
	section 1	1.38	section 2	1.7
	organic phase inlet	0.16	section 1	1.8

*Table A.18: Drop swarm extractor: fluiddynamics and mass transfer of drop swarms in an agitated extractor with rotating discs **"RDC-extractor"**; liquid/liquid-system: **butyl acetate (d)/acetone/water** (continued)*

column type:	concentration profile		hold-up profile	
RDC-extractor				
liquid/liquid-system:	aqueous phase	x [%]	measuring position	h_d [-]
bu-ac (d)/a/w	water inlet	4.98		
mass transfer direction:	section 3	3.95	section 3	0.243
c to d	section 2	3.22	section 2	0.263
rotational speed:	section 1	2.15	section 1	0.258
n_R = 400 1/min	water outlet	0.91		
volume flow $\dot{V}_c$ [l/h]:			sauter diameter profile	
80.0	organic phase	y [%]		
volume flow $\dot{V}_d$ [l/h]:	organic phase outlet	3.69	measuring position	$d_{1,2}$ [mm]
96.0	section 3	2.81		
	section 2	2.35	section 3	2.0
	section 1	1.33	section 2	1.9
	organic phase inlet	0.15	section 1	2.1

*Table A.19: Drop swarm extractor: fluiddynamics and mass transfer of drop swarms in an agitated extractor with Kühni blade agitators **"Kühni-extractor"**; liquid/liquid-system: **toluene (d)/acetone/water***

column type:	concentration profile		hold-up profile	
Kühni-extractor				
liquid/liquid-system:	aqueous phase	x [%]	measuring position	h_d [-]
t (d)/a/w	water inlet	5.27		
mass transfer direction:	section 3	4.52	section 3	0.108
c to d	section 2	3.67	section 2	0.111
rotational speed:	section 1	2.04	section 1	0.129
n_R = 150 1/min	water outlet	1.01		
volume flow $\dot{V}_c$ [l/h]:			sauter diameter profile	
40.0	organic phase	y [%]		
volume flow $\dot{V}_d$ [l/h]:	organic phase outlet	3.86	measuring position	$d_{1,2}$ [mm]
48.0	section 3	3.11		
	section 2	2.50	section 3	2.9
	section 1	1.12	section 2	3.3
	organic phase inlet	0.04	section 1	3.2

column type:	concentration profile		hold-up profile	
Kühni-extractor				
liquid/liquid-system:	aqueous phase	x [%]	measuring position	h_d [-]
t (d)/a/w	water inlet	5.08		
mass transfer direction:	section 3	4.53	section 3	0.108
c to d	section 2	3.76	section 2	0.111
rotational speed:	section 1	2.18	section 1	0.120
n_R = 150 1/min	water outlet	0.99		
volume flow $\dot{V}_c$ [l/h]:			sauter diameter profile	
40.0	organic phase	y [%]		
volume flow $\dot{V}_d$ [l/h]:	organic phase outlet	3.71	measuring position	$d_{1,2}$ [mm]
48.0	section 3	3.34		
	section 2	2.74	section 3	2.8
	section 1	1.26	section 2	3.1
	organic phase inlet	0.02	section 1	3.2

column type:	concentration profile		hold-up profile	
Kühni-extractor				
liquid/liquid-system:	aqueous phase	x [%]	measuring position	h_d [-]
t (d)/a/w	water inlet	5.31		
mass transfer direction:	section 3	4.79	section 3	0.224
c to d	section 2	4.06	section 2	0.188
rotational speed:	section 1	2.73	section 1	0.209
n_R = 150 1/min	water outlet	1.00		
volume flow $\dot{V}_c$ [l/h]:			sauter diameter profile	
60.0	organic phase	y [%]		
volume flow $\dot{V}_d$ [l/h]:	organic phase outlet	3.89	measuring position	$d_{1,2}$ [mm]
72.0	section 3	3.55		
	section 2	2.95	section 3	2.7
	section 1	1.56	section 2	3.2
	organic phase inlet	0.04	section 1	3.2

*Table A.19: Drop swarm extractor: fluiddynamics and mass transfer of drop swarms in an agitated extractor with Kühni blade agitators **"Kühni-extractor"**; liquid/liquid-system: **toluene (d)/acetone/water** (continued)*

column type:	concentration profile		hold-up profile	
Kühni-extractor				
liquid/liquid-system:	aqueous phase	x [%]	measuring position	h_d [-]
t (d)/a/w	water inlet	5.07		
mass transfer direction:	section 3	4.55	section 3	0.185
c to d	section 2	3.90	section 2	0.182
rotational speed:	section 1	2.64	section 1	0.197
n_R = 150 1/min	water outlet	0.96		
volume flow $\dot{V}_c$ [l/h]:			sauter diameter profile	
60.0	organic phase	y [%]		
volume flow $\dot{V}_d$ [l/h]:	organic phase outlet	3.72	measuring position	$d_{1,2}$ [mm]
72.0	section 3	3.32		
	section 2	2.79	section 3	2.6
	section 1	1.57	section 2	3.1
	organic phase inlet	0.02	section 1	3.2

column type:	concentration profile		hold-up profile	
Kühni-extractor				
liquid/liquid-system:	aqueous phase	x [%]	measuring position	h_d [-]
t (d)/a/w	water inlet	5.45		
mass transfer direction:	section 3	4.83	section 3	0.274
c to d	section 2	4.24	section 2	0.298
rotational speed:	section 1	3.04	section 1	0.316
n_R = 150 1/min	water outlet	1.18		
volume flow $\dot{V}_c$ [l/h]:			sauter diameter profile	
70.0	organic phase	y [%]		
volume flow $\dot{V}_d$ [l/h]:	organic phase outlet	3.92	measuring position	$d_{1,2}$ [mm]
84.0	section 3	3.54		
	section 2	3.01	section 3	3.0
	section 1	1.83	section 2	2.8
	organic phase inlet	0.00	section 1	3.1

column type:	concentration profile		hold-up profile	
Kühni-extractor				
liquid/liquid-system:	aqueous phase	x [%]	measuring position	h_d [-]
t (d)/a/w	water inlet	5.44		
mass transfer direction:	section 3	4.79	section 3	0.286
c to d	section 2	4.18	section 2	0.291
rotational speed:	section 1	2.89	section 1	0.337
n_R = 150 1/min	water outlet	1.08		
volume flow $\dot{V}_c$ [l/h]:			sauter diameter profile	
70.0	organic phase	y [%]		
volume flow $\dot{V}_d$ [l/h]:	organic phase outlet	4.02	measuring position	$d_{1,2}$ [mm]
84.0	section 3	3.59		
	section 2	3.04	section 3	2.7
	section 1	1.80	section 2	2.9
	organic phase inlet	0.04	section 1	3.0

*Table A.19: Drop swarm extractor: fluiddynamics and mass transfer of drop swarms in an agitated extractor with Kühni blade agitators **"Kühni-extractor"**; liquid/liquid-system: **toluene (d)/acetone/water** (continued)*

column type:	concentration profile		hold-up profile	
Kühni-extractor				
liquid/liquid-system:	aqueous phase	x [%]	measuring position	h_d [-]
t (d)/a/w	water inlet	5.23		
mass transfer direction:	section 3	4.63	section 3	0.168
c to d	section 2	3.83	section 2	0.163
rotational speed:	section 1	1.91	section 1	0.173
n_R = 200 1/min	water outlet	0.90		
volume flow $\dot{V}_c$ [l/h]:			sauter diameter profile	
40.0	organic phase	y [%]		
volume flow $\dot{V}_d$ [l/h]:	organic phase outlet	3.89	measuring position	$d_{1,2}$ [mm]
48.0	section 3	3.50		
	section 2	2.82	section 3	2.2
	section 1	1.19	section 2	2.5
	organic phase inlet	0.06	section 1	3.2

column type:	concentration profile		hold-up profile	
Kühni-extractor				
liquid/liquid-system:	aqueous phase	x [%]	measuring position	h_d [-]
t (d)/a/w	water inlet	5.26		
mass transfer direction:	section 3	4.61	section 3	0.191
c to d	section 2	4.09	section 2	0.178
rotational speed:	section 1	2.04	section 1	0.154
n_R = 200 1/min	water outlet	0.85		
volume flow $\dot{V}_c$ [l/h]:			sauter diameter profile	
40.0	organic phase	y [%]		
volume flow $\dot{V}_d$ [l/h]:	organic phase outlet	3.98	measuring position	$d_{1,2}$ [mm]
48.0	section 3	3.57		
	section 2	2.96	section 3	1.9
	section 1	1.28	section 2	2.3
	organic phase inlet	0.02	section 1	3.0

column type:	concentration profile		hold-up profile	
Kühni-extractor				
liquid/liquid-system:	aqueous phase	x [%]	measuring position	h_d [-]
t (d)/a/w	water inlet	5.56		
mass transfer direction:	section 3	5.17	section 3	0.246
c to d	section 2	4.44	section 2	0.237
rotational speed:	section 1	2.55	section 1	0.286
n_R = 200 1/min	water outlet	0.89		
volume flow $\dot{V}_c$ [l/h]:			sauter diameter profile	
50.0	organic phase	y [%]		
volume flow $\dot{V}_d$ [l/h]:	organic phase outlet	4.29	measuring position	$d_{1,2}$ [mm]
60.0	section 3	3.66		
	section 2	3.01	section 3	2.2
	section 1	1.26	section 2	2.6
	organic phase inlet	0.04	section 1	3.0

*Table A.19: Drop swarm extractor: fluiddynamics and mass transfer of drop swarms in an agitated extractor with Kühni blade agitators **"Kühni-extractor"**; liquid/liquid-system: **toluene (d)/acetone/water** (continued)*

column type:	concentration profile		hold-up profile	
Kühni-extractor				
liquid/liquid-system:	aqueous phase	x [%]	measuring position	h_d [-]
t (d)/a/w	water inlet	5.45		
mass transfer direction:	section 3	5.12	section 3	0.246
c to d	section 2	4.19	section 2	0.228
rotational speed:	section 1	2.15	section 1	0.262
n_R = 200 1/min	water outlet	0.85		
volume flow $\dot{V}_c$ [l/h]:			sauter diameter profile	
50.0	organic phase	y [%]		
volume flow $\dot{V}_d$ [l/h]:	organic phase outlet	4.14	measuring position	$d_{1,2}$ [mm]
60.0	section 3	3.75		
	section 2	3.18	section 3	2.0
	section 1	1.55	section 2	2.6
	organic phase inlet	0.00	section 1	2.9

column type:	concentration profile		hold-up profile	
Kühni-extractor				
liquid/liquid-system:	aqueous phase	x [%]	measuring position	h_d [-]
t (d)/a/w	water inlet	6.28		
mass transfer direction:	section 3	5.85	section 3	0.268
c to d	section 2	4.92	section 2	0.284
rotational speed:	section 1	2.93	section 1	0.304
n_R = 200 1/min	water outlet	0.98		
volume flow $\dot{V}_c$ [l/h]:			sauter diameter profile	
59.7	organic phase	y [%]		
volume flow $\dot{V}_d$ [l/h]:	organic phase outlet	4.63	measuring position	$d_{1,2}$ [mm]
72.1	section 3	4.02		
	section 2	3.36	section 3	2.0
	section 1	1.69	section 2	2.6
	organic phase inlet	0.00	section 1	2.8

column type:	concentration profile		hold-up profile	
Kühni-extractor				
liquid/liquid-system:	aqueous phase	x [%]	measuring position	h_d [-]
t (d)/a/w	water inlet	5.62		
mass transfer direction:	section 3	5.14	section 3	0.311
c to d	section 2	4.41	section 2	0.289
rotational speed:	section 1	2.60	section 1	0.311
n_R = 200 1/min	water outlet	0.90		
volume flow $\dot{V}_c$ [l/h]:			sauter diameter profile	
60.0	organic phase	y [%]		
volume flow $\dot{V}_d$ [l/h]:	organic phase outlet	4.32	measuring position	$d_{1,2}$ [mm]
72.0	section 3	3.84		
	section 2	3.24	section 3	2.1
	section 1	1.57	section 2	2.7
	organic phase inlet	0.04	section 1	3.0

*Table A.20: Drop swarm extractor: fluiddynamics and mass transfer of drop swarms in an agitated extractor with Kühni blade agitators **"Kühni-extractor"**; liquid/liquid-system: **butyl acetate (d)/acetone/water***

column type:	concentration profile		hold-up profile	
Kühni-extractor				
liquid/liquid-system:	aqueous phase	x [%]	measuring position	h_d [-]
bu-ac (d)/a/w	water inlet	5.36		
mass transfer direction:	section 3	3.25	section 3	0.050
c to d	section 2	2.02	section 2	0.049
rotational speed:	section 1	0.61	section 1	0.047
n_R = 100 1/min	water outlet	0.58		
volume flow $\dot{V}_c$ [l/h]:			sauter diameter profile	
20.0	organic phase	y [%]		
volume flow $\dot{V}_d$ [l/h]:	organic phase outlet	4.18	measuring position	$d_{1,2}$ [mm]
24.0	section 3	2.36		
	section 2	1.40	section 3	1.9
	section 1	0.37	section 2	2.3
	organic phase inlet	0.00	section 1	2.0

column type:	concentration profile		hold-up profile	
Kühni-extractor				
liquid/liquid-system:	aqueous phase	x [%]	measuring position	h_d [-]
bu-ac (d)/a/w	water inlet	5.01		
mass transfer direction:	section 3	3.34	section 3	0.049
c to d	section 2	2.14	section 2	0.046
rotational speed:	section 1	0.83	section 1	0.048
n_R = 100 1/min	water outlet	0.63		
volume flow $\dot{V}_c$ [l/h]:			sauter diameter profile	
20.0	organic phase	y [%]		
volume flow $\dot{V}_d$ [l/h]:	organic phase outlet	3.98	measuring position	$d_{1,2}$ [mm]
24.0	section 3	2.45		
	section 2	1.08	section 3	2.1
	section 1	0.42	section 2	2.4
	organic phase inlet	0.00	section 1	2.1

column type:	concentration profile		hold-up profile	
Kühni-extractor				
liquid/liquid-system:	aqueous phase	x [%]	measuring position	h_d [-]
bu-ac (d)/a/w	water inlet	5.13		
mass transfer direction:	section 3	3.57	section 3	0.088
c to d	section 2	2.42	section 2	0.094
rotational speed:	section 1	1.00	section 1	0.088
n_R = 100 1/min	water outlet	0.66		
volume flow $\dot{V}_c$ [l/h]:			sauter diameter profile	
30.0	organic phase	y [%]		
volume flow $\dot{V}_d$ [l/h]:	organic phase outlet	4.01	measuring position	$d_{1,2}$ [mm]
36.0	section 3	2.67		
	section 2	1.74	section 3	1.8
	section 1	0.54	section 2	2.2
	organic phase inlet	0.00	section 1	2.3

*Table A.20: Drop swarm extractor: fluiddynamics and mass transfer of drop swarms in an agitated extractor with Kühni blade agitators **"Kühni-extractor"**; liquid/liquid-system: **butyl acetate (d)/acetone/water** (continued)*

column type:	concentration profile		hold-up profile	
Kühni-extractor				
liquid/liquid-system:	aqueous phase	x [%]	measuring position	h_d [-]
bu-ac (d)/a/w	water inlet	5.27		
mass transfer direction:	section 3	3.58	section 3	0.097
c to d	section 2	2.42	section 2	0.088
rotational speed:	section 1	1.10	section 1	0.091
n_R = 100 1/min	water outlet	0.66		
volume flow $\dot{V}_c$ [l/h]:			sauter diameter profile	
30.0	organic phase	y [%]		
volume flow $\dot{V}_d$ [l/h]:	organic phase outlet	3.92	measuring position	$d_{1,2}$ [mm]
36.0	section 3	2.68		
	section 2	1.75	section 3	1.8
	section 1	0.53	section 2	2.1
	organic phase inlet	0.00	section 1	2.2

column type:	concentration profile		hold-up profile	
Kühni-extractor				
liquid/liquid-system:	aqueous phase	x [%]	measuring position	h_d [-]
bu-ac (d)/a/w	water inlet	5.01		
mass transfer direction:	section 3	3.70	section 3	0.127
c to d	section 2	2.63	section 2	0.117
rotational speed:	section 1	1.30	section 1	0.123
n_R = 100 1/min	water outlet	0.83		
volume flow $\dot{V}_c$ [l/h]:			sauter diameter profile	
40.0	organic phase	y [%]		
volume flow $\dot{V}_d$ [l/h]:	organic phase outlet	3.72	measuring position	$d_{1,2}$ [mm]
48.0	section 3	2.50		
	section 2	1.93	section 3	1.8
	section 1	0.64	section 2	1.8
	organic phase inlet	0.06	section 1	2.2

column type:	concentration profile		hold-up profile	
Kühni-extractor				
liquid/liquid-system:	aqueous phase	x [%]	measuring position	h_d [-]
bu-ac (d)/a/w	water inlet	4.96		
mass transfer direction:	section 3	3.64	section 3	0.139
c to d	section 2	2.63	section 2	0.133
rotational speed:	section 1	1.39	section 1	0.112
n_R = 100 1/min	water outlet	0.86		
volume flow $\dot{V}_c$ [l/h]:			sauter diameter profile	
40.0	organic phase	y [%]		
volume flow $\dot{V}_d$ [l/h]:	organic phase outlet	3.69	measuring position	$d_{1,2}$ [mm]
48.0	section 3	2.51		
	section 2	1.89	section 3	1.7
	section 1	0.61	section 2	2.0
	organic phase inlet	0.05	section 1	2.4

*Table A.20: Drop swarm extractor: fluiddynamics and mass transfer of drop swarms in an agitated extractor with Kühni blade agitators **"Kühni-extractor"**; liquid/liquid-system: **butyl acetate (d)/acetone/water** (continued)*

column type:	concentration profile		hold-up profile	
Kühni-extractor				
liquid/liquid-system:	aqueous phase	x [%]	measuring position	h_d [-]
bu-ac (d)/a/w	water inlet	5.36		
mass transfer direction:	section 3	4.05	section 3	0.158
c to d	section 2	2.91	section 2	0.153
rotational speed:	section 1	1.45	section 1	0.149
n_R = 100 1/min	water outlet	0.70		
volume flow $\dot{V}_c$ [l/h]:			sauter diameter profile	
50.0	organic phase	y [%]		
volume flow $\dot{V}_d$ [l/h]:	organic phase outlet	4.01	measuring position	$d_{1,2}$ [mm]
60.0	section 3	3.04		
	section 2	2.19	section 3	2.0
	section 1	0.81	section 2	1.9
	organic phase inlet	0.00	section 1	2.4

column type:	concentration profile		hold-up profile	
Kühni-extractor				
liquid/liquid-system:	aqueous phase	x [%]	measuring position	h_d [-]
bu-ac (d)/a/w	water inlet	5.23		
mass transfer direction:	section 3	3.90	section 3	0.178
c to d	section 2	2.82	section 2	0.166
rotational speed:	section 1	1.43	section 1	0.163
n_R = 100 1/min	water outlet	0.60		
volume flow $\dot{V}_c$ [l/h]:			sauter diameter profile	
50.0	organic phase	y [%]		
volume flow $\dot{V}_d$ [l/h]:	organic phase outlet	4.01	measuring position	$d_{1,2}$ [mm]
60.0	section 3	3.01		
	section 2	2.17	section 3	1.8
	section 1	0.81	section 2	2.1
	organic phase inlet	0.00	section 1	2.2

column type:	concentration profile		hold-up profile	
Kühni-extractor				
liquid/liquid-system:	aqueous phase	x [%]	measuring position	h_d [-]
bu-ac (d)/a/w	water inlet	5.64		
mass transfer direction:	section 3	3.91	section 3	0.216
c to d	section 2	2.81	section 2	0.223
rotational speed:	section 1	1.57	section 1	0.197
n_R = 100 1/min	water outlet	0.70		
volume flow $\dot{V}_c$ [l/h]:			sauter diameter profile	
60.0	organic phase	y [%]		
volume flow $\dot{V}_d$ [l/h]:	organic phase outlet	4.28	measuring position	$d_{1,2}$ [mm]
72.0	section 3	3.17		
	section 2	2.19	section 3	1.8
	section 1	0.95	section 2	2.1
	organic phase inlet	0.00	section 1	2.3

*Table A.20: Drop swarm extractor: fluiddynamics and mass transfer of drop swarms in an agitated extractor with Kühni blade agitators **"Kühni-extractor"**; liquid/liquid-system: **butyl acetate (d)/acetone/water** (continued)*

column type:	concentration profile		hold-up profile	
Kühni-extractor				
liquid/liquid-system:	aqueous phase	x [%]	measuring position	h_d [-]
bu-ac (d)/a/w	water inlet	5.51		
mass transfer direction:	section 3	4.19	section 3	0.231
c to d	section 2	2.88	section 2	0.215
rotational speed:	section 1	1.59	section 1	0.200
n_R = 100 1/min	water outlet	0.78		
volume flow $\dot{V}_c$ [l/h]:			sauter diameter profile	
60.0	organic phase	y [%]		
volume flow $\dot{V}_d$ [l/h]:	organic phase outlet	4.30	measuring position	$d_{1,2}$ [mm]
72.0	section 3	3.16		
	section 2	2.21	section 3	1.8
	section 1	0.95	section 2	2.2
	organic phase inlet	0.18	section 1	2.4

column type:	concentration profile		hold-up profile	
Kühni-extractor				
liquid/liquid-system:	aqueous phase	x [%]	measuring position	h_d [-]
bu-ac (d)/a/w	water inlet	5.00		
mass transfer direction:	section 3	2.64	section 3	0.092
c to d	section 2	1.42	section 2	0.092
rotational speed:	section 1	0.38	section 1	0.089
n_R = 150 1/min	water outlet	0.31		
volume flow $\dot{V}_c$ [l/h]:			sauter diameter profile	
20.0	organic phase	y [%]		
volume flow $\dot{V}_d$ [l/h]:	organic phase outlet	4.03	measuring position	$d_{1,2}$ [mm]
24.0	section 3	2.27		
	section 2	1.14	section 3	1.4
	section 1	0.14	section 2	1.6
	organic phase inlet	0.00	section 1	1.9

column type:	concentration profile		hold-up profile	
Kühni-extractor				
liquid/liquid-system:	aqueous phase	x [%]	measuring position	h_d [-]
bu-ac (d)/a/w	water inlet	4.98		
mass transfer direction:	section 3	2.84	section 3	0.086
c to d	section 2	1.52	section 2	0.092
rotational speed:	section 1	0.42	section 1	0.077
n_R = 150 1/min	water outlet	0.28		
volume flow $\dot{V}_c$ [l/h]:			sauter diameter profile	
20.0	organic phase	y [%]		
volume flow $\dot{V}_d$ [l/h]:	organic phase outlet	4.19	measuring position	$d_{1,2}$ [mm]
24.0	section 3	2.38		
	section 2	1.24	section 3	1.4
	section 1	0.15	section 2	1.7
	organic phase inlet	0.00	section 1	1.9

*Table A.20: Drop swarm extractor: fluiddynamics and mass transfer of drop swarms in an agitated extractor with Kühni blade agitators **"Kühni-extractor"**; liquid/liquid-system: **butyl acetate (d)/acetone/water** (continued)*

column type:	concentration profile		hold-up profile	
Kühni-extractor				
liquid/liquid-system:	aqueous phase	x [%]	measuring position	h_d [-]
bu-ac (d)/a/w	water inlet	5.03		
mass transfer direction:	section 3	3.26	section 3	0.234
c to d	section 2	1.70	section 2	0.222
rotational speed:	section 1	0.54	section 1	0.199
n_R = 150 1/min	water outlet	0.30		
volume flow $\dot{V}_c$ [l/h]:			sauter diameter profile	
30.0	organic phase	y [%]		
volume flow $\dot{V}_d$ [l/h]:	organic phase outlet	4.13	measuring position	$d_{1,2}$ [mm]
36.0	section 3	2.64		
	section 2	1.36	section 3	1.6
	section 1	0.25	section 2	1.7
	organic phase inlet	0.00	section 1	1.6

column type:	concentration profile		hold-up profile	
Kühni-extractor				
liquid/liquid-system:	aqueous phase	x [%]	measuring position	h_d [-]
bu-ac (d)/a/w	water inlet	4.81		
mass transfer direction:	section 3	3.26	section 3	0.194
c to d	section 2	2.05	section 2	0.227
rotational speed:	section 1	0.61	section 1	0.202
n_R = 150 1/min	water outlet	0.29		
volume flow $\dot{V}_c$ [l/h]:			sauter diameter profile	
30.0	organic phase	y [%]		
volume flow $\dot{V}_d$ [l/h]:	organic phase outlet	4.09	measuring position	$d_{1,2}$ [mm]
36.0	section 3	2.76		
	section 2	1.63	section 3	1.5
	section 1	0.40	section 2	1.7
	organic phase inlet	0.00	section 1	2.0

column type:	concentration profile		hold-up profile	
Kühni-extractor				
liquid/liquid-system:	aqueous phase	x [%]	measuring position	h_d [-]
bu-ac (d)/a/w	water inlet	5.04		
mass transfer direction:	section 3	3.55	section 3	0.274
c to d	section 2	2.17	section 2	0.262
rotational speed:	section 1	0.62	section 1	0.243
n_R = 150 1/min	water outlet	0.32		
volume flow $\dot{V}_c$ [l/h]:			sauter diameter profile	
40.0	organic phase	y [%]		
volume flow $\dot{V}_d$ [l/h]:	organic phase outlet	4.22	measuring position	$d_{1,2}$ [mm]
48.0	section 3	2.89		
	section 2	1.73	section 3	1.6
	section 1	0.39	section 2	1.8
	organic phase inlet	0.00	section 1	1.9

*Table A.20: Drop swarm extractor: fluiddynamics and mass transfer of drop swarms in an agitated extractor with Kühni blade agitators **"Kühni-extractor"**; liquid/liquid-system: **butyl acetate (d)/acetone/water** (continued)*

column type:	concentration profile		hold-up profile	
Kühni-extractor				
liquid/liquid-system:	aqueous phase	x [%]	measuring position	h_d [-]
bu-ac (d)/a/w	water inlet	5.03		
mass transfer direction:	section 3	3.46	section 3	0.262
c to d	section 2	2.04	section 2	0.279
rotational speed:	section 1	0.58	section 1	0.254
n_R = 150 1/min	water outlet	0.29		
volume flow $\dot{V}_c$ [l/h]:			sauter diameter profile	
40.0	organic phase	y [%]		
volume flow $\dot{V}_d$ [l/h]:	organic phase outlet	4.17	measuring position	$d_{1,2}$ [mm]
48.0	section 3	2.87		
	section 2	1.64	section 3	1.6
	section 1	0.36	section 2	1.8
	organic phase inlet	0.00	section 1	1.9

column type:	concentration profile		hold-up profile	
Kühni-extractor				
liquid/liquid-system:	aqueous phase	x [%]	measuring position	h_d [-]
bu-ac (d)/a/w	water inlet	5.44		
mass transfer direction:	section 3	4.19	section 3	0.355
c to d	section 2	3.07	section 2	0.368
rotational speed:	section 1	0.92	section 1	0.332
n_R = 150 1/min	water outlet	0.39		
volume flow $\dot{V}_c$ [l/h]:			sauter diameter profile	
50.0	organic phase	y [%]		
volume flow $\dot{V}_d$ [l/h]:	organic phase outlet	4.29	measuring position	$d_{1,2}$ [mm]
60.0	section 3	3.44		
	section 2	2.41	section 3	1.8
	section 1	0.40	section 2	1.9
	organic phase inlet	0.00	section 1	2.1